Cardiovascular Autonomic Dysfunction in Chronic Kidney Disease

Ibrahim M. Salman, *BSc (Pharmacy), MSc (Pharmacology)*

A thesis of The Australian School of Advanced Medicine, Faculty of Human Sciences, Macquarie University, submitted in fulfilment of the requirements for the degree of Doctor of Philosophy.

Supervisor:

Professor Jacqueline K. Phillips

Co-supervisor:

Doctor Cara M. Hildreth

June 2014

Declaration of originality

I hereby declare that the work presented in this thesis has not been submitted for a higher degree to any other university or institution. To the best of my knowledge this submission contains no material previously published or written by another person, except where due reference is stated otherwise. Any contribution made to the research by others is explicitly acknowledged.

Ibrahim M. Salman (42270790)

Australian School of Advanced Medicine
Faculty of Human Science
Macquarie University

June 2014

Declaration of contributions

Chapter 3

Candidate performed all experiments, analysed data and interpreted results. Candidate was the major contributor to the manuscript. Jacqueline Phillips and Cara Hildreth contributed to conception and design of experiments, data analysis, interpretation of results and editing, revision and final approval of manuscript. Omar Ziad Ameer Al-adhami (42270707), a PhD candidate, assisted with the preparation of aortic histological sections, imaging and data analysis and contributed to final approval of manuscript.

Chapter 4

Candidate performed all experiments, analysed data and interpreted results. Candidate was the major contributor to the manuscript. Jacqueline Phillips and Cara Hildreth contributed to conception and design of experiments, data analysis, interpretation of results and editing, revision and final approval of manuscript. Omar Ziad Ameer Al-adhami, a PhD candidate, assisted with the preparation of aortic histological sections, imaging and data analysis and contributed to final approval of manuscript. Divya Sarma Kandukuri (42185262), a PhD candidate, assisted with urine samples collection.

Chapter 6

Candidate contributed to experimental design, performed all experiments, analysed data, and interpreted results. Candidate was the major contributor to the manuscript. Jacqueline Phillips and Cara Hildreth contributed to interpretation of results and editing, revision and final approval of manuscript.

Chapter 7

Candidate performed all experiments, analysed data and interpreted results. Candidate was the major contributor to the manuscript. Jacqueline Phillips and Cara Hildreth contributed to conception and design of experiments, data analysis, interpretation of results and editing, revision and final approval of manuscript. Joanna Harrison contributed to the design of experiments. Divya Sarma Kandukuri assisted with anaesthetic and animal monitoring during recovery surgical procedures, record keeping and weekend check of instrumented animals.

This thesis is dedicated to

my beloved family

Acknowledgements

Completing my PhD degree is probably the most challenging activity I have ever embarked upon. The best and worst moments of my doctoral journey have been shared with many people who deserve a special mention. It has been a great privilege to spend the last three and a half years in the Australian School of Advanced Medicine at Macquarie University, and its members will always remain dear to me.

First and foremost, I would like to express my special appreciation and thanks to my advisor Professor Jacqueline Phillips, you have been a tremendous mentor for me. I would like to thank you for encouraging my research and for allowing me to grow as a research scientist. Your advice, support and understanding over these past years have been priceless, and your warm welcoming smile every time I meet you is something that I have always admired. I hope that I could be as lively, enthusiastic, and energetic as you, to someday be able to command an audience as well as you can. I am also very grateful to my co-supervisor Dr Cara Hildreth for her valuable advice, constructive criticism and her extensive discussions around my work. Without her assistance and dedicated involvement in every step throughout the process, this thesis would have been a lot harder to accomplish.

Thank you to Drs Anita Turner, Willian Korim, Mark Butlin, Simon McMullan, Ahmed Rahman, Israt Shahid, Branimir Zogovikj, Eyitemi Egwuenu and Qi Jian Sun (Macquarie University) for excellent technical advice. Your highly skilled experimental abilities were extremely valuable for me during the early learning process of my PhD. Of a great benefit was the many and varied discussion I had with Dr Sarah-Jane Guild (University of Auckland). Special thanks must go to her for answering my countless enquiries regarding recording of nerve activity in conscious animals described in this thesis.

I thank all the present and former staff at the Australian School of Advanced Medicine, Ms Carmel Warsop, Ms Gabrielle Dunn, Ms Jaime Perry, Ms Kathryn Clark, Ms Laura Newey and Ms Shanna O'Connor for their kind help with all my administrative work, Ms Tamara Leo, Ms Leonie Diment, Mr Cameron McClement, and Ms Lucy Lu, for their various forms of support in making the laboratory always a safe and ready-to-use research environment for all postgraduate students. In the absence of the kind help provided by Ms Christine Sutter, Mr Wayne McTegg and other technical staff at the animal house facility of Macquarie University, it would have been extremely hard to deal with matters pertaining to animal care during my studies. If I have forgotten anyone, I apologize.

Getting through my PhD required more than academic support, and I have mainly two people to thank for listening to and, at times, having to tolerate me over the past three and a half years. I cannot begin to express my gratitude and appreciation for their friendship. Omar Al-adhami and Divya Kandukuri have been unwavering in their personal and professional support during the time I spent at the university. These two friends have always picked me up during my down time and I couldn't have survived my PhD nor stayed sane without them. Omar, who I would like to think of him as the older brother I never had, has literally shared every moment of this tough journey with me. Thanks for not only being my closest friend for over a decade now but also for being such a wonderfully sincere person and great flatmate. Divya, who I would like to think of as a travelling encyclopaedia, is a wonderful and generous friend. I admire her positive outlook, her ability to smile despite the situation and the diverse topics she always discusses. Thanks are due to the two of you for not only your contribution to this thesis but also for all the wonderful lunches and memorable evenings out and in.

I thank my friends and colleagues in Professor Phillips's group. In particular, I would like to convey a special acknowledgment to Alice Ding, the best party planner and the glue that has always held our lab group together. Thank you for opening your home time and time again for our group to hang out and have fun. Ben Wyse has been a good friend and I thank him for all great dinners, having our group staying over at his house after the High Blood Pressure Research Council 2011 meeting in Perth, taking us to the beaches there and the lovely time we spent with his remarkable parents. I would like to especially thank Rochelle Boyd and Jin Ko Quek, very nice and kind friends who were always willing to lend their service whenever I approached them. Thank you for all the lovely Hungry Jacks nights I have had with you guys. How would I ever get my beef burger fix without you? Big thanks also go to Justyna Ozimek-Kulik and YiminYao for being two of the nicest people one could meet. I thoroughly enjoyed my time with you and will always value your friendship.

Most importantly, none of this could have happened without my family. There are no words to convey how grateful I am to my parents, who have sacrificed their lives for my bother and myself and provided unconditional love and care. You have both been instrumental in instilling confidence in me and giving me my fighting spirit. I love you so much, and I would not have made it this far without you and without your prayers. My brother Harith, who I failed to attend his marriage or witness the birth of his first child baby Zayed while busy with my PhD, has been my best friend all my life and I love him dearly and thank him for all his care and support. I know I always have my family to count on when times are rough. Special thanks also go to a special someone who, with her kind words and support, has without fail helped cheer me up during tough times over the last year of my PhD (You know who you are).

Finally, I would like to acknowledge the financial support form the Higher Degree Research office and the Australian School of Advanced Medicine at Macquarie University for offering me the prestigious Macquarie University Research Excellence Scholarship, the Postgraduate Research Fund and the generous funding received from the Skipper's Foundation.

Ibrahim M. Salman

June 2014

"It had long since come to my attention

that people of accomplishment rarely sat

back and let things happen to them. They

went out and happened to things."

Leonardo da Vinci (1452 – 1519)

Publications arising from this thesis

Journal Publications

SALMAN, I. M., HILDRETH, C. M., AMEER, O. Z. AND PHILLIPS, J. K. (2014). Differential contribution of afferent and central pathways to the development of baroreflex dysfunction in chronic kidney disease. *Hypertension*, 63**,** 804-10.

Conference Proceedings

SALMAN, I. M., HILDRETH, C. M., HARRISON, J. L. & PHILLIPS, J. K. (2013). Blunted pressor and renal sympathetic nerve stress response in a conscious rodent model of chronic kidney disease. *The 43rd Society for Neuroscience Conference*, 9–13 November, San Diego Convention Centre, San Diego, California, USA. (Poster presentation)

SALMAN, I. M., HILDRETH, C. M. & PHILLIPS, J. K. (2013). Direct long-term assessment of renal sympathetic nerve activity in the conscious Lewis polycystic kidney rat model of chronic kidney disease. *Central Cardiovascular & Respiratory Control: Future Directions meeting, Neuroscience Research Australia*, 16–17 September, Sydney, New South Wales, Australia. (Poster presentation)

SALMAN, I. M., HILDRETH, C. M. & PHILLIPS, J. K. (2012). Temporal impairment of baroreflex control of renal sympathetic nerve activity in the Lewis polycystic kidney model of chronic kidney disease. *The Neurophathophysiology of Hypertension - a satellite scientific meeting of the International Society of Hypertension*, 25–28 September, Palm Cove, Queensland, Australia. (Oral presentation)

SALMAN, I. M., HILDRETH, C. M. & PHILLIPS, J. K. (2012). Renal sympathetic nerve activity in a rodent model of chronic kidney disease. *The* 32nd *Annual Meeting of the Australian Neuroscience Society*, 29 January–1 February, Gold Coast, Queensland, Australia. (Poster presentation)

SALMAN, I. M., HILDRETH, C. M. & PHILLIPS, J. K. (2011). Baroreflex control of the renal sympathetic nerve in autosomal recessive cystic kidney disease. *The 33rd Annual Scientific Meeting of the High Blood Pressure Research Council of Australia*, 7–9 December, Perth Convention Exhibition Centre, Perth, Western Australia. (Oral presentation)

HILDRETH, C. M., **SALMAN, I. M.**, WYSE, B. F., HARRISON, J. L. & PHILLIPS, J. K. (2011). Evidence for increased renal sympathetic outflow in renal failure. *Central Cardiovascular Control: Future Directions meeting*, 20–21 October, Florey Neuroscience Institutes, Melbourne Brain Centre, University of Melbourne, Melbourne, Victoria, Australia. (Oral presentation)

SALMAN, I. M., HILDRETH, C. M. & PHILLIPS, J. K. (2011). Impaired baroreflex control of heart rate and sympathetic nerve activity is not associated with altered baroreceptor afferent processing in the Lewis cystic kidney model of chronic kidney disease. *Central Cardiovascular Control: Future Directions meeting*, 20–21 October, Florey Neuroscience Institutes, Melbourne Brain Centre, University of Melbourne, Melbourne, Victoria, Australia. (Oral presentation)

Conference abstracts published in journals

PHILLIPS, J.K., **SALMAN, I.M.**, HARRISON, J.L. & HILDRETH, C.M. (2013). Long-term telemetry recordings demonstrate increased renal sympathetic nerve activity and blood pressure in rats with chronic kidney disease. *J Hypertens*, 31, P e141. *Abstract of the 23rd Scientific meeting of the European Society of Hypertension*. 14–17 June Mico Milano Congress, Milan, Italy. (Oral presentation)

SALMAN, I. M., HILDRETH, C. M. & PHILLIPS, J. K. (2012). Impaired renal sympathoinhibitory responses to vagal afferent stimulation in chronic kidney disease. *J Hypertens*, 30, e86–7. Abstract of the 24th Scientific Meeting of the International Society of Hypertension, 30 September–4 October, Sydney Convention & Exhibition Centre, Sydney, NSW, Australia. (Poster presentation)

Publications arising from period of candidature

Journal Publications

AMEER, O. Z., **SALMAN, I. M.**, AVOLIO, A. P., PHILLIPS, J. K. & BUTLIN, M. 2014. Opposing changes in thoracic and abdominal aortic biomechanical properties in rodent models of vascular calcification and hypertension. *Am J Physiol Heart Circ Physiol.*, 307**,** H143-51.

Abstract

Autonomic dysfunction is a major complication of chronic kidney disease (CKD) (Dursun et al., 2004, Rubinger et al., 2009), likely contributing to the high incidence of cardiovascular mortality in this patient population. In addition to sympathetic overdrive, evidenced by increased sympathetic nerve activity (SNA) (Neumann et al., 2007, Schlaich et al., 2013) and plasma noradrenaline levels (Zoccali et al., 2002), baroreflex control of heart rate (HR) is impaired (Hildreth et al., 2013, Johansson et al., 2007). Whether or not baroreflex control of SNA is impaired in CKD is unclear, with mixed reports of normal (Ligtenberg et al., 1999) and impaired (Tinucci et al., 2001) responses. Moreover, the mechanisms underlying baroreceptor dysfunction in CKD are unknown. Therefore, the aims of this thesis were to: first, identify if a temporal impairment in baroreflex control of SNA occurs in a novel rodent model of CKD, the Lewis Polycystic Kidney (LPK) rat, and if deficits in the afferent, central and/or efferent components of the baroreflex exist; second, assess whether baroreflex dysfunction in CKD is differentially expressed in male and female genders and is contributed to by sex-dependent deteriorations in different components of the baroreflex pathway; third, investigate whether altered reflex control of the heart and sympathetic vasomotor tone relates to deficits in the vagal afferent pathway, a baroreceptor-independent mechanism that can similarly modulate efferent autonomic nerve activity; and fourth, to examine the hypothesis that ongoing elevation of SNA is a key pathological feature of CKD using conscious dual recording of blood pressure (BP) and SNA in the LPK,.

In the first study (Chapter 3), under anaesthesia, baroreflex control of renal SNA (RSNA) and HR were investigated in juvenile (7–8 weeks old) and adult (12–13 weeks old) male LPK and Lewis control rats and the functionality of the afferent, central and efferent components of the baroreflex circuit examined. A major finding was that RSNA was markedly elevated early in the LPK and high tonic activity persisted throughout adulthood. The study also demonstrated a temporal impairment of the baroreceptor afferent function which correlated with vascular remodelling and hypertrophy, suggesting altered vascular stretch as a key contributor to diminished afferent neurotransmission in CKD. It was further concluded that a deficit in the afferent component of the baroreflex precedes the development of impaired central regulation of HR and RSNA in CKD and that progressive impairment of both components is associated with marked dysfunction of the baroreflex pathway.

The second study (Chapter 4) was designed to characterise baroreflex functions in the female LPK model of CKD and similarly assess the integrity of the afferent, central and efferent components of the baroreflex arc and their ability to evoke baroreflex-mediated changes in HR and sympathetic outflow. The data demonstrated that in female LPK cardiac and sympathetic baroreflex function becomes impaired during adulthood, and that attenuated baroreflexes, unlike male LPK, are solely driven by altered central mechanisms rather than deficits in the responsiveness of aortic baroreceptors to BP.

Given the association between autonomic dysfunction and increased cardiovascular mortality in CKD (Chesterton and McIntyre, 2005, Thapa et al., 2010) and the fact that cardiovascular risk is higher in

men with CKD than women (National Kidney Foundation, 2013), data from the first and second studies were directly compared in order to elucidate if sexes differences in the expression of cardiac and sympathetic baroreflex dysfunction exist in CKD and relate to a differential influence of sex on the functionality of the afferent, central and efferent drives of the baroreflex pathway (Chapter 5). Upon CKD progression, in addition to similar elevations in RSNA, male and female LPK expressed comparatively similar deficits in the baroreflex control of HR and RSNA despite greater deteriorations in the afferent and central components of the baroreflex arc in the male. Impairments within the sensory afferent arm of the baroreceptor reflex appeared to have a minimal impact upon the development of baroreflex dysfunction in CKD, as despite a temporal decline in the functionality of the afferent drive in the male LPK, this was not encountered with the female LPK, and yet both male and female LPK rats displayed relatively similar deficits in cardiac and sympathetic baroreflex function during adulthood, suggesting that a central deficit in the processing of autonomic outflows to the heart and vasculature, which is perhaps linked to a complex interplay between high BP and loss of renal function, primarily underpins baroreflex dysfunction in CKD.

The third study (Chapter 6) was aimed at identifying if the central processing of vagal afferent input was altered in the male and female LPK and associated with an age-related decline in the ability to evoke reflex changes in RSNA, HR and BP. Consistent with altered central baroreflex function in adult LPK animals, impaired central integration of vagal afferent outflow was only evident during adulthood and differentially expressed in both male and female LPK. While centrally-evoked changes in SNA were reduced in LPK rats of either sex, reflex control of HR by the vagal afferents was blunted in the female LPK only, suggesting that, specific to this pathway, females exhibit greater autonomic deficits. Taken together with our previous studies, this shows that central processing of other cardiovascular reflexes besides the baroreflex pathway may become impaired in CKD, resulting in an inability to reflexively control autonomic outflows and maintain optimal BP homeostasis.

The fourth and last study (Chapter 7) was designed to measure RSNA in conscious LPK rats and investigate whether similar elevations in RSNA baseline levels to those we saw under anaesthetic would be seen. Responses to acute stress and peripheral and central chemoreflex activation were also measured. The data demonstrated that, similar to our previous anaesthetised studies, conscious recording of RSNA showed increased levels in the LPK, revealing the capacity of this technique to determine ongoing alterations in SNA in CKD. The LPK further exhibited blunted sympathetic and BP responses to acute stress and peripheral and central chemoreflex activation, indicating deficits in the neural processing of sympathetic outflow driven by these pathways. Diminished sympathetic responses to acute stress and activation of the central chemoreflex supported our previous demonstration of a central deficit in the LPK and further suggested that impaired autonomic neuroregulation in CKD is promoted by a state of generalised central dysfunction.

Table of Contents

List of Figures

List of Tables

List of Abbreviations

%	Per cent
α	Alpha adrenergic receptor
ACE	Angiotensin-converting enzyme
ACEi	Angiotensin-converting enzyme inhibitors
ACh	Acetylcholine
ACTH	Adrenocorticotrophic hormone
ADN	Aortic depressor nerve
ADNA	Aortic depressor nerve activity
$ADNA_{sat}$	Saturation aortic depressor nerve activity
$ADNA_{thr}$	Threshold aortic depressor nerve activity
ADPKD	Autosomal dominant polycystic kidney disease
AMB	Nucleus ambiguus
$ANDA_{50}$	Aortic depressor nerve activity at midpoint of the curve
Ang II	Angiotensin II
ANOVA	Analysis of variance
ANP	Atrial natriuretic peptide
ANS	Autonomic nervous system
ARB	Angiotensin receptor blockers
ARPKD	Autosomal recessive polycystic kidney disease
AT_1	angiotensin type 1 receptors
ATP	Adenine triphosphate
AUC	Area under the curve
AV	Atrioventricular
β	Beta adrenergic receptors
BEI	Baroreceptor effectiveness index
BP	Blood pressure
BPM	Beats per minute
BRS	Baroreflex sensitivity
BRS_{PE}	Baroreflex sensitivity to phenylephrine-induced bradycardia
BRS_{SNP}	Baroreflex sensitivity to sodium nitroprusside-induced tachycardia
BW	Body weight
BZJ	Bezold-Jarisch reflex
^0C	Degree Celsius
Ca^{2+}	Calcium
cAMP	Cyclic adenosine monophosphate
^{51}Cr	Chromium isotope
CKD	Chronic kidney disease
cm	Centimetre
CNS	Central nervous system
CO_2	Carbon dioxide
CSN	Carotid sinus nerve
CVD	Cardiovascular disease
CVLM	Caudal ventrolateral medulla
CVPN	Cardiac vagal preganglionic neurons
DBP	Diastolic blood pressure

DMH	Dorsomedial hypothalamus
DMNV	dorsal motor nucleus of the vagus
DPX	Di-N-butyl phthalate in xylene
EAA	Excitatory amino acid
EDTA	Ethylenediaminetetraacetic acid
ESRD	End-stage renal disease
fMRI	Functional magnetic resonance imaging
g	Gram
GABA	Gamma amino butyric acid
GFR	Glomerular filtration rate
h	Hour
HF	High frequency
HPA	Hypothalamo-pituitary-adrenocortical axis
HR	Heart rate
HRV	Heart rate variability
5-HT_3	Serotonin type 3 receptors
Hz	Hertz
i.p.	Intraperitoneal
i.v.	Intravenous
IML	intermediolateral cell column
jck	Juvenile cystic kidney
J-receptors	juxtapulmonary capillary receptors
K^+	Potassium
2K-1C	2 kidney-1 clip
KDOQI	Kidney Disease Outcomes Quality Initiative
kHz	Kilohertz
L	Litre
L-NAME	N^{ω}-nitro-L-arginine methyl ester
LSNA	Lumbar sympathetic nerve activity
LVH	Left ventricular hypertrophy
µV	Microvolt
M	Muscarinic cholinergic receptors
m^2	Square meter
MAP	Mean arterial pressure
MAP_{50}	Mean arterial pressure at midpoint of the curve
MAP_{sat}	Saturation mean arterial pressure
MAP_{thr}	Threshold mean arterial pressure
ME	Median eminence
min	Minute
ml	Millilitre
mmHg	Millimetre of mercury
ms	Millisecond
MSB	Martius Scarlet Blue
MSNA	Muscle sympathetic nerve activity
N_2	Nitrogen
NA	Noradrenaline
Na^+	Sodium

NADPH	Nicotinamide adenine dinucleotide phosphate
Nek8	Never in mitosis gene A-related kinase 8
NIMA	Never in mitosis gene A
NMDA	N-methyl-D-aspartate
NO	Nitric oxide
NOS	Nitric oxide synthase
NPHP	Nephronophthisis
NPY	Neuropeptide Y
ns	No significance
NTS	Nucleus tractus solitarius
O_2	Oxygen
P	Pressure
P_2	Purinoceptor type 2
PCO_2	Carbon dioxide partial pressure
PE	Phenylephrine
PKD	Polycystic kidney disease
pNN50	Proportion of differences in consecutive normal-to-normal intervals that are longer than 50 milliseconds
PO_2	Oxygen partial pressure
PP	Pulse pressure
PVN	Paraventricular nucleus
PWV	Pulse wave velocity
RAAS	Renin-angiotensin-aldosterone system
rMSDD	Square root of the mean squared differences of successive normal-to-normal intervals
RP	Raphe pallidus
RPM	Revolution per minute
RSNA	Renal sympathetic nerve activity
RVLM	Rostral ventrolateral medulla
s	Second
s.c.	Subcutaneous
SA	Sinoatrial
sat	Saturation
SBP	Systolic blood pressure
SBPV	Systolic blood pressure variability
SDANN	Standard deviation of the average normal-to-normal intervals
SDNN	Standard deviation of normal-to-normal intervals
SEM	Standard error of the mean
SHR	spontaneously hypertensive rat
SLE	Systemic lupus erythematosus
SNA	Sympathetic nerve activity
SNP	Sodium nitroprusside
SNS	Sympathetic nervous system
SPN	Sympathetic preganglionic neurons
thr	Threshold
TRPV1	transient receptor potential vanilloid 1
U_{Cr}	Urinary creatinine
UPC	Urinary protein:creatinine ratio
U_{Pro}	Urinary protein

v/v	Volume by volume
VLF	Very low frequency
WKY	Wistar-Kyoto

1 Literature Review

1.1 Introduction

Chronic kidney disease (CKD) is a growing public health problem, affecting 5–7% of the world population (Couser et al., 2011) and responsible for a high incidence of premature mortality in Australia (Kidney Health Australia, 2012). It is estimated that 1 in 3 Australians is at an increased risk of developing CKD (Australian Bureau of Statistics, 2013) and approximately 1.7 million Australians aged 18 years and over have indicators of CKD such as reduced renal function and/or the presence of albumin in the urine (Australian Institute of Health and Welfare, 2011).

Individuals with CKD are more likely to die of cardiovascular complications than to develop kidney failure (Sarnak et al., 2003, Tonelli et al., 2006) due to the high prevalence of cardiovascular disease (CVD) in this patient population (Schiffrin et al., 2007). Hypertension in and of itself, which is almost invariably present in ~80–85% of CKD patients (U.S. renal data system, 2013, Wong et al., 2006), is a powerful indicator of CVD and an independent risk factor for disease progression in both adult and paediatric patients with CKD (Schiffrin et al., 2007, Wuhl and Schaefer, 2011). Several mechanisms have been implicated in the pathogenesis of hypertension and CVD in CKD, including sodium retention and fluid overload due to defects in the pressure natriuresis relationship, activation of the renin-angiotensin-aldosterone system (RAAS) (Guyton and Coleman, 1999, Morgado and Neves, 2012, Neumann et al., 2007), sympathetic nervous system (SNS) hyperactivity (Klein et al., 2001, Neumann et al., 2007, Schlaich et al., 2009b), autonomic dysfunction (Klein et al., 2003a, Lugon et al., 2003, Robinson and Carr, 2002), endogenous and environmental stress (Oparil et al., 2003, Schiffrin et al., 2007), impaired endothelial function, vascular remodelling and arterial calcification (Foley et al., 1996, Locatelli et al., 2003, Passauer et al., 2005), thus highlighting a complex interplay of neural, hormonal and vascular mechanisms which links kidney disease to high blood pressure (BP) and the associated cardiovascular problems that arise as a consequence.

Among the myriads of factors contributing to or arising from CKD, cardiovascular autonomic dysfunction is a serious, yet poorly understood long-term clinical problem in the CKD population. Autonomic dysfunction as a broad term mainly refers to a condition where tonic and reflex control of autonomic outflows is altered, favouring increased SNS activity and depressed parasympathetic function (Hildreth, 2011, Phillips, 2012). Indeed, CKD patients with cardiovascular autonomic dysfunction have consistently been shown to have an enhanced risk of premature death (Dursun et al., 2004, Ranpuria et al., 2008, Shamseddin and Parfrey, 2011), suggesting direct detrimental effects on clinical prognosis of renal failure. Dysfunctional vagal control of heart rate (HR), as assessed by reductions in HR variability (HRV) and spontaneous baroreflex sensitivity (BRS), is also prevalent and poses increased risk of sudden cardiac death (Johansson et al., 2007, Vita et al., 1999).

Sympathetic nervous system activity is elevated in patients with CKD, as evidenced by increased plasma catecholamine levels (Grassi et al., 2011a, Ksiazek and Zaluska, 2008, Zoccali et al., 2002) and increased muscle sympathetic nerve activity (SNA) (Converse et al., 1992, Grassi et al., 2011a, Neumann et al., 2007). Sympathetic overactivity is implicated in the development, maintenance and progression of renal disease (Campese and Krol, 2002, Converse et al., 1992, Rump et al., 2000) and has been recognised as an important mechanism contributing to the strong association between CKD and increased cardiovascular morbidity and mortality (Collins, 2003, Grassi et al., 2011a, Zoccali et al., 2002). While contribution of autonomic neural mechanisms to the development of hypertension and CVD in CKD is now well established, the exact mechanisms contributing to altered sympathetic and parasympathetic tone in patients with CKD are unclear. Abnormalities in cardiovascular reflexes central to the control of autonomic function, such as baroreceptor, chemoreceptor and cardiopulmonary reflexes have been put forward as possible underlying mechanisms (La Rovere et al., 1998, Neahring et al., 1995, Rassaf et al., 2012, Tinucci et al., 2001). However, deficits in these reflex pathways and more importantly the mechanisms that underpin those deficits (e.g., altered afferent, central or efferent signalling pathway, inability of target organ such as the heart or vasculature to respond to autonomic inputs, etc.) are incompletely understood. Current evidence also suggests that autonomic deficits are driven by the diseased kidneys, since nephrectomy, renal denervation or kidney transplantation has been shown to correct BP, lower sympathetic overdrive and improve vagal control of HR in humans and experimental animals (Boero et al., 2001, Esler et al., 2012, Hering et al., 2012, Schlaich et al., 2012, Weinstock et al., 1996, Yildiz et al., 1998).

One of the ultimate goals of clinical and experimental research in the hypertension field is the identification of innovative diagnostic and advanced treatment approaches that limit hypertension and target end-organ damage. However, this is restricted by the fact that our crux of understanding of the mechanisms that bind the complex interaction between the autonomic, cardiovascular, and renal systems is still far from being completely understood, and our current therapeutic strategies for primary or secondary prevention of CVD in patients with CKD remains nonspecific. At present, in the absence of solid evidence, clinical judgment suggests effective control of modifiable and uraemia specific risk factors at an early stage of renal disease, with maintenance of optimal or near optimal BP control being recognised as a priority (Harris and Rangan, 2005, Parmar, 2002, Schiffrin et al., 2007).

Accordingly, the main aim of this thesis was to assess autonomic reflexes in CKD and investigate mechanisms underlying autonomic dysfunction and altered sympathovagal balance. This chapter reviews in further detail concepts in relation to the important determinants of BP control and the involvement of the autonomic nervous system in this process, and the role of altered tonic and reflex control of BP in CKD-mediated hypertension.

1.2 Autonomic control of the circulation

The autonomic nervous system (ANS) is a collection of afferent and efferent neurons that link the central nervous system (CNS) with the effector organs and is responsible for involuntary control of various visceral structures including the heart and vasculature. Autonomic motor control comprises a set of highly differentiated and closely regulated pathways made up of:

(1) Thin, lightly myelinated cholinergic preganglionic neurons which arise from the cranial [cranial nerves III (oculomotor), VII (facial), IX (glossopharyngeal) and X, (vagus)] and sacral spinal cord regions [sacral nerves S2, S3 and S4 (pelvic splanchnic nerves)] for the parasympathetic nervous system, and the thoracolumbar (T1–L3) spinal cord regions for the SNS. Preganglionic neurons of parasympathetic nervous system innervate the autonomic ganglia while those of the sympathetic division innervate both the autonomic ganglia and adrenal glands. All preganglionic neurons use a nicotinic receptor-modulated neurotransmission.

(2) Very thin, unmyelinated cholinergic postganglionic neurons (parasympathetic) which innervate the heart and other visceral organs.

(3) Very thin, unmyelinated sympathetic postganglionic neurons (noradrenergic) which innervate the heart, vascular smooth muscle, kidneys, etc (Loewy and Spyer, 1990, Thomas, 2011, Waugh and Grant, 2010).

The autonomic ganglionic neurons that control the heart are both sympathetic and parasympathetic, whereas the vasculature is primarily controlled by sympathetic postganglionic neurons (Loewy and Spyer, 1990, Thomas, 2011).

Blood pressure is a function of cardiac output and total peripheral resistance; two variables that are controlled by the ANS. Cardiac output is dependent upon three regulated variables: end-diastolic volume, cardiac contractility, and HR. End-diastolic volume, the volume of blood in the ventricular chamber before contraction, is determined by venous pressure. Venous pressure is related to blood volume and venous smooth muscle tone; both of which are regulated by the SNS. Cardiac contractility and HR, in turn, are under control of both the sympathetic and parasympathetic divisions of the ANS, whereas total peripheral resistance is modulated by the SNS (Guyenet, 2006). Autonomic neuroregulation (tonic and reflex) of BP is accomplished in the short-term through a series of differentiated neural pathways that integrate chemical and mechanical inputs to modify efferent sympathetic and parasympathetic activities to the different target organs. Humoral factors such as circulating hormones, noradrenaline (NA), adrenaline, angiotensin II (Ang II), endothelin, histamine, bradykinin, nitric oxide (NO) can modulate these neuronal pathways and impact long-term BP regulation.

1.2.1 Neural control of the heart

The heart receives dual innervation from the parasympathetic (vagal postganglionic neurons) and sympathetic (sympathetic postganglionic neurons) divisions of the ANS. These components exert a powerful antagonistic influence on the heart by modulating cardiac rate (chronotropy), conduction velocity (dromotropy), contraction (inotropy), and relaxation (lusitropy) (Thomas, 2011). Cardiac vagal preganglionic neurons (CVPN) project onto cardiac vagal postganglionic neurons located within the intracardiac ganglia, sinoatrial (SA), atrioventricular (AV), and cranioventricular ganglia (Gray et al., 2004). Sympathetic postganglionic neurons similarly project through the intracardiac ganglia or directly innervate atrial and ventricular myocardium (Ardell et al., 1988, Hirakawa et al., 1993). The chronotropic and dromotropic effects are mediated by both cardiac vagal and sympathetic postganglionic neurons innervating the SA and AV nodes, whereas the inotropic and lusitropic effects are primarily mediated by sympathetic and parasympathetic nerve fibres innervating atrial and ventricular myocytes. Increased vagal discharge can reduce HR (bradycardia), prolong AV conduction, lower cardiac contractility and stroke volume, and decrease cardiac output (Garcia Perez and Jordan, 2001, Thomas, 2011), whereas higher sympathetic discharge can increase HR (tachycardia), shorten AV conduction, enhance cardiac contractility, and increase stroke volume and cardiac output (Furukawa et al., 1990, Thomas, 2011). Conversely, withdrawal of tonic vagal or sympathetic discharge has opposing effects to increase or decrease cardiac output, respectively.

Cardiac vagal postganglionic nerve terminals release the cholinergic neurotransmitter acetylcholine (ACh), which activates G_i-coupled M_2 muscarinic cholinergic receptors, thereby inhibiting adenylate cyclase, lowering intracellular cyclic adenosine monophosphate (cAMP), and increasing potassium conductance of nodal cells. This results in membrane hyperpolarization and reductions in the spontaneous firing rate of the SA and AV nodes, thereby slowing the intrinsic HR (Belardinelli and Isenberg, 1983, Brodde et al., 2001, Guimaraes and Moura, 2001). The sympathetic postganglionic nerve terminals release the noradrenergic neurotransmitter NA, which binds to the predominant G_s-coupled β_1-adrenergic receptors to activate adenylate cyclase, increase intracellular cAMP, and activate protein kinase A (Brodde et al., 2001, Guimaraes and Moura, 2001). Activation of β_1-adrenoreceptors increases the slope of diastolic depolarization in the SA node and accelerates AV nodal conduction, triggering an increase in HR. In cardiac myocytes, β-adrenoceptor activation increases intracellular calcium content and membrane depolarisation currents. This is accomplished through sarcoplasmic reticulum-mediated calcium release in response to each action potential, which results in increased force of cardiac contraction (Guimaraes and Moura, 2001, Thomas, 2011). Enhancements of calcium reuptake into the sarcoplasmic reticulum, on the other hand, accelerate relaxation (Thomas, 2011). Efferent vagus nerve activity also has tonic and basal effects that inhibit sympathetic activation and NA release at a presynaptic site of action. This facilitation of cardiac vagal input explains why cardiac vagal activity dominates over those of cardiac sympathetic postganglionic neurons at rest; a response known as “accentuated antagonism” (Stramba-Badiale et al., 1991,

Uijtdehaage and Thayer, 2000). In a static or dynamic state, elevated cardiac sympathetic drive can be overridden by intense vagus nerve discharge (Kawada et al., 1999).

Given the ability to modulate both HR and stroke volume, the autonomic innervation of the heart provides an important remote mechanism to rapidly adjust cardiac output to meet short-term changes in the body needs: e.g., responding to changes in BP, volume or composition [pH, oxygen partial pressure (PO_2), carbon dioxide partial pressure (PCO_2), endogenous mediators or toxins], or reacting to environmental challenges such as exercise or stress (Thomas, 2011).

1.2.2 Sympathetic neural control of the blood vessels

Blood vessels receive sympathetic inputs but mostly lack parasympathetic innervation. Postganglionic sympathetic nerve fibres are confined to the adventitial-medial junction of most arteries, arterioles, and veins supplying muscle, viscera and skin (Bevan and Su, 1971, Nilsson et al., 1986). The arterioles are the major contributors to total peripheral resistance, which makes sympathetic control of those vascular beds critical to the regulation of systemic BP. In contrast to arteries, veins contain less smooth muscle and receive limited sympathetic innervation, yet they can still contract in response to sympathetic activation (Nilsson et al., 1986). They serve primarily as capacitance vessels as they are more distensible and able to accommodate large volumes of blood. Venules and capillaries, however, lack smooth muscle and are not directly innervated by sympathetic nerves (Thomas, 2011).

Postganglionic sympathetic nerve terminals release NA which binds to the G-protein coupled α_1- and α_2-adrenergic receptors located on vascular smooth muscle cells. This leads to a cascade of downstream events that involve the activation of a phospholipase and the release of calcium from intracellular stores. Increased intracellular calcium concentration ultimately causes activation of the calmodulin-dependent myosin light-chain kinase, and thus the subsequent phosphorylation of the myosin light chain which is required for the development of muscle tension (Guimaraes and Moura, 2001, Sweeney et al., 1993). In addition to NA, vascular sympathetic nerve endings may also release substances such as neuropeptide Y (NPY) or adenine triphosphate (ATP) as cotransmitters. These are capable of producing vasoconstriction by activating vascular NPY Y1 receptors or purinergic P2X receptors, respectively, and increasing intracellular calcium concentration (Pablo Huidobro-Toro and Veronica Donoso, 2004). Neuropeptide Y may also potentiate the vasoconstrictor-effecting properties of NA and ATP (Pablo Huidobro-Toro and Veronica Donoso, 2004).

Cardiovascular sympathetic efferent nerves are classified into 3 populations: thermosensitive, glucosensitive and barosensitive (Guyenet, 2006). The thermosensitive group consists primarily of vasoconstrictor neurons supplying the tail artery in the rat (Gilbey, 2007), analogous to those supplying cutaneous vascular beds in humans, recruited to cope with changes in body temperature, but can also be activated by emotional stimuli or hyperventilation (Jänig and Habler, 2003). The glucosensitive group of sympathetic neurons control adrenaline release from the adrenal gland in response to hypoglycaemia or exercise activity (Cao and Morrison, 2001, Morrison and Cao, 2000).

These two groups of neurons are weakly, if at all, coupled to the cardiac cycle or inhibited by the baroreceptor reflex; thus suggesting a less important role in the control of BP (Guyenet, 2006, Jänig and Habler, 2003, Morrison and Cao, 2000). The last and by far largest class of cardiovascular sympathetic efferents is the barosensitive group. These neurons, which innervate the blood vessels supplying the heart, kidneys, muscle and other visceral organs, show ongoing activity at rest (sympathetic tone), are subject to numerous reflex regulatory pathways that operate in feedback or feedforward manner, and their activity are strongly coupled to the cardiac cycle and respiration, which consequently suggests a primary role for these nerves in short- and/or long-term BP stability (Dampney et al., 2002, Dorward et al., 1987, Guyenet, 2006, Jänig and Habler, 2003, Ootsuka et al., 2002). Increasing sympathetic outflow beyond this tonic level causes more vasoconstriction, whereas withdrawing sympathetic tone causes vasodilation.

Although most vascular beds are innervated by sympathetic nerve fibres, their responsiveness to sympathetic neural input can either be selective depending on the type of stimulus, or vary in intensity according to the vessel anatomical location (Guyenet, 2006). Regardless of the type of vascular sympathetic efferent, arterioles of the skin, muscle, renal and splanchnic circulations appear to show robust constriction in response to factors triggering sympathetic activation such as anxiety (Brown et al., 2012), exercise (Ichinose et al., 2006), heat stress (DiBona and Jones, 2003a, Low et al., 2011), low salt intake (DiBona and Sawin, 1985) and hypoxia (Silva and Schreihofer, 2011), whereas cerebral and coronary arterioles seem to be less responsive (Thomas, 2011). Target specific differences in the level of sympathetic activity suggest that efferent sympathetic activity to various vascular beds is differentially regulated, as shown in numerous studies (Ardell et al., 1988, Morrison and Cao, 2000, Ramchandra et al., 2012, Turner et al., 2013, Yoshimoto et al., 2010). For instance, Yoshimoto and colleagues (2010) showed that an infusion of Ang II in rats kept on high salt diet decreased renal SNA (RSNA) by 40% during the first 7 days and then returned toward control levels by day 10 of Ang II (Fig. 1.1A). Lumbar SNA, by contrast, remained at control levels throughout the Ang II period (Fig. 1.1B). Such differential responsiveness is important to redistribute cardiac output mainly through constricting nonessential vascular beds, while preserving flow to vital organs in the setting of global SNS activation (Thomas, 2011).

1.2.3 Sympathetic neurohumoral control

The SNS also exerts more prolonged, indirect cardiovascular effects via activation of several powerful hormonal systems which mainly include:

1) *The sympathoadrenal system:* chromaffin cells of the adrenal medulla receive sympathetic preganglionic neurons (SPN) that promote the synthesis and release of mainly adrenaline along with NA into the bloodstream (Morrison and Cao, 2000, Reid, 1992). These circulating catecholamines play a major role in cardiovascular regulation through modulating cardiac and vascular adrenergic receptor responses (Guimaraes and Moura, 2001).

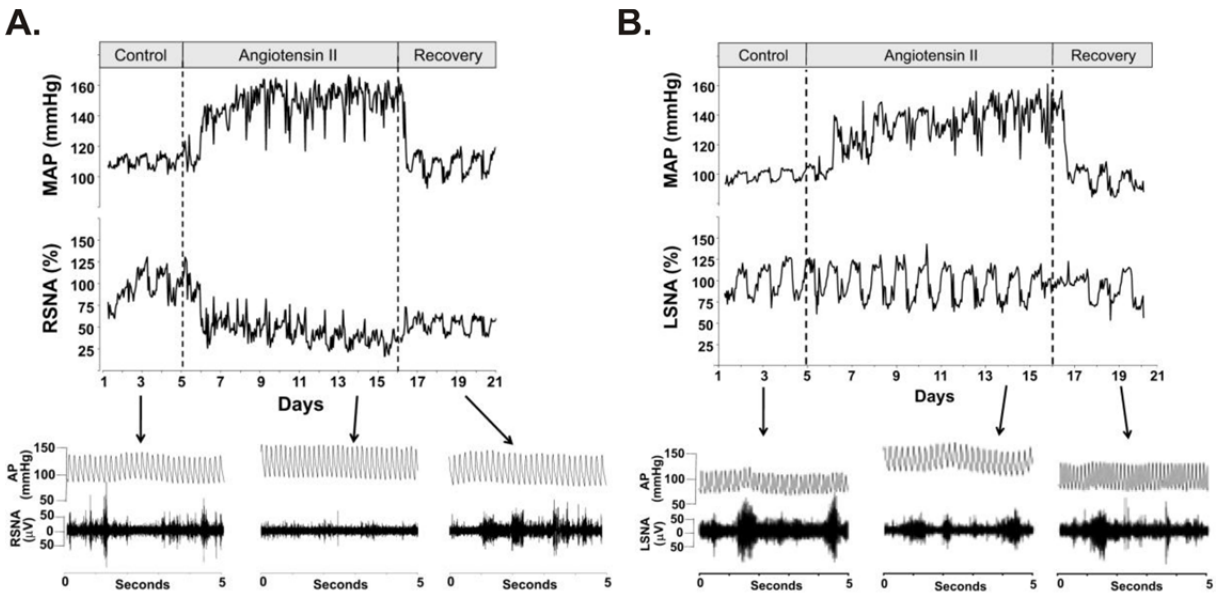

Figure 1.1: Mean arterial pressure (MAP) and renal sympathetic nerve activity (RSNA) responses (A), and MAP and lumbar sympathetic nerve activity (LSNA) responses (B) before, during, and after angiotensin II (Ang II) administration in a single conscious Sprague-Dawley rat. Bottom shows 5 second traces for arterial pressure (AP) and RSNA or AP and LSNA on indicated days. Taken from (Yoshimoto et al., 2010).

2) *The renin-angiotensin-aldosterone system (RAAS):* The RAAS exerts powerful effects on determining long-term level of SNA. Postganglionic sympathetic nerves synapse onto renin-producing juxtaglomerular cells in the walls of the renal afferent arterioles. Increased RSNA stimulates β_1-adrenergic receptors on the juxtaglomerular cells to evoke renin release into the bloodstream. Circulating renin works in concert with angiotensin-converting enzyme (ACE), a proteolytic enzyme found in the endothelial cells of the lung, vascular endothelium, and cell membranes of the kidneys, heart, and brain, to convert angiotensinogen, a globulin produced by the liver, into Ang II. The action of the latter on angiotensin type 1 (AT_1) receptors modulates cardiovascular function through either directly promoting systemic vasoconstriction action which increases peripheral resistance and BP, or stimulating adrenocortical secretion of aldosterone, a hormone which increases renal tubular sodium and water reabsorption, thereby increasing blood volume and BP (Brewster and Perazella, 2004, DiBona, 1994, DiBona, 2000b, Peti-Peterdi and Harris, 2010). A crosstalk relationship between the activity of SNS and RAAS has also been identified, whereby Ang II acts to evoke NA release through a presynaptic site of action on postganglionic sympathetic nerve terminals, enhance synaptic transmission through sympathetic ganglia (DiBona, 2000a, Reid, 1992), or influence central neural processing via the circumventricular organs, particularly the subfornical organ and the area postrema (Dampney et al., 2002, Reid, 1992), hence evoking activation of central sympathetic outflow and increasing BP.

1.3 Reflex control of blood pressure

Maintenance of BP and cardiovascular homeostasis at levels adequate to perfuse body tissues and organs is an essential requirement for the constancy of the internal environment and survival. Regulation of BP is accomplished via a series of differentiated arterial and non-arterial reflex pathways that integrate a variety of sensory afferent inputs (pressure, volume, chemical, etc.) to tightly maintain autonomic balance and correct changes in BP. Here, major autonomic reflexes responsible for BP control are reviewed.

1.3.1 The arterial baroreceptor reflex

The baroreceptor reflex buffers moment-to-moment changes in BP by altering parasympathetic and sympathetic outflow, thereby producing reflex changes in HR and total peripheral resistance. Baroreceptors, stretch receptors located within the aortic arch and carotid sinus, detect changes in vascular distensibility and send sensory afferent impulses to the cardiovascular regulatory centre in the brain stem (Dampney et al., 2002, Guyenet, 2006). Specifically, these receptors represent a complex arrangement of sensory terminals located mostly in the inner adventitia of the arterial wall (Fig.1.2), where strain develops most effectively and deforms nerve endings responsible for generation of the sensory signals (Krauhs, 1979). In the rat, the sensory terminal region of aortic baroreceptors is located between two elastic laminae which are arranged in concentric layers within the arterial wall. The nerve cell membrane of the sensory terminal is attached to a basal lamina which connects vascular smooth muscle cells in the media and the elastic lamina in the adventitia (Krauhs, 1979). The precise molecular mechanism for impulse generation at the sensory nerve terminal is not completely known; however, various cellular elements are thought to play a role including voltage-gated ion (Na^+, K^+ or Ca^{2+}) channels (Tu et al., 2010), transient receptor potential vanilloid 1 (TRPV1) (Sun et al., 2009) or P_2 purinoceptors (Song et al., 2012).

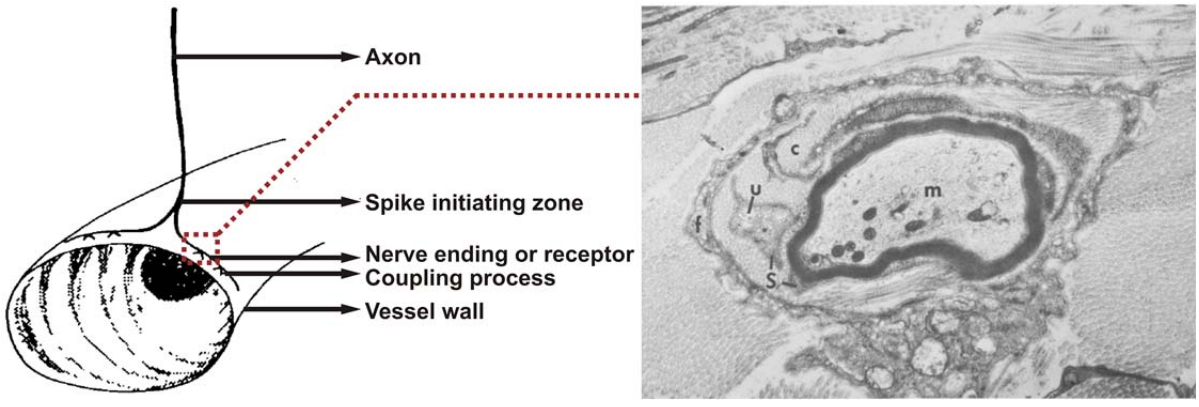

Figure 1.2: Diagrammatic representation of the mechanical and electrical components of a baroreceptor. The mechanical components are the vessel wall consisting of collagen, elastin, and a small amount of smooth muscle and the processes of that couple the vessel wall and the receptor (Brown, 1980). The electrical components are the receptor, spike-initiating zone, and axon through which action potential travels. The transmission electron microscope image (right) shows a typical fibre bundle in the outer adventitia from a Wistar-Kyoto rat. It is bounded by fibroblast-like perineurtal processes (f). A group of unmyelinated fibres (u) and a myelinated fibre (m) are sheathed in Schwann cells (S) and embedded in collagen (c) (Krauhs, 1979).

The baroreceptor afferent signal, which directly correlates with the stretch of the vessel wall in which those receptors are located (Andresen et al., 1978), is conveyed via specialised nerve fibres – low pressure threshold myelinated A-fibres and high pressure threshold unmyelinated C-fibres (Fan and Andresen, 1998, Fan et al., 1999, Kumada et al., 1990) – within the vagus nerve and carotid sinus nerve in humans (Dampney et al., 2002, Thomas, 2011), or the aortic depressor nerve (ADN) and carotid sinus nerve in rodents and rabbits (Easton and Howe, 1983, Ninomiya et al., 1971, Sapru et al., 1981, Sapru and Krieger, 1977). Cell bodies of aortic baroreceptor and carotid sinus baroreceptor neurons are located in the nodose ganglion and the petrosal ganglion, respectively (Kumada et al., 1990).

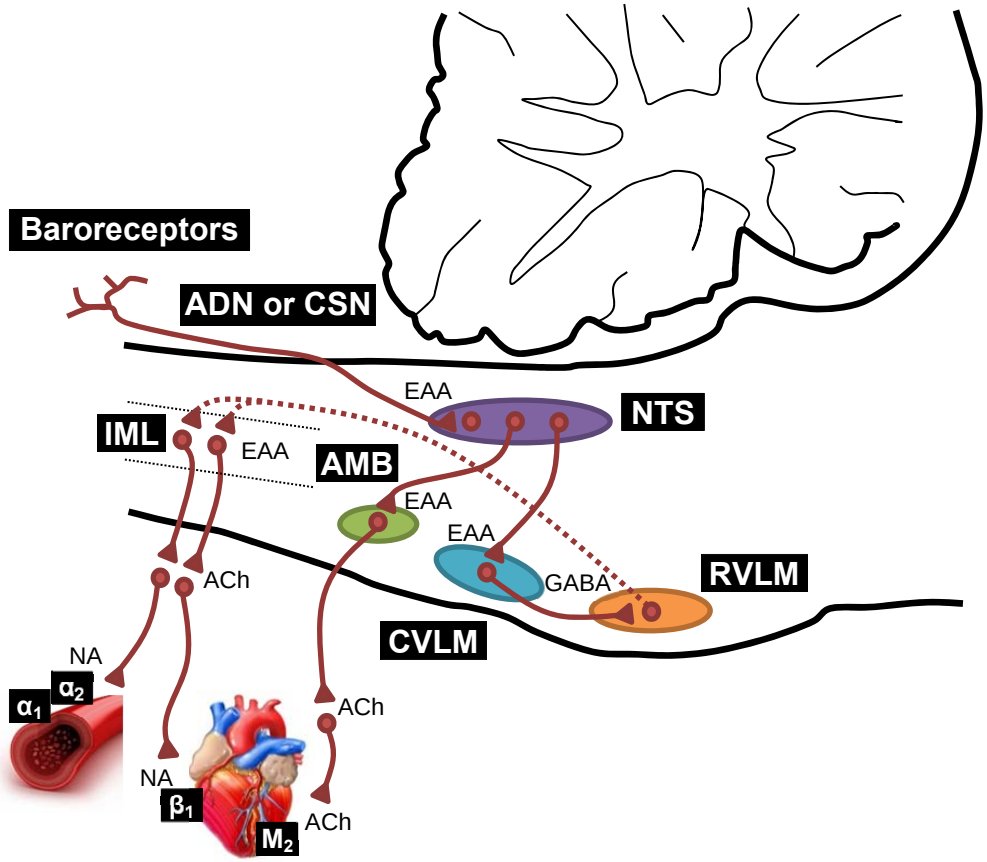

Figure 1.3: Baroreceptor reflex pathway within the lower brainstem region. ADN, aortic depressor nerve; CSN, carotid sinus nerve; NTS, nucleus tractus solitarius; CVLM, caudal ventrolateral medulla; RVLM, rostral ventrolateral medulla; AMB, nucleus ambiguus; IML, intermediolateral cell column in the spinal cord; EAA, an excitatory amino acid; GABA, γ-aminobutyric acid; ACh, acetylcholine and NA, noradrenaline. Figure modified from (Dampney et al., 2002).

Baroreceptor afferents terminate within the nucleus tractus solitarius (NTS) and excite, via a glutamatergic synapse, second-order neurons (Fig. 1.3) (Andresen et al., 2001, Dampney, 1994, Guyenet et al., 1987, Pilowsky and Goodchild, 2002), located within the intermediate and caudal NTS (Mendelowitz et al., 1992). The NTS represents a principle integrative centre for circulatory control. For example, it receives direct inputs from higher brain centres (e.g., inhibitory inputs from the paraventricular nucleus, PVN) (Bailey et al., 2006) which may play a role in modulating the baroreflex arc or controlling BP in the long term, and it is the region where sensory afferent fibres innervating the

large systemic arteries and cardiopulmonary region; and polysynaptic inputs from many sympathetic and somatic afferents terminate (Kawabe et al., 2008, Potts et al., 2003, Sun and Guyenet, 1987, Vardhan et al., 1993). The NTS is essential for the transmission of baroreceptor information, since lesions of the NTS completely abolish the baroreflex in rats (Akemi Sato et al., 2001) and humans (Biaggioni et al., 1994). Similarly, bilateral blockade of excitatory amino acid receptors, N-methyl-D-aspartate (NMDA), in the NTS by microinjection of kynurenate, a glutamate receptor antagonist, abolishes the baroreflex (Leone and Gordon, 1989). In contrast, microinjection of glutamate into the NTS simulates baroreceptor activation, with a fall in arterial BP and HR (Talman et al., 1980).

Sympathetic outflow to the heart and vasculature is modulated through a relay circuit involving the NTS, caudal ventrolateral medulla (CVLM) and rostral ventrolateral medulla (RVLM) (Fig. 1.3). The NTS neurons conveying baroreceptor signals send glutamatergic projections to the CVLM (Miyawaki et al., 1997). Neurons within the CVLM use an inhibitory GABAergic synapse which exerts a continuous and powerful restraining influence on the discharge properties of sympathoexcitatory neurons within the RVLM (Dampney et al., 2002, Guyenet, 2006, Pilowsky and Goodchild, 2002, Schreihofer and Guyenet, 2002). Evidence supporting a sympathoinhibitory effect for the CVLM brain stem region was deduced based on numerous studies showing that lesions of the CVLM (Cravo and Morrison, 1993) and inhibition with the $GABA_A$ receptor agonist muscimol (Horiuchi et al., 2004) or with the glutamate receptor antagonist kynurenate (Guyenet et al., 1987) produce long lasting pressor and sympathoexcitatory responses, whereas stimulation of the CVLM results in depressor and sympathoinhibitory responses (Agarwal et al., 1989). Interestingly, neurons within the CVLM have been shown to exhibit a tonic activity that is independent of baroreceptor drive (Cravo and Morrison, 1993, Sved et al., 2000) and may serve a potential role in long-term regulation of BP (Schreihofer and Guyenet, 2002).

Barosensitive inhibitory neurons of the CVLM project monosynaptically to bulbospinal sympathoexcitatory neurons in the RVLM bilaterally (Jeske et al., 1995). The RVLM neurons synapse on the SPN in the intermediolateral (IML) cell column of the spinal cord (Dampney, 1994, Pilowsky and Goodchild, 2002). Due to their direct projection to cardiac and vasomotor SPN in the thoracic and lumbar spinal cord, sympathoexcitatory neurons in the RVLM are also called presympathetic neurons (Dampney et al., 2002). The RVLM presympathetic neurons are inhibited by baroreceptor activation during ADN electrical stimulation or BP elevations when recorded intracellularly (Lipski et al., 1995) or extracellularly (Schreihofer and Guyenet, 1997, Verberne et al., 1999). Microinjection of bicuculline, a $GABA_A$ receptor antagonist, in the RVLM blocks the baroreceptor mediated inhibition of RVLM sympathoexcitatory neurons (Sun and Guyenet, 1985). Activity of the RVLM presympathetic neurons is believed to be a major factor in driving tonic activity in the SPN (Dampney et al., 2000). It has been hypothesised that RVLM barosensitive neurons preferentially regulate SNA to the skeletal muscle arteries, splanchnic arteries, heart and kidneys (Campos and McAllen, 1997, McAllen and Dampney, 1990, McAllen et al., 1995). However, anatomical studies have yet to provide

convincing evidence in support of this hypothesis (Guyenet, 2006, Guyenet et al., 2010). Importantly, the RVLM is also the region where inputs from other brain regions converge (e.g., sympathoexcitatory inputs from the PVN which is driven by AT_1 receptors in the RVLM) and may therefore contribute to long-term BP regulation (Dampney et al., 2002, Guyenet, 2006, Tagawa and Dampney, 1999).

Vagal efferent outflow to the heart (Fig. 1.3) is modulated through a neuronal circuit involving the NTS and CVPNs principally located within the nucleus ambiguus, the intermediary zone and the dorsal motor nucleus of the vagus (DMNV) (Izzo et al., 1993, Nosaka et al., 1979, Stuesse, 1982). Bilateral blockade of the NMDA receptors in the NTS by microinjection of kynurenate abolishes baroreflex mediated bradycardia (Leone and Gordon, 1989). Stimulation of the pathway from the NTS activates excitatory NMDA and non-NMDA receptor-mediated postsynaptic currents in vagal cardiac neurons in the nucleus ambiguus (Neff et al., 1998). There is also a tonically active GABAergic input to the CVPN that plays an important role in the tonic and reflex control of HR (Wang et al., 2001). Blockade of $GABA_A$ receptors by microinjection of bicuculline into the nucleus ambiguus produces a dose-dependent bradycardia, which can be reversed by the $GABA_A$ receptor agonist, muscimol (DiMicco et al., 1979). $GABA_A$ agonists microinjected in the nucleus ambiguus prevent the reflex slowing of the heart in response to BP increases evoked with phenylephrine (PE) (DiMicco et al., 1979).

As shown above, two separate pathways are responsible for regulating vagal and sympathetic outflow, both of which are recruited to alter HR and SNA, and counteract changes in BP. Increases in arterial BP stimulate afferent baroreceptor discharge, triggering reflex inhibition of efferent sympathetic outflow to the heart and vasculature, and activation of parasympathetic outflow to the heart. The resultant decreases in vascular resistance, stroke volume, and HR then reduce arterial BP back to baseline levels. Decreases in arterial BP have the opposite effect, evoking reflex increases in peripheral vascular resistance, stroke volume, and HR to restore arterial BP. Given the high sensitivity of baroreceptors to altered vascular stretch, the firing pattern of arterial baroreceptors increases rapidly during early systole and decreases during late systole/early diastole (Thomas, 2011). These phasic responses become more apparent at lower pressures, a time when baroreceptor discharge frequency is reduced, and less apparent at higher pressures, when the baroreceptor discharge frequency is increased (Thomas, 2011). An inability for the baroreflex to adequately buffer changes in BP may be due to various factors, such as an inability of the baroreceptor afferents to sense changes in BP, the central relay nuclei to produce changes in vagal or sympathetic outflow, or the heart or vasculature to respond to autonomic inputs.

Function and strength of the arterial baroreflex is often represented by a sigmoid logistic function, with a direct relationship existing between afferent baroreceptor discharge and arterial pressure, and an inverse relationship existing between BP and either efferent SNA or HR (Kent et al., 1972, Ma et al., 2002). An important property of the arterial baroreceptor reflex is the ability to operate around a new

baseline BP; a phenomenon known as "baroreceptor resetting" (Fig. 1.4). Any component (e.g., afferent, central, or efferent) of the baroreceptor reflex is able to reset and influence reflex control of BP (Andresen, 1984, Andresen et al., 1978, Gonzalez et al., 1983, Mccubbin et al., 1956, Sapru and Wang, 1976, Wallin and Sundlof, 1979). In other words, the afferent signal may become modified in the face of sustained elevations or reductions in BP, the CNS may "re-wire" its connections that regulate sympathetic and parasympathetic outflows, and/or the amount of SNA to different vascular beds may reset to varying degrees. The degree to which target-organs, especially the kidney, respond to reset reflex control of SNA may also help determine the long-term level of BP and development of hypertension.

A resetting of arterial baroreflex can be acute or chronic. Acute resetting is a reversible process where receptors reset only partially, demonstrated within ≤20 minutes after arterial pressure has been elevated (Krieger, 1988, Munch et al., 1983) and often occurs during conditions such as nociception, emotional stimuli or increased physical activity during exercise (Hatton et al., 1997, Ichinose et al., 2006, Kanbar et al., 2007, Smith et al., 2003). Here, the efferent baroreflex function curve shifts to the right and upward, in the absence of an evident reduction in sensitivity (the slope of the steepest portion of the baroreflex relationship). This adaptive response allows BP, efferent SNA, and HR to stay at higher levels and then fall back to baseline levels when the stimulus is ceased. The transient nature of baroreflex resetting in these settings indicates that alterations in the central components of the baroreflex arc are not related to neuroanatomic changes in the acute settings.

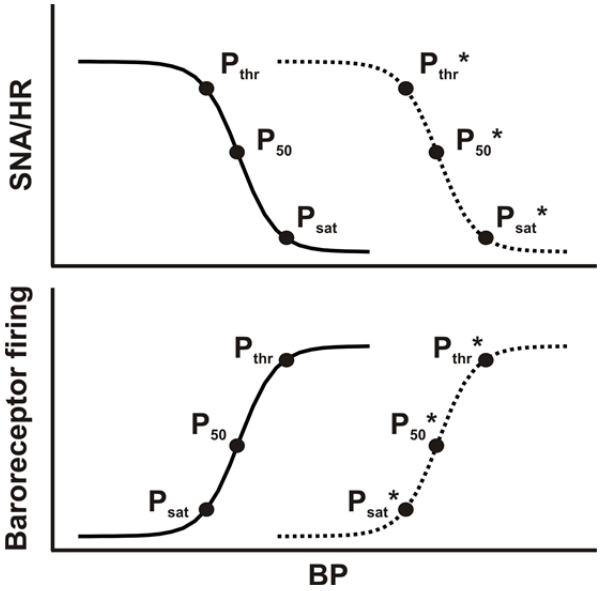

Figure 1.4: Baroreflex function curves of efferent sympathetic nerve activity (SNA)/heart rate (HR) (upper panel) and afferent activity (bottom panel) illustrating resetting of the baroreflex relationship in response to increased blood pressure (BP). Note the rightward shift resetting in all the pressure parameters of the baroreflex function to higher BP. Pressure threshold (P_{thr}), pressure at midpoint of the curve (P_{50}), pressure saturation (P_{sat}), reset pressure threshold (P_{thr}*), reset pressure at midpoint of the curve (P_{50}*) and reset pressure saturation (P_{sat}*).

Chronic resetting, on the other hand, results from a sustained elevation in arterial pressure that lasts for longer than a few weeks and is often associated with the development of hypertension (Andresen, 1984, Head and Burke, 2001, Huber and Schreihofer, 2010, Ligtenberg et al., 1999). Under such conditions, the baroreflex function curve gradually shifts to the right to operate around the new prevailing BP set point (Fig. 1.4). Over time, as elevated BP persists, the sensitivity of the baroreflex mechanism may become impaired, rendering it less capable of buffering acute BP fluctuations. Baroreflex resetting is thought to be governed by neurohumoral mechanisms (Guyenet, 2006), with a reduction in baroreceptor feedback due to a biasing of the transmission between baroreceptor afferents

and second-order neurons in the NTS being a proposed mechanism (Andresen et al., 2001). In the latter, GABAergic transmission within the NTS driven by inputs from higher brain regions (e.g., hypothalamus and other forebrain regions) or factors such as circulating/brain Ang II can pre- or postsynaptically dampen baroreceptor afferent-mediated glutamatergic excitation of the NTS second-order neuron (Andresen et al., 2001, Paton et al., 2001a, Potts et al., 2003).

Under pathological conditions, baroreceptor resetting is thought to be driven by thickening of the arterial wall, a reduction of its distensibility, and diminished sensitivity of baroreceptors, leading to impaired afferent traffic (Andresen et al., 1978). However, chronic resetting that develops in a few weeks as observed during the early stages of hypertension in spontaneously hypertensive rats (SHR) is not accompanied by vascular hypertrophy and reduced distensibility of the arterial wall (Brown et al., 1976). It is therefore possible that, at this stage, resetting is attributed to changes in the baroreceptors themselves and/or other neural elements within the reflex arc as described above. At this point, when vascular remodelling is not established in the SHR, Sparu and Krieger (1979) were able to show that antihypertensive therapy is fully capable of reversing baroreceptor resetting, suggesting that early interventional strategies that lower BP can preserve BRS.

1.3.2 Cardiopulmonary reflex

Despite the central role of the arterial baroreceptors in the rapid stabilization of BP, research has shown that reflex control of the cardiovascular functions is not only dependent upon the arterial baroreceptor reflex, but also to a great extent on cardiopulmonary reflex function. Cardiopulmonary reflexes, which are major yet diverse cardiovascular reflex pathways, originate in the heart and lungs, and play a critical role in the control of sympathetic cardiovascular drive, HR, peripheral vascular resistance, sodium and water excretion, and the release of humoral substances such as vasopressin, renin and atrial natriuretic peptide (ANP) (Grassi et al., 2006, Kashihara, 2009, Mancia et al., 1985, Merrill et al., 1999, Thomas, 2011). This reflex pathway consists of the following: (1) cardiopulmonary receptors, which are a unique set of chemosensitive and mechanosensitive receptors located within the heart, aorta and lungs (Aviado and Guevara Aviado, 2001), and respond either by exposure to chemical irritant (chemosensitization) or increases in pressure or stress (mechanostimulation) (Aviado and Guevara Aviado, 2001, Kashihara, 2009, Merrill et al., 1999, Vasquez et al., 1997); (2) sensory afferent fibres within the parasympathetic cranial nerve X, including myelinated A-fibres which are activated at lower intensities, and unmyelinated C-fibres which are activated at higher intensities. Both are thought to play a central role in the tonic depression of SNA, HR, vascular tone, and renin secretion, as their severing evokes an increased SNA, HR, renin release and vasoconstrictions of the skeletal muscle, renal and mesenteric vascular beds (Aviado and Guevara Aviado, 2001, Hainsworth, 2014, Mancia et al., 1985); (3) medullary regions regulating visceral function by modulation of efferent sympathetic and parasympathetic innervations; and (4) efferent pre-

and postganglionic sympathetic and parasympathetic nerve fibres supplying the periphery (Aviado and Guevara Aviado, 2001).

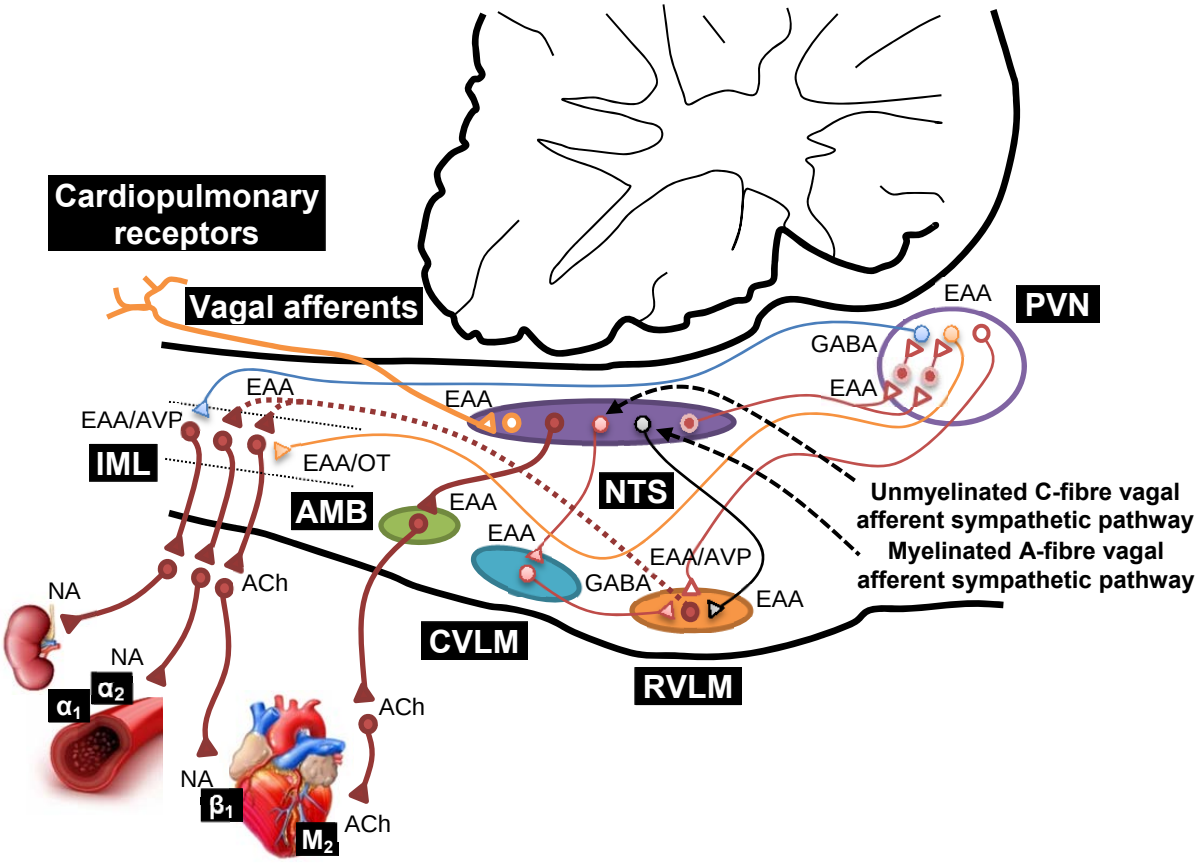

Figure 1.5: Cardiopulmonary reflex pathway within the lower brainstem region. NTS, nucleus tractus solitarius; CVLM, caudal ventrolateral medulla; RVLM, rostral ventrolateral medulla; AMB, nucleus ambiguus; IML, intermediolateral cell column in the spinal cord; EAA, an excitatory amino acid; OT, oxytocin; AVP, arginine vasopressin; GABA, γ-aminobutyric acid; ACh, acetylcholine and NA, noradrenaline. Pathway description taken from (Coote, 2005, Verberne and Guyenet, 1992). Figure modified from (Dampney et al., 2002).

The cardiopulmonary reflex, evoked by the unmyelinated C-fibre vagal afferents, and the baroreceptor reflex use common central pathways (Fig.1.5) in the brainstem regions to stabilise BP (Kashihara, 2009, Verberne and Guyenet, 1992, Verberne et al., 1999). The vagal afferent fibres terminate in the NTS and act by inducing reflex responses in sympathetic and parasympathetic outflows to the periphery (Lee et al., 1972, Sun and Guyenet, 1987, Vardhan et al., 1993). Sympathetic outflow to the heart and vasculature is then modulated via the CVLM, RVLM and SPN in the spinal cord (Su et al., 1996, Verberne et al., 1999). Efferent parasympathetic outflow to the heart is modulated through the nucleus ambiguus and DMNV (Lee et al., 1972, Toader et al., 2007). Like the baroreceptor reflex, unmyelinated C-fibre vagal afferent stimulation evokes sympathoinhibition, whereas myelinated A-fibre vagal afferent pathways (Fig. 1.5), like the chemoreceptor reflex (see below), is thought to be sympathoexcitatory and its responses are modulated through a direct projection from the NTS to the RVLM (Verberne and Guyenet, 1992). As reviewed by Coote (2005), there is also evidence that vagal afferent neurons terminating in the NTS project to the PVN (Lovick and Coote, 1988, Pyner et al.,

2002), where there is a discrete targeting of spinally projecting oxytocin neurons that innervate cardiac SPNs (Yang et al., 2002) and a specific pool of GABA inhibitory interneurons (Yang and Coote, 2003) that innervate a population of spinally projecting vasopressin neurons that synapse with the renal SPNs (Yang et al., 2002). There is also a vasopressin/glutamate projection from the PVN to RVLM spinally projecting vasomotor neurons (Yang et al., 2001), although the involvement of this projection in the reflex is still unclear.

Several specific cardiopulmonary reflexes have been identified based on the type of sensory afferent fibre types recruited during activation of the reflex:

(A) *Reflexes mediated by myelinated A-fibres of the vagal afferents:*

1) The best defined cardiopulmonary reflex mediated by the myelinated A-fibre type of the vagal afferent is the Bainbridge reflex. This reflex is initiated by mechanoreceptor activation at the pulmonary vein-atrial junctions in response to increased atrial volume and pressure (Ledsome and Linden, 1964). Activation of this reflex leads to sympathetically mediated reflex tachycardia (Bainbridge, 1915, Karim et al., 1972), with minimal or no apparent effect on cardiac inotropic activity (Furnival et al., 1971). The reflex differentially affects sympathetic outflow to different target organs, with cardiac SNA reflexively increased, RSNA decreased, adrenal SNA increased, splanchnic SNA increased or unchanged but lumbar remaining unaffected (Deering and Coote, 2000, Karim et al., 1972). Systemic vascular resistance remains unaltered (Carswell et al., 1970a); however, decreases in antidiuretic hormone (vasopressin) (Bennett et al., 1983), cortisol (Drinkhill and Mary, 1989) and renin (Drinkhill et al., 1988) secretions and consequent diuresis are observed (Carswell et al., 1970b).
2) Mechanoreceptors within the pulmonary trunk and the proximal part of the pulmonary arteries (pulmonary baroreceptors) are also endowed with myelinated A-fibre vagal afferents. These pulmonary pathways are activated in response to venous infusions and vena caval occlusions, causing reflex vasoconstriction and an increase in respiratory activity (Hainsworth, 2014).

(B) *Reflexes mediated by unmyelinated C-fibres of the vagal afferents:* these include reflexes initiated in the atria, ventricles, coronary arteries and lungs:

1) Atrial mechanoreceptors respond to increased atrial volume and pressure by causing bradycardia and vasodilation (Campagna and Carter, 2003, Hainsworth, 2014).
2) Mechanoreceptors in the left ventricle and coronary arteries respond to increased ventricular diastolic pressure and afterload by causing vasodilation (Hainsworth, 2014).
3) Ventricular chemoreceptors are stimulated by toxic and irritant chemicals including plant alkaloids (e.g., veratridine, veriloid and protoveratrine, initially described as anithypertensives before the 1960s), nicotine, capsaicin, venoms (e.g., snake, insects and marine animals), and synthetic organic compounds (e.g., ethylacetoacetate, thioureas, halogenated anaesthetics and the serotonin 5-HT_3 receptor agonist phenylbiguanide). Endogenously occurring substances stimulating these receptors are potassium chloride,

bradykinin, prostaglandins, prostacyclin, histamine, serotonin and reactive oxygen species (Aviado and Guevara Aviado, 2001, Chapleau and Sabharwal, 2011, Kaufman et al., 1980, Vasquez et al., 1997). Chemostimulation of these receptors evokes what is often referred to as the Bezold-Jarisch (BZJ) reflex, the activation of which is characterised by a powerful reflex sympathoinhibition, bradycardia, widespread vasodilation and hypotension (Aviado and Guevara Aviado, 2001, Schultz, 2001, Vasquez et al., 1997). Clinically, this reflex can be triggered during intracoronary injection of contrast agent or myocardial ischaemia, which releases endogenous chemical factors (e.g., bradykinin and prostaglandins) that can contribute to the activation of this reflex, which is therefore thought to have a cardioprotective action (Chapleau and Sabharwal, 2011, Hainsworth, 2014, Schultz, 2001). There is also evidence that mechanical stimulation of afferents by strong contractions of an under-filled left ventricle can also evoke the BJZ reflex (Chapleau and Sabharwal, 2011, Hainsworth, 2014).

4) Marked lung inflation (e.g., mechanical stimulation, pulmonary oedema or congestion) activates juxtapulmonary capillary receptors (J-receptors) in the lungs, leading to respiratory sinus arrhythmia, bradycardia, sympathoinhibition, peripheral vasodilation, and hypotension (Asanoi, 2009, Ashton and Cassidy, 1985, Hayano et al., 1996, Shepherd, 1981).

1.3.3 Chemoreceptor reflex

The chemoreceptor reflex mechanism is primarily involved in the control of ventilation; however, it can also modulate neural pathways regulating mean arterial BP. Stimulation of this reflex is triggered by hypoxia, hypercapnia, and/or acidosis, leading to increases in parasympathetic, sympathetic and phrenic nerve activities (Braga et al., 2006, Cao and Morrison, 2001, Silva and Schreihofer, 2011, Wenker et al., 2013). The peripheral chemoreceptors, which are located in the carotid bodies at the bifurcation of the common carotid arteries and in aortic bodies in the region of the aortic arch, are highly specialised receptors; the activation of which is primarily evoked by a reduction in PO_2 of the arterial blood (Chapleau and Sabharwal, 2011, Dampney et al., 2002, Guyenet et al., 2010, Marshall, 1994, Thomas, 2011, Vasquez et al., 1997). Arterial chemoreceptors are thought to be type 1 glomus cells that contain and release multiple neurotransmitters into the synaptic cleft activating presynaptic (i.e. on the type 1 glomus cells) and postsynaptic (i.e. chemoafferent terminals) receptors, utilising catecholamines (especially dopamine), acetylcholine, met- and leuenkaphalins, substance P, NPY, galanin, calcitonin-gene-related peptide, serotonin, and endothelins (Gonzalez et al., 1994). Similar to baroreceptor afferent fibres, chemoreceptor afferents are located within the vagus nerve in humans and the carotid sinus nerve in humans and rats (Dampney et al., 2002, Guyenet et al., 2010, Sapru and Krieger, 1977, Timmers et al., 2003) and relay sensory signals to the brain that reflexively elicit hyperventilation, bradycardia and sympathetically-mediated vasoconstriction in most vascular beds. The increase in ventilation tends to increase oxygen saturation of the blood, while the bradycardia and sympathetic vasoconstriction acts to reduce oxygen consumption by the tissues to thus maintain the

oxygen reserve and vital organ perfusion (Dampney et al., 2002, de Burgh Daly and Scott, 1962, Marshall, 1994, Paton et al., 2001b, Thomas, 2011). The initial bradycardic response to arterial chemoreceptor activation is then usually followed by tachycardia at steady-state as hyperventilation inhibits efferent vagal outflow to the heart (Marshall, 1994). If BP is within the normal range, the chemoreflex does not exert a powerful cardiovascular response because of the predominant inhibitory effect of the arterial baroreceptor reflex. However, if BP falls below 80 mmHg, activation of the chemoreflex potentiates the baroreflex-mediated vasoconstriction to restore BP to normal levels (Thomas, 2011).

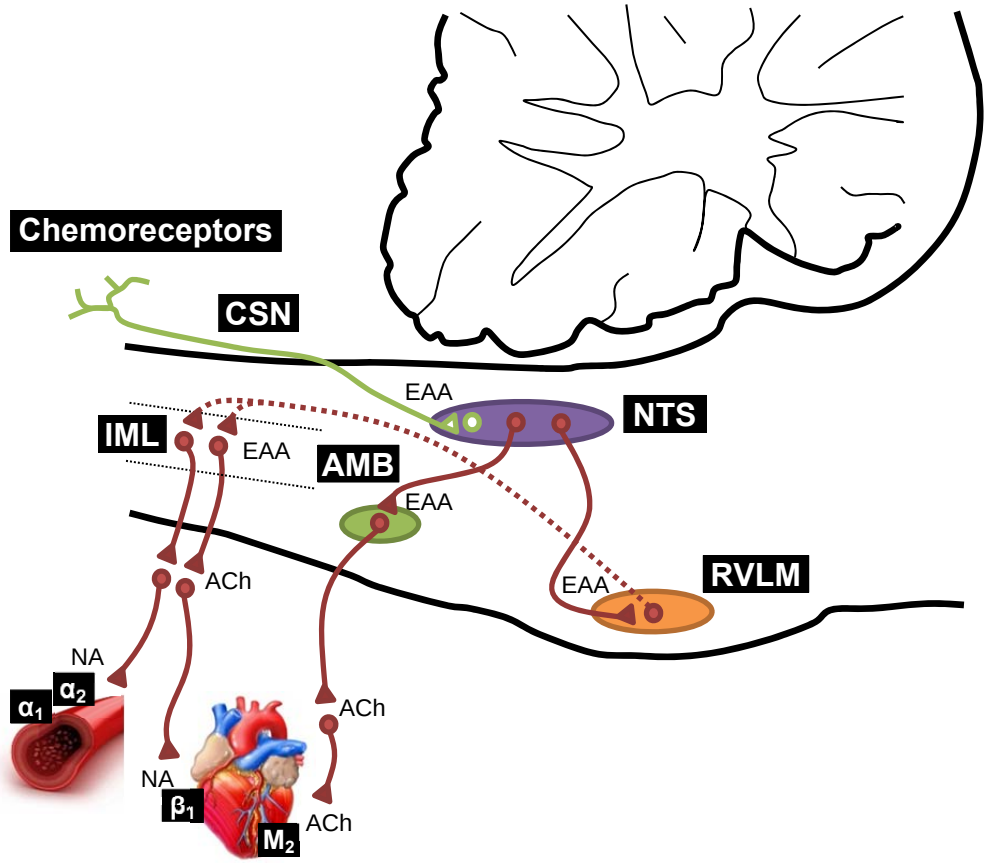

Figure 1.6: Peripheral chemoreceptor reflex pathway within the lower brainstem region. CSN, carotid sinus nerve; NTS, nucleus tractus solitarius; RVLM, rostral ventrolateral medulla; AMB, nucleus ambiguus; IML, intermediolateral cell column in the spinal cord; EAA, an excitatory amino acid; GABA, γ-aminobutyric acid; ACh, acetylcholine and NA, noradrenaline. Figure modified from (Dampney et al., 2002).

Like baroreceptor afferent fibres, chemoreceptor primary afferent fibres terminate in the NTS (Fig. 1.6); however, in contrast to the baroreflex pathways, chemoreceptor signals are transmitted to the RVLM via a direct excitatory glutamatergic projection (Aicher et al., 1996, Callera et al., 1999, Guyenet and Koshiya, 1995), increasing the activity of the SPNs. Bilateral microinjections of the glutamate receptor antagonist kynurenate into the RVLM abolish the sympathoexcitatory and pressor responses following peripheral chemoreceptor activation (Koshiya et al., 1993). A non-glutamatergic neurotransmission of the sympathoexcitatory component of the chemoreflex at the NTS level has also been suggested (Machado and Bonagamba, 2005). Cardiac vagal efferent activity and chemoreflex-induced bradycardia, which share similar yet separate neurochemical mechanisms in the NTS to those

of baroreflex-mediated bradycardia, is regulated via relay circuit which involves the NTS and nucleus ambiguus and/or DMNV; all of which are recruited to increase the activity of CVPN (Callera et al., 1999, Haibara et al., 1995). Evidence supporting a common neuroanatomical pathway for the parasympathetic component of chemoreflex and baroreflex in the NTS came from studies demonstrating that activation of 5-HT_3 serotonin receptors in the NTS abolished the cardiovagal component of both the baroreflex and chemoreflex (Callera et al., 1997). However, microinjection of baclofen, a $GABA_B$ agonist, into the NTS affected the bradycardic response to baroreflex (Callera et al., 2000) but not chemoreflex activation (Callera et al., 1999), suggesting that the parasympathetic component of baroreflex and chemoreflex are regulated by two different inhibitory mechanisms.

There is also evidence that the pontomedullary region may contain multiple sites for central chemoreception, including the NTS, retrotrapezoid nucleus, pre-Bötzinger complex, and raphe (Guyenet et al., 2009, Guyenet et al., 2010, Mulkey et al., 2004, Richerson et al., 2005, Sun et al., 2001). Importantly, the two major chemoreception locales (peripheral and central) that drive breathing are hypothesized to be combined at the retrotrapezoid nucleus (Guyenet et al., 2009). A rise in CNS PCO_2 has also been shown to evoke marked increases in SNA to the heart and blood vessels in both humans and experimental animals (Huang et al., 2009, Somers et al., 1991). The effect of hypercapnia is generally linked to series of events, whereby brain extracellular fluid acidification stimulates central chemoreceptors to activate the respiratory pattern generator. This ultimately drives the sympathetic generating network by phasically exciting the RVLM (Guyenet and Koshiya, 1992, Guyenet et al., 2009, Millhorn, 1986), the sympathoexcitatory neurons of which are known to be intrinsically pH-sensitive and receive excitatory synaptic inputs from the retrotrapezoid nucleus (Moreira et al., 2006). During central chemoreceptor stimulation, RVLM sympathoexcitatory neurons exhibit patterns of central respiratory-related activity that are similar to those of barosensitive sympathetic ganglionic neurons (Guyenet et al., 1990, Miyawaki et al., 1995).

1.4 Short-term feedforward regulation: activation of central stress pathways

Autonomic cardiovascular responses can also be evoked as part of a more complex behavioural response: for example, exercise or stress (Dampney et al., 2002). These changes are orchestrated by a complex supramedullary network of neurons in the limbic cortex, amygdala, and hypothalamus via synaptic projections to the central autonomic control centres. Among the various behavioural responses, autonomic and cardiovascular responses to stressful stimuli are of particular importance. It is well established that acute emotional stress or threatening stimuli evoke marked cardiovascular responses (fight-or-flight response) characterised by increased SNA, HR and BP (Dampney et al., 2002, DiMicco et al., 2002, Fontes et al., 2011, Fontes et al., 2014). Activation of limbic system structures including the amygdala, which is involved in the processing of emotions and memory (LeDoux, 2007), is evoked in response to a stressful stimulus (Dampney et al., 2002, Fontes et al., 2011, Fontes et al., 2014). Excitatory projections from the amygdala to the dorsomedial hypothalamus

(DMH) (Soltis et al., 1998), a nucleus corresponding with the hypothalamic defence area (Dampney et al., 2002, DiMicco et al., 2002) which when disrupted leads to panic like response in rats (Johnson and Shekhar, 2006), are thought to be the primary generator for endocrine and autonomic responses to stress (Fig. 1.7):

1) *The endocrine response:* Central regulation of the hypothalamo-pituitary-adrenocortical (HPA) axis plays a critical role in the processing of the hormonal response to a stressful stimulus (DiMicco et al., 2002). Here, the DMH signals excitation of the PVN (Cullinan et al., 1996, Ulrich-Lai and Herman, 2009), whose neurons project down to the median eminence (ME) (Koegler-Muly et al., 1993). Neurons within the ME release corticotrophin releasing hormone (CRH) (Evanson et al., 2009, Merchenthaler et al., 1984), which stimulates anterior pituitary production of adrenocorticotrophic hormone (ACTH) (Bailey and Dimicco, 2001, Makara et al., 1986, Ulrich-Lai and Herman, 2009). ACTH then acts on the adrenal glands to trigger cortical release of glucocorticoids, which have widespread effects to cope with stress (DiMicco et al., 2002, Smith and Vale, 2006).
2) *The autonomic response:* Apart from its primary role in the endocrine response, activation of the PVN neurons was initially thought to play no role in the tachycardic and pressor response to stress (Stotz-Potter et al., 1996). However, Busnardo and co-workers showed that bilateral inhibition of the PVN reduced the pressor response to acute restraints in rats, suggesting that local PVN neurotransmission is involved in the neural pathway that controls autonomic responses to stress (Busnardo et al., 2010). Furthermore, the DMH signals excitation of the RVLM and the raphe pallidus, regions which independently influence the cardiac and vasomotor component of stress reactivity as well as adrenaline release from the adrenal medulla. Synaptic connections between the DMH and RVLM appear to trigger discharge from the sympathetic premotor neurons involved in the maintenance of sympathetic vasomotor activity (Fontes et al., 2001), and hence contribute to vasoconstriction and BP elevation. The cardiac sympathoexcitatory component of the stress pathway is evoked by a DMH-mediated excitation of the raphe pallidus (Fontes et al., 2001, Samuels et al., 2002), whose sympathetic premotor neurons may project directly to the spinal cardiac sympathetic preganglionic neurons (Cao and Morrison, 2003). This activation occurs independently of excitation of the sympathetic premotor neurons in the RVLM which normally drives increases in cardiac SNA and contributes to tachycardia. In support of the role of the raphe pallidus in mediating the tachycardic response to stress are studies showing that inhibition of the raphe pallidus abolished the tachycardic response to stress, but not to baroreceptor unloading (Zaretsky et al., 2003). Further evidence comes from reports demonstrating a comparable tachycardia in response to activation of the DMH and raphe pallidus neurons (Samuels et al., 2002). It is important to note, however, that the pattern of sympathetic response preferentially involves the heart, as evidenced by measurements of regional NA spillover during a cognitive challenge (Esler et al., 1989). In support of this view is also the finding that the arterial BP

response, which is dependent upon the intensity of the stressor, is primarily influenced by the intensity of the tachycardic response – even more so than responses of the vasomotor SNA (Callister et al., 1992).

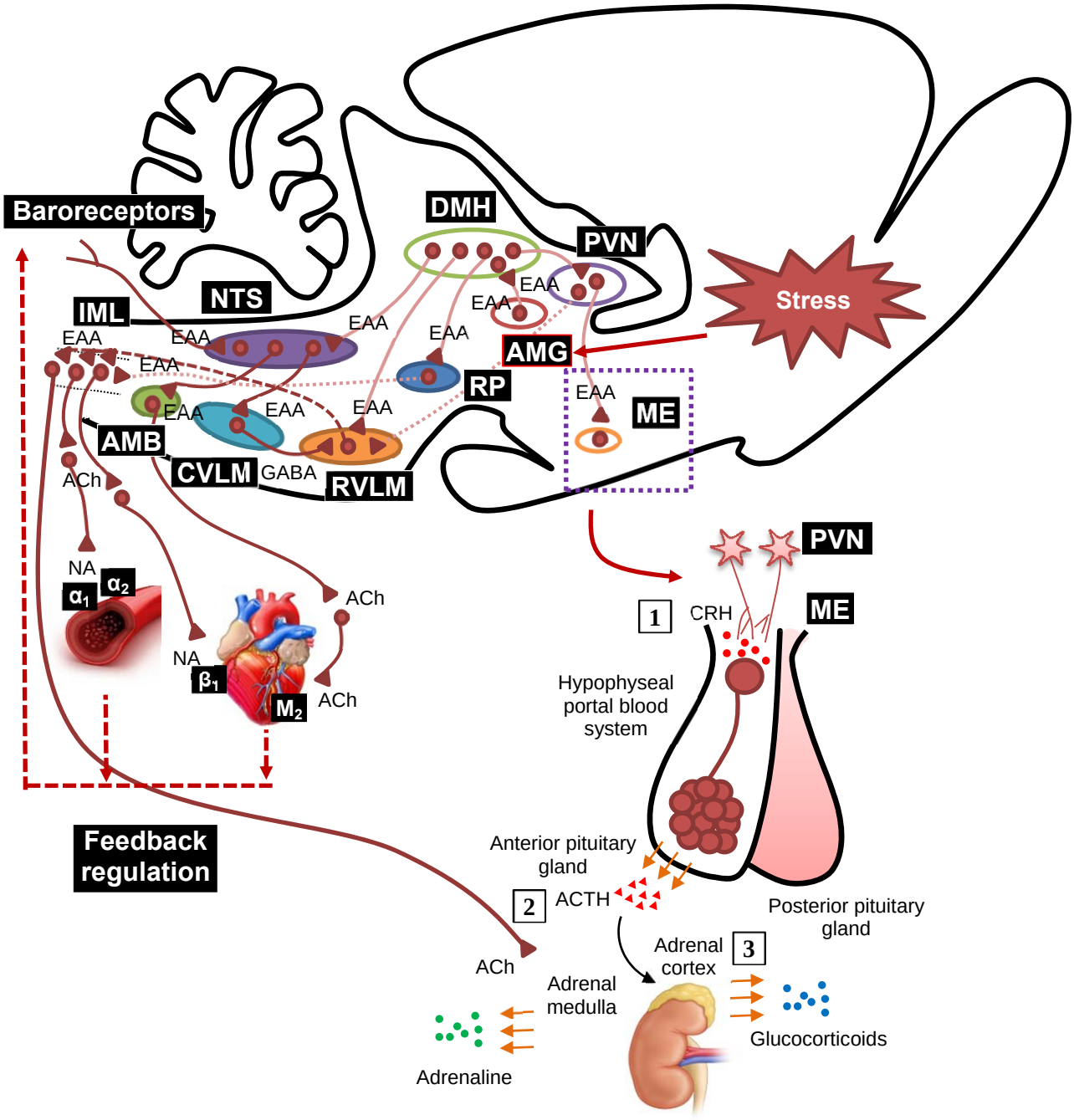

Figure 1.7: The neuroendocrine stress pathway. AMG, amygdala, DMH, dorsomedial hypothalamus; PVN, paraventricular nucleus; ME, median eminence; RP, raphe pallidus; NTS, nucleus tractus solitarius; CVLM, caudal ventrolateral medulla, RVLM; rostral ventrolateral medulla; AMB, nucleus ambiguus; IML, intermediolateral cell column in the spinal cord; EAA, an excitatory amino acid; GABA, γ-aminobutyric acid; CRH, corticotrophin releasing hormone; ACTH, adrenocorticotrophic hormone; ACh, acetylcholine and NA, noradrenaline. Pathway description taken from (Busnardo et al., 2010, Dampney et al., 2002, Fontes et al., 2001, Fontes et al., 2011, Fontes et al., 2014, Samuels et al., 2002).

Stress-induced stimulation of the DMH neurons can also modulate the baroreceptor reflex through not only descending pathways from the DMH to the RVLM (Fontes et al., 2001) but also via

possible direct excitatory projections from the DMH to the NTS neurons (Kunos and Varga, 1995). This modulation appears to be critical during defence reactions to stress to ensure that changes in HR and BP can occur simultaneously (Fontes et al., 2011). The reaction is also associated with resetting of the HR and SNA baroreflex relationship to higher BP, with unaltered HR BRS (Hatton et al., 1997), but increased SNA BRS (Kanbar et al., 2007), have been reported. Most recently, Furlong and colleagues have also shown that sympathetic activity during psychological stress is not driven primarily by RVLM sympathetic premotor neurons, and that neurons in the PVN, perifornical area, ventrolateral periaqueductal gray may contribute to the resetting of the baroreceptor-sympathetic reflex that is associated with psychological stress (Furlong et al., 2014).

1.5 Methods of assessment of autonomic nervous system function in humans and experimental animals

Disorders of autonomic regulation are described in a range of cardiovascular and non-cardiovascular diseases. Many methods assessing the functionality of the ANS have therefore been developed to characterise changes in autonomic functions in humans and laboratory animals. Here, some of the methods used to assess tonic and reflex function of the ANS and their use in clinical practice and scientific studies are briefly reviewed.

1.5.1 Measurements of tonic sympathetic and parasympathetic nervous activity

These include the following:

1.5.1.1 Pharmacological agents targeting autonomic receptors and ganglia

The ongoing parasympathetic activity to the heart (cardiovagal tone) can be quantified by measuring increases in HR in response to muscarinic receptor (mainly M_2 cholinergic receptors) blockers such as methylatropine (Harrison et al., 2010, Head and McCarty, 1987, Mircoli et al., 2003). Tonic cardiac sympathetic activity, on the other hand, can be measured by estimating changes in the bradycardic response to β-adrenoceptor (mainly β_1 adrenergic receptors on the SA node) blockers such as atenolol (Badve et al., 2011, Harrison et al., 2010, Head and McCarty, 1987). Intrinsic pacemaker properties of the heart (i.e. intrinsic HR) can be evaluated by measuring HR responses after dual pharmacological blockade of both muscarinic and β-adrenergic receptors (Harrison et al., 2010). Sympathetic vasomotor tone can be quantified by measuring depressor response to centrally acting α_2-adrenoceptor agonists (e.g., clonidine and moxonidine) (Iriuchijima, 1997, Neumann et al., 2004, Nikolic and Agbaba, 2012), α_1-adrenoceptor antagonists (e.g., prazosin) (Oates et al., 1977), or ganglionic blockers (e.g., hexamethonium and pentolinium) (Burke et al., 2008, Phillips et al., 2007). These methods are relatively easy to implement and can be applied in human and/or animal subjects.

1.5.1.2 Analysis of heart rate and systolic blood pressure variability

Analysis of HRV and systolic BP variability (SBPV) has become one of the most common methods of assessing ANS function. These methods are based on quantifying spontaneous fluctuations in HR and BP to derive information regarding sympathetic, parasympathetic and non-neuronal (e.g., hormonal, thermoregulatory, etc.) influence (Diedrich et al., 2003, Head, 2003, Hildreth et al., 2013a, Zygmunt and Stanczyk, 2010), and are not direct indices of tonic activity of the sympathetic or parasympathetic nervous system, but rather the result of their influence on the effector organs (e.g., heart and vasculature) (Chapleau and Sabharwal, 2011, Zygmunt and Stanczyk, 2010).

HRV: Heart rate variability is based on the observation that even at rest, the duration of R-R intervals is not constant but continually fluctuates around the mean value. Heart rate variability is generally assessed based on time-domain or frequency-domain analysis. Parameters of time-domain analysis include: 1) the standard deviation of normal-to-normal intervals (SDNN) which describes overall HRV, 2) the standard deviation of the average normal-to-normal intervals (SDANN) which evaluates slow changing components of HRV, and 3) the square root of the mean squared differences of successive normal-to-normal intervals (rMSDD) and the proportion of differences in consecutive normal-to-normal intervals that are longer than 50 ms (pNN50), both of which describe short-term variation and are reflective of parasympathetic activity (Electrophysiology, 1996, Hildreth et al., 2013a, Zygmunt and Stanczyk, 2010).

Parameters of frequency domain analysis, which concentrates on revealing the cyclical nature hidden in the series of changing R-R intervals, are: 1) very low frequency (VLF) band (below 0.04 Hz humans, 0.04–0.2 Hz rats) which relates to hormonal and thermoregulatory influences on the heart, 2) low frequency (LF) band (0.04–0.15 Hz humans, 0.2–0.75 Hz rats, 0.15–0.6 Hz mice) which is modulated by both the sympathetic and parasympathetic nervous system and also associated with baroreceptor activity, 3) high frequency (HF) band (HF; 0.15–0.4 Hz humans, 1–3 Hz rats, 2.5–5 Hz mice) which is modulated by the parasympathetic nervous system and connected with respiration and BP changes, and 4) LF/HF ratio which reflects interactions of both types of autonomic modulation and measures are regarded as a marker of sympathovagal balance (Hildreth et al., 2013a, Zygmunt and Stanczyk, 2010).

SBPV: The frequency components of SBPV detected by power spectral analysis are: 1) VLF (0.02–0.20Hz in rats, 0.02–0.07Hz in humans) which is modulated by myogenic vascular function, RAAS, and endothelium-derived NO, 2) LF (0.2–0.6Hz in rats, 0.077–0.15Hz in humans) which is modulated by sympathetic vasomotor tone, 3) HF (1‑4Hz in rats and 0.15‑0.40Hz in humans) which is influenced by cardiac output, and 4) LF/HF which is a marker of sympathetic vascular activity (Höcht, 2013, Stauss, 2007).

1.5.1.3 Measurements of neurotransmitter levels or spillover

Tonic sympathetic autonomic activity can also be quantified by measurement of circulating neurotransmitters. While ACh, the principle neurotransmitter of the parasympathetic nervous system, cannot be quantified precisely as it is quickly disintegrated by the enzyme acetylcholinesterase (Chapleau and Sabharwal, 2011), tonic activity of the SNS can be assessed based on plasma or urine NA concentration (Sinski et al., 2006, Vink et al., 2013). However, such measurements do have limitations, as NA is subjected to changeable presynaptic reuptake and circulating NA represents only a small fraction of the amount of neurotransmitter secreted from nerve endings (Esler, 1992, Sinski et al., 2006). Nonetheless, the measurement of plasma NA is seen to be an improvement over assessment of its urine levels (Sinski et al., 2006).

Noradrenaline spillover rate, an assessment which mirrors the secretion of NA from the sympathetic nerve terminals (Sinski et al., 2006), allows for assessment of total body as well as regional NA spillover from for example, the heart, splanchnic and renal circulations, skeletal muscle or the brain (Esler et al., 1989, Mitchell et al., 2009, Wallin et al., 1996, Yoshimoto et al., 2010); hence making this method more specific than quantifying plasma or urine NA levels. The method involves administration of an intravenous (i.v.) infusion of a small amount of radiolabelled NA, then calculating the difference between tissue clearance of this substance and plasma NA measures, which represents a marker of NA "spillover" from neuroeffector junctions (Esler et al., 2003, Sinski et al., 2006).

1.5.1.4 Heart rate recovery after exercise

During exercise training, parasympathetic inhibition and sympathetic activation mediate increases in basal HR. When exercise is terminated, HR falls exponentially, and this rapid fall in HR has been linked to effective parasympathetic reactivation (Coote and Bothams, 2001). This view is supported by the fact that post-exercise HR recovery is markedly blunted after muscarinic receptor blockade (Chapleau and Sabharwal, 2011), which therefore makes this measure a useful indirect tool to assess cardiac vagal tone.

1.5.1.5 Direct measurement of sympathetic and parasympathetic nerve activity

Several factors may dissociate the indirect measurements described thus far from the true level of sympathetic and parasympathetic nerve activity, including local modulation of neurotransmitter release within synaptic neurons, changes in neurotransmitter degradation or reuptake and altered target organ responsiveness (Chapleau and Sabharwal, 2011). Accordingly, more direct recording techniques can be used to measure actual nerve activity levels

Microneurography: This method, which utilizes the postganglionic sympathetic fibres going to muscles, is used in humans to directly record multi-unit SNA from the large peripheral nerves located superficially under the skin (peroneal, tibial or median nerve) by means of tungsten microelectrodes

inserted selectively into muscle or skin fascicles (Brown et al., 2012, Esler et al., 2003, Grassi et al., 2011a, Sundlof and Wallin, 1977). Muscle SNA represents the vasoconstrictor signal to the skeletal muscle vasculature. It is highly sensitive to BP changes and is regulated by means of baroreflexes and cardiopulmonary reflexes (Sinski et al., 2006). These reflexes, however, do not affect skin SNA, the activity of which merely reflects vasomotor neural traffic to skin blood vessels (Hagbarth et al., 1972). Muscle SNA often correlates with whole body, renal and cardiac NA spillover, and together these measures are considered as the only "gold standard" methods to quantify sympathetic activity in humans (Vink et al., 2013, Wallin et al., 1992, Wallin et al., 1996). Though within-subject reproducibility of the basal supine muscle SNA signal is very high (Fagius and Wallin, 1993), this procedure is associated with major limitations which include lengthy time duration and the need for extensive training (Vink et al., 2013). In a series of carefully executed experiments, James and co-workers have recently been able to record multi-unit muscle or skin SNA while performing functional magnetic resonance imaging (fMRI) of the brain in order to identify central regions responsible for generating increases in sympathetic outflow during rest and emotional engagement (James et al., 2013a, James et al., 2013b).

A superior method to recording multi-unit SNA is quantifying firing frequency, firing probability, and the number of spikes generated per cardiac interval using single-unit SNA recordings (Hering et al., 2013, Macefield et al., 1994). Of note, it has been shown that a high level of multi-unit muscle SNA does not accurately reflect underlying pathology (Burke et al., 2011). For example, in patients with mild hypertension, sympathetic discharge from single muscle vasoconstrictor neurons is more pronounced than in moderate to severe hypertension, whereas multi-unit muscle SNA is comparable across all grades of the disease (Greenwood et al., 1999). Despite permitting a more detailed examination of SNA, this method is still technically challenging (Burke et al., 2011).

Invasive measurements in experimental animals: Animal studies enable more precise dissection of neuronal pathways and therefore more accurate characterisation of autonomic functions.

Parasympathetic activity: Parasympathetic nerve activity can be assessed directly from efferent nerve fibres within the cervical vagus nerve or its cardiac branches. Typically, the right vagus is used due to its prominent role in control of HR. Repeated splitting of nerve fibres is required to obtain single-fibre or few-fibre preparations where the activity can be shown to be cardiovagal. Section of the vagus nerve distal to the recording electrodes eliminates the activity of sensory signals from the recordings (Chapleau and Sabharwal, 2011, Jones et al., 1998).

Sympathetic activity: Whole-nerve activity recordings have been obtained from various sympathetic nerve beds in conscious and anaesthetised sheep, dogs, cats, rabbits, rats and mice (Montano et al., 2009). The rat has been, and still is, the most frequently used species in cardiovascular research (Montano et al., 2009). In unconscious or conscious animals, multi-fibre recordings have been

obtained from a variety of sympathetic nerve beds that subserve quite different functions. These nerves are:

a) Splanchnic sympathetic nerve: The splanchnic nerve contains post-ganglionic axons supplying the splanchnic circulation as well as glands and muscles in the gut (Montano et al., 2009). An example of the splanchnic nerve recording is the work of Huber and Schreihofer who showed elevated tonic levels of SNA and impaired sympathetic baroreflex function in obese Zucker rats (Huber and Schreihofer, 2010). Conscious recording of splanchnic SNA has also been attempted in the work of Ricksten et al. who used this technique to show marked excitations of SNA in response to spontaneous BP drop (baroreceptor-pattern) and natural behaviour (centrally-mediated pattern) in the SHR relative to Wistar-Kyoto (WKY) rats (Ricksten et al., 1984).
b) Renal sympathetic nerve: The most preferred for recording because, as with the splanchnic nerve recorded after the adrenal branch, it is, with little doubt, of purely post-ganglionic nature (Scislo et al., 1998). The renal nerve contains axons of neurons that innervate blood vessels, tubules and juxtaglomerular cells in the kidney (DiBona, 2000b, Johns et al., 2011). An example of RSNA recording is the work of Vitela et al., who demonstrated in anaesthetised rats resetting of RSNA baroreflex function to higher BP four weeks following the induction of renal wrap hypertension (Vitela et al., 2005). In the work of Kanbar and others, conscious short-term recording of RSNA in rats were carried out to assess sympathetic baroreflex responses to air-jet stress. Their result showed that emotional stress was associated with enhanced RSNA baroreflex responses (Kanbar et al., 2007). Successful short-term recordings of RSNA in conscious mice have also been reported (Hamza and Hall, 2012).
c) Adrenal sympathetic nerve: The adrenal nerve contains pre-ganglionic axons supplying the adrenal glands which regulate the release of adrenaline and NA (Cao and Morrison, 2000). An example of the adrenal SNA recording is the work of Scislo et al. who recorded this nerve bed simultaneously with RSNA and lumbar SNA to assess differential baroreflex responses in anaesthetised rats. In this work, adrenal SNA baroreflex function exhibited greater range and sensitivity relative to those of RSNA and lumbar SNA (Scislo et al., 1998). In the work of Zhang et al. exaggerated adrenal SNA responses to ganglionic blockade, air-jet stress and glucopenia were reported in the conscious SHR compared with WKY (Zhang and Thoren, 1998).
d) Lumbar sympathetic nerves: The lumbar sympathetic chain contains axons of both pre- and postganglionic sympathetic neurons. However, the proportion of pre-ganglionic axons is low (Scislo et al., 1998). The fibres contained within predominantly supply skeletal muscle and skin of the hindlimb. The predominance of muscle over cutaneous SNA in resting lumbar SNA is suggested by its strong barosensitivity, where muscle SNA is strongly pulse modulated by the arterial baroreflex while skin SNA is not (Habler et al., 1994). An example of lumbar SNA recording is the work of Mueller and co-workers who, using concurrent recording of lumbar,

adrenal and renal SNA in anaesthetised rats, demonstrated significantly smaller increases in lumbar SNA in response to microinjection of glutamate into the RVLM relative to RSNA and adrenal SNA (Mueller et al., 2011). Short-term recording of lumbar SNA has also been described in the work of Chen and others who used this technique to show that daily spontaneous running for 8–9 weeks reduced lumbar SNA baroreflex range, maximum and gain, in conscious Sprague-Dawley rats (Chen and DiCarlo, 1996).

e) Cardiac sympathetic nerve: The sympathetic cardiac nerves are six postganglionic branches of the SNS which run from the cervical ganglia of the sympathetic trunk to the cardiac plexus. They are named after the ganglion from which they emerge, incorporating the superior cardiac nerve, middle cardiac nerve and inferior or stellate cardiac nerve (Janes et al., 1986). An example of cardiac SNA recording is the work of Turner et al. who used dual recording of cardiac and splanchnic SNA in anaesthetised rats to assess differential nerve responses driven by the baroreceptor reflex. In these experiments they were able to show that rapid changes in baroreceptor pressure input resulted in a smaller response in cardiac SNA compared with splanchnic SNA (Turner et al., 2013). Cardiac SNA has also been recorded simultaneously with RSNA in conscious sheep models of heart failure (Ramchandra et al., 2013, Ramchandra et al., 2012) and sepsis (Booth et al., 2014, Ramchandra et al., 2009).

A common limitation to recordings from all these nerves is that when the nerve is not cut distal to the recording electrode, a contribution from the afferent neuronal activity cannot be ruled out (Montano et al., 2009). With the renal nerve, however, this contribution is perhaps negligible as RSNA levels recorded after ganglionic blockade are no different to post-mortem levels (Bertram et al., 2005).

With regard to recording SNA in conscious animals, a limitation is the ability to maintain a viable nerve signal for a prolonged period. Traditionally, conscious recording in rats were performed within hours of recording electrode implantation (Koepke and DiBona, 1985, Neahring et al., 1995, Ricksten et al., 1984, Zhang and Thoren, 1998), while recording in rabbits typically lasts longer (Armitage et al., 2012, Burke et al., 2008, Burke and Head, 2003, Guild et al., 2012, Head and Burke, 2001, Ramchandra et al., 2006). With advances in technology and the revisited concept of differential central control of sympathetic outflow to different target organs (Head and Burke, 2001, Ramchandra et al., 2013, Yoshimoto et al., 2010), there has been a growing interest in obtaining long-term recordings of organ-specific SNA (e.g., lumbar and renal SNA) in conscious rats (Hart et al., 2013, Muntzel et al., 2012, Yoshimoto et al., 2010). This approach has re-emerged to resolve issues related to unconscious recordings of SNA, including the effects of anaesthesia, surgical stress, and the inability to identify temporal changes in the SNS during disease due to short-term nerve viability. Without a doubt, the ability to record SNA chronically will greatly impact our understanding of the mechanisms pertaining to the functional role of the SNS in health and disease.

1.5.2 Measurements of reflex sympathetic and parasympathetic nervous activity

A wide range of methods have been devised to test sympathetic and parasympathetic reflex function in research laboratories and clinics.

1.5.2.1 Arterial baroreflex function

Arterial baroreflex function can be tested in humans and experimental animals using both invasive and non-invasive methods.

Invasive methods:

1) *Pharmacological methods:* Pharmacologically-induced changes in BP using vasoactive drugs are used to assess sympathetic and cardiovagal baroreflex function in humans and experimental animals. This method, also known as the Oxford method, involves recording of HR and/or SNA baroreflex response to evoked changes in BP using i.v. bolus injections or infusions of a vasoconstrictor (e.g., PE) and vasodilator (e.g., sodium nitroprusside, SNP; nitroglycerine) drug (Chapleau and Sabharwal, 2011, Parati et al., 2000, Smyth et al., 1969). Phenylephrine-induced rise in BP generates bradycardia and sympathoinhibition, which enables calculation of BRS as the slope of the linear regression between HR/SNA versus BP (Chapleau and Sabharwal, 2011, Parati et al., 2000, Smyth et al., 1969). Bolus injection of PE selectively interrogates the vagal efferent limb of the baroreflex due to the rapidity of the reflex response (Abdel-Rahman, 1999, Chapleau and Sabharwal, 2011). This notion is supported by studies showing elimination of changes in HR following muscarinic receptor blockade, reaffirming that the response is primarily mediated by parasympathetic modulation (Coleman, 1980). However, this selectivity is lost with the infusion protocol, as inhibition of SNA may contribute to the reflex decrease in HR (Head and McCarty, 1987). Under such circumstances, β-adrenoceptor blockade is required to selectively interrogate the parasympathetic limb of the reflex (Chapleau and Sabharwal, 2011). Another potential factor that may confound estimation of BRS in response to PE is the magnitude of BP increase. This method may potentially underestimate BRS if BP increases beyond the linear range of the baroreflex function, or overestimate BRS if BP and cardiac afterload rise sufficiently to increase intracardiac pressures, with subsequent activation of cardiopulmonary vagal afferents (Dibner-Dunlap and Thames, 1989, DiBona and Sawin, 1994, Hunt and Farquhar, 2005). Baroreflex response to SNP, which is characterised by a compensatory tachycardia and sympathoexcitation in response to BP fall, is more difficult to interpret, rendering estimation of BRS rather challenging (Zygmunt and Stanczyk, 2010). However, combined peak changes in HR or SNA in response to PE and SNP enable the construction of a sigmoidal baroreflex function curve, and therefore the calculations of

threshold, midpoint and saturation pressures, maximum slope (gain) and the range of the HR/SNA versus BP relationship (Head and McCarty, 1987, Hunt and Farquhar, 2005, Kent et al., 1972, Wallin and Sundlof, 1979).

2) *Electrical stimulation of the baroreceptor afferents:* Direct electrical activation of the baroreceptor afferent fibres projecting from the carotid sinus or aortic arch enables defined control of the afferent input into the CNS, and therefore assessment of the central component of the baroreflex arc (de Paula et al., 1999, Ma et al., 2002). This technique bypasses BP-mediated activation of the mechanoreceptors in the carotid sinus and aortic arch, and avoids distortion of the sensory nerve endings within the viscoelastic element of the arterial wall (Chapleau and Sabharwal, 2011, DiBona and Jones, 2003b). A major additional advantage of this method is that it enables variation of the stimulus frequency and/or intensity, which allows for selective activation of myelinated A-fibre and unmyelinated C-fibre afferents, and investigation of differential baroreflex responses triggered by those fibres. Essentially, low voltage (<5V) or high frequency (>10Hz) stimulation selectively activates A-fibre type, while high voltage (20V) or low frequency (<10Hz) stimulation predominantly activates C-fibre type (Fan and Andresen, 1998, Fan et al., 1999). This method, however, does not reproduce the natural recruitment pattern of afferent fibres with different pressure thresholds that occurs with the spontaneous increases in BP (Chapleau and Sabharwal, 2011). An additional limitation is the presence of chemoreceptor afferents in the carotid sinus nerve (and the ADN in some species); however, the negligible number of chemoreceptor fibers within the ADN of species such as rabbits, rats, and mice (Easton and Howe, 1983, Sapru et al., 1981, Sapru and Krieger, 1977), overcomes this limitation and encourages the use of this preparation to selectively study baroreflex function in these species. Electrical stimulation of baroreceptor afferent fibre is most commonly carried out in anaesthetised animals (Gu et al., 2009, Huber and Schreihofer, 2010, Ma et al., 2002). However, there are reports demonstrating conscious stimulation of the ADN (Salgado et al., 2007) or carotid sinus nerve (Lohmeier et al., 2007, Lohmeier et al., 2010). Carotid baroreceptor stimulation has been shown to produce a sustained reduction in SNA and BP in humans (Heusser et al., 2010, Scheffers et al., 2010), with a number of controlled clinical trials have been undertaken to approve widespread use of this novel tool to treat patients with resistant hypertension (Doumas et al., 2014, Menne et al., 2013). This promising approach will therefore provide new insights into baroreflex mechanisms in humans.

3) *Isolated carotid sinus preparation (Moisejeff preparation):* In this method, the carotid sinus is isolated functionally from the circulation, which allows for more control of the stimulus applied to the baroreceptors (i.e., mean pressure, rate of change in pressure, frequency, amplitude, and shape of pulsatile waveforms). This technique is reserved for experimental animals and has been performed in both conscious and anaesthetised preparations (Chapleau et al., 1989, Melcher and Donald, 1981, Pickering et al., 2008).

Non-invasive methods:

1) *Spontaneous BRS testing:* Advances in beat-to-beat BP and HR monitoring methods have now made it possible to quantify BRS non-invasively in humans and animals using only autogenic changes in BP. This method only evaluates BRS under resting conditions however, and provides no information about modulation of BP in response to baroreceptor activation (Zygmunt and Stanczyk, 2010). Two techniques that provide comparable estimates of BRS have been described; namely, the sequence method and α-index. The sequence method assumes that spontaneous fluctuations in BP are opposed by baroreflex-mediated changes in HR, using an algorithm that seeks out patterns of three consecutive lengthening or shortening pulse intervals associated with an increase or decrease in BP, with BRS then derived from the linear regression of the relationship between BP and pulse interval across these fragments (Hildreth et al., 2013a, Parati et al., 2000). Baroreflex sensitivity calculated by this method has been found to correlate very closely with that calculated using the Oxford method (Stauss et al., 2006, Watkins et al., 1996). The ratio of the number of baroreflex sequences to the total number of linear SBP sequence provides a measure of the extent of engagement of the reflex and is referred to as the baroreflex effectiveness index (BEI) (Di Rienzo et al., 2001). The α-index method, on the other hand, provides a BRS estimate based on spectral analysis of HR and BP. With this method, BRS is assessed by analysing changes in the pulse interval associated with rhythmic BP oscillations over a range of frequencies reported to reflect baroreflex function (Hildreth et al., 2013a, Parati et al., 2000). Baroreflex sensitivity calculated using αLF and αHF estimates correlate with that derived using the Oxford and the sequence methods (Laude et al., 2004).
2) *Other clinical tests:* In clinical settings, most of the tests assessing baroreflex function are based on the evaluation of cardiovascular responses triggered by performing specific provocative manoeuvres. Table 1.1 provides details on some of the tests used to assess baroreflex mechanisms in humans. Blood pressure increases evoked by stimuli, such as the Valsalva manoeuvre, orthostatic testing, isometric exercise, or neck suction, activate predominantly sympathetic outflow. Changes in HR during Valsalva manoeuvre, orthostatic testing, or neck suction, on the other hand, reflect mainly parasympathetic modulation. It is important to note that the specificity of these tests to a particular reflex pathway cannot be confirmed, because there are reports suggesting the engagement of other autonomic reflexes (Zygmunt and Stanczyk, 2010).

1.5.2.2 Cardiopulmonary reflexes involving activation of vagal afferents

Various methods testing the chemosensory and mechanosensory components of the cardiopulmonary reflex have been established, including:

1) *Assessment of the chemosensitive reflex (BZJ reflex):* In laboratory animals, this reflex is most commonly assessed by measuring cardiovascular responses to i.v., or preferably, intracoronary

injection of a range of chemicals such as veratridine, prostacyclin, reactive oxygen species, serotonin, capsaicin or the serotonin 5-HT_3 receptor agonist phenylbiguanide (Aviado and Guevara Aviado, 2001, Chapleau and Sabharwal, 2011, Huber and Schreihofer, 2010, Kaufman et al., 1980, Ma et al., 1999). Injection of these chemicals into the pulmonary circulation, which evokes a comparable autonomic response, has also been used to evaluate pulmonary chemoreflex function (Chapleau and Sabharwal, 2011).

2) *Assessment of the mechanosensitive reflex:* Clinically, prolonged upright tilt or upright tilt combined with lower body negative pressure, which triggers the mechanosensitive component of the cardiopulmonary reflex, is used to assess orthostatic tolerance (vasovagal event) (Table 1.1) (Cooper and Hainsworth, 2008). Manoeuvres that manipulate the central venous pressure are also used in clinical practice to assess cardiopulmonary reflex function. Here, changes in HR, SNA, BP or vascular resistance are monitored while cardiopulmonary receptors are activated via passive leg raising, and deactivated through application of nonhypotensive lower body negative pressure (Grassi et al., 1988). In experimental animals, extracellular fluid volume expansion induced by saline, dextran, albumin or polygeline solution is used to evoke stimulation of the mechanosensitive cardiopulmonary reflex and assess autonomic response output (Ferrari et al., 1984, Hinojosa-Laborde et al., 1994, Neahring et al., 1995, Ramchandra et al., 2006). Invasive inflation of small balloons at the junctions of the pulmonary veins and left atrium is also used in experimental animals to selectively stimulate the mechanosensitive component of the cardiopulmonary reflex (Dibner-Dunlap and Thames, 1992).
3) *Electrical stimulation of the vagal afferents:* Like stimulation of the baroreceptor afferents, direct electrical stimulation of the vagal afferent allows for selective activation of the myelinated A-fibre or unmyelinated C-fibre of the vagal afferents and the assessment of central processing of the vagal afferent input. The advantage of this approach is that it eliminates the confounding effects related to peripheral stimulation of the chemosensitive and mechanosensitive cardiopulmonary receptors (Merrill et al., 1999, Neahring et al., 1995).

1.5.2.3 Chemoreceptor reflex

Factors such as hypoxia, hypercapnia, and/or acidosis can trigger the activation of the chemoreceptor reflex and consequently upregulate sympathetic and cardiovagal outflows. Various methods have been developed to assess these responses in human and/or laboratory animals, including:

1) *Alterations of inspired gas composition:* Chemoreceptor reflex sensitivity can be assessed in humans and animals by measuring ventilatory and cardiovascular responses to a controlled reduction in the inspired oxygen concentration. Alterations in the inspired gas composition can differentially affect peripheral versus central chemoreceptors. The peripheral chemoreceptor reflex is often triggered by dropping the concentration of inhaled oxygen to 10–15% (isocapnic

hypoxia) (Huang et al., 2009, Steinback et al., 2009, Trombetta et al., 2013). This translates to a reduction of ~35–40 mmHg (normal 80–100 mmHg) in the PO_2, which causes near maximum activation of arterial chemoreceptors (Chapleau and Sabharwal, 2011, Steinback et al., 2009). A few seconds of exposure to 100% nitrogen can also be used to stimulate the peripheral chemoreflex (Makeham et al., 2005). Central chemoreflex activation, on the other hand, is achieved by increasing carbon dioxide (CO_2) in the inspired gas to 3.5–10% (hypercapnia) (Huang et al., 2009, Miyamoto et al., 2004, Sabino et al., 2013, Trombetta et al., 2013). Alternatively, the contribution of tonic chemoreceptor activity to ventilation, BP, and HR can be evaluated using inhalation of 100% oxygen to inhibit chemoreceptor activity (Hering et al., 2007, Meyer et al., 2009, Rassaf et al., 2012, Rassaf et al., 2010). Responses to chemoreflex stimulation can be mitigated by compensatory hyperventilation, rendering the ability to achieve peak cardiovascular response less attainable. This issue can be overcome in the anaesthetised preparation, whereby mechanical ventilation after the administration of neuromuscular blocking agents enables responses to hypoxia to be quantified in the absence of hyperventilation (Chapleau and Sabharwal, 2011).

2) *Chemical-induced activation:* This is a frequently used method in animal studies to stimulate the chemoreceptor reflex, which is reserved for anaesthetised or conscious animals. Here, cardiovascular responses to a bolus injection of cyanide administered intravenously or into the common carotid artery proximal to the carotid chemoreceptors are recorded (Barros et al., 2002, Braga et al., 2008). Despite its powerful chemoreceptor stimulant properties, cyanide can evoke peripheral vasodilation which has the potential to confound the interpretation of the reflex haemodynamic responses to chemoreceptor activation. Vagally mediated bradycardia, however, occurs very rapidly, thereby enabling its measurement before the delayed depressor responses to cyanide (Chapleau and Sabharwal, 2011).
3) *Isolated carotid sinus preparation:* As with the carotid sinus baroreceptors, chemoreceptors within the carotid sinus can be activated by perfusing the isolated carotid sinus region with hypoxic blood, buffer, or cyanide. The preparation is again limited to laboratory animals in which the confounding effects of systemic hypoxemia, peripheral vascular resistance, cardiac function, and the CNS can be avoided by stripping all visible neural connections among the carotid sinus, the superior cervical, and nodose ganglia (Franchini and Krieger, 1992, Li et al., 2006).

1.5.2.4 Other tests used to assess autonomic functions in clinic

Table 1.1 provides additional tests that are used in the clinic to assess sympathetic and parasympathetic functions triggered by some other reflex pathways.

Table 1.1: A selection of autonomic function tests commonly used in clinical practice to assess both sympathetic and parasympathetic activities

Test	Definition	Major reflex pathway engaged	Comments	References
Valsalva manoeuvre	Refers to voluntary forced expiration of a subject against a resistance (e.g., closed glottis or elevated airway pressure) for sustained period of time followed by resumption of breathing while recording HR and BP.	Baroreflex	This test can be used to assess both sympathetic and parasympathetic functions. Four phases of the response to the manoeuvre have been described with the baroreflex being engaged during phase 2 when BP decreases and HR increases, and phase 4 when BP rises and HR falls. Valsalva manoeuvre is thought to not only activate the baroreflex arc but also the cardiopulmonary reflex pathway.	(Chapleau and Sabharwal, 2011, Heidbreder et al., 1985, Mathias, 2003, Parati et al., 2000, Sahin et al., 2006, Zygmunt and Stanczyk, 2010)
Orthostatic test	Refers to measurements of haemodynamic responses to active standing. The subject is rested in a supine position.	Baroreflex	This test can be used to assess both sympathetic and parasympathetic functions. Evaluation of changes in HR is performed during the initial phase of adaptation to orthostasis (first 45 seconds). Fluctuations of BP are assessed based on somewhat later responses to standing (first 4 minutes)	(Sahin et al., 2006, Zygmunt and Stanczyk, 2010)
Neck suction	Refers to the application of external negative and positive pressures to the cervical region while recording HR and BP.	Baroreflex	This test can be used to assess both sympathetic and parasympathetic functions. A mouldable lead collar is used to evoke carotid sinus baroreflexes by changing the transmural pressure across the carotid sinus wall. In contrast to pharmacological activation of the baroreflex, neck suction determines not only HR responses to baroreceptor stimulation but also BP responses. A modification of this method is a carotid sinus massage with assessment of the subject's response to direct, mechanical activation of baroreceptors.	(Chapleau and Sabharwal, 2011, Kim et al., 2011, Parati et al., 2000, Zygmunt and Stanczyk, 2010)
Head-up tilt test	Evaluates adaptation to orthostasis and subsequent changes in haemodynamic parameters after passive tilting on a special motorized table.	Cardiopulmonary reflex (BZJ reflex)	This test can be used to assess both sympathetic and parasympathetic functions. A provocative tilt test is performed on an automated tilt test table, which allows a consistent slow tilt to 60–80 degrees. HR and BP recordings are obtained prior to the test and during 30–45 minutes of tilting. Prolonged upright tilt or upright tilt combined with lower body negative pressure can evoke vasovagal response.	(Cooper and Hainsworth, 2008, Di Leo et al., 2005, Mallat et al., 1997, Schroeder et al., 2004, Zygmunt and Stanczyk, 2010)

Isometric handgrip test	Refers to measurement of BP rise during isometric pressing of a handgrip dynamometer.	Unclear. Interaction between baroreflex and cardiopulmonary reflex has been reported.	This test is mainly used to assess sympathetic functions. The test is performed at approximately one third of the maximum contraction strength for 3–5 minutes. BP measurements are taken at the other arm at 1 minute interval. The test result is presented as the difference between the highest diastolic pressure during the examination and the average diastolic pressure at rest. The difference should normally be greater than 15 mmHg.	(Mathias, 2003, Sahin et al., 2006, Sanders et al., 1989, Wallin et al., 1992)
Passive leg raising	Records haemodynamic responses to leg raising at an angle with the application of lower body negative pressure.	Cardiopulmonary reflex	The reflex is activated by passive elevation of the legs and the lower pelvis of the supine subject to 60 degrees. Reflex deactivation is achieved through the application of lower body negative pressure, where the supine subject's legs and lower abdomen were enclosed in a Plexiglas box that is sealed at the level of the anterosuperior iliac crests.	(Grassi et al., 1988)
Deep breathing test	Measures HR responses to deep breathing.	Cardiopulmonary Reflex (Bainbridge reflex)	This test is mainly used to assess parasympathetic functions. The test is based on the phenomenon of respiratory arrhythmia, which is most pronounced at the respiration rate of 6 breaths per minute. The subject is asked to breathe at this rate (with 5 seconds of inhalation and 5 seconds of exhalation per breath).	(Cashion et al., 2000, Sahin et al., 2006, Vita et al., 1999, Zygmunt and Stanczyk, 2010)
Cold pressor test	Evaluates BP and/or SNA responses to immersion of hands or feet in cold water.	Somatosensory-sympathetic reflex pathway	This test is mainly used to assess sympathetic functions. The test involves immersion of hands or feet for about 60–120 seconds in cold water (4°C). The test evokes activation of the afferent pain and temperature fibres from the skin as well as emotional arousal, leading to sympathetic activation and increase in BP and HR.	(Mathias, 2003, Narkiewicz et al., 1998)
Mental arithmetic test	Refers to performing serial subtraction while recording BP.	Stress pathways	This test is mainly used to assess sympathetic functions. This test is based on performing serial subtraction (usually 100 minus 7 or 1000 minus 13) which aims at activating sympathetic outflow.	(Hjemdahl et al., 1989, Wallin et al., 1992, Zhang and Thoren, 1998, Zygmunt and Stanczyk, 2010)

Diving reflex	Evaluates HR responses to immersion of the face in cold water.	Trigeminocardiac reflex*	This test is mainly used to assess parasympathetic functions. The test involves immersion of the face in water (~ 30–40 seconds) while breath holding. Regardless of water temperature, bradycardia is observed. Cold face test is a slight modification where a cold compress (1–2°C) is applied to the subject's face for a period of 1–3 minutes. It has similar sensitivity in evaluating parasympathetic response. Activation of chemoreceptor afferents are thought to be involved too. This test can be performed in experimental animals too, by either local stimulation of the nerve or submerging the animal in water.	(Chapleau and Sabharwal, 2011, Khurana and Wu, 2006, McCulloch et al., 2010, Saino et al., 2000, Saino et al., 1997)

BP, blood pressure and HR, heart rate.

Trigeminocardiac reflex*: activation of the sensory nerve endings of the trigeminal nerve send neuronal signals to the sensory nucleus of the trigeminal nerve, forming the afferent pathway of the reflex arc. This afferent pathway later connects with the efferent pathway in the motor nucleus of the vagus nerve (Schaller, 2004).

1.6 Chronic kidney disease

Chronic kidney disease (CKD) refers to an irreversible deterioration in renal function which classically develops over a period of years (Table 1.2) (National Kidney Foundation, 2013). Chronic kidney disease represents a significant medical problem globally, affecting 5–7% of the world population (Couser et al., 2011) and with the number of clinical cases eventuating in end-stage renal disease (ESRD) growing at an alarming rate of 3% annually (Collins et al., 2009). Mortality in patients with ESRD remains up to 14% higher than that in the general population (ANZDATA Registry, 2012) and in most cases is related to cardiovascular complications rather than actual renal shutdown (U.S. renal data system, 2013). This has therefore shifted the focus in the recent year to optimising the care of patients during the phase of CKD, before the onset of ESRD (National Kidney Foundation, 2013).

Table 1.2: Stages of chronic kidney disease (CKD). Adapted from (National Kidney Foundation, 2013)

Stage	Description	GFR (ml/min/1.73 m^2)	Action
1	Kidney damage with normal or high GFR	≥90	Investigate, e.g., haematuria and proteinuria
2	Kidney damage with slightly low GFR	60–89	Renoprotection, e.g., BP control and dietary modification
3	Moderately low GFR	30–59	
4	Severe low GFR	15–29	Prepare for renal replacement therapy
5	Kidney failure	<15 or dialysis	

GFR, glomerular filtration rate. Chronic kidney disease is defined as either kidney damage or GFR <60 ml/min/1.73 m^2 for ≥3 months. Kidney damage is defined as pathologic abnormalities or marker of damage, including abnormalities in blood or urine tests or imaging studies.

1.6.1 Aetiology

Chronic kidney disease can be caused by a variety of aetiologies that destroy the normal structure and function of the kidney, including genetic and environmental factors, autoimmune and infectious diseases, diet or medications (Table 1.3).

Variations in the disease expression are related partly to the main underlying cause, pathology, severity, and rate of disease progression. However, despite different aetiologies and diverse primary outcomes, the endpoint is eventually the same – CKD/ESRD (Levey and Coresh, 2012, National Kidney Foundation, 2013, Yang et al., 2010a).

Table 1.3: Common causes of chronic kidney disease (CKD) (Goddard and Turner, 2014, ANZDATA Registry, 2012, National Kidney Foundation, 2013)

Disease	Proportion of ESRD	Comments
Congenital and inherited	3–6%	e.g., Polycystic kidney disease (PKD)
Renal artery stenosis	5%	
Hypertension	5–25%	
Glomerular disease	10–24%	e.g., Autoimmune diseases. IgA nephropathy is the most common
Interstitial disease	5–15%	
Systemic inflammatory disease	5%	e.g., vasculitis and systemic lupus erythematosus (SLE)
Diabetes mellitus	20–40%	
Unknown	5–20%	

1.6.2 Assessment of chronic kidney disease

Renal excretory functions can be assessed by measuring plasma or serum levels of compounds excreted by the kidney, commonly the products of protein catabolism (creatinine and urea) (Goddard and Turner, 2014). Blood urea is a poor guide to renal excretory functions as it varies with protein intake, liver metabolic capacity and renal perfusion (Goddard and Turner, 2014). Serum creatinine appears to be a more reliable measure as it is produced from muscle at a constant rate and is almost completely filtered at the glomerulus. In the presence of constant muscle mass, changes in creatinine concentration reflect changes in the glomerular filtration rate (GFR) (Goddard and Turner, 2014). However, Kidney Disease Outcomes Quality Initiative (KDOQI) guidelines for CKD evaluation do not recommend reporting serum creatinine concentration alone when assessing the level of kidney function, as this may give a misleading impression of renal function if muscle mass is unusually small or large (Goddard and Turner, 2014, National Kidney Foundation, 2013). Instead, serum creatinine measure must be combined with estimates of GFR, which is regarded as the best index of kidney functioning (National Kidney Foundation, 2013, Parmar, 2002). Using urinary creatinine measurements to derive creatinine clearance provide a reasonable approximation of GFR. In clinical practice, however, more accurate measurements can now be undertaken using chromium (^{51}Cr)-labelled ethylenediamine tetraacetic acid (EDTA) or inulin (Goddard and Turner, 2014, National Kidney Foundation, 2013). Urine sediment examination or dipstick for red blood cells, white blood cells, fat and granular casts and epithelial cells are also recommended for patients with CKD or high risk individuals to investigate intrinsic renal disease (Goddard and Turner, 2014, Levey and Coresh, 2012).

Proteinuria, which refers to persistently increased protein excretion with reference most commonly to total protein usually in the urine, is another reliable marker of kidney damage (Levey and Coresh, 2012, National Kidney Foundation, 2013) and a known risk factor for CVD in CKD individuals (Iseki, 2008). It is also regarded as an important predictor of ESRD (Iseki et al., 1996). The excretion of specific types of protein in the urine, such as albumin (albuminuria or microalbuminuria when albumin excretion is above the normal range but below the level of detection by tests for total protein) or low molecular weight globulins, depends mainly upon the type of kidney disease present. Albuminuria is a sensitive marker for CKD due to diabetes, glomerular disease, and hypertension (National Kidney Foundation, 2013). Increased excretion of low molecular weight globulins is a sensitive marker for some tubulointerstitial diseases (National Kidney Foundation, 2013). A 24-hour urine collection has long been considered the "gold standard" for quantitative measurements of proteinuria, accounting for the issue that hourly protein excretion rates vary during different times during the day (National Kidney Foundation, 2013). An alternative method for quantitative evaluation of proteinuria, which is gradually replacing the old 24-hour urinary protein analysis, is measurement of the ratio of protein or albumin to creatinine in an untimed urine specimen. These ratios correct for variations in urinary concentration due to hydration and provide a more convenient method of assessing protein and albumin excretion than that involved with timed urine collections (Levey and Coresh, 2012, National Kidney Foundation, 2013).

Other investigations of renal disease include assessment of tubular excretory functions by measuring the kidney ability to excrete water or acid load, or by comparing blood and urine ratios of electrolytes to creatinine (e.g., fractional sodium excretion) (Goddard and Turner, 2014); or the use of various imaging techniques that enable visualisation of the kidney, such as X-ray, ultrasound, computed tomography (CT), magnetic resonance imaging (MRI), or radionuclide studies to diagnose a range of kidney abnormalities (Goddard and Turner, 2014).

1.6.3 Cardiovascular disease in chronic kidney disease

Cardiovascular disease is prevalent in patients with CKD and ESRD, with a range of traditional cardiovascular risk factors including hypertension, hyperlipidaemia, diabetes, obesity, old age, male sex and uraemia-specific risk factors (anaemia, volume overload, hyperphosphataemia and hyperparathyroidism) most commonly underlying the development and progression of renal disease (Hildreth, 2011, National Kidney Foundation, 2013, Parmar, 2002, Schiffrin et al., 2007). Cardiovascular disease in CKD/ESRD occurs due to functional and structural adaptive modifications to chronically elevated BP triggered by factors such as increased sympathetic vasomotor tone, altered autonomic control of HR, activation of RAAS, enhanced production of reactive oxygen species, endothelial dysfunction, atherosclerosis, arteriosclerosis and vascular calcification (Klein et al., 2003b, Locatelli et al., 2003, Neumann et al., 2007, Passauer et al., 2005, Schiffrin et al., 2007).

Vascular injury and resultant vasculopathies can in turn contribute to the increased prevalence of coronary artery disease, heart failure, stroke, and peripheral vascular disease in this patient population (Schiffrin et al., 2007). Consequently, subjects with CKD are exposed to increased morbidity and mortality as a result of cardiovascular events (Table 1.4) and, indeed, sudden cardiac death is a major cause of cardiac mortality in ESRD patients, with the incidence increasing with the stage of renal failure (Herzog, 2003, U.S. renal data system, 2013). Therefore, prevention and treatment of CVD are critical considerations in the management of individuals with CKD.

Table 1.4: Cardiovascular (CV) risk according to stages of chronic kidney disease (CKD). Adapted from Schiffrin *et al.* (2007)

Stage	CV Risk (Odds Ratio, Univariate)
1	Depending on degree of proteinuria
2	1.5
3	2–4
4	4–10
5	10–50
ESRD	20–1000

The increase in risk in comparison with people free of CKD depends on the age of the population studied: The younger the person, the higher the relative risk. Microalbuminuria increases the CV risk by 2–4 folds.

1.6.4 Chronic kidney disease and hypertension

There is a strong relationship between CKD and hypertension, with renal insufficiency contributing to half of the cases of all forms of secondary hypertension (Kaplan, 2006, Morgado and Neves, 2012). Although kidney disease can cause hypertension, hypertension in its own right is also a key driver of ESRD, contributing to the disease itself or, most commonly, underlying the progressive decline in GFR and hence renal function (Morgado and Neves, 2012, National Kidney Foundation, 2013, Parmar, 2002, Young et al., 2002). Hypertension is almost invariably encountered in patients with CKD, with 80% of the cases beginning renal replacement therapy presenting with elevated BP (Ridao et al., 2001, Schiffrin et al., 2007). High BP in CKD plays a powerful role in the greater cardiovascular morbidity and mortality seen in this particular population, predisposing affected individuals to cardiac arrhythmias, myocardial damage, coronary ischaemia and eventually left ventricular hypertrophy (LVH) (Locatelli et al., 2001, Morgado and Neves, 2012, Shamseddin and Parfrey, 2011).

The pathogenesis of hypertension in CKD is very complex and multifactorial, with patients suffering from vascular disease, diabetes and polycystic kidney disease (PKD) being more prone to developing hypertension (Morgado and Neves, 2012, Ridao et al., 2001). Besides the classical factors that promote BP increase in CKD, including sodium retention, intravascular hypervolemia and excessive RAAS activity (Guyton and Coleman, 1999, Kashihara and Satoh, 2008, Klein et al., 2003b), there are newly recognized key players such as SNS hyperactivity (Klein et al., 2001, Masuo et al., 2010, Neumann et al., 2007, Schlaich et al., 2007, Schlaich et al., 2009b), autonomic imbalance (Klein et al., 2003a, Lugon et al., 2003, Robinson and Carr, 2002), endothelial

dysfunction and vascular remodelling (Foley et al., 1996, Locatelli et al., 2003, Passauer et al., 2005).

1.6.5 Altered autonomic control of cardiovascular function in chronic kidney disease

Autonomic neuroregulation of cardiovascular function, which controls periodic fluctuations in HR and BP, is dependent upon a balance between sympathetic and parasympathetic (vagal) activity to the heart and vasculature (Li, 2011, Pal et al., 2013). During CKD, a state of functional disharmony between sympathetic and vagal components of the ANS, with altered tonic and reflex control of autonomic outflows, is observed, contributing to autonomic dysfunction (Cashion et al., 2000, Di Leo et al., 2005, Dursun et al., 2004, Lugon et al., 2003, Robinson and Carr, 2002, Rubinger et al., 2009). Cardiovascular autonomic dysfunction is a serious yet poorly understood long-term complication in CKD, and, in most cases, is associated with SNS hyperactivity and a blunted parasympathetic nervous system (Hildreth, 2011, Phillips, 2012), further aiding the deleterious impact of sympathetic activation. Nevertheless, reports have also shown that vagal withdrawal could also be the principal mechanism in initiating sympathovagal imbalance (Pal et al., 2013). Empirically, sympathovagal imbalance has been recognised as a major mechanism underlying many cardiovascular morbidities and comorbidities in general (Thayer et al., 2010), and could possibly be the final common pathway of sudden cardiac death in CKD in particular (Dursun et al., 2004, Ranpuria et al., 2008, Shamseddin and Parfrey, 2011).

Sympathetic nervous system overactivity is implicated in the development and progression of renal disease (Campese and Krol, 2002, Converse et al., 1992, Koomans et al., 2004, Rump et al., 2000) and has been recognised as an important mechanism contributing to the poor prognosis in CKD patients and consequent cardiovascular morbidity and mortality (Collins, 2003, Collins et al., 2001, Schlaich et al., 2009b). Various clinical studies have demonstrated increased concentrations of plasma NA in CKD patients and suggested this measure as not only a first indicator of increased SNS activity in those patients, but also a powerful predictor of both survival and incidents of cardiovascular complications (Masuo et al., 2010, Masuo et al., 1995, Schohn et al., 1985, Zoccali et al., 2002). These observations were further substantiated by evidence from human studies showing enhanced depressor responses to central sympathoinhibition by clonidine (Levitan et al., 1984) or debrisoquine (Schohn et al., 1985), and a pronounced hypotensive effect in response to ganglionic blockade in animal models of CKD (Haywood et al., 1984, Phillips et al., 2007). In addition to elevated catecholamine levels, directed measurements of SNA, as assessed clinically using microneurography to record muscle SNA are also elevated (Grassi et al., 2011a, Klein et al., 2003b, Ligtenberg et al., 1999, Neumann et al., 2007, Tinucci et al., 2001) and increased levels are independent of resting BP (Masuo et al., 2010) or circulating uraemia-related toxins (Bruno et al., 2012, Schlaich et al., 2009b). Further evidence of altered sympathetic activity in CKD patients has come from reports showing abnormal BP responses to standing up or handgrip exercise (Sahin et al.,

2006), and augmented LF oscillations of SBPV, which is suggestive of increased sympathetic vasomotor tone (Lewanski and Chrzanowski, 2003). Similarly, upregulated adrenergic control of cardiac function has also been documented in CKD, with evidence of enhanced bradycardic responses to β-adrenergic receptor blockade (Badve et al., 2011, Furgeson and Chonchol, 2008).

Sympathetic hyperactivity has considerable adverse consequences on both renal and cardiovascular systems, and can further aggravate hypertension and proteinuria in CKD individuals. Indeed, in stage 2–4 CKD patients (Fig. 1.8), Grassi et al. demonstrated a strong negative association between increased muscle SNA and decline in GFR and a significant positive correlation between high muscle SNA and proteinuria (Grassi et al., 2011b). Interstitial fibrosis, glomerulosclerosis (Adamczak et al., 2002), accelerated atherosclerosis, vasoconstriction, and proliferation of smooth muscle cells and adventitial fibroblasts in the vessel wall are further deleterious consequences of sympathetic overactivity related to progression of renal damage (Erami et al., 2002, Zhang and Faber, 2001).

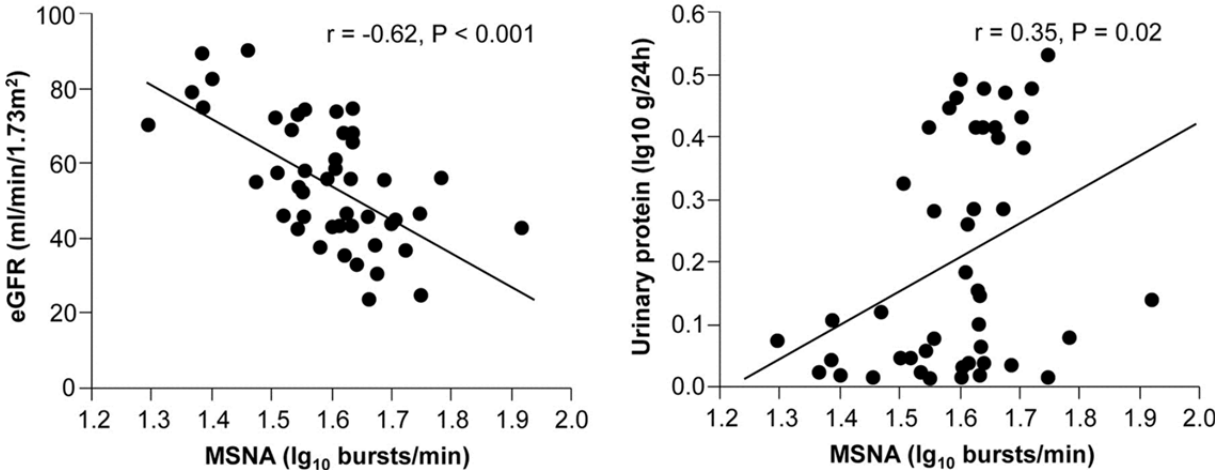

Figure 1.8: Relationships between muscle sympathetic nerve activity (MSNA) and estimated glomerular filtration rate (eGFR) or proteinuria in 48 stage 2–4 chronic kidney disease (CKD) patients. The data are Pearson product moment correlation coefficient (r) and P values. Because proteinuria allows 0 values, 1 was added to each patient's value before log transformation. Taken from (Grassi et al., 2011b).

Noradrenaline released by the sympathetic nerve endings can 1) directly induce proliferation of smooth muscle cell and adventitial fibroblasts in the vascular wall and exert a trophic influence upon cardiac myocytes (Erami et al., 2002, Zhang and Faber, 2001), or 2) indirectly evoke cardiac and vessel wall remodelling (Raizada et al., 2012) via activating RAAS pathway and Ang II formation (Grisk and Rettig, 2004, Johansson et al., 1999). Studies have also demonstrated that cardiac sympathetic activity is related to LVH in patients with primary (Schlaich et al., 2003) or CKD-mediated hypertension (Guizar-Mendoza et al., 2006).

Besides increased sympathetic control of the heart in CKD individuals, cardiac vagal tone, by contrast, is reduced, as evaluated by decreased measures of vagal tachycardic reserve in response to the nonspecific muscarinic receptor antagonist, atropine (Mircoli et al., 2003), reduced HF oscillations of HRV (Lerma et al., 2004, Tory et al., 2004), and low HR scores to

forceful exhalation against a closed airway (valsalva manoeuvre), deep breathing and standing up (Agarwal et al., 1991, Sahin et al., 2006). Vagal withdrawal, alongside sympathetic activation, is closely linked to cardiac arrhythmias (de Ferrari et al., 1991, Facchini et al., 1991) and, at least partly, is responsible for the higher incidence rate of sudden cardiac death in CKD patients (Herzog, 2003, Herzog et al., 1998).

1.6.5.1 Possible mechanisms contributing to autonomic imbalance in chronic kidney disease

The contribution of autonomic neural mechanisms to the development of hypertension and CVD in CKD are well established; however, the exact mechanisms contributing to altered sympathetic and parasympathetic tone in patients with CKD remain unclear. Here, a number of not mutually exclusive or thoroughly characterised mechanisms can be advanced (Fig. 1.9):

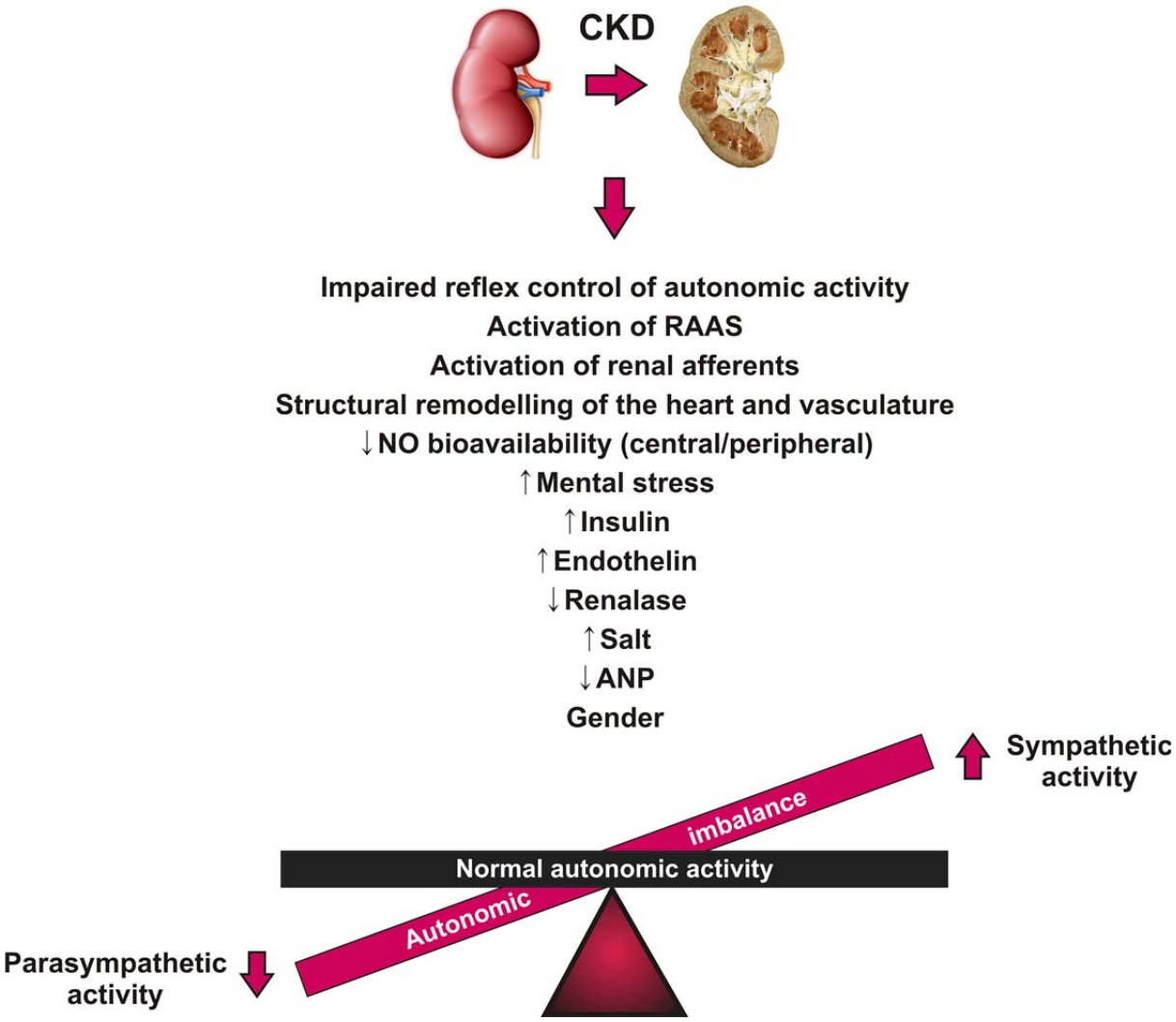

Figure 1.9: Diagram illustrating possible mechanisms contributing to cardiovascular autonomic dysfunction in chronic kidney disease (CKD). RAAS, renin-angiotensin aldosterone system; NO, nitric oxide; and ANP, atrial natriuretic peptide.

1.6.5.1a Altered reflex control mechanisms of autonomic outflows in chronic kidney disease

As reviewed earlier, a number of autonomic reflexes are involved in the modulation of sympathetic and parasympathetic outflows to the heart and vasculature to provide an effective fine-tuning of BP. Deficits in the regulatory influence, physiologically exerted by a range of cardiovascular reflexes, have been demonstrated in hypertension and CKD. However, in comparison to studies describing altered sympathetic and parasympathetic tones in CKD, little is known about reflex control of autonomic function in CKD and how this could ultimately impact sympathovagal imbalance. One major mechanism that has long been thought to underlie altered autonomic outflow and elevated BP in CKD is reduced functionality of the arterial baroreflex. In clinical practice, prognostic information regarding cardiovascular morbidity and mortality in CKD can be derived from measurements of: 1) cardiac BRS, an independent predictor of sudden cardiac death accompanying CKD (Johansson et al., 2007); and 2) BEI, a more recently established measure of the number of times baroreflex is active in controlling HR in response to BP fluctuations (Di Rienzo et al., 2001), that has been recognised as strong independent predictor of long-term survival in the CKD population (Johansson et al., 2005, Johansson et al., 2007). Indeed, HR BRS, either spontaneous (Johansson et al., 2007, Johnson and Shekhar, 2006, Lacy et al., 2006, Studinger et al., 2006) or evoked by pharmacological manipulation of BP (Agarwal et al., 1991, Studinger et al., 2006, Tinucci et al., 2001, Tomiyama et al., 1980), and BEI (Johansson et al., 2005, Johansson et al., 2007) are reduced in CKD, and, most importantly, deficits correlate with reductions in the GFR (Lacy et al., 2006), suggesting a direct association between deteriorations in renal function and altered cardiac baroreflex mechanism and usefulness of these markers in assessing cardiovascular risk in CKD.

In contrast to HR baroreflex, reports assessing sympathetic baroreflex function in CKD patients are still inadequate, perhaps due to a more technically challenging experimental setup as opposed to the ease with which HR is acquired. To date, only two human reports have assessed baroreflex control of SNA in CKD (Ligtenberg et al., 1999, Tinucci et al., 2001), the results from which were dissimilar. Ligtenberg and colleagues (1999) assessed baroreflex control of muscle SNA in 14 hypertensive CKD patients and 14 normotensive control subjects. Their results demonstrated a comparable sympathetic BRS in both groups, albeit a reset sympathetic baroreflex function to higher BP range in the CKD group. A similar experimental approach was used by Tinucci and others (2001) to measure muscle SNA baroreflex in 7 hypertensive CKD patients and 7 hypertensive controls with normal renal function. Their data, in contrast to Ligtenberg et al. (1999), and despite that individuals from both studies showed comparably low GFR, high serum creatinine levels and elevated plasma renin activity, revealed markedly blunted sympathetic BRS in CKD patients relative to hypertensive controls. These findings, with the added absence of data assessing SNA baroreflex in animal models of CKD, suggest the need for more studies to elucidate the role of altered sympathetic baroreflex control in mediating sympathetic overactivity in CKD.

Deficits in the reflex control of autonomic outflow in CKD may not be limited to defects in the regulatory pathways that operate the baroreceptor reflex only, but may also be due to other reflex mechanisms known to be impaired in CKD including the cardiopulmonary and chemoreceptor reflexes. Intact cardiopulmonary reflex control of autonomic outflow is required to maintain normal fluid volume regulation (Ferrari et al., 1984, Merrill et al., 1999). A few studies have illustrated deficits in the mechanosenstive (volume-dependent) cardiopulmonary reflex control of sympathetic but not parasympathetic activity in both CKD patients (Frank et al., 2004, Grassi et al., 1987) and animal models of nephrotic syndrome (Hinojosa-Laborde et al., 1994, Neahring et al., 1995). An inability to properly restrain SNA by cardiopulmonary reflexes, which has been suggested as a potential predisposing factor to salt and water retention, inappropriately high levels of systemic vascular resistance and reduced GFR (Neahring et al., 1995), may provide another mechanistic explanation to altered autonomic balance and maintenance of hypertension in CKD. Whether a similar deficit extends to the chemosensitive cardiopulmonary reflex (BZJ reflex) control of autonomic outflow remains undetermined; however, activation of this pathway has been proposed as the main mechanism underlying dialysis-induced hypotension in CKD patients, in which hypovolemia and consequent tissue hypoperfusion provokes adenosine release to activate the BZJ reflex (Daugirdas, 2001, Ligtenberg, 1999).

The chemoreceptor reflex plays a pivotal role in monitoring changes in arterial blood oxygen concentration, and chemosensation is also mechanistically linked to cardiorespiratory control by the ANS (Rassaf et al., 2010). Dysfunctional chemoreflex control of HR and SNA is also evident in CKD, suggesting impaired chemoreflex function as another principle contributor to autonomic imbalance in CKD. Supporting this notion, Rassaf and co-workers demonstrated depressed cardiac chemoreflex sensitivity in CKD/ESRD patients (Rassaf et al., 2012, Rassaf et al., 2010), indicative of altered autonomic control of HR in response to chemoreflex activation in renal disease. Recent evidence also suggested that tonic arterial chemoreceptor activation is involved in sympathetic overactivity of CKD, since deactivation of the arterial chemoreceptors by inhalation of 100% oxygen noticeably reduces muscle SNA (Fig. 1.10) in renal failure patients (Despas et al., 2009, Hering et al., 2007). Various mechanisms which impair the oxygen carrying capacity of blood and therefore sensitize the carotid bodies have been suggested with respect to chemoreceptor-induced activation of SNA including sleep apnea, metabolic acidosis (Kotanko, 2006) and anaemia associated with chronic renal failure (Schlaich et al., 2009b).

Despite that altered cardiovascular reflexes are thought to underlie sympthovagal imbalance in CKD, the exact cause by which these reflexes become impaired is unclear. Clearly, every site within the baroreceptor, cardiopulmonary and chemoreceptor reflex may be responsible for blunted reflex autonomic activity and altered sympathovagal balance in CKD. However, there is only a fragmentary experimental evidence to support this assumption owing to the inability of clinical cardiovascular autonomic function tests to differentiate the role of the afferent, central and efferent

components of individual reflex arcs. It is possible that deficits in the afferent arm of these reflexes and impaired sensory afferent traffic conveyed via the ADN, carotid sinus nerve and vagal afferent neurons to the brain may relate to: (1) altered mechanostimulation of baroreceptors within the carotid sinus and aortic arch due to arterial stiffening; (2) impaired responsiveness of the volume- and/or chemosensitive receptors located within the cardiac chambers due to altered cardiac structure and LVH; and/or (3) structural changes of arterial chemoreceptors located within the carotid and aortic bodies. Alternatively, abnormal central mechanisms [e.g., altered central processing of vagal afferent input of the cardiopulmonary reflex as shown in a nephrotic syndrome model of CKD (Dibona et al., 1997, Hinojosa-Laborde et al., 1994, Neahring et al., 1995)] may be responsible. This may be due to 1) deficits within key medullary regions common to these reflex pathways including NTS, CVLM, RVLM and nucleus ambiguus (see page 8); 2) altered neuronal activity of higher brain areas such as the paraventricular and hypothalamic supraoptic nuclei and their subsequent regulation of these medullary nuclei; or 3) an inability of the heart and vasculature to respond to autonomic inputs. A comprehensive investigation of overall reflex function in CKD is still lacking and more experiments are required to delineate the role of altered reflex function in skewing normal control of sympathetic and vagal outflows.

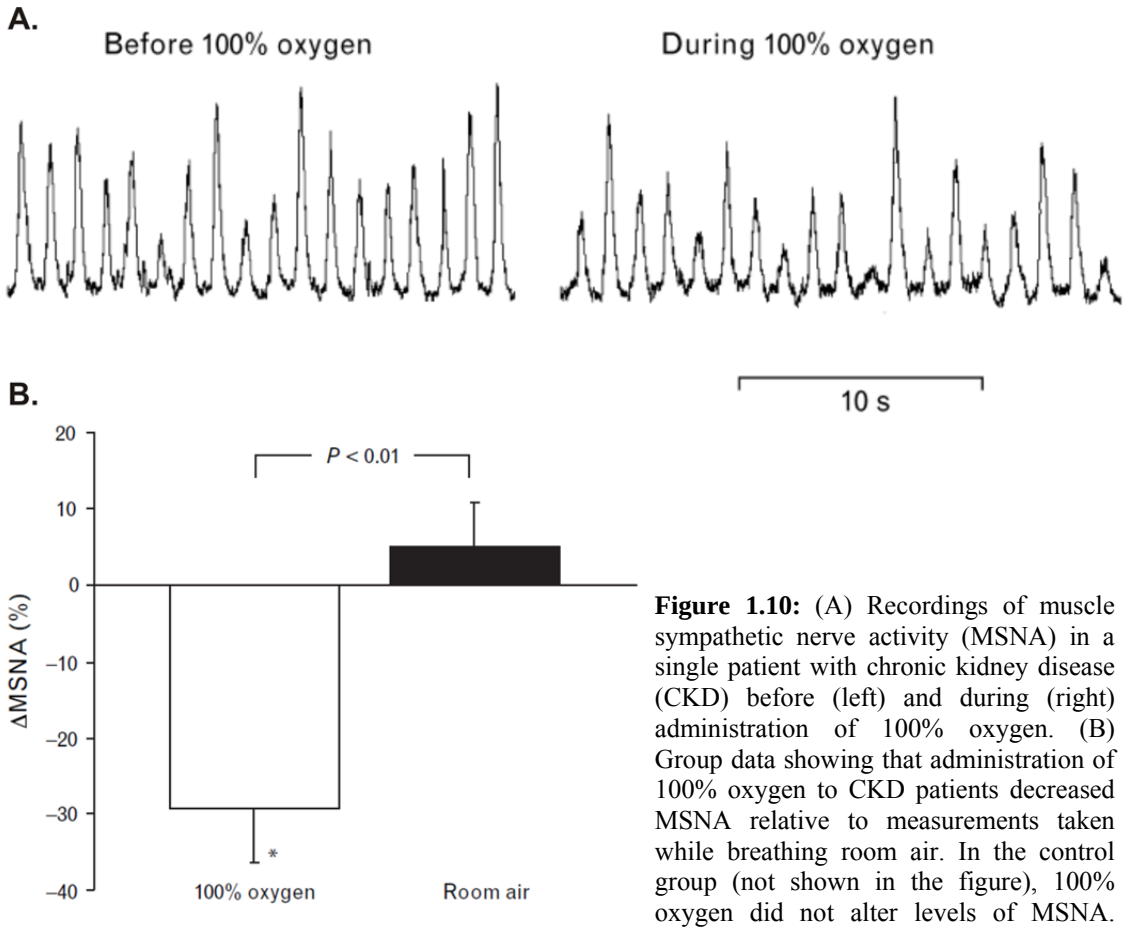

Figure 1.10: (A) Recordings of muscle sympathetic nerve activity (MSNA) in a single patient with chronic kidney disease (CKD) before (left) and during (right) administration of 100% oxygen. (B) Group data showing that administration of 100% oxygen to CKD patients decreased MSNA relative to measurements taken while breathing room air. In the control group (not shown in the figure), 100% oxygen did not alter levels of MSNA. Taken from (Hering et al., 2007).

1.6.5.1b Activation of renin-angiotensin-aldosterone system in chronic kidney disease

Central and peripheral activation of RAAS occurs in many forms of renal disease (Schiffrin et al., 2007) and is a leading cause of potentiating SNS activity (Grassi, 2001). Central action of Ang II on AT_1 receptors has been implicated in determination of baroreceptor set point of BP regulation and upregulation of central sympathetic outflow (Grassi, 2001, Pal et al., 2013). These effects were substantiated by experimental evidence showing that intracerebral infusion of Ang II was associated with systemic vasoconstriction and resetting of the baroreflex towards higher BP range (Reid, 1992). The mechanism by which Ang II is believed to alter sympathetic outflow to the heart and vasculature involves activation of a nicotinamide adenine dinucleotide phosphate (NADPH) oxidase and increased levels of reactive oxygen species in neuroanatomical regions within the brain central to sympathetic stimulation such as the RVLM, circumventricular organs and PVN (Gao et al., 2005, Gao et al., 2008, Li et al., 2006, Zucker, 2006).

A similar crosstalk relationship exists between RAAS and SNS at the peripheral levels. Ang II modulates regional sympathetic outflow via presynaptic facilitation of NA release and inhibition of neuronal reuptake, a mechanism known to enhance neuronal transmission within sympathetic ganglia and amplify α-adrenoceptor-mediated vasoconstriction (Grassi, 2001, Reid, 1992, Saino et al., 2000). This view was supported by studies showing marked attenuation of muscle SNA in CKD patients treated with angiotensin-converting enzyme inhibitors (ACEi) or angiotensin receptor blockers (ARB) (Klein et al., 2003b, Ligtenberg et al., 1999, Neumann et al., 2007), suggesting an imperative role for RAAS activation in mediating autonomic imbalance in CKD.

1.6.5.1c Role of the renal afferents in chronic kidney disease

The kidney contains afferent sensory nerve fibres that are located primarily in the corticomedullary connective tissue of the renal pelvic wall and the major vessels, where they sense stretch or chemostimulation (Barajas and Wang, 1978, Recordati et al., 1981). The afferents project to the ipsilateral dorsal root ganglia and the dorsal horn in the spinal cord (Donovan et al., 1983). They synapse onto neurons within medullary and hypothalamic regions including the NTS, RVLM and PVN (Solano-Flores et al., 1997). Stretch activation of renal afferent fibres evokes an inhibitory renorenal reflex response whereby a compensatory natriuresis and diuresis due to diminished efferent RSNA is observed in the contralateral kidney. This is important in the coordination of renal excretory function and facilitation of homeostatic regulation of sodium and water balance (Johns et al., 2011, Kopp et al., 1985). There is also a negative feedback loop in which efferent RSNA facilitates increases in afferent renal nerve activity that in turn triggers a reflex renal sympathoinhibitory response. This mechanism is crucial for regulation of excess renal sodium (Johns et al., 2011, Kopp et al., 1987). In states of renal insult, activation of excitatory renal afferent nerve fibres and impaired inhibitory renorenal reflex ensue, contributing to increased peripheral

SNA, vasoconstriction, and increased arterial BP (Campese and Krol, 2002, Ciriello and de Oliveira, 2002, Johns et al., 2011, Kopp and Buckley-Bleiler, 1989).

In CKD, signals arising in the failing kidneys seem to mediate sympathetic activation (Campese and Kogosov, 1995, Converse et al., 1992), hence constituting another mechanism by which autonomic imbalance can be driven in renal disease. The role of the renal afferents in driving sympathetic overactivity in CKD remains an area of active investigation, however current evidence from animal studies suggest that abrogation of the afferent sensory signals by nephrectomy or dorsal rhizotomy, a selective severing of the afferent renal nerves at the entrance to the ganglionic dorsal root, prevents increases in the turnover rate and secretion of NA from the posterior hypothalamic nuclei, reduces SNA, ameliorates elevations in BP, improves renal function and slows down CKD progression (Bigazzi et al., 1994, Campese and Kogosov, 1995, Campese et al., 1995, Hausberg et al., 2002, Wyss et al., 1986, Ye et al., 1997b). These findings indicate that afferent impulses from the diseased kidney to central integrative structures in the brain elicit increased sympathetic nerve discharge and contribute to hypertension and deterioration of renal function in CKD.

Various factors are thought to play a role in the activation of the renal afferents and consequent upregulation of the neuroadrenergic drive. Animal studies have shown that circulating uraemia-related toxins are likely to cause excitation of the renal afferent nerves, provoking a sustained activation of SNA and increasing BP (Recordati et al., 1981, Converse et al., 1992, Schlaich et al., 2009b). However, Hausberg and others have shown that correction of uraemia in patients who had received renal transplantation did not alter baseline levels of muscle SNA relative to patients on regular haemodialysis therapy (Hausberg et al., 2002). This data indicates that increased SNA appears to be mediated by signals arising in the native kidneys that are possibly independent of circulating uraemia-related toxins.

Another possible activator of the renal afferent neurons and perhaps one of the most important primary events in sympathetic nerve activation is renal ischaemic damage (Schlaich et al., 2009b) and resultant fibroproliferative scarring in the failing kidneys (Ye et al., 1998). This notion is supported by animal studies where normal BP was restored upon deafferentation of the clipped kidney in the 2 kidney-1 clip (2K-1C) rat model of hypertension (Katholi et al., 1982). Further evidence comes from human studies showing normalization of BP and muscle SNA responses following amelioration of impaired renal perfusion and local tissue ischaemia in humans with renal artery stenosis (Miyajima et al., 1991). A similar ischaemic injury due to expansion of renal cyst growth is observed in hypertensive PKD patients, of which increases in muscle SNA are thought to be driven by stimulation of the renal afferent fibres (Fall and Prisant, 2005, Koomans et al., 2004, Valvo et al., 1985). The mechanism by which renal ischaemia activates the renal afferents is complex, however a role for mechano- and chemoreceptor-mediated secretion of adenosine, a chemical mediator, in response to local hypoxia has been proposed. This was based on studies

showing that an infusion of adenosine in humans and experimental animals stimulated sympathetic nervous activity (Costa et al., 2001, Katholi et al., 1982). Activation of RAAS pathway is also triggered by local ischaemia and this can further contribute to sympathetic stimulation (Schlaich et al., 2009b).

1.6.5.1d Cardiovascular remodelling in chronic kidney disease

Thus far, we have reviewed how altered autonomic function and particularly increased SNS activity could contribute to changes in cardiovascular structure and function in CKD. However, it is also important to consider the fact that the relationship between changes in autonomic outflows and cardiovascular remodelling is bidirectional, and that altered structure of the heart and vasculature can similarly influence sympathetic and cardiovagal tones during renal disease (Fig. 1.11).

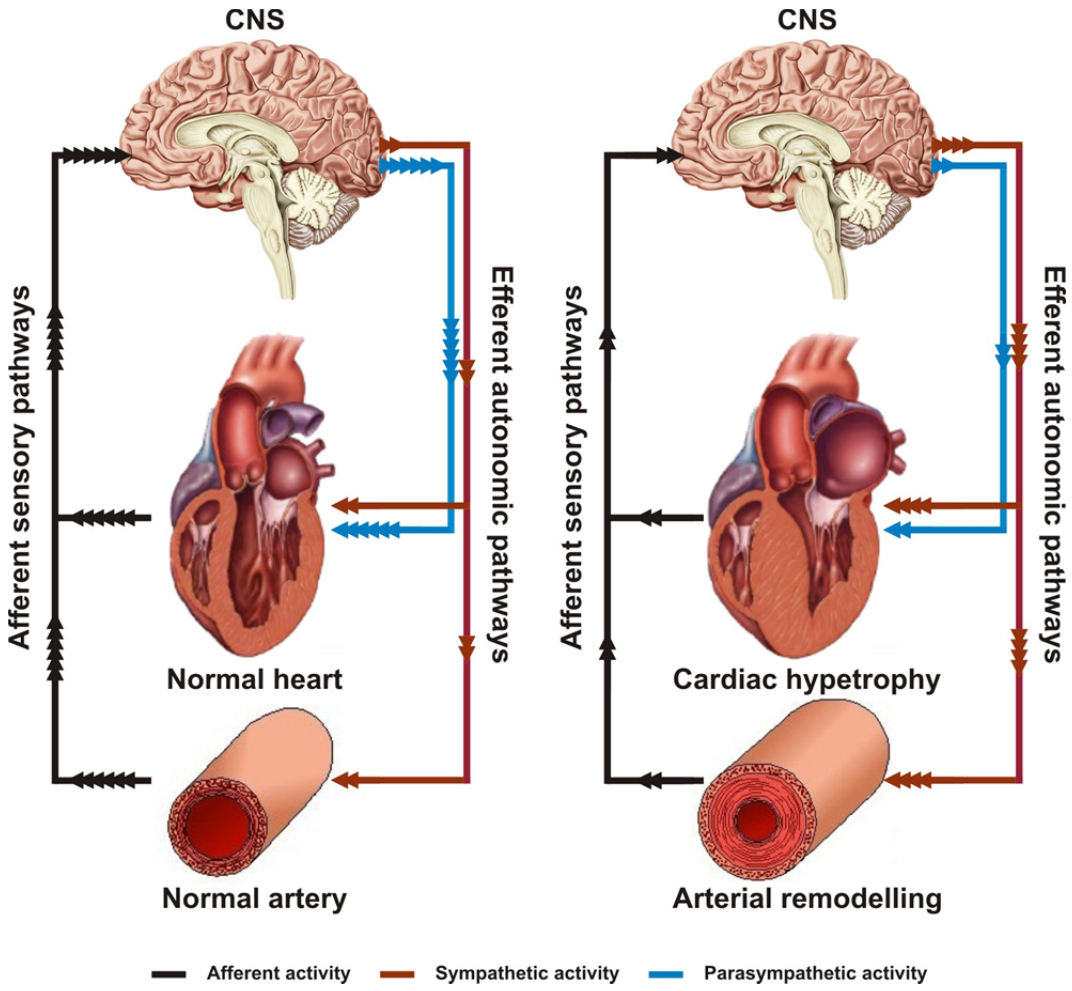

Figure 1.11: Effects of cardiovascular remodelling on sensory afferent and reflex efferent activities in chronic kidney disease (CKD). Note that the ability to evoke a reflex change in sympathetic and parasympathetic outflows is dependent upon the magnitude of the sensory afferent signal travelling to the brain. With arterial remodelling and cardiac hypertrophy, there is a reduction in the afferent nerve traffic which corresponds with a parallel reduction in reflex sympathetic and parasympathetic nerve activity.

Vascular remodelling and arterial stiffness are evident in both animal models of CKD (Ng et al., 2011a, Ng et al., 2011b, Pai et al., 2011, Sutliff et al., 2011) and humans with chronic renal failure (Blacher et al., 2001, Chesterton et al., 2005, Temmar et al., 2010). The process is mainly characterised by arterial hypertrophy and calcification, elevated tissue collagen deposition and

increased focal rupture of elastin fibres within the vascular wall (Ng et al., 2011b, Pai et al., 2011, Temmar et al., 2010). These effects can negatively impact upon arterial distensibility and the velocity of BP pulse wave propagation (Bruno et al., 2012), which ultimately impairs the ability of arterial baroreceptors to effectively signal BP to the CNS. An inability to transduce BP changes to the brain is then associated with defective baroreflex control of autonomic outflows and altered tonic levels of sympathetic and vagal efferent activity. Indeed, studies have shown a negative association between BRS and the magnitude of vascular calcification (Chan et al., 2005, Chesterton et al., 2005) and arterial stiffness (Studinger et al., 2006) in chronic haemodialysis patients. In patients receiving renal transplant, increased levels of muscle SNA were correlated with impaired arterial distensibility (Kosch et al., 2002). Together, these observations indicate an imperative role for vascular remodelling in cardiovascular autonomic dysfunction in CKD.

In addition to vascular abnormality, cardiac structural changes can also be identified in CKD patients, leading to LVH or dilated cardiomyopathy (Diwan et al., 2014, Fedecostante et al., 2014, Mencarelli et al., 2013). Factors increasing myocardial oxygen demand including volume overload (Wang et al., 2004), sympathetic overstimulation (Despas et al., 2009, Wang et al., 2004), anaemia (Frank et al., 2004, Wang et al., 2004) and hypertension (Fedecostante et al., 2014), or trophic effects exerted by catecholamines (Schlaich et al., 2009b, Zoccali et al., 2002), Ang II (Raizada et al., 2012) and aldosterone (Edwards et al., 2009, Moody et al., 2013) on cardiac myocytes have been implicated in the pathogenesis of cardiac damage in CKD, leading to fibroblast proliferation, interstitial accumulation of collagen, and microvessel disease (Raizada et al., 2012). As far as reflex regulation of autonomic outflow is concerned, cardiac structural abnormalities can also influence reflex control of sympathetic and parasympathetic nerve activity, perhaps through interfering with the normal function of autonomic reflexes (e.g., the cardiopulmonary reflex) initiated at the level of the heart. This view is supported by studies showing greater cardiopulmonary reflex deficits, evidenced by impaired reflex changes in forearm vascular resistance, to passive leg raising and manipulation of central venous and body negative pressures in hypertensive patients with LVH relative hypertensive subjects with no evidence of altered cardiac structure (Grassi et al., 1988), suggesting impaired cardiopulmonary reflex control of sympathetic vasomotor tone in LVH. In the SHR, where LVH is evident, cardiopulmonary reflexes activated via changes in cardiac filling pressure (volume-sensitive reflex) and chemical stimulation (chemosensitive reflex), are impaired (Uggere et al., 2000). Regression of LVH with ACEi therapy restores the volume-sensitive, but not the chemosensitive, reflex control of SNA and HR in those animals (Uggere et al., 2000). It is therefore possible that LVH mediated abnormalities in the reflex control of autonomic outflow may relate to polymorphic changes in the mechanosensitive and chemosensitive receptors within the cardiac chambers, which renders them less efficient in detecting and/or signalling changes in ventricular filling pressures and blood composition in CKD.

1.6.5.1e Altered nitric oxide bioavailability in chronic kidney disease

Nitric oxide is perhaps the most important molecule produced by the vascular endothelium (Furchgott and Jothianandan, 1991). It is synthesised from the amino acid L-arginine by the action of the enzyme NO synthase (NOS) (Bruno et al., 2012). Evidence suggests an interaction between NO and the ANS at both central and peripheral levels (Bruno et al., 2012), hence the importance of this molecule in the regulation of autonomic activity.

It is now well accepted that NO retains a tonic sympthoinhibitory effect within the CNS (Hirooka et al., 2011, Patel et al., 2001). Intravenous or intracerebroventricular administration of NOS inhibitors increases plasma NA levels and/or SNA (Nurminen et al., 1997, Sakuma et al., 1992), and these effects are abolished by cervical spine section (Sakuma et al., 1992, Togashi et al., 1992), ganglionic blockade (Cunha et al., 1993), sympathectomy (Sander et al., 1995) and β-adrenoceptor blockade (Nurminen et al., 1997). Further confirmation of the putative dependency of the ANS on the modulatory effect of NO was derived from experiments showing increased sympathetic nerve responses to microinjection of NOS inhibitors within the NTS (Harada et al., 1993) and RVLM (Zanzinger et al., 1995). NOS-positive neurons capable of modulating SNA were also identified within the PVN (Zhang et al., 1997).

Nitric oxide also plays a key role in the autonomic control of HR as NOS inhibition increases sympathetic drive to the heart, yet virtually blunts cardiac vagal tone (Cunha et al., 1993). A role for NO in regulating baroreflex function has been described in studies reporting impaired baroreflex control of HR, but not SNA, in human subjects following NOS inhibition (Spieker et al., 2000).

Many lines of evidence suggest the presence of endothelial dysfunction, progressive attenuation of NOS activity and therefore reduced NO bioavailability in CKD (Endemann and Schiffrin, 2004, Schiffrin et al., 2007, Schmidt and Baylis, 2000, Wever et al., 1999). A reduction in NO bioavailability in CKD patients may relate to reduced availability of the NO precursor L-arginine, impaired NOS activity or accumulation of natural inhibitory metabolites of NO synthesis such as asymmetric dimethyl arginine and elevated cholesterol levels (Grassi et al., 2011b, Schiffrin et al., 2007, Schlaich et al., 2009b). Despite reports emphasising a key action for NOS and NO in restraining central sympathetic outflow in normotensive (Nurminen et al., 1997, Sakuma et al., 1992) and hypertensive conditions (Chan et al., 2001, Shinohara et al., 2012), little is known about its central action in CKD. In 5/6 nephrectomised rats, in which NOS was inhibited with N^{ω}-nitro-L-arginine methyl ester (L-NAME), Ye and co-workers (1997) demonstrated a significant increase in NA turnover rate in the posterior hypothalamic nuclei, the locus coeruleus, and the NTS, and a marked increase in BP. Enhanced local NOS gene expression partially mitigated these effects and L-arginine supplementation produced an opposite effect on brain NA turnover rate (Ye et al., 1997a). This data suggests an imperative role for NO in the central regulation of sympathetic outflow and neurogenic control of BP. The mechanism by which NO depletion triggers activation of the SNS in

CKD is incompletely understood; however, it is likely to be due to increased production of reactive oxygen species and oxidative stress (Montezano and Touyz, 2012, Shinohara et al., 2012, Vaziri et al., 2002).

1.6.5.1f Mental stress in chronic kidney disease

Emotional, psychosocial and environmental stressors are major, yet modifiable risk factors for hypertension and CVD (Pal et al., 2013, Thayer et al., 2010), with augmented reactivity to (Matthews et al., 1993) and delayed recovery from (Schuler and O'Brien, 1997) stress associated with increased morbidity and mortality. Impaired autonomic control of HR, evidenced by a reduction in HRV (Chandola et al., 2008), and increased sympathetic activity (Hjemdahl et al., 1989, Niebylski et al., 2012), possibly due to a primary central sympathetic excitation (Wallin et al., 1992), have been associated with stress exposure. Adrenergic stimulation during psychological stress is governed by a complex mechanism, with central neuropeptides not only believed to evoke direct sympathetic activation but also induce the release of other stress hormones that can feed forward sympathetic activation including glucocorticoids and renin (Black, 2002). Accordingly, observations from these studies suggest a pivotal role for stress factors in mediating autonomic imbalance and CVD.

Altered autonomic activity and psychological distress are known to be related to increased cardiovascular morbidity and mortality in CKD patients (Kouidi et al., 2010). However, research has perhaps not given enough credit to the role of mental stress in driving altered sympathovagal balance in CKD. Given the feasibility by which stress can be modified in CKD relative to other modifiable risk factors, more investigations are required to characterise the role of stress in driving CVD in CKD patients. Most recently, in 4/6 nephrectomised rats, Palkovits et al. have been able to demonstrate that CKD elicits high activity in several stress- and pain-related brain regions including the limbic system, the hypothalamus and the circumventricular organs (Palkovits et al., 2013). However, whether stress-mediated activation of those brain regions promotes altered autonomic function in CKD and subsequent cardiovascular complications remain undetermined.

1.6.5.1g Other factors contributing to autonomic imbalance in chronic kidney disease

Other potential factors which may impact autonomic balance in CKD are:

Insulin: Insulin resistance and compensatory hyperinsulinemia are common in both diabetic and non-diabetic CKD patients, and increase as the GFR decreases over the course of the disease (Sit et al., 2006, Svensson and Eriksson, 2006). There is evidence that insulin resistance and elevated circulating plasma insulin levels cause sympathetic activation, impaired BRS and hypertension, or potentiate the hypertensive effects of other pressor agents including Ang II (Hall et al., 1995, Ryan et al., 2013, Vollenweider et al., 1993). It is therefore possible that insulin resistance can promote increased sympathetic activity and altered autonomic balance in CKD.

Endothelin: Endothelin, a vasoconstrictor peptide produced by endothelial cells, plays an important role in the regulation of vascular tone and renal function (Schneider and Mann, 2014), and levels are elevated in hypertensive CKD and non-CKD patients (Shichiri et al., 1990). A role for endothelin in the regulation of SNA was proposed based on studies illustrating heightened sympathetic and BP responses to intracerebral administration of endothelin in normotensive (Gulati et al., 1997) and hypertensive (Nakamura et al., 1999) animals. Further evidence supporting a role for endothelin in the regulation of autonomic function has come from studies reporting an action for endothelin on carotid bodies and cervical superior and nodose ganglia to influence baroreflex and chemoreflex regulation (Mortensen, 1999). A role for endothelin in modulating catecholamine release from sympathetic nerve terminals and the adrenal gland has also been shown (Mortensen, 1999). Activation of endothelin synthesis is linked to autonomic dysfunction in CKD (Smirnov et al., 2011), however further studies are required to further characterise these findings.

Renalase: Renalase is an established regulator of sympathetic activity, whose discovery has made the participation of SNS in the pathogenesis of autonomic imbalance in CKD more complex. Renalase is a soluble monoamine oxidase predominantly expressed in the glomeruli and proximal renal tubules as well as cardiomyocytes and skeletal muscle (Xu et al., 2005). Renalase, whose secretion is regulated by renal function, renal perfusion and catecholamine levels, metabolizes catecholamines in the following order: dopamine → adrenaline → NA (Desir and Peixoto, 2014, Xu et al., 2005). Under basal conditions, renalase lacks significant amine oxidase activity; however, when a modest increase in BP is evoked by adrenaline, a 10-fold increase in renalase activity is observed (Li et al., 2008). Interestingly, renalase is readily detectable in venous plasma of healthy individuals but not in the plasma of uraemic patients (Desir and Peixoto, 2014, Schiffrin et al., 2007, Schlaich et al., 2009b, Xu et al., 2005), suggesting that normal kidneys are a prerequisite for renalase secretion and a loss the protective effects of renalase against SNS overactivity in CKD patients. The latter view was supported by evidence demonstrating that renalase activation induced by adrenaline was significantly reduced in magnitude and duration in a 5/6 nephrectomy rat model of CKD (Li et al., 2008). More recent reports have also shown decreased renalase secretion in the ischaemic kidney compared with the non-ischaemic side in a rat model of unilateral renal artery stenosis (Gu et al., 2011), hence implicating changes in renal perfusion as a determinant. Accordingly, alterations in renalase secretion, expression and/or enzyme activity may play a causative role in increased plasma catecholamine and sympathetic hyperactivity in CKD. However, to what extent the impairment of renalase production contributes to sympathetic overstimulation and BP elevation in CKD remains to be elucidated.

Salt: Derangements in mechanisms regulating central sympathetic inhibition and consequent peripheral sympathetic activation have been linked to high salt content (Brooks et al., 2005, Strazzullo et al., 2001), suggesting a crucial role for salt intake/retention in mediating altered sympathetic control of cardiovascular function and evoking autonomic imbalance. The exact

mechanism by which high salt intake aggravates sympathetic stimulation and hypertension in CKD is an active area of research, with salt restriction now being more frequently considered as a mean of controlling BP in CKD/ESRD patients (Kidney Health Australia, 2012, Mailloux, 2000). In non-dialysis CKD patients, a linear relationship between salt intake and systolic BP has been identified, with salt sensitivity of BP rising with a decline in renal function (Meng et al., 2014). An inhibitory action for salt on neuronal NOS expression in the posterior hypothalamic nuclei, the locus coeruleus and the PVN was suggested by Campese and others (Campese et al., 2002) as one possible mechanism relating high-salt mediated action of the SNS. A role for brain oxidative stress in driving sympathoexcitation in response to salt load in uninephrectomised rats has also been shown (Fujita et al., 2012).

Atrial natriuretic peptide: Atrial natriuretic peptide is a powerful vasodilator produced by the atrial myocytes, and its circulating levels are elevated in both hypertensive (Wambach et al., 1987) and CKD (Akiba et al., 1995) patients. Studies have suggested a critical role for ANP in inhibiting hypothalamic NA release (Peng et al., 1996, Vatta et al., 1993) and enhancing cardiac vagal baroreflex and cardiopulmonary reflex function (Toader et al., 2007, Woods et al., 1994), suggesting a potential role for ANP in modulating autonomic function. In the SHR, ANP-mediated facilitation of cardiac baroreflex is absent, indicating altered ANP-ANS interaction during disease (Woods et al., 1994, Hood and Woods, 2004). The relationship between ANP and autonomic neuroregulation in health and disease is far from being completely understood, and clearly CKD is no exception.

1.6.6 The effect of sex on autonomic functions

A number of epidemiological studies reveal that the prevalence, incidence and severity of CVD in premenopausal women are markedly lower than that in men of the same age (Burt et al., 1995, Maric, 2005, Reckelhoff, 2001). As those differences are lost after the onset of menopause, it has been proposed that those effects are mainly related to sex hormones which act to protect women against cardiovascular complications. A key question is whether the relative protection of the female sex against the development of CVD is due to a hormone-driven neuromodulatory effect on cardiovascular homeostasis. There is a substantial literature to suggest that the functioning of the ANS and its pivotal role in cardiovascular regulation varies between men and women in health and disease. However, to date, consistent evidence has not been forwarded regarding differences in autonomic functions in both males and females, perhaps due to limited number of investigations in humans and animal models which have compared autonomic functions in males and females or differences in time of the oestrous cycle during which autonomic function was assessed.

Under normal conditions, healthy men and women appear to have similar resting BP and HR (Hogarth et al., 2007b, Kim et al., 2011, Sevre et al., 2001, Shoemaker et al., 2001, Tank et al., 2005). Indices of SNS activity show either similar baseline levels in men and women, or reduced levels in women

(Hogarth et al., 2007b, Jones et al., 1996, Ng et al., 1993). Relative to males, and perhaps depending on the time of the reproductive cycle when measurements were taken (Brooks et al., 2012), baroreflex control of HR in females has been shown to be enhanced (Chen and DiCarlo, 1996, Kim et al., 2011), depressed or comparable (Crofton et al., 1988, Tank et al., 2005), while measures of sympathetic baroreflex function are either enhanced (Hogarth et al., 2007b) or unchanged in both males and females (Tank et al., 2005). It has been shown in clinical studies that women respond with greater changes in HR and/or total peripheral resistance when the cardiopulmonary baroreflex is activated by a head-up tilt (Shoemaker et al., 2001) or deactivated by orthostasis (Frey et al., 1994), and that deactivation of the cardiopulmonary reflex by the application of lower negative pressure results in a lower HR change in women relative to men (Convertino, 1998). Cardiopulmonary reflex control of SNA triggered by chemical and mechanical activation of the cardiopulmonary receptors in rats exhibit a greater response range in females compared with males; phenomena which may, in turn, contribute to greater renal excretory functions in females (Scislo and DiCarlo, 1994).

Despite this range of findings, research has, however, consistently shown that hormone replacement therapy improves baroreflex control of HR and vascular sympathetic outflow in postmenopausal women (Huikuri et al., 1996, Hunt et al., 2001). Likewise, ovariectomy enhances sympathetic activation and attenuates HR BRS, which can be ameliorated by oestrogen replacement therapy (Fadel et al., 2003, Mohamed et al., 1999). These observations therefore support sexual dimorphism in the control of autonomic outflows to the heart and vasculature. Likely underpinning these dissimilarities between males and females are developmental and functional variations in the baroreflex arc, including differences in the sensory afferent pathways (baroreceptors, cardiopulmonary receptors or chemoreceptors), central neurotransmission, or efferent and postsynaptic signalling pathways. Indeed, cumulative evidence confirms an impact for ovarian hormones on central mediation of vagal and sympathetic outflow (Mohamed et al., 1999, Saleh and Connell, 2000), peripheral efferent nerves (Du et al., 1994) and signalling pathways of effector organs that respond to neurotransmitters (Schroeder et al., 2004). In support of the sexual dimorphism in the central processing of autonomic outflows is the demonstration that women elicit greater reductions in plasma NA and BP in response to central inhibition of sympathetic outflow by the α_2-adrenoceptor agonist clonidine (Esler et al., 1990). Accordingly, an appreciation of sex differences in function of the ANS is critical to fully understand a number of common and important clinical presentations in men and women.

In hypertensive conditions, women and female animal models of hypertension, including SHRs (Reckelhoff et al., 2000), Dahl salt-sensitive rats (Crofton et al., 1993), deoxycorticosterone acetate/salt hypertensive rat (Ouchi et al., 1987), renal wrap (Haywood and Hinojosa-Laborde, 1997) and Ang II hypertension animals (Xue et al., 2005), have lower BP readings compared with hypertensive males. In some of these models where ovariectomised females were used, removal of the ovaries augmented hypertension. As far as autonomic functions are concerned, Hogarth and others (2007) showed that hypertensive women have lower muscle SNA but comparable resting HR

relative to hypertensive men (Hogarth et al., 2007a). On the other hand, HRV and HR BRS are markedly lower in hypertensive women compared with hypertensive men (Pavithran et al., 2008, Sevre et al., 2001). However, in rat and mice models of hypertension, females show lower or unchanged resting HR, greater HRV and HR BRS, as well as lower resting BP and BPV and/or lower sympathetic vasomotor tone, as assessed by ganglionic blockade (Johnson et al., 2011, Xue et al., 2005).

In CKD, sexual dimorphism appears to play a significant yet ill-defined role in the incidence, prevalence and progression of renal disease. Data from clinical and animal studies have provided some conflicting results, reporting both a slower (Coggins et al., 1998, Cowley et al., 1997, Eriksen and Ingebretsen, 2006) and faster (Jafar et al., 2003, Rosenmann et al., 1984) decline in renal function in females relative to males. These discrepancies are perhaps borne from the fact that little attention is paid to the importance of sex differences in CKD pathology, and that clearly, studies with more standardised experimental criteria are required to accurately characterise these findings. With respect to CVD in CKD, current evidence suggests that women are at relatively lower risk of developing CVD and related complications compared with men (National Kidney Foundation, 2013); however, whether these effects, as shown in hypertension, are driven by a differential influence for sex on cardiovascular neuroregulatory function in CKD is still unknown. Despite the large number of studies that have assessed autonomic functions in CKD, it appears that sex effects are not well accounted for. Likely underlying this scarcity of information is also the fact that most CKD women, being postmenopausal, may have contributed to the overlooking of this issue (Carrero, 2010). Thus, undoubtedly, there is still plenty of work to be done, as our current knowledge indicates that males and females behave differently in CKD.

1.6.7 Current interventional strategies targeting the autonomic nervous system in chronic kidney disease

Cardiovascular autonomic dysfunction is a major contributor to CVD in CKD patients and likely underlies the high morbidity and mortality in this patient population (Cashion et al., 2000, Dursun et al., 2004). Current evidence suggest that deficits in the autonomic function and elevated BP are driven by the diseased kidneys, since nephrectomy, renal denervation, kidney transplantation or pharmacotherapy targeting sympathetic activation has been shown to correct BP, lower sympathetic overdrive, improve vagal control of HR and/or limit the progression of renal damage in humans and experimental animals (Boero et al., 2001, Esler et al., 2012, Hering et al., 2012, Schlaich et al., 2012, Schlaich et al., 2009b, Weinstock et al., 1996, Yildiz et al., 1998).

1.6.7.1 Pharmacological treatment

Various classes of pharmacological agents that have the ability to directly or indirectly modulate autonomic function are currently being used to limit hypertension and progression of renal disease in CKD. Based on the suggested reciprocal potentiation of RAAS and SNS in renal disease (Vink et al.,

2013), inhibition of the RAAS pathway seems to be a logical step in the treatment of CKD. Indeed, RAAS inhibitors including both ACEi and ARB are recommended as a first line therapy in patients with CKD (Masuo et al., 2010, Weir, 2009). Apart from counteracting direct cardiovascular manifestations of Ang II, ACEi and ARB are both capable of indirectly supressing the stimulated SNA in CKD patients (Ligtenberg et al., 1999, Neumann et al., 2007) and providing comparable sympathoinhibitory and antihypertensive effects (Klein et al., 2003b). A combination therapy of an ACEi plus ARB has been found to provide more effective RAAS inhibition, better BP control and superior reductions in serum creatinine levels and proteinuria (Weir, 2007). An additive sympathoinhibition, however, has never been described in the literature with the combined therapy. Blockers of RAAS have also been shown to reset sympathetic baroreflex function towards a lower BP range without altering sympathetic BRS (Ligtenberg et al., 1999), and HRV appears to improve in patients receiving ACEi and ARB (Sato et al., 2013, Ranpuria et al., 2008); however, a worsening of HRV with ACEi has also been shown (Ondocin and Narsipur, 2006). The extent to which RAAS inhibitors can reduce SNA in CKD, on the other hand, has been a subject of debate. Lightenberg and colleagues (1999) measured muscle SNA response in CKD patient treated with an i.v. infusion of the ACEi, enalapril. Their result showed that enalapril was able to normalise muscle SNA to levels comparable to controls. In a series of studies by Neumann et al. a normalised muscle SNA was only attainable when the ARB, eprosartan was combined with the central sympatholytic agent, moxonidine (Neumann et al., 2004), but not when an ACEi or ARB monotherapy was given (Neumann et al., 2007). The reasons underlying these controversial findings remain incompletely understood; however, it may relate to differences in drug potency, dose and/or route of administration. More recently, a similar sympathoinhibitory effect to the renin inhibitor aliskiren has been demonstrated in CKD individuals when used with statin therapy (Siddiqi et al., 2011); however, like findings from Neumann et al., normalised muscle SNA responses were not observed with aliskiren alone nor did statins improve HRV in ESRD renal disease patients receiving chronic haemodialysis (Narsipur et al., 2011).

Studies evaluating the effects of adrenergic blockers and central sympatholytics in CKD are scarce, with reports highlighting their beneficial effects only when combined with RAAS blockers or calcium channel antagonists (Suzuki et al., 2001, Vonend et al., 2003, Palkovits et al., 2013, Neumann et al., 2004). β-blockers and central imidazoline α_2-adrenoceptor agonists have been shown to slow deteriorations of renal structure and function in CKD. This is based upon findings showing reduced glomerulosclerosis and progression of renal failure in 5/6 or subtotal nephrectomised rats (Amann et al., 2001, Amann et al., 2000), and a reduction in albuminuria in hypertensive CKD patients (Bakris et al., 2006, Strojek et al., 2001). Current evidence also suggests that β-blockers, relative to RAAS inhibitors, are underutilized in CKD (Bakris et al., 2006), despite data reporting a cardioprotective action (Cice et al., 2003) and comparable renoprotective effects to those of ACEi (Brooks et al., 1993, Suzuki et al., 2001). As far as autonomic function is concerned, β-receptor blockade seems to markedly improve HRV and cardiac autonomic balance in ESRD patients (Tory et al., 2004).

Likewise, moxonidine appears to lower muscle SNA in ESRD on pre-existing antihypertensive therapy (Hausberg et al., 2010). What is surprising though is the lack of reports that have directly assessed SNA in CKD patients treated with adrenoceptor blockers. In patients with essential hypertension, however, long-term β-adrenoceptor blockade with metaprolol (Wallin et al., 1984), but not atenolol (Burns et al., 2004), seems to lower muscle SNA.

Long-term treatment with calcium channel blockers (e.g., amlodipine) appears to increase muscle SNA in CKD patients (Ligtenberg et al., 1999), which is perhaps mediated by the baroreflex induced activation of SNA in the face of the significant drop in BP elicited by this class of compounds.

1.6.7.2 Percutaneous renal denervation

We have now reviewed that afferent signalling derived from the native kidney can play a causal role mediating efferent sympathoexcitation in CKD. Consequently, interruption of the efferent and afferent renal nerve fibres by renal denervation can offer an attractive approach to mitigate sympathetic hyperactivity and reverse autonomic imbalance in CKD. Accordingly, percutaneous renal denervation, a catheter-based approach that specifically disrupts the renal sympathetic nerves in the adventitia of the renal arteries using radiofrequency bursts, has emerged as one promising treatment for sympathetic excitation in CKD (Vink et al., 2013).

The concept of renal denervation is not new and has substantially been used to study the influence of the SNS on renal function in experimental animals. Smithwick *et al.* was the first to bring surgical renal denervation into clinical practice in 1953 when he used this procedure to treat patients with resistant hypertension (Smithwick and Thompson, 1953). Despite the compelling benefits of the procedure and improved survival, the invasive nature of the surgery and the later discovery of more effective antihypertensive drugs rendered the procedure obsolete. To date, our knowledge of and renewed interest in renal denervation are principally based on decades long of refining of what was first known to be an extremely invasive procedure that carries a high risk of intraoperative mortality and long-term complications. The unresponsive BP to conventional pharmacotherapy in the hypertensive population and the substantial risks associated with polypharmacy have lately renewed interest in this surgical approach as a mean of lowering BP, counteracting the sympathetic overdrive observed in patients with essential hypertension and CKD, and limiting cardiovascular complications and end-organ damage.

Aside from lowering BP, which on its own can slow down the progression of kidney disease (Ravera et al., 2006), renal denervation seems to offer a range of invaluable therapeutic benefits independent of BP reduction, including lowering renin production, improving renal haemodynamics, enhancing GFR and reducing albuminuria (Hering et al., 2013, Hering et al., 2012, Kiuchi et al., 2013, Schlaich et al., 2009a). However, the question of whether renal denervation retains the ability to reduce muscle SNA or improve reflex control of HR and SNA in CKD long-term remains unanswered. Reports on basal muscle SNA in renally denervated hypertensive subjects has yielded controversial results, with mixed

reports of lowered (Hering et al., 2013, Hering et al., 2014) or unchanged (Brinkmann et al., 2012) muscle SNA in denervated CKD patients. Similar controversial findings have also been identified with respect to the effect of renal denervation on HR and SNA baroreflex function in hypertensive humans and animals. When tested using pharmacological manipulation of BP, baroreflex control of HR and muscle SNA, on the other hand, remains unaltered in hypertensive patients (Brinkmann et al., 2012). Spontaneous BRS, by contrast, appears to be improved in the SHR and resistant hypertensive individual following renal denervation (Hart et al., 2013).

The reimplementation of this procedure in clinical practice is relatively new. Most recently, the SYMPLICITY HTN-3 trial, a controlled trial for renal denervation for resistant hypertension, has shown no significant reduction in systolic BP in patients with resistant hypertension 6 months after renal artery denervation relative to sham controls (Bhatt et al., 2014); however, conclusive evidence regarding long-term safety was not provided. Therefore, more studies are required to determine the safety, feasibility, efficacy, and durability of this approach (Jin et al., 2013). Intriguingly, however, preliminary data shows that the BP lowering effect of renal denervation seems to inversely correlate with kidney function at baseline, suggesting renal denervation in CKD patients may have more pronounced therapeutic advantages relative to hypertensive subjects with normal renal functions.

1.6.7.3 Carotid baroreceptor stimulation

Carotid baroreceptor stimulation is a successfully developed invasive procedure that involves the implantation of a device capable of electrically stimulating the baroreceptors within the carotid sinus of a hypertensive subject. The result is a baroreflex mediated sympathoinhibition and enhanced reflex control of vagal drive. Accordingly, this surgical technique serves the dual purpose of not only providing information on the functioning of baroreflex mechanisms in hypertensive patients, but also achieving a satisfactory control of BP in patients with resistant hypertension including those with CKD (Grassi et al., 2012). Indeed, research has shown that carotid stimulation of baroreceptors evokes a profound sympathoinhibitory response and sustained reductions in BP (Heusser et al., 2010, Lohmeier et al., 2010, Scheffers et al., 2010). These observations suggest the importance of adrenergic overdrive in the maintenance of high BP in hypertensive subjects and the potent BP lowering effects of the intervention in resistant hypertensive states. The reflex mediated sympathoinhibition, which is evidenced by reductions in plasma NA and muscle SNA, is not associated with changes in plasma renin activity or differences in sympathetic and HR baroreflex function (Heusser et al., 2010). The technique is yet to be trialled in CKD patients or animal models of renal disease. However, preliminary findings in hypertensive subjects suggest the potential of this technique to become a new treatment option for resistant hypertension in CKD patients.

1.6.7.4 Renal replacement therapy

Renal replacement therapy is not a direct treatment method for uraemic autonomic disturbances in CKD; rather, relative correction of autonomic parameters emerges as an inherent consequence. Renal

replacement therapy, including haemodialysis (nocturnal and home short daily haemodialysis), peritoneal dialysis (continuous ambulatory peritoneal dialysis, automated peritoneal dialysis, and a combination of the two) and kidney transplantation, aims to correct and/or maintain plasma biochemistry (uraemic toxins, electrolytes and acid-base balance) within acceptable limits and is reserved for patients with advanced renal failure (Berger et al., 2009, Goddard and Turner, 2014). Transplantation is superior to chronic dialysis and offers the best chance of long-term survival (Goddard and Turner, 2014, Wolfe et al., 1999).

Dialysis therapy can trigger sympathetic overactivity and vagal withdrawal as a result of intradialytic hypotension caused by acute fluid removal (Chan et al., 2010, Chesterton et al., 2010). The efficacy of long-term dialysis in ameliorating abnormalities in the autonomic nervous system, on the other hand, has been a subject of considerable debate. In patients receiving chronic haemodialysis or continuous ambulatory peritoneal dialysis, Dursun and others (2004) showed significant improvements in cardiac vagal tone and HRV parameters, with patients receiving continuous ambulatory peritoneal dialysis displaying better treatment outcomes (Dursun et al., 2004). In non-diabetic, but not diabetic, ESRD patients receiving chronic haemodialysis therapy, Giordano and co-workers (2001) reported a marked improvement in HRV, which correlated negatively with uraemia (Giordano et al., 2001). Mylonopoulou et al. (2010), in contrast, observed enhanced HRV parameters in both diabetic and non-diabetic ESRD patients, but the effect was more pronounced in the non-diabetic population (Mylonopoulou et al., 2010). Conversion from conventional to nocturnal haemodialysis, which allows for more efficient removal of uraemic toxins, was associated with improved BRS, increased HF (vagal) power of HRV and normalised LF/HF ratio of HRV (Chan et al., 2014, Chan et al., 2004, Chan et al., 2005). A marked drop in muscle SNA in patients receiving frequent haemodialysis has also been reported (Zilch et al., 2007). While it is possible that removal of toxic effects of uraemia could explain ameliorative action of dialysis on tonic levels and/or reflex control of autonomic function in CKD, reports which failed to demonstrate any beneficial effects suggest otherwise (Agarwal et al., 1991, Korejwo et al., 2002, Vita et al., 1992, Vlachojannis et al., 2000). In support of the latter view is the fact that bilaterally nephrectomized haemodialysis patients show muscle SNA levels comparable to controls (Converse et al., 1992), providing a substantive proof that signals arising from the diseased kidneys, rather than uraemic toxins, drive changes in autonomic functions in CKD. Nonetheless, the main reasons behind discrepant results obtained in the dialysis-dependent patients with respect to autonomic function remain incompletely understood; however, differences may at least in part be related to factors such as age, severity of renal dysfunction, existing co-morbid conditions, dialysis technique and/or composition of the dialysate solution (Robinson and Carr, 2002). Clearly, further studies are required to delineate the mechanisms by which longer-term dialysis therapy may or may not improve autonomic dysfunction in CKD individuals.

Reports describing beneficial effects of renal transplantation on parasympathetic functions appear to be more consistent. Indeed, a significant improvement in tonic and reflex control of parasympathetic

functions, as assessed by HF power of HRV (Yang et al., 2010b, Yildiz et al., 1998), spontaneous BRS (Rubinger et al., 2009), BRS phenylephrine test (BRS_{PE}) (Agarwal et al., 1991, Korejwo et al., 2002), and HR responses to respiration, orthostatic change and Valsalva manoeuvre (Agarwal et al., 1991, Heidbreder et al., 1985), has often been observed in renal transplant receipts. Muscle SNA does not differ following renal transplantation (Hausberg et al., 2002); however, LF power of SBPV is markedly reduced (Rubinger et al., 2009), perhaps suggestive of a differential effect for renal transplantation on various sympathetic beds (Agarwal et al., 1991). Reflex sympathetic function tests, as assessed by BP responses to orthostatic change, sustained handgrip, cold pressor, mental arithmetic and/or sudden loud noise, were shown to be either improved (Agarwal et al., 1991) or unchanged (Heidbreder et al., 1985) following a kidney transplant. Chemoreflex sensitivity derived from HRV responses to chemoreceptor deactivation by 100% oxygen, on the other hand, is improved in kidney transplant patients relative to patients on maintenance haemodialysis (Rassaf et al., 2010).

1.6.7.5 Treatment limitations

There is significant consensus regarding autonomic dysfunction in CKD; however, current interventional strategies to contain this condition provide less clear-cut conclusions with respect to efficacy, specificity and reproducibility. Several pharmacological treatments have been developed to decrease sympathetic activity and BP; however, these medications still have their limitations. Clinical practices are mainly limited by the feasibility of present-day diagnostic technologies and the ability to standardize test conditions, which makes identifying critical pathways driving autonomic dysfunction within the nervous system a formidable challenge. Most of the current methods classically used to assess autonomic functions in the clinic are indirect and rely mostly on simple acquisition of an ECG signal, HR and/or BP. Perhaps the only direct, yet time consuming, measurement of autonomic activity to date is muscle or skin SNA, which in its own right may not necessarily predict changes in other sympathetic nerve beds key to the regulation of BP (see section 1.5.1.5, page 23). It is clear from the above that the pathogenesis of autonomic dysfunction in CKD is far from being completely understood and current human studies provide limited scope for specific mechanisms to be investigated. The underlying mechanisms require further work before specific treatment options can be developed.

1.6.8 Polycystic kidney disease as a cause of chronic kidney disease

Polycystic kidney disease, a predominant cause of ESRD in children and adults, is a genetic disorder characterised by accumulation of fluid-filled cysts in the kidney and other organs (Fall and Prisant, 2005, Igarashi and Somlo, 2002). The renal cysts originate from the epithelia of the nephrons and renal collecting duct and are lined by a single layer of cells that exhibit vigorously higher rates of cellular proliferation and are relatively less differentiated than normal tubular cells (Comperat et al., 2006, Nadasdy et al., 1995). Abnormalities in gene expression, fluid secretion, cell polarity,

extracellular matrix and apoptosis have been shown in PKD, yet the critical underlying mechanism of cyst formation remains elusive (Guay-Woodford, 2003, Igarashi and Somlo, 2002).

Two hereditary forms of PKD have been identified in human: adult onset autosomal dominant (ADPKD) and autosomal recessive (ARPKD), a major cause of early childhood nephropathy (Guay-Woodford, 2003, Zerres et al., 2003). Hypertension develops in 60% of ADPKD patients prior to deterioration in renal function (Gabow et al., 1990). In ARPKD, however, hypertension occurs in up to 80% of affected children, with nearly all who survive the neonatal period requiring anti-hypertensive therapy (Capisonda et al., 2003, Sweeney and Avner, 2006). With a high incidence of LVH, PKD has been described as a hypertensive heart disease (Bardaji et al., 2001).

Several mechanisms have been implicated in the pathogenesis of hypertension in PKD including volume overload associated with an abnormal pressure-natriuresis response, activation of RAAS associated with renal cyst formation, induction of local tissue ischaemia and increased SNS activity (Augustyniak et al., 2002, Fall and Prisant, 2005, Klein et al., 2001, Locatelli et al., 2003, Valvo et al., 1985).

Muscle SNA is increased in hypertensive PKD patients, regardless of renal function (Klein et al., 2001) and blockade of RAAS does not return muscle SNA to normal levels (Klein et al., 2003b). Furthermore, several lines of evidence have demonstrated elevated plasma catecholamine levels (Cerasola et al., 1998) and increased renin release play a central role in the development of hypertension in the disease. A number of studies suggest that this increase in SNS activity is due to stimulation of the renal afferents (Klein et al., 2001, Wang and Strandgaard, 1997). In PKD patients with ESRD, bilateral renal nephrectomy (Converse et al., 1992) and total renal denervation (Prejbisz et al., 2014) have been found to significantly attenuate the hypertension, consistent with studies in animal models of PKD where total renal denervation has been shown to reduce BP, renal enlargement and cystic pathology (Gattone et al., 2008).

A severe form of autosomal recessive cystic kidney disease and one of the most frequent genetic causes of ESRD in children and young adults is nephronophthisis (NPHP) (Hildebrandt et al., 2009, Wolf and Hildebrandt, 2011). Nephronophthisis is a hereditary condition where disintegration of nephrons is present, contributing to a critical tubulointerstitial nephropathy (Hildebrandt and Otto, 2005). Eleven different genes (NPHP1–11, NPHP1L) are believed to underlie NPHP (Wolf and Hildebrandt, 2011); however, the exact causative gene in approximately 70% of all individuals with NPHP is unknown (Hildebrandt et al., 2009). Positional cloning of these genes and functional characterization of their encoded proteins (nephrocystins) has shown that all proteins mutated in humans or animal models of NPHP are expressed in primary cilia or centrosomes of renal epithelial cells (Hildebrandt et al., 2009, Otto et al., 2003, Otto et al., 2008). Accordingly, this identifies NPHP as a disease that affects ciliary functions “ciliopathy”, epithelial cell polarity and cell-cycle control (Hildebrandt et al., 2009), consistent with both ADPKD and ARPKD.

Nephronophthisis has been distinguished based on onset of ESRD into infantile (Gagnadoux et al., 1989), juvenile (Hildebrandt et al., 1992), and adolescent NPHP (Omran et al., 2000), in which ESRD becomes evident at a median age of 1, 13, and 19 years, respectively. Among these, juvenile NPHP is the most common, accounting for 5–10% of cases of ESRD in affected children (Salomon et al., 2009). Clinical presentation of the disease is mainly characterized by anaemia, polyuria, polydipsia, isosthenuria, impaired urinary concentrating ability, progressive renal dysfunction, hypertension and LVH (Ala-Mello et al., 1996, Hildebrandt et al., 2009, O'Toole et al., 2010, Wolf and Hildebrandt, 2011). Histological features of the diseased kidneys involve: tubular basement membrane disintegration, tubular cyst formation, and tubulointerstitial inflammation and fibrosis (Wolf and Hildebrandt, 2011, Zollinger et al., 1980). The histological characteristics of the infantile form of NPHP differ from those seen in juvenile NPHP, with the former combining features of NPHP (e.g., tubular cell atrophy, tubular cysts, and interstitial fibrosis) with features of PKD including enlarged kidneys and widespread cyst development (Gagnadoux et al., 1989, Wolf and Hildebrandt, 2011).

1.6.9 The Lewis Polycystic Kidney rat: an animal model of chronic kidney disease

Our current understanding of human renal disease has progressed significantly based on studies carried out in animal models of disease. The rapid onset of disease in experimental models offers an efficient mean of investigating pathogenesis, since decades may elapse between kidney injury and clinical manifestations in human renal disease. Furthermore, in most cases the pathological process in the human form of CKD is multifactorial. Therefore, careful use of animal models offers the opportunity to study disease-specific mechanisms, investigate molecular pathogenesis, and assess potential novel therapies.

The Lewis Polycystic Kidney (LPK) model is a new rodent model of cystic kidney disease that expresses cardiovascular and renal complications analogous to the human form of ARPKD (Phillips et al., 2007). The LPK rat, which arises from a spontaneous genetic mutation in the NIMA (never in mitosis gene A)-related kinase 8 (*Nek8*) (Fig. 1.12), develops renal cysts at 3 weeks of age, displays hypertension by 6 weeks of age, manifests moderate impairments of renal function by 12 weeks of age, and presents with end-organ damage, including ESRD and cardiomyopathy, by 18–24 weeks of age (Phillips et al., 2007, McCooke et al., 2012). Given the similarity of the LPK course of the disease to that of human CKD, the LPK model greatly facilitates investigation of various mechanisms underlying cardiovascular and renal dysfunctions accompanying both PKD and CKD, and provides a useful tool critical to identifying interventional strategies aimed at limiting morbidity and mortality associated with those complex medical conditions. With the spontaneous nature of CKD in the LPK, the model seems relatively superior to other renal disease models including 5/6 nephrectomy (Liu et al., 2003) and unilateral ureteric obstruction (Chevalier, 2006) CKD models, whereby animals are subjected to surgical stress to create the model; and drug or nephrotoxin (e.g., cyclosporine, adenine,

adriamycin, puromycin, streptozotocin, etc.) induced models (Jia et al., 2013, Jones et al., 1991, Kelly et al., 1998, Kinzler et al., 1991), in which drug/toxin effects on other target organs besides the kidneys cannot be ruled out.

1.6.9.1 Molecular genetics

Nek8 plays a key role in normal communication between the cilia and the processes of renal epithelial cell differentiation and proliferation, such that when its expression or localization is inadequate, renal cilia elongation, kidney cysts formation and renal fibrosis ensue (McCooke et al., 2012, Phillips et al., 2007, Salomon et al., 2009). In humans, *Nek8* mutation contributes to the development of NPHP 9, which as described above, belongs to a family of mutations which together are a leading cause of renal failure in children and young adults (Frank et al., 2013, Hildebrandt and Zhou, 2007, Otto et al., 2008, Salomon et al., 2009). Accordingly, this classifies the LPK rat as a genetic rodent model of NPHP9 (Salomon et al., 2009) that can be used to delineate the complex disease processes associated with NPHP, including hypertension and cardiac disease as previously shown (Harrison et al., 2010, Hildreth et al., 2013b). The LPK phenotype resembles that described for the juvenile cystic kidney (jck) mouse *Nek8* model (Atala et al., 1993, Liu et al., 2002, Trapp et al., 2008), which not only presents with similarly elongated renal cilia and altered ciliary *Nek8* expression (Atala et al., 1993, Smith et al., 2006) but also with a comparable phenotypic presentation of cystic kidney disease that resembles human ARPKD (Smith et al., 2006).

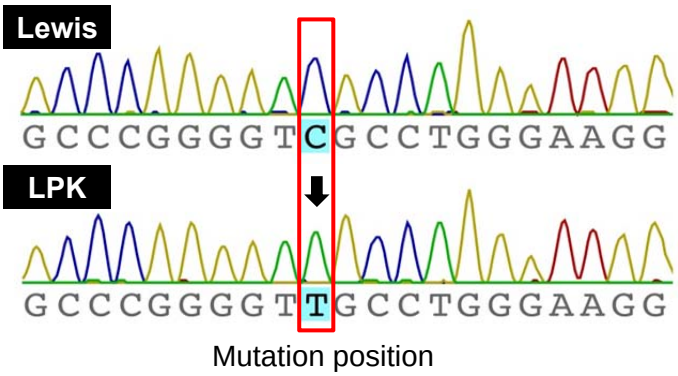

Figure 1.12: Chromoatographic sequencing of the Lewis Polycystic Kidney (LPK) rat *Nek8* gene mutation on Chromosome 10. Note the base change from cystosine to thymidine resulting in an amino acid change of arginine to cysteine. Figure modified from (McCooke et al., 2012).

1.6.9.2 Structural and functional characteristics of the LPK kidney

The LPK rat demonstrates a progressive polyuria (Ding et al., 2012), which reflects an accelerated deficit in urine concentrating mechanisms. As previously described by Phillips and others (2007), a progressive nephromegaly (Fig. 1.13) is also observed in the LPK. These cysts are primarily due to fusiform dilatation of, predominantly, the collecting ducts, and to a lesser extent the distal convoluted tubule, thick ascending or thin descending limbs of the nephron (Phillips et al., 2007).

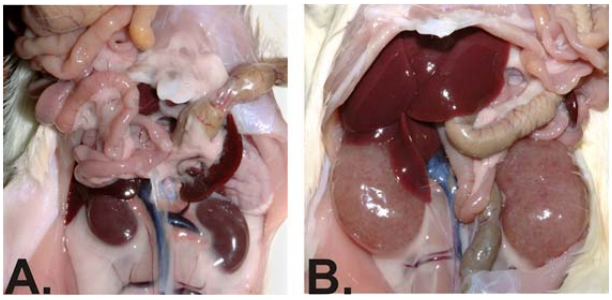

Figure 1.13: Gross kidney features in 12-week-old Lewis control (A) and Lewis Polycystic Kidney (LPK, B) rats. Figure illustrates the dramatic increase in size of the kidneys in LPK and their pale and nodular appearance. Figure taken from (Phillips et al., 2007) .

Cystic lesions (Fig. 1.14) are limited to the kidney. Three structural-functional phases have been identified by analysis of the renal histopathology correlated with phenotype in the LPK model (Phillips et al., 2007):

Phase I

This phase, which is known as the precursor cystic phase, is evident at week 1, where precursor cystic lesions, namely focal dilations of proximal and distal tubules, are observed prior to hypertension. This indicates that cystogenesis and subsequent renal structural abnormalities are key events in the genesis of hypertension and end-organ damage in PKD.

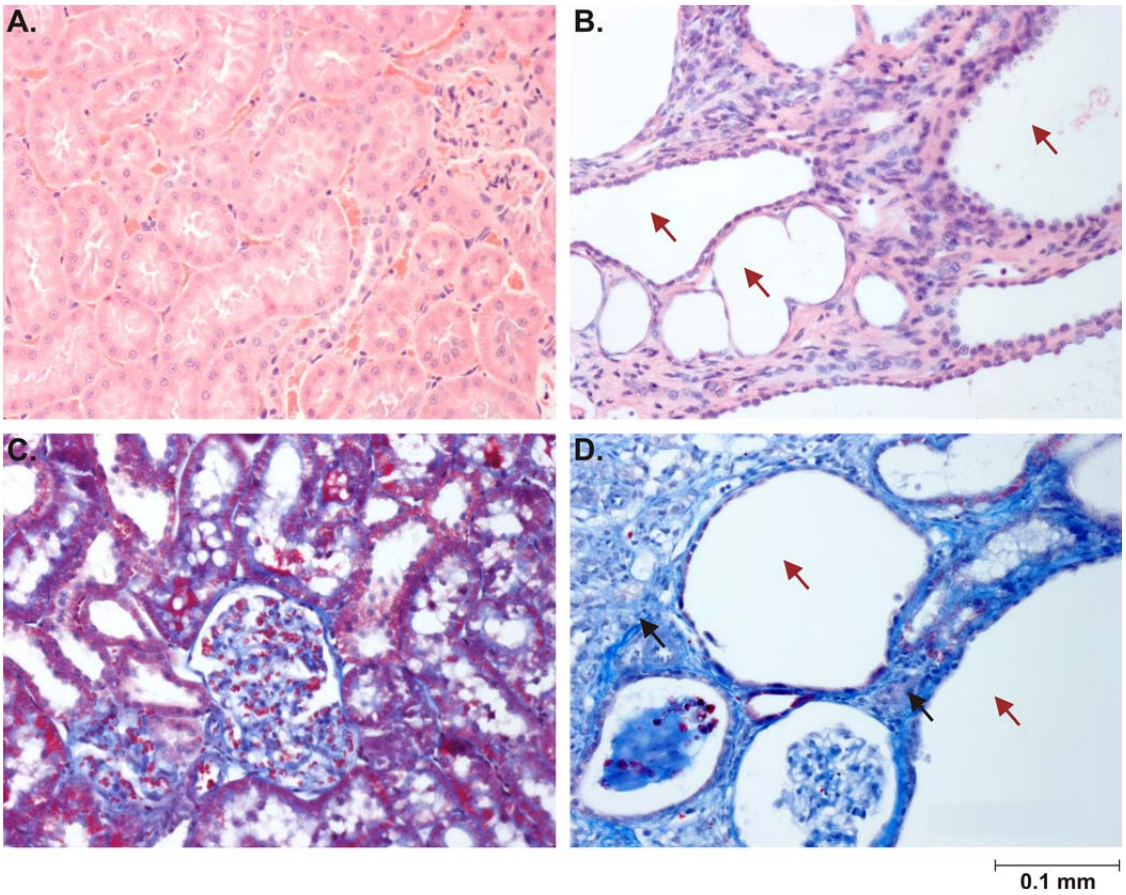

Figure 1.14: Light microscopy of kidney histological sections stained with haematoxylin and eosin (H&E, upper panels) and Masson's Trichrome (lower panels) in Lewis (A & C) and Lewis Polycystic Kidney (LPK, B & D) rats at 12 weeks of age. Images illustrate the cystic phenotype (red arrows in B & D) and fibrosis (black arrows in D blue showing areas of blue staining) in kidneys of the LPK. Images acquired at 20x magnification.

Phase II

This cystic phase is expressed at 3–6 weeks of age and is mainly characterised by gross derangement of the kidney cortex and medulla, where tubular epithelial cell proliferation and dedifferentiation, distal tubular dilatation and interstitial inflammation with compensatory preservation of renal function are present.

Phase III

Cystic phase III is characterised by tubulointerstitial fibrosis (Fig. 1.14) correlating with progressive significant deteriorations of renal function seen at 12 weeks of age. Cystic enlargement continues until week 24 but at slower rate, and normally precedes the development of any other typical histological features of ESRD, including interstitial macrophage and myofibroblast accumulation, interstitial fibrosis and tubular cell dedifferentiation.

Typical to CKD, deteriorations of renal function in the LPK are progressive and eventually lead to ESRD and death. During Phase II, serum creatinine levels remain within the normal/high range, while significantly higher levels are identified from 12 weeks of age onward. In addition to changes in serum creatinine, other functional markers of kidney function are also consistent with progression of renal dysfunction, including marked elevated serum urea, isosthenuria, decreased serum protein, increased urinary protein:creatinine ratio (UPC) and reduced packed cell volume of blood (Phillips et al., 2007).

1.6.9.3 Cardiovascular features of the Lewis Polycystic Kidney rat

Hypertension is a common finding in cystic kidney disease in humans (Gonzalo et al., 1996, Zerres et al., 2003) and is an important factor that not only accelerates renal failure but also drives a spectrum of cardiovascular changes including cardiomyopathy and LVH (Chapman et al., 1997, Ecder and Schrier, 2004). In the LPK, BP increases after early cystogenesis when changes in indicators of renal function are still undetectable. In this regard, the LPK rat model shows a strong similarity to human PKD, as described earlier. The model is also distinct to other rodent models of ARPKD which show no or only very mild to moderate elevations in BP (Al-Nimri et al., 2003, Braun et al., 1996, Lager et al., 2001, Nauta et al., 2000, Stringer et al., 2005).

Impairment of vascular structure and function as a result of hypertension and renal insufficiency is a major feature of both PKD (Kocaman et al., 2004, Kocyigit et al., 2012, Moorhead et al., 1974) and CKD (Blacher et al., 2001, Blacher et al., 2003) in humans. The LPK model demonstrates similar progressive functional and structural abnormalities of the vascular wall, including increased arterial stiffness, aortic wall hypertrophy and vascular remodelling (Ng et al., 2011a, Ng et al., 2011b). Functionally, increased arterial stiffening in the LPK has been proven experimentally by elevated pulse pressure readings and increases in pulse wave velocity (PWV) (Ng et al., 2011a, Ng et al., 2011b), a strong and independent predictor of cardiovascular risk in both hypertensive and CKD patients (Blacher et al., 2003). Structurally, altered aortic wall composition in the LPK is likewise suggestive of a stiff vasculature, demonstrating increased medial thickness, reduction in the elastin component of the arterial wall and marked arterial calcification (Ng et al., 2011a, Ng et al., 2011b) (Fig. 1.15).

The RAAS is also altered in the LPK, with animals showing suppressed plasma renin activity and Ang II at 10–12 weeks of age (Phillips et al., 2007). However, suppression of RAAS with perindopril, an

ACEi, from 6 weeks of age significantly reduces BP and limits vascular remodelling (Ng et al., 2011a).

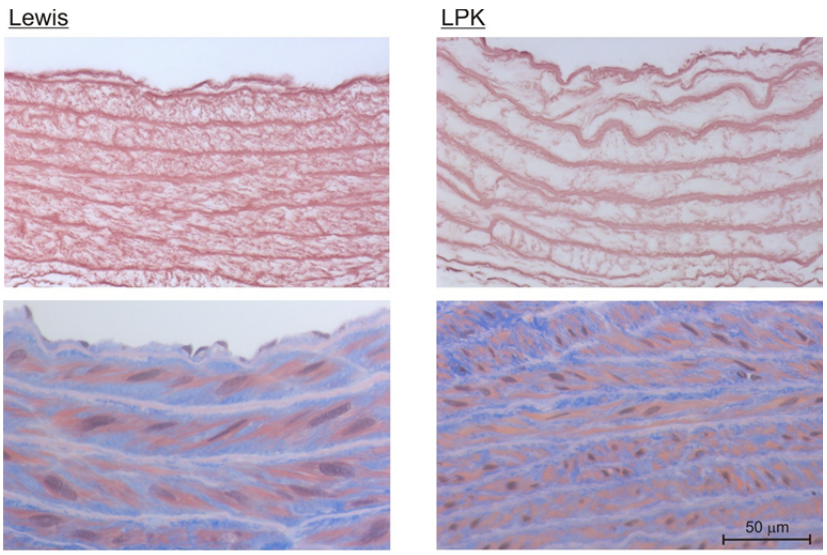

Figure 1.15: Typical histological sections of the thoracic aorta in Lewis (left) and Lewis Polycystic Kidney (LPK, right) rats at 12 weeks of age, stained with Shitaka's orcein (*top*), showing the elastin component in red, and Martius Scarlet Blue (*bottom*), showing the collagen component in blue and the nuclei in black. A reduction in elastin density can be observed in the LPK compared with Lewis rat. Figure taken for (Ng et al., 2011).

Apart from deficits in the vascular and hormonal systems of the LPK, defects also extend to the ANS, showing a classical presentation of altered sympathovagal balance and autonomic dysfunction. As observed in human PKD (Klein et al., 2001, Neumann et al., 2002) and CKD (Converse et al., 1992, Grassi et al., 2011a, Klein et al., 2003a, Koomans et al., 2004, Neumann et al., 2007), several lines of evidence suggest increased SNS activity in the LPK, a likely contributor to the hypertensive state, including enhanced depressor responses to ganglionic blockade (Phillips et al., 2007), increased bradycardic responses to β_1-adrenergic receptor blockade with atenolol (Harrison et al., 2010), elevated LF band of SBPV (Harrison et al., 2010, Hildreth et al., 2013b), an upward shift in the baroreflex function of splanchnic SNA and an inability to maximally suppress SNA in response to increases in BP (Harrison et al., 2010). In addition to sympathetic overactivity, the LPK exhibit reduced cardiac vagal tone and impaired baroreflex control of HR by 12 weeks of age, findings evidenced by depressed tachycardic responses to muscarinic receptor blockade with methylatropine, blunted HR BRS (spontaneous or pharmacologically driven) and reductions in the HF and/or LF components of HRV, under both conscious or unconscious settings (Harrison et al., 2010, Hildreth et al., 2013b). Collectively, this data support the use of the LPK rat model as an excellent experimental tool to understand the mechanisms of cardiovascular autonomic dysfunction in CKD.

1.7 Thesis objectives

Chronic kidney disease is worldwide public health problem that carries an increasing risk of cardiovascular morbidity and mortality (Couser et al., 2011, Schiffrin et al., 2007). Autonomic dysfunction is a major complication of CKD (Cashion et al., 2000, Dursun et al., 2004, Rubinger et al., 2009), possibly underpinning the high incidence of CVD in this patient population. Sympathetic overdrive (Klein et al., 2001, Neumann et al., 2007, Zoccali et al., 2002) and impaired HR baroreflex function (Johansson et al., 2007, Studinger et al., 2006, Tinucci et al., 2001) are often observed in

CKD patients; however, the principle underlying mechanisms are incompletely understood. While the presence of impaired HR baroreflexes is well established in CKD, deficits in the baroreflex control of SNA are not. Therefore, a key objective **(Aim 1)** of this thesis was to investigate sympathetic baroreflex function in the genetic rat model of CKD, the LPK rat, using recordings of RSNA.

The cause of impaired baroreflex function in CKD may relate, at least in part, to an inability of the aortic arch or carotid sinus baroreceptors to properly detect changes in BP (i.e., impaired sensory afferent neurotransmission); effects which are probably driven by altered vascular distensibility and structural remodelling of the arteries in CKD. Alternatively, impaired central processing of baroreceptor afferent input and an inability to induce effective reflex changes in sympathetic and vagal outflow to the heart and vasculature may potentially underlie baroreflex deficits in CKD. Accordingly, another key objective **(Aim 2)** was to localise the site of deficit within the baroreflex arc responsible for generating altered baroreflex functions in CKD. Given the progressive nature of CKD (Campese et al., 1995, Grassi et al., 2011a), this study also aimed to identify the time course over which baroreflex dysfunction is expressed in CKD, and whether this relates to temporal deteriorations in the afferent, central and efferent components of the baroreflex pathway **(Aim 3)**.

The association between autonomic dysfunction and increased cardiovascular mortality in CKD is well described (Chesterton and McIntyre, 2005, Thapa et al., 2010). However, women with CKD appear to have a relatively lower risk of developing CVD and related complications (National Kidney Foundation, 2013). In view of this, the next series of studies were designed to characterise temporal changes in baroreflex function in the female sex and assess the integrity of the afferent and central drives of the baroreflex arc, and their ability to evoke baroreflex-mediated changes in HR and sympathetic outflow **(Aim 4)**. A further aim that consequently emerged was to establish whether baroreflex dysfunction in CKD is differentially expressed in males and females and contributed to by sex-dependent deteriorations in different components of the baroreflex pathway **(Aim 5)**.

Impairments of baroreflex function and resultant pathologic manifestations in autonomic neuroregulation are consistently encountered in CKD. However, whether deficits in the autonomic functions relate to baroreceptor-independent mechanisms that can similarly modulate autonomic outflows such as the vagal afferent pathway have never been reported. Therefore, this thesis also aimed to investigate if deficits in the central processing of vagal afferent input could possibly underlie impaired reflex regulation of vagal and sympathetic outflow to the heart and vasculature, hence contributing to autonomic dysfunction in CKD **(Aim 6)**.

A large body of evidence indicates increased SNA in CKD; however, these reports were mainly based on acute recording of SNA (Grassi et al., 2011a, Hausberg et al., 2002, Klein et al., 2001, Klein et al., 2003b, Neumann et al., 2007). Sympathetic nerve activity specifically to the kidney has the potential to have a much larger influence on long-term levels of arterial BP, given the role of

RSNA in not only altering blood flow but also regulating salt and water reabsorption (DiBona and Kopp, 1997, Johns et al., 2011). Accordingly, the last aim of this thesis was to establish dual recording of BP and RSNA in the LPK model of CKD using telemetry in conscious animals, examining the hypothesis that elevation of RSNA is a key pathological feature of CKD **(Aim 7)**.

2 Additional Methodology

The following section details methodology not otherwise provided in thesis Chapters 3–5 in association with their presentation in publication format.

2.1 Ethical approval

All studies were approved by the Macquarie University Animal Ethics Committee and carried out in accordance with the Australian Code of Practice for the Care and Use of Animals for Scientific Purposes.

2.2 Animals

For non-recovery experiments, juvenile (7–8 weeks old) and adult (12–13 weeks old) Lewis and Lewis Polycystic kidney (LPK) rats of either sex were used. For recovery telemetry probe implantation experiments, male Lewis and LPK rats (10–11 weeks old) were used. All animals were purchased from the Animal Resource Centre (ARC) in Western Australia and housed in the Animal House Facility of Macquarie University. Rats were habituated for at least a week prior to the conduction of any experimental procedure. All animals were kept under a 12-hour light/dark cycle and received a standard pellet diet and water *ad libitum*. Cystic kidney disease in the LPK was confirmed macroscopically at surgery or post-mortem by the presence of grossly enlarged kidneys with pale and nodular appearance (Phillips et al., 2007) or otherwise by palpation from age 6 weeks onwards.

2.3 Detailed histological staining procedure

Aortic arch vascular tissues were fixed as detailed in the relevant method section of Chapters 3 and 4. Five-µm thick aortic sections were mounted on glass slides and incubated at 37°C overnight. Sections were then deparaffinised by immersing in HistoChoice® clearing agent (AMRESCO, Inc., USA, 3×10 minutes). Sections were subsequently rehydrated by dipping in descending grades of alcohol (100%: 2×5 minutes, 85%: 2×3 minutes and 70%: 1×1 minute) followed by rinsing under running tap water (3 minutes).

Following completion of specific staining protocols (see below), all section were dehydrated by immersing in ascending grades of alcohol (70%: several dips, 85%: 2×3 minutes and 100%: 3×10 dips) followed by HistoChoice (3×5 minutes). For long-term storage and maintenance of a high refractive index for microscope examination, dehydrated sections were then mounted with a coverslip using DPX mounting media (Sigma-Aldrich, Spain).

Shikata's orcein staining procedure: Deparaffinised and hydrated aortic sections were first treated with 0.15% potassium permanganate (Sigma-Aldrich, Germany) in 3% aqueous sulphuric acid (Univar,

Ajax Finechem Pty Ltd, Australia) solution for 3 minutes then rinsed with running water. The sections were then decolorized with 1% aqueous oxalic acid (Sigma-Aldrich, Germany) (5 dips) then washed in water. Subsequently, all sections were stained with 5% Shikata orcein (Sigma-Aldrich, Germany) in 1% (v/v) alcoholic (70%) hydrochloric acid (Univar, Ajax Finechem Pty Ltd, Australia) solution for 15 minutes. The tissue slides were then rinsed, dehydrated and mounted in DPX. Stained sections would subsequently show elastin fibres as red, purple or brown.

Martius Scarlet Blue (MSB) staining procedure: Deparaffinised and hydrated aortic sections were first immersed in a preheated (60 °C) Bouin's fixative [a 0.9% aqueous solution of picric acid (Sigma-Aldrich, Germany), 5% glacial acetic acid (Univar, APS Asia pacific speciality chemicals Ltd, Australia) and 0.9% of 40% formaldehyde (Univar, Ajax Finechem Pty Ltd, Australia)] and placed in a 60°C oven for 1 hour. The fixative was then removed from slides by washing under running tap water. Nuclei in the aortic section were stained with 1% aqueous solution of Celestine blue (Sigma-Aldrich, USA), to which a 5% ferric ammonium sulphate (Sigma-Aldrich, USA) and 14% (v/v) glycerine (Sigma-Aldrich, USA) were added, for 8 minutes followed by immersion in Harris's haematoxylin solution (Clinipure stains & reagents for pathology, HD scientific supplies, Australia) for additional 5 minutes. Sections were then rinsed in water followed by 95% alcohol (Sigma-Aldrich, Germany), and subsequently treated with 0.5% Martius Yellow (Sigma-Aldrich, USA) in 2% alcoholic (95%) phosphotungstic acid (Sigma-Aldrich, Germany) solution for 3 minutes. Rinsed sections were then stained for smooth muscle and mature fibrin by treating with 1% Brilliant Crystal Scarlet (Sigma-Aldrich, Germany) in 2.5% aqueous acetic acid (Univar, APS Asia pacific speciality chemicals Ltd, Australia) solution for 10 minutes. Sections were then washed in water to remove excess Brilliant Crystal Scarlet stain and subsequently immersed in 1% aqueous phosphotungstic acid for 10 minutes. Rinsed sections were lastly treated with 0.5% soluble blue (Sigma-Aldrich, Germany) in 1% aqueous acetic acid solution for 15 minutes to stain collagen. All slides were rinsed, dehydrated then mounted in DPX. Stained sections would subsequently show nuclei in black, muscle in red and collagen in blue.

Von Kossa staining procedure: To stain calcium salts, deparaffinised and hydrated aortic sections were first incubated with 1% aqueous silver nitrate (Sigma-Aldrich, USA) solution maintained under ultraviolet light for 60 minutes. Sections were then rinsed in several changes of distilled water and excess unreacted silver nitrate removed by submerging section in a 5% aqueous sodium thiosulfate (Sigma-Aldrich, Germany) for 5 minutes. The sections were again washed in distilled water then counterstained with a 0.1% nuclear fast red (Sigma-Aldrich, USA) in 5% aqueous aluminium sulphate (Univar, APS Asia pacific speciality chemicals Ltd, Australia) for 5 minutes. Stained sections were then rinsed in water to remove excess stain, dehydrated then mounted in DPX. Stained section would subsequently show calcium salts in black or brown, cytoplasm in pink and nuclei in red.

3 Differential Contribution of Afferent and Central Pathways to the Development of Baroreflex Dysfunction in Chronic Kidney Disease

Ibrahim M. Salman, Cara M. Hildreth, Omar Z. Ameer, Jacqueline K. Phillips

Australian School of Advanced Medicine, Macquarie University, Sydney, NSW, Australia

The following Chapter is a modified version of the published paper: Salman, I.M., Hildreth, C.M., Ameer, O.Z. and Phillips, J.K. (2014). Differential contribution of afferent and central pathways to the development of baroreflex dysfunction in chronic kidney disease. *Hypertension*, 63, 804-10.

Abstract

The effects of chronic kidney disease (CKD) on baroreflex control of renal sympathetic nerve activity (RSNA) and deficits in afferent, central and/or efferent components of the baroreflex were studied in juvenile and adult male Lewis Polycystic Kidney (LPK) and control Lewis rats under anaesthesia (n = 35). Blood pressure (BP), heart rate (HR), aortic depressor nerve activity (ADNA) and RSNA were determined after pharmacological manipulation of BP. Responses to ADN and vagal efferent stimulation (4.0V, 2.0-ms, ADN: 1–24Hz and vagal efferent: 1–48Hz) were determined and the aortic arch collected for histomorphometry. In juvenile LPK versus age-matched Lewis, gain of RSNA (-1.5 ± 0.2 vs. -2.8 ± 0.2 %/mmHg; P<0.05) and ADNA (2.5 ± 0.3 vs. 5.0 ± 0.6 %/mmHg; P<0.05), but not HR barocurves was reduced. BP, HR and RSNA responses to ADN stimulation were normal and/or enhanced in juvenile LPK. HR responses to vagal efferent stimulation remained unchanged. In adult LPK versus age-matched Lewis, the gain and range of RSNA (gain: -1.2 ± 0.1 vs. -2.2 ± 0.2 %/mmHg, range: 62 ± 8 vs. 98 ± 7%) and HR (gain: -0.7 ± 0.1 vs. -3.5 ± 0.7 bpm/mmHg, range: 44 ± 8 vs. 111 ± 19 bpm) barocurves were reduced (P<0.05). The gain and range of the ADNA barocurves were also reduced in adult LPK versus Lewis [1.5 ± 0.4 vs. 5.2 ± 1.1 (%/mmHg) and 133 ± 35 vs. 365 ± 61 (%); P<0.05] and correlated with aortic arch vascular remodelling. BP, HR and RSNA responses to ADN stimulation were significantly reduced in adult LPK, whereas their HR responses to vagal efferent stimulation were comparable to controls and juvenile LPK. Our data demonstrates a deficit in the afferent component of the baroreflex that precedes the development of impaired central regulation of RSNA and HR in CKD, and that progressive impairment of both components is associated with marked dysfunction of the baroreflex pathway.

Key words: heart rate, renal sympathetic nerve activity, aortic depressor nerve activity, baroreflex, hypertension, chronic kidney disease

3.1 Introduction

Autonomic dysfunction is a major complication of chronic kidney disease (CKD) (Cashion et al., 2000, Dursun et al., 2004) and is likely a key contributor to the high incidence of cardiovascular mortality in this patient population. In addition to sympathetic overdrive, evidenced by increased sympathetic nerve activity (SNA) (Converse et al., 1992, Hausberg et al., 2002, Klein et al., 2001) and plasma noradrenaline levels (Zoccali et al., 2002), baroreflex control of heart rate (HR) is impaired (Harrison et al., 2010, Johansson et al., 2007, Tinucci et al., 2001). Impaired baroreflex control of HR

is directly correlated with the severity of CKD (Lacy et al., 2006) and is an independent risk factor for sudden cardiac death in people with CKD (Johansson et al., 2007). Whether or not baroreflex control of SNA is impaired in CKD is unclear, with mixed reports of normal (Ligtenberg et al., 1999) and impaired (Tinucci et al., 2001) responses. Moreover, the mechanisms underlying baroreceptor dysfunction in CKD are unknown and could relate to an inability for the baroreceptor afferents, including the aortic depressor nerve (ADN) and carotid sinus nerve (Ninomiya et al., 1971), to sense changes in blood pressure (BP), influenced by factors such as altered vascular distensibility and mechanotransduction at the receptor level. Alternatively, central relay nuclei such as the nucleus tractus solitarius (NTS), nucleus ambiguus or ventrolateral medullary sites may fail to produce sufficient change in vagal or sympathetic outflow, or the heart and/or vasculature may inadequately respond to these autonomic inputs.

Previously we demonstrated that the Lewis Polycystic Kidney (LPK) rat, an animal model of autosomal recessive cystic kidney disease arising from a mutation in the *Nek8* gene (McCooke et al., 2012), develops impaired baroreflex control of HR between 10 and 12 weeks of age (Hildreth et al., 2013b). In the present study we wished to identify if a temporal impairment in baroreflex control of renal SNA (RSNA) also occurs in the LPK, and at what point within the baroreflex arc dysfunction occurs. We therefore compared the functionality of the afferent, central and efferent components of the baroreflex in LPK and control Lewis rats, at 7–8 weeks of age, when the heart rate reflex is intact, and 12–13 weeks of age, when the heart rate reflex is impaired (Hildreth et al., 2013b) and renal function has deteriorated (Phillips et al., 2007). As progressive remodelling occurs along the thoracic aorta in the LPK between 6 and 12 weeks of age (Ng et al., 2011b), we hypothesised that similar vascular remodelling would occur along the aortic arch, a site of origin of baroreceptors, and be associated with reduced functionality of the afferent component of the baroreflex.

3.2 Methods

3.2.1 Animals

Male juvenile (7–8 weeks old) and adult (12–13 weeks old) LPK (n = 32) and Lewis (n = 31) were sourced from the Animal Resource Centre, Murdoch, Western Australia, Australia. All experiments were approved by the Animal Ethics Committee of Macquarie University and carried out in accordance with the Australian Code of Practice for the Care and Use of Animals for Scientific Purposes.

The LPK model is a result of a mutation in *Nek8* (McCooke et al., 2012), which in humans is responsible for nephronophthisis (NPHP)9 (Frank et al., 2013, Otto et al., 2008). Multiple NPHP genes have been identified that encode for the nephrocystin protein family and overall they constitute a group of autosomal-recessive cystic kidney disorders that are the leading genetic cause of end-stage renal disease in children and young adults (Frank et al., 2013). In the juvenile cystic kidney (jck) mouse (Liu et al., 2002) and LPK rat (Phillips et al., 2007) the *Nek8* mutation leads to a phenotypic

presentation of cystic kidney disease that resembles human autosomal recessive polycystic kidney disease.

3.2.2 Anaesthesia and surgical procedures

For in-vivo studies, animals (n = 35 total) were anaesthetised with ethyl carbamate (urethane, 1.3 g/kg i.p., Sigma Aldrich, Australia). Depth of anaesthesia was confirmed by absence of reflex response to tactile (corneal stroking) and noxious (hindpaw pinch) stimuli. Supplemental doses of urethane (10–20 mg i.v.) were administered as required. Immediately following induction of anaesthesia, rectal temperature was monitored and maintained at 37ºC using a thermostatically controlled heating blanket and infrared heating source, and supplemental oxygen provided. A tracheostomy was performed and if required, the animal was artificially ventilated with oxygen enriched room air and ventilation adjusted to maintain pH at 7.40 ± 0.05 and PCO_2 at 40 ± 5 mmHg.

The right jugular vein and both femoral veins were cannulated for the administration of fluids (Ringer's solution, 5 ml/kg/hr) and drugs respectively. The right carotid artery was cannulated and connected to a pressure transducer for the recording of BP, which was sampled at 250 Hz and acquired using a CED 1401 plus (Cambridge Electronic Designs Ltd, Cambridge, UK) and Spike 2 (v7, Cambridge Electronic Designs Ltd., Cambridge, UK). Heart rate was derived online from the BP signal.

The left ADN was isolated as it joined the cervical vagus nerve near the superior laryngeal nerve. Isolation of the ADN was confirmed using the following criteria: 1. audio confirmation that the nerve had a bursting discharge pattern; 2. pulse synchronous discharge of nerve activity with the systolic phase of the cardiac cycle; and 3. an increase and a decrease in activity following administration of phenylephrine (PE) and sodium nitroprusside (SNP), respectively.

The left renal nerve was isolated retroperitoneally. Both the renal nerve and ADN were dissected by the same investigator, maintained in paraffin oil and recorded whole using bipolar silver wire recording electrodes, amplified, band-pass filtered (10–1000Hz, CWE Inc., Ardmore, PA, USA) and sampled at 5 kHz using a CED 1401 plus and Spike2, using the same bioamplifier calibrated to a pre-set 50 µV setting.

3.2.3 Experimental protocols

Following stabilisation of baseline parameters, rats underwent at least one of the protocols detailed below to assess the different components of the baroreflex arc. Baroreflex control of HR and sympathetic outflow were examined by measuring changes in HR and RSNA in response to changes in mean arterial pressure (MAP). The afferent component of the baroreflex arc was assessed by determining changes in ADN activity (ADNA) in response to changes in MAP. The central component of the baroreflex arc was tested by measuring the changes in HR and RSNA to direct stimulation of the ADN and also by correlating changes in ADNA and RSNA in response to

alterations in MAP. The efferent arm of HR baroreflex was assessed by measuring changes in HR in response to direct stimulation of the vagal efferent nerve.

Protocol I: Assessment of the relationship between BP and ADNA, RSNA and HR. Blood pressure was manipulated using sequential bolus injections of PE (10–50 µg/kg i.v.) and SNP (50–70 µg/kg i.v.) administered over ~5 seconds, in order to increase MAP to 200–250 mmHg maximum and reduce it down to 50 mmHg, respectively. This was repeated at least 3 times. Changes in ADNA, RSNA and HR were recorded in response to each drug administration and all variables were allowed to return to baseline levels prior to subsequent drug administration. Where possible the relationship between MAP and ADNA was assessed simultaneously to the relationship between MAP and RSNA. In animals that subsequently underwent Protocol II (see below), the ADN was cut distal to the recording electrode and background ADNA recorded. Animals that did not undergo Protocol II were euthanased with an overdose of sodium pentobarbital (60 mg/kg i.v., Virbac® Pty Ltd., Australia) and background ADNA recorded.

Protocol II: Assessment of the RSNA, HR and BP response to ADN stimulation. The ADN was cut and the proximal end stimulated sequentially using a 5-second train (4.0V, 2.0-ms pulses) of 1, 2, 4, 8, 16 and 24 Hz separated by a period of 3–5 minutes, as described previously (Huber and Schreihofer, 2010, Ma et al., 2002, Salgado et al., 2007). Peak RSNA, HR and BP responses were observed within the first two seconds of ADN stimulation and were sustained until the stimulation was ceased. Responses were continuously recorded.

Protocol III: Assessment of the HR response to cervical vagal efferent stimulation. The left vagus nerve was cut and the peripheral end stimulated sequentially using a 5-second train (4.0V, 2.0-ms pulses) of 1, 2, 4, 8, 16, 24, 32, 40 and 48 Hz separated by a period of 3–5 minutes. Peak HR responses were continuously recorded.

At the end of the experiment, the renal nerve was cut proximally to the recording electrode and background RSNA recorded. The animal was then either euthanased with an overdose of 60 mg/kg sodium pentobarbital i.v. or transcardially perfused with heparinised 0.9% saline followed by 4% formalin in saline and the aortic arch removed and stained with Shikata's orcein, Martius Scarlet Blue (MSB) or Von Kossa for histomorphometry.

Urinary protein:creatinine (UPC) ratio: A separate cohort of age-matched animals (n = 25 total) were individually held in metabolic cages for at least 4 hours to collect urine samples. Urine was then centrifuged at 3000 rpm for 5 minutes and stored at -20^{0}C until further assayed for urinary protein (U_{Pro}), urinary creatinine (U_{Cr}) and UPC using an IDEXX VetLab analyser (IDEXX Laboratories Pty Ltd., NSW, Australia).

3.2.4 Data analysis

All data was analysed offline using Spike 2 software, GraphPad Prism (GraphPad Prism software v6 Inc., La Jolla, CA, USA) and/or Axiovision software (AxioVs40 v4.8.2.0, Carl Zeiss Microimaging, Gottingen, Germany).

Baseline data: Mean arterial pressure, systolic BP (SBP), diastolic BP (DBP) and HR were derived from the arterial pressure waveform. Both RSNA and ADNA waveforms were full-wave rectified, a 1-second smoothing constant applied and the level of activity following nerve transection or euthanasia subtracted.

Baseline measurements of MAP, SBP, DBP, pulse pressure (PP), HR, RSNA and ADNA were taken over a 30-second period immediately prior to commencement of the experimental protocol.

In order to confirm the integrity of the RSNA signal and eliminate renal afferent nerve activity as a confounding variable, a pilot study using adult LPK (n = 3) was undertaken where RSNA recordings were assessed before and after ganglionic blockade [hexamethonium (20 mg/kg i.v.)] and then compared to levels after euthanasia. RSNA was significantly reduced after ganglionic blockade (6.4 ± 0.8 vs. 2.2 ± 0.2 μV, P = 0.003) and did not change any further after euthanasia (2.3 ± 0.3 μV, P>0.99 vs. after hexamethonium). P values are the outcomes of one-way ANOVA and Bonferroni post-hoc analysis.

Baroreceptor afferent, central and reflex function curves: Baroreceptor reflex regulation of ADNA, RSNA and HR were examined by comparing changes in ADNA, RSNA and HR, in response to pharmacologically-evoked increases and decreases in BP using PE and SNP, respectively (Figure 3.1). In animals where simultaneous recordings of ADNA and RSNA were made, indirect assessment of the central component of the baroreceptor reflex was evaluated by comparing RSNA (efferent output) with ADNA (afferent input) over the pharmacologically-evoked increase and decrease in BP achieved using PE and SNP.

Both RSNA and ADNA were normalised, setting a 30-second period immediately prior to PE and SNP administration as 100% and the level of background nerve activity, which was subtracted from the original recordings, as 0%. The baseline levels of RSNA, ADNA and HR prior to administration of PE or SNP were compared to ensure that resting levels of nerve activity and HR did not differ between drug administrations; however, due to a range in the time intervals between PE and SNP administration, nerve activity immediately prior to each drug administration was used to normalise to 100%.

The relationship between the active phase of MAP change (from resting level of BP through to the peak BP change induced by PE or SNP) and induced responses in HR (beats per minute, bpm), RSNA (% and μV) or ADNA (%) were fitted to a four-parameter sigmoid logistic function curve (GraphPad Prism software) using the following equation:

$$y = \frac{A_1}{1 + \exp[A_2(MAP - A_3)]} + A_4$$

where A_1 is the y axis range of the curve, A_2 is the gain coefficient, A_3 is midpoint of the curve and A_4 is the lower plateau. Curves with a R^2 value less than 0.9 were not included in the data set (see Figure 3.2 for example curves showing goodness of fit). In order to account for the time delay between a change in BP and the reflex change in HR, the relationship between an increase and a decrease in BP and the concomitant change in HR was shifted by 10 beats with respect to their corresponding R-R interval as described previously (Kellett et al., 2005).

From each individual non-linear regression curve generated, the following parameters were obtained: range of the curve (A_1), the gain coefficient (A_2), midpoint of the curve (A_3) and lower plateau (A_4). Using these parameters, the range of the reflex (i.e. HR range, RSNA range and ADNA range), the gain of the reflex, MAP_{50}, MAP threshold (MAP_{thr}) and MAP saturation (MAP_{sat}), MAP operating range and HR, RSNA and ADNA values at MAP_{thr} and MAP_{sat} were calculated as described previously (Kent et al., 1972). Each individual parameter was then averaged to create a mean value for each group of animals (juvenile LPK, juvenile Lewis, adult LPK and adult Lewis).

Using the same equation described above, the relationship between ADNA and RSNA was fitted to a sigmoid regression curve as described previously (DiBona and Sawin, 1994) and parameters of the curve fit calculated. Curves with a R^2 value less than 0.85 were not included in the data set.

Each individual non-linear regression curve was averaged to obtain single logistic function curve per group. The MAP and HR, RSNA or ADNA relationships were then plotted over a fixed range of 50–200 mmHg in the Lewis and 50–250 mmHg in the LPK, reflecting the maximal PE and SNP-induced changes in MAP evoked in these two strains. The ADNA-RSNA curves were plotted over the range of ADNA evoked in response to these same BP ranges in each strain.

Heart rate baroreflex function was further examined by separately calculating the sensitivity of the relationship between an increase and decrease in BP and the reciprocal reflex bradycardia (BRS_{PE}) or tachycardia (BRS_{SNP}), respectively, as follows:

$$sensitivity = \frac{\text{change in HR (bpm)}}{\text{change in MAP (mmHg)}}$$

ADN stimulation: Reflex responses to ADN stimulation were determined by measuring peak changes in RSNA (% and μV), HR (bpm) and MAP (mmHg) relative to an immediate 30-second baseline prior to the application of each electrical stimulus.

Vagal efferent stimulation: Reflex responses to vagal efferent stimulation were determined by measuring peak changes in HR (bpm) relative to an immediate 30-second baseline prior to the application of each electrical stimulus.

Histomorphometry: After perfusion with fixative, the aortic arch from each animal was excised, cleaned of adherent fat and connective tissue, and stored in 70% ethanol. The aortic arch was then dehydrated and fixed, as described previously (Ng et al., 2011b), embedded in paraffin and transverse sections (5 μm) cut using a microtome (Leica Microm HH325, Germany), and mounted onto glass slides. Sections were stained for Shikata's orcein, MSB, and Von Kossa. Photos were captured using a video camera mounted on a microscope (Carl Zeiss Microimaging, Gottingen, Germany) and processed with Zeiss Axiovision. Images were corrected for brightness and contrast only and analysis performed using Image J (v1.47d, National Institute of Health, USA). Evaluation of aortic thickness, elastin lamellae fracture points, calcium density and average size of calcium deposits was performed on the whole aortic segment (captured at 10x magnification) for each animal. All other histomorphometric parameters were calculated from an average of 4 fields equally distributed around the circumference of the aorta from each segment of the aortic arch (captured at 20 x magnifications). Wall thickness was measured on at least eight separate aortic arch regions for each animal and averaged. Specific analysis for each stain was as follows:

Shikata's orcein: Analogue images were digitized and separated into 3 coloured images (red, blue and green). Subsequent image processing was performed on the red image only, indicating the elastin component of the aortic arch. The images were then binarized to extract relative measures of elastin in the field examined.

The number of elastin lamellae fracture points was normalised using the following equation:

$$\frac{\text{number of fracture points}}{\text{average of inner and outer circumfence} \times \text{number of lamellae}}$$

Martius Scarlet Blue (MSB): The MSB stained images were analysed by setting a threshold, which allowed for visualisation and quantification of the blue colour, indicating the total collagen density. All images were then binarized to extract relative measures of collagen and the smooth muscle cell nuclei in the studied field. Nuclei were detected by setting a minimum threshold on the binarized image and the total number of nuclei summated.

Von Kossa: The total calcium density and average size of calcium deposit in the media on Von Kossa-stained sections was quantified by setting a minimum threshold on the binarized image to visualise the black calcium deposits in the aortic media.

All binarized images were visually inspected by two investigators and compared with the original image to ensure that all parameters were detected accurately.

Correlation analysis: The gain and range of the MAP-ADNA function curves were correlated with the aortic arch histomorphometrical indices detailed above including medial wall thickness and measures of elastin, collagen and calcium content. Correlation analysis was performed using a Pearson correlation followed by linear regression.

3.2.5 Statistical analysis

All data are expressed as mean ± standard error of the mean (SEM). Statistical analysis was performed using GraphPad Prism software. A two-way ANOVA with Bonferroni's correction was used to identify differences between groups (strain and age). A Brown-Forsythe test was used to determine if there were any differences in the variance, and if so, the data was log-transformed before statistical analysis. Significance was defined as $P \leq 0.05$.

3.3 Results

3.3.1 Baseline data

Baseline levels of MAP, SBP, pulse pressure (PP), HR and RSNA were elevated in the LPK compared to age-matched controls (Table 3.1). SBP were overall significantly higher in the adult versus juvenile animals. An age-related increase in PP was observed in the LPK. No difference in aortic depressor nerve activity (ADNA) was observed between LPK and age-matched controls but there was an age-related increase in the LPK, despite no concomitant increase in HR. Regardless of age, U_{Pro} was elevated and U_{Cr} was reduced in the LPK versus Lewis. Urinary protein: creatinine ratio was also elevated in both juvenile and adult LPK versus age-matched controls and further elevated in adult versus juvenile LPK (Table 3.1).

3.3.2 Baroreceptor reflex control of HR, RSNA and ADNA

Reflex HR, RSNA and ADNA responses to pharmacologically-evoked increases and decreases in BP following administration of PE and SNP, respectively, are illustrated in Figure 3.1. Representative curves showing the sigmoidal fit of the MAP-HR, MAP-RSNA and MAP-ADNA relationship in adult Lewis and LPK rats are shown in Figure 3.2, and group data in Figure 3.3.

(i) Baroreflex control of HR: In both juvenile and adult LPK there was a rightward shift in the HR baroreflex function curve compared with age-matched controls (Figure 3.3A), as indicated by an increase in the MAP_{50} (Table 3.2). In the juvenile LPK, the curve was shifted upward as demonstrated by an increase in the upper plateau of the curve. However, both the lower plateau and the range of the curve were not significantly different between the juvenile LPK and Lewis (Tables 3.2). In the adult LPK, the upper plateau of the curve did not differ compared with age-matched controls. The lower plateau, however, was higher and therefore there was a reduction in the range of the curve in the adult LPK compared with adult Lewis (Tables 3.2). The gain of the reflex was comparable in the juvenile LPK and Lewis, but was reduced in the adult LPK versus Lewis (Table 3.2). Consequently, there was an age-related reduction in both the range and the gain of the HR baroreflex in the LPK (Table 3.2).

When the reflex bradycardic and tachycardic components were assessed separately, the sensitivity of the relationship between an increase in MAP and decrease in HR (BRS_{PE}) was not significantly different in the juvenile LPK versus Lewis (1.61 ± 0.23 vs. 0.99 ± 0.10 bpm/mmHg, $P = 0.08$) but was reduced in the adult LPK (0.50 ± 0.10 bpm/mmHg) compared with both age-matched Lewis (1.38 ±

0.22 bpm/mmHg, $P<0.01$) and juvenile LPK ($P<0.01$). In the Lewis, by contrast, BRS_{PE} did not significantly change with age ($P = 0.32$). The sensitivity of the reflex tachycardic component (BRS_{SNP}) was reduced overall in the LPK versus Lewis ($P = 0.04$), but was uninfluenced by age in either strains (Lewis: 0.45 ± 0.08 vs. 0.59 ± 0.14 and LPK: 0.29 ± 0.04 vs. 0.27 ± 0.05 bpm/mmHg, juvenile vs. adult, both $P>0.05$).

(ii) Baroreflex control of RSNA: RSNA baroreflex function curves were shifted to the right in both the juvenile and adult LPK (Figure 3.3B). Accordingly $MAP_{50,}$ MAP_{thr} and MAP_{sat} were higher in the LPK versus age-matched Lewis (Tables 3.2). In juvenile LPK, there was no difference in the upper and lower plateau, and therefore range, of the reflex compared to juvenile Lewis (Tables 3.2). In adult LPK, the upper plateau was comparable; however, the lower plateau and therefore RSNA at MAP_{sat} were higher versus Lewis and juvenile LPK rats (Table 3.2). Consequently, the range of RSNA (%) was reduced in adult LPK versus adult Lewis and juvenile LPK (Table 3.2). The gain of the RSNA baroreflex was reduced in both juvenile and adult LPK and an overall age-related decline in the adult versus juvenile was observed (Table 3.2).

As baseline RSNA was elevated in the LPK, baroreflex function curves were also generated using microvolt RSNA (Figure 3.4). Accordingly, there was an increase the upper plateau of the reflex and RSNA at MAP_{thr} and MAP_{sat} in the juvenile LPK versus age-matched Lewis (Table 3.3). Compared to age-matched Lewis, the lower plateau was shifted upward in adult LPK and this was associated with markedly higher measures of RSNA at MAP_{sat}. An overall age effect influenced values of the upper plateau, being lower in the adult versus juvenile rats. The gain and range of the reflex expressed in microvolts was not different between the LPK and Lewis at any age; however, both parameters declined with age in the LPK (Table 3.3).

(iii) Baroreflex control of ADNA: Administration of SNP markedly reduced ADNA while PE resulted in an increase in ADNA (Figure 3.1). For ADN burst frequency analysis see Appendix 1.

Baroreflex control of ADNA was shifted to the right in both the juvenile and adult LPK (Figure 3.3C). Accordingly, MAP_{50} and MAP_{sat} were higher in the LPK versus Lewis (Tables 3.2). The range of the curves was comparable between the juvenile LPK and Lewis; however, in the adult LPK the upper plateau, range and ADNA at MAP_{sat} were reduced relative to Lewis and an age-related decrease in the range was evident. The gain of the reflex was also reduced in both juvenile and adult LPK versus Lewis controls, and this reduction tended to be greater ($P = 0.065$) in adult versus juvenile LPK (Table 3.3).

3.3.3 Central component of baroreflex arc

(i) Indirect assessment: The ADNA-RSNA relationship (Figure 3.5) was comparable in the juvenile Lewis and LPK (Table 3.4). Adult LPK, however, showed higher measures of RSNA at the lower plateau relative to age-matched Lewis and juvenile LPK. RSNA range was significantly smaller in the

adult LPK compared with juvenile LPK, with values also tended to be lower (P = 0.083) relative to adult Lewis. $ADNA_{50}$, $ADNA_{sat}$ and the ADNA range over which reflex control of RSNA was achieved were also smaller in the adult LPK compared with age-matched Lewis (Table 3.4). In adult Lewis, $ADNA_{50}$ and $ADNA_{sat}$ increased with age.

(i) Direct assessment: A representative data trace showing reflex RSNA, HR and MAP responses to direct electrical stimulation of the ADN in adult Lewis and LPK animals is shown in Figure 3.6. Electrical stimulation of the ADN between 1–24 Hz reduced RSNA, HR and MAP in all groups in frequency-dependent fashion (P<0.001, Figure 3.7). In juvenile LPK, the reflex sympathoinhibition was comparable to Lewis controls. Reflex bradycardic and depressor responses were, however, enhanced in juvenile LPK (Figure 3.7). In adult LPK, reflex responses were reduced compared with Lewis controls and juvenile LPK. This was most noticeable at the higher frequencies (Figure 3.7). An age-related decline in the reflex depressor response was also observed in the Lewis.

Sympathoinhibitory responses to ADN stimulation were also analysed as microvolt data (Figure 3.7). Results were comparable to those described in terms of % change, with no difference between juvenile LPK and Lewis controls, but reduced RSNA reflex responses in the adult LPK, and an age-related reduction evident.

3.3.4 Efferent baroreflex function

In both LPK and Lewis, regardless of age, stimulation of the vagus nerve produced a frequency-dependent reductions in HR (P<0.001, Figure 3.8). Bradycardic responses to vagal efferent stimulation remained comparable between LPK and age-matched Lewis and an age-related difference in both strains was not evident.

3.3.5 Histomorphometry of the aortic arch and correlation with afferent baroreflex function

Vascular remodelling along the aortic arch was evident in both the juvenile and adult LPK (Figure 3.9, Table 3.5). Notably, at both ages, the aortic arch was characterised by an increase in medial wall thickness, reduction in elastin content, elastin-to-collagen ratio, an increase in the number of elastin lamellae fractures and collagen density in the tunica media. Aortic medial calcium deposition was markedly elevated in adult LPK. These parameters progressively changed with age, indicating an age-related increase in vascular hypertrophy and arteriosclerotic remodelling along the aortic arch.

There was a significant negative correlation between the gain of the ADNA baroreflex function curves and medial wall thickness, number of elastin lamellae fractures, collagen density and nucleus cross-sectional area, and a significant positive correlation with the total elastin density and elastin-to-collagen ratio (Table 3.6, Figure 3.10). The range of the ADNA baroreceptor function curve was negatively correlated with aortic medial wall thickness, number of elastin lamellae fractures and total calcium density, while a positive association was seen with total elastin density and elastin-to-collagen ratio (Table 3.6, Figure 3.10).

3.4 Discussion

The major goal of this study was to identify if any temporal change in baroreflex control of HR and/or RSNA in CKD is associated with a deficit in the afferent or central component of the baroreflex circuit. The important new findings are that: (1) there is a temporal decline in baroreflex control of RSNA in the LPK; (2) in juvenile LPK, a deficit in the afferent component of the baroreflex is the primary deficit; (3) in adult LPK, further reduced afferent function and a decrease in central processing is associated with markedly impaired RSNA and HR baroreflexes; (4) a decline in the functionality of the afferent component of the reflex is correlated with vascular remodelling of the aortic arch. Together this shows that in CKD, full expression of baroreflex dysfunction is dependent upon both impaired afferent signaling and abnormal central processing.

Afferent signalling: An early deficit in the afferent component of the baroreflex was observed in the LPK evidenced by a reduction in the gain of the ADNA baroreflex function curves in the juvenile LPK. This impairment worsened with age in the LPK, with the adult animals exhibiting a marked reduction in the range of the reflex. This indicates that in the adult LPK, in response to changes in BP, the ADN does not respond as fast or as effectively in comparison to either juvenile LPK or age-matched Lewis. Dysfunctional baroreceptor afferent function has been previously shown in the spontaneously hypertensive rat (SHR) (Sapru and Wang, 1976) and Dahl salt-sensitive hypertensive rat (Gordon and Mark, 1984). To our knowledge this is the first report of impaired baroreceptor afferent function in CKD.

Hypertension and increased SNA are known to cause vascular hypertrophy and loss of vessel structure, leading to the loss of aortic receptor function (Grassi et al., 2006). Previously we demonstrated vascular remodelling in the thoracic aorta of the LPK and an associated functional increase in pulse wave velocity (PWV), indicating aortic stiffness (Ng et al., 2011b). In CKD patients, impaired baroreflex function directly correlates with a reduction in arterial distensibility, as evidenced by increased PWV (Chesterton et al., 2005). In PKD patients, this has been further demonstrated to be apparent before the onset of hypertension or reduced renal function (Kocyigit et al., 2012). Here, we demonstrate that vascular remodelling occurs along the aortic arch, the site of aortic baroreceptor afferents, correlating with a decline in baroreceptor afferent function. These findings strongly support the hypothesis that in the LPK, hypertrophy and a reduction in elastic properties reduce aortic wall distensibility and hence impair the ability of the aortic baroreceptors to effectively transduce changes in BP.

Central processing: Altered afferent baroreceptor function preceded any decline in the functionality of the central component of the baroreceptor reflex in the LPK. In juvenile LPK, the central component of the baroreceptor reflex was intact, and greater reductions in HR could be evoked by ADN stimulation when compared to juvenile Lewis. This enhancement may indicate a compensatory mechanism, such that in response to a reduction in afferent input, the HR baroreceptor reflex is able to

buffer changes in BP. In adulthood, the LPK demonstrated blunted RSNA-ADNA relationship and reduced reflex responses to stimulation of the ADN, indicating a decline in the central component of the reflex. The impairment in central processing appears independent of the afferent fibre type as the reflex responses to both low (<10Hz) and high (>10Hz) frequency stimulation were reduced in the LPK, indicating that both A- and C- fibre input is impaired (Fan and Andresen, 1998). Altered central processing of the baroreceptor reflex is a feature of other models of hypertension, including the SHR (Gonzalez et al., 1983), renal wrap hypertensive rats (Zhang and Mifflin, 2000) and obese Zucker rats (Huber and Schreihofer, 2010) and while the exact location of the deficit cannot be elucidated from the present study, it is plausible that key medullary nuclei, such as the rostral ventrolateral medulla, responsible for generating changes in SNA in accordance with the baroreflex, are abnormal in the LPK, as seen in other hypertensive rodent models (Huber and Schreihofer, 2010, Smith and Barron, 1990).

Efferent signalling: To strengthen our assertion that deficits within the baroreflex circuit in the LPK is localised to the afferent and central components of the reflex arc, the ability of the heart to respond to vagal nerve input was examined. Indeed, reflex bradycardic responses to vagal efferent stimulation were comparable between Lewis and LPK and remained uninfluenced by age in both strains. While it has been suggested that lateralisation exists with respect to vagal control of HR, such that right vagal nerve stimulation produces greater changes in HR (Mace and Levy, 1983, Minami and Head, 2000), the fact that the chronotropic responses to left vagal nerve stimulation were comparable in both juvenile and adult LPK and Lewis rats implies that the responsiveness of the heart to vagal inputs is adequate in the LPK.

Baroreflex function: Previously we demonstrated that, under conscious conditions, the LPK develops a temporal decline in the sensitivity of the HR baroreflex between 10 and 12 weeks of age (Hildreth et al., 2013b). In the present study we replicate and extend upon this finding under anaesthesia by showing that there is also a temporal decline in the range of the HR baroreflex in the LPK. In keeping with this were the observations that the reflex bradycardic response to a PE-induced increase in BP, which is mediated through an increase in cardiac vagal activity (Head and McCarty, 1987), is intact in juvenile LPK but impaired in adult LPK. Baroreflex control of cardiac sympathetic outflow, as indicated by the reflex tachycardic response to SNP-induced hypotension (Head and McCarty, 1987), was slightly reduced in the LPK, indicating a mild impairment of baroreflex control of cardiac sympathetic outflow. Here we further show that there is a temporal decline in baroreflex control of RSNA in CKD, which is associated with an increase in resting RSNA. This renal sympathetic overactivity was already evident in juvenile LPK, but interestingly, despite a decline in renal function over the same time-frame, RSNA did not further increase. This suggests that, analogous to the human condition, RSNA is increased early in the disease-course and may contribute to the further deterioration in renal function (Grassi et al., 2011).

In the juvenile LPK, the RSNA baroreflex gain (%) was reduced; however, the range (% or μV) of the reflex was comparable. This suggests that at this age, the baroreflex is capable of producing a full range of RSNA change, albeit at a slower rate. The decreased gain of the RSNA baroreflex is potentially contributed to by the decreased responsiveness of the ADN that we describe. In contrast, in adult LPK, the gain and range of the RSNA (%) baroreceptor function curves was impaired in comparison with both adult Lewis and juvenile LPK. We believe that this change reflects a temporal decline in baroreflex control of RSNA rendering the reflex impaired in adulthood as (1) there was no further increase in RSNA in the adult LPK that could potentially bias this data; (2) the ability to produce reflex inhibition of RSNA in response to ADN stimulation was reduced when RSNA was expressed in both normalised and absolute units; and (3) there was an age-related reduction in the gain and range of the RSNA (μV) baroreceptor curves in the LPK that was not observed in the Lewis rats. The deficit in baroreflex control of RSNA in the adult LPK observed in this study contrasts with previous findings that baroreflex control of splanchnic sympathetic outflow, while unable to maximally suppress nerve activity, is comparable in the LPK and Lewis in terms of the sensitivity of the reflex (Harrison et al., 2010). Our finding of reduced baroreflex control of RSNA suggests that the reflex control of sympathetic outflow may be differentially regulated and/or impaired in CKD.

In conclusion, our findings indicate that in the juvenile LPK, a deficit in baroreceptor afferent function is compensated for by the central component of the baroreflex and consequently HR baroreflex function is preserved and only a minimal impairment in baroreflex control of RSNA is observed. In the adult LPK, however, there is a loss of function in the central component of the baroreflex, which together with a reduction in afferent baroreflex function, results in markedly impaired baroreflex control of both HR and RSNA.

3.5 Perspectives and significance

Cardiovascular autonomic dysfunction is a major cause of morbidity and mortality in CKD patients (Cashion et al., 2000, Dursun et al., 2004), however the critical underlying mechanisms are not fully understood. Herein, we provide direct evidence of sympathetic overactivity, compounded with impaired baroreflex control of HR and SNA, thus emphasizing the complexity of this pathological condition. The study further highlights key pathways within the baroreflex arc that explain the mechanisms involved and could potentially be targeted for future therapeutics. We suggest that early interventional measures to treat CKD that reduce SNA, lower BP and limit vascular remodelling may well serve to ameliorate autonomic dysfunction and therefore reduce overall cardiovascular risk in these patients.

Table 3.1: Baseline parameters in juvenile (7–8 weeks old) and adult (12–13 weeks old) male Lewis and Lewis Polycystic Kidney (LPK) rats

Group	Juvenile		Adult		Two-way ANOVA adjusted *P* value	
	Lewis *(7)*	LPK *(6)*	Lewis *(6)*	LPK *(6)*	Strain	Age
Parameter						
BW (g)	214 ± 11	167 ± 6*	361 ± 8†	239 ± 7$^{*\dagger\#}$	<0.0001	<0.0001
U_{Pro} (g/L)	0.05 ± 0.00	0.31 ± 0.06*	0.05 ± 0.00	1.04 ± 0.42*	0.0061	0.0889
U_{Cr} (g/L)	1.30 ± 0.22	0.37 ± 0.08*	1.10 ± 0.05	0.29 ± 0.07*	<0.0001	0.3050
UPC	0.05 ± 0.01	0.94 ± 0.25*	0.05 ± 0.00	4.12 ± 1.43$^{*\dagger\#}$	0.0018	0.0328
MAP (mmHg)	86 ± 3	108 ± 4*	85 ± 2	111 ± 6*	<0.0001	0.8468
SBP (mmHg)	116 ± 5	165 ± 4*	123 ± 5	179 ± 6*	<0.0001	0.0374
DBP (mmHg)	65 ± 3	76 ± 4*	64 ± 2	69 ± 5	0.0263	0.2586
PP (mmHg)	51 ± 4	89 ± 6*	59 ± 6	111 ± 6*†	<0.0001	0.0139
HR (BPM)	363 ± 11	439 ± 14*	350 ± 16	402 ± 13*	0.0001	0.0994
RSNA (μV)	3.6 ± 0.7	7.3 ± 1.5*	2.7 ± 0.4	5.3 ± 0.8*	0.0008	0.1199
ADNA (μV)	0.4 ± 0.1	0.4 ± 0.1	0.7 ± 0.3	1.2 ± 0.3†	0.1822	0.0070

BW, body weight; U_{Pro}, urinary protein; U_{Cr}, urinary creatinine; UPC, urinary protein:creatinine ratio; MAP, mean arterial pressure; SBP, systolic blood pressure; DBP, diastolic blood pressure; PP, pulse pressure; HR, heart rate; RSNA, renal sympathetic nerve activity; and ADNA, aortic depressor nerve activity. Results are expressed as mean ± SEM.

$^{*}P<0.05$ vs. age-matched Lewis.

$^{\dagger}P<0.05$ vs. strain-matched juvenile rat.

$^{\#}P<0.05$ indicates strain × age interaction.

(n) values denoted in subscript and represent the minimum number in each group.

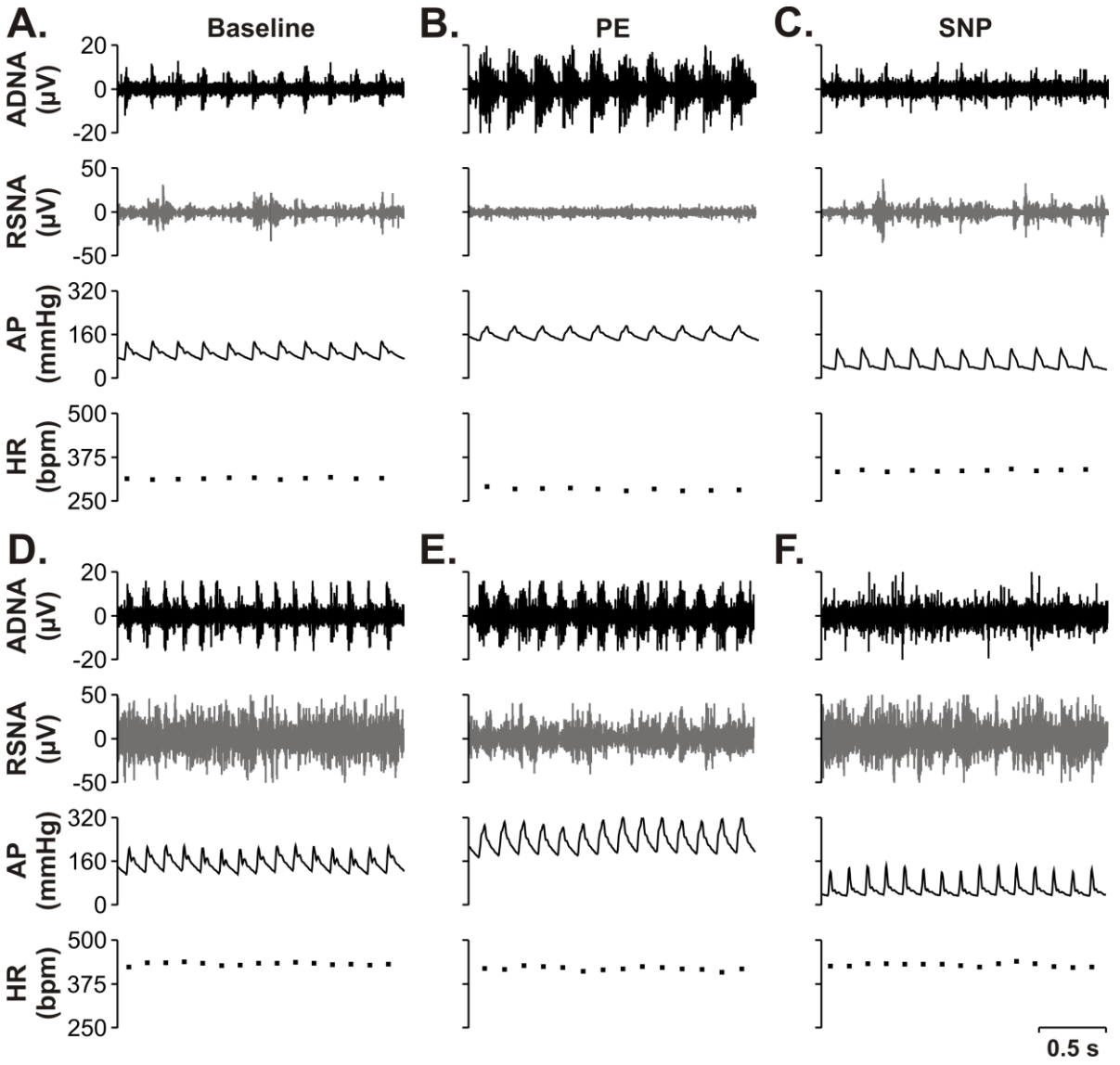

Figure 3.1: Representative raw data traces, illustrating responses of aortic depressor nerve activity (ADNA), renal sympathetic nerve activity (RSNA) and heart rate (HR) to evoked changes in arterial pressure (AP) from an (A–C) adult male (12–13 weeks old) Lewis and (D–E) adult Lewis Polycystic Kidney (LPK) rat. Bursts of ADNA can be seen in association with each pulse of AP in both Lewis and LPK. In response to phenylephrine (PE, 10–50 μg/kg), RSNA is silenced and HR reduced in the Lewis (B); however, in the LPK (E), reflex sympathoinhibition and bradycardia is reduced. Significant reductions in ADNA and reflex tachycardia are observed when AP is reduced by sodium nitroprusside (SNP, 50–70 μg/kg; C and F). bpm: beats per minute.

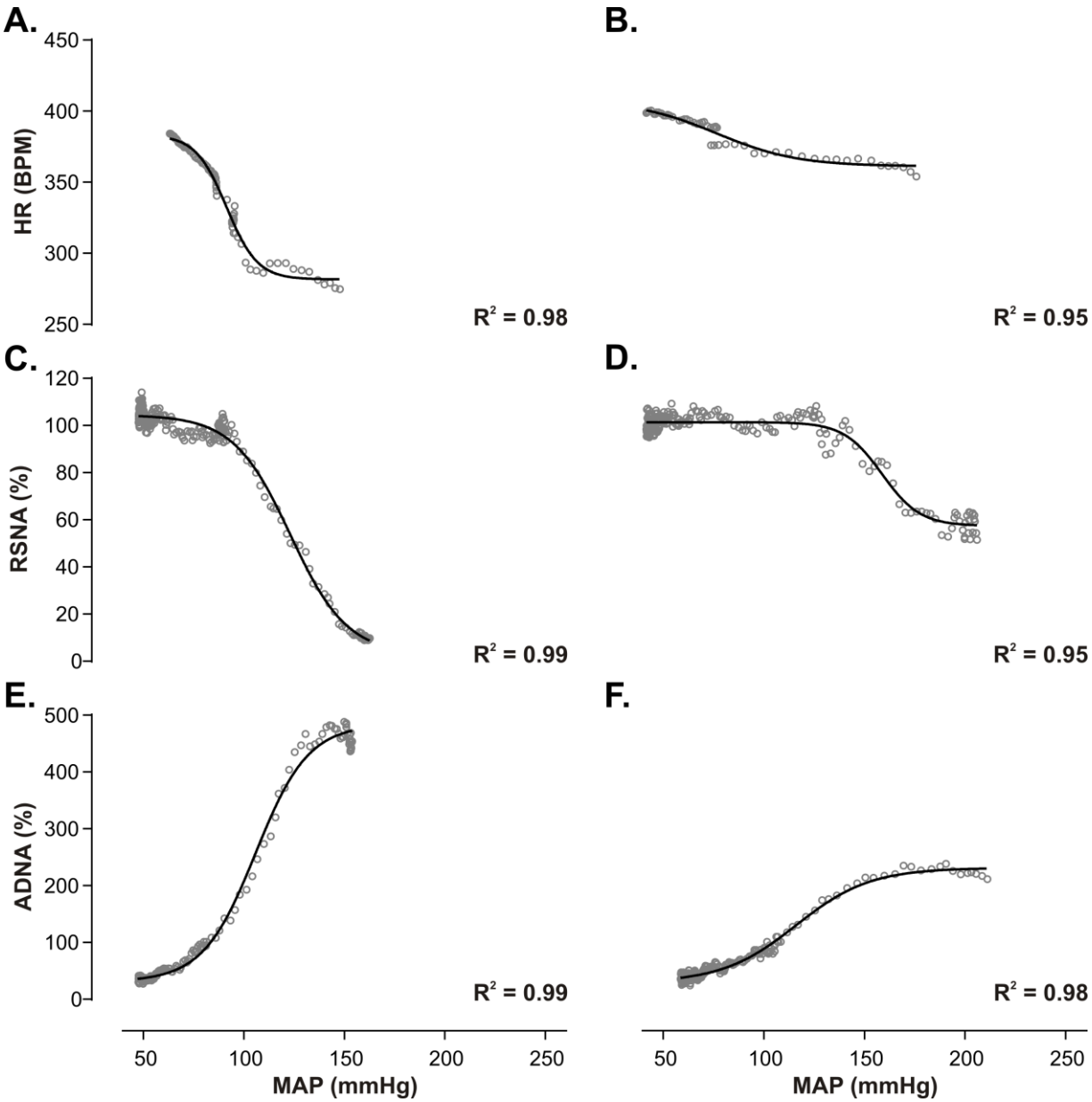

Figure 3.2: Representative raw data curves from individual animals showing the sigmoidal relationship between mean arterial pressure (MAP) and heart rate (HR; A–B), renal sympathetic nerve activity (RSNA; C–D) and aortic depressor nerve activity (ADNA; E–F) in adult male (12–13 weeks old) Lewis (left panels) and Lewis Polycystic Kidney (LPK) rats (right panels).

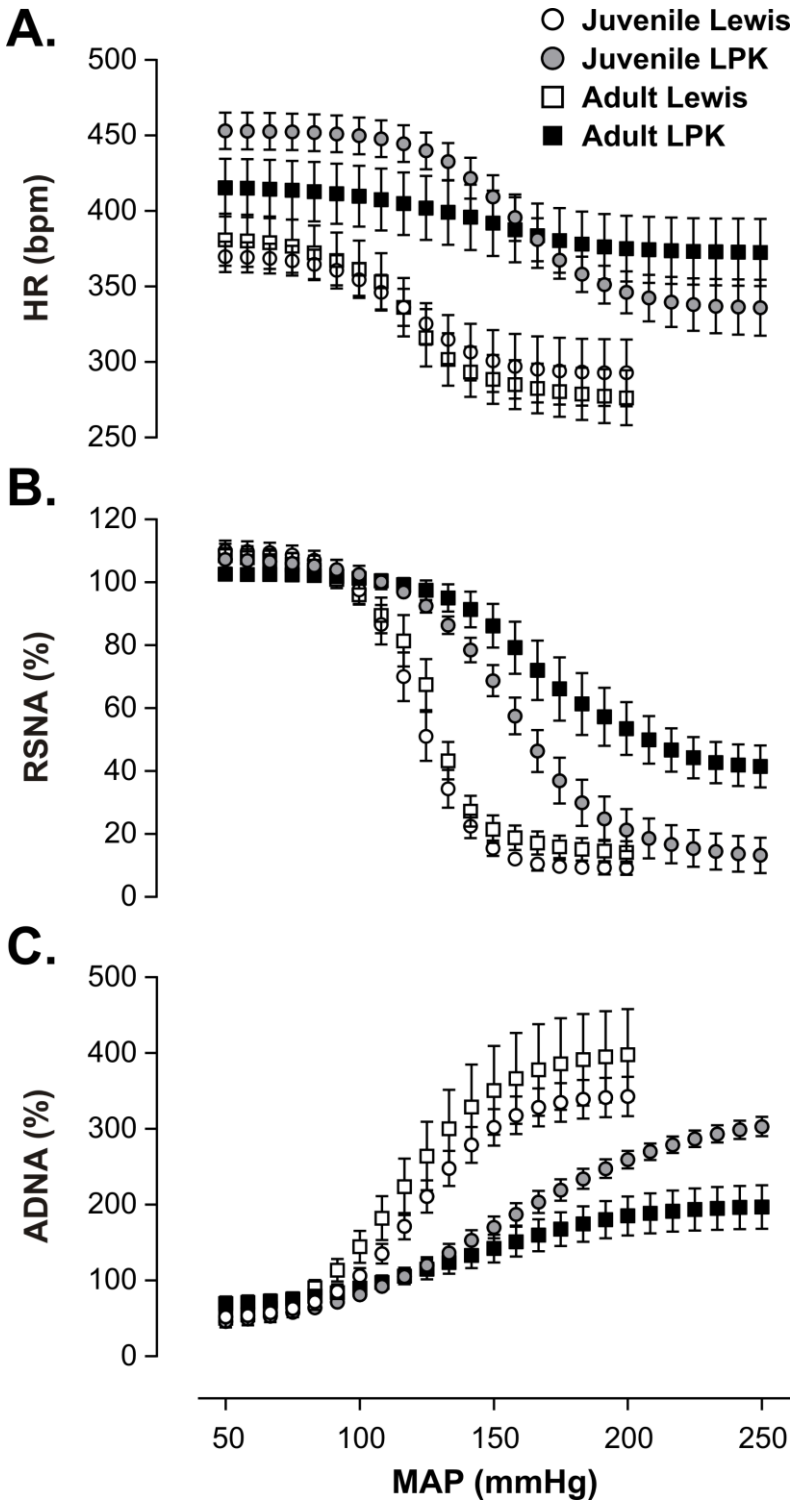

Figure 3.3: Logistic function curves illustrating the relationship between mean arterial pressure (MAP) and heart rate (HR; A), renal sympathetic nerve activity (RSNA; B) and aortic depressor nerve activity (ADNA; C) in juvenile (7–8 weeks old) and adult (12–13 weeks old) male Lewis and Lewis Polycystic Kidney (LPK) rats. Results are expressed as mean ± SEM. *n* values are detailed in Table 3.2. bpm: beats per minute. (HR: R^2 = 0.96 ± 0.1, RSNA: R^2 = 0.95 ± 0.01 and ADNA: R^2 = 0.97 ± 0.01, all groups).

Table 3.2: Parameters describing the relationship between mean arterial pressure (MAP) and heart rate (HR), renal sympathetic nerve activity (RSNA) and aortic depressor nerve activity (ADNA) in the juvenile (7–8 weeks old) and adult (12–13 weeks old) male Lewis and Lewis Polycystic Kidney (LPK) rats

Groups	Juvenile		Adult		Two-way ANOVA adjusted P value	
	Lewis	LPK	Lewis	LPK	Strain	Age
Parameter						
HR barocurve *(n)*	*7*	*8*	*11*	*7*	-	-
Upper plateau (bpm)	370 ± 10	463 ± 8*	383 ± 17	415 ± 19	0.0003	0.2836
Lower plateau (bpm)	283 ± 24	331 ± 21	272 ± 21	372 ± 22*	0.0024	0.5082
Range (bpm)	88 ± 16	132 ± 24	111 ± 19	44 ± 8$^{*\dagger\#}$	0.2198	0.0411
Gain (bpm/mmHg)	-3.0 ± 1.3	-2.8 ± 0.6	-3.5 ± 0.9	-0.7 ±0.1$^{*\dagger\#}$	0.0326	0.1005
MAP_{50} (mmHg)	116 ± 6	153 ± 6*	116 ± 6	140 ± 8*	0.0001	0.3197
MAP_{thr} (mmHg)	102 ± 6	135 ± 8*	101 ± 5	118 ± 10	0.0014	0.2119
HR at MAP_{thr} (bpm)	352 ± 12	435 ± 7*	359 ± 16	407 ± 19	0.0002	0.5062
MAP_{sat} (mmHg)	131 ± 7	171 ± 6*	131 ± 9	161 ± 9*	0.0002	0.5652
HR at MAP_{sat} (bpm)	301 ± 8	359 ± 16*	295 ± 18	382 ± 21*	0.0006	0.6552
MAP operating range (mmHg)	29 ± 5	37 ± 5	31 ± 7	44 ± 10	0.1641	0.5641
RSNA barocurve *(n)*	*8*	*9*	*9*	*7*	-	-
Upper plateau (%)	110 ± 3	108 ± 4	111 ± 5	103 ± 1	0.1751	0.5291
Lower plateau (%)	9 ± 2	12 ± 6	13 ± 4	41 ± 7$^{*\dagger\#}$	0.0030	0.0016
Range (bpm)	101 ± 4	96 ± 8	98 ± 7	62 ± 8 $^{*\dagger\#}$	0.0069	0.0123
Gain (bpm/mmHg)	-2.8 ± 0.2	-1.5 ± 0.2*	-2.2 ± 0.2	1.2 ± 0.1*	<0.0001	0.0267
MAP_{50} (mmHg)	121 ± 3	159 ± 5*	127 ± 5	171 ± 11*	<0.0001	0.1701
MAP_{thr} (mmHg)	109 ± 4	136 ± 6*	106 ± 7	153 ± 12*	<0.0001	0.3247
RSNA at MAP_{thr} (%)	89 ± 3	88 ± 3	90 ± 4	90 ± 1	0.7503	0.5672
MAP_{sat} (mmHg)	134 ± 3	183 ± 5*	143 ± 2	189 ± 10*	<0.0001	0.1766

RSNA at MAP_{sat} (%)	30 ± 2	32 ± 4	34 ± 2	54 ± 5$^{*\dagger\#}$	0.0040	0.0013
MAP operating range (mmHg)	25 ± 2	47 ± 6*	37 ± 8	36 ± 3$^{\#}$	0.0704	0.9632
ADNA barocurve *(n)*	*7*	*6*	*7*	*7*	-	-
Upper plateau (%)	346 ± 26	324 ± 26	406 ± 60	199 ± 29$^{*\#}$	0.0076	0.4171
Lower plateau (%)	48 ± 15	37 ± 8	40 ± 5	66 ± 9	0.4799	0.3066
Range (bpm)	297 ± 31	287 ± 33	265 ± 61	133 ± 35$^{*\dagger\#}$	0.0088	0.3239
Gain (bpm/mmHg)	5.0 ± 0.6	2.5 ± 0.3*	5.2 ± 1.1	1.5 ± 0.4*	0.0009	0.0782
MAP_{50} (mmHg)	123 ± 2	155 ± 8*	119 ±3	147 ±9*	<0.0001	0.2982
MAP_{thr} (mmHg)	103 ± 3	116 ± 7	93 ± 2	108 ± 11	0.0605	0.2207
ADNA at MAP_{thr} (%)	111 ± 11	98 ± 5	117 ± 12	94 ± 7	0.0814	0.8821
MAP_{sat} (mmHg)	143 ± 3	195 ± 13*	145 ± 6	176 ± 8*	<0.0001	0.2690
ADNA at MAP_{sat} (%)	283 ± 21	263 ± 19	328 ± 47	171 ± 22$^{*\#}$	0.0078	0.4526
MAP operating range (mmHg)	40 ± 4	80 ± 13*	52 ± 6	67 ± 9	0.0020	0.9841

MAP_{50}, mean arterial pressure at the midpoint of the curve; MAP_{thr}, threshold mean arterial pressure to trigger a change in HR, RSNA or ADNA; and MAP_{sat}, saturation mean arterial pressure at which there is no further change in HR, RSNA or ADNA.
Results are expressed as mean ± SEM.
$^{*}P<0.05$ vs. age-matched Lewis.
$^{\dagger}P<0.05$ vs. strain-matched juvenile rat.
$^{\#}P<0.05$ indicates strain × age interaction.
(n) = number in each group.

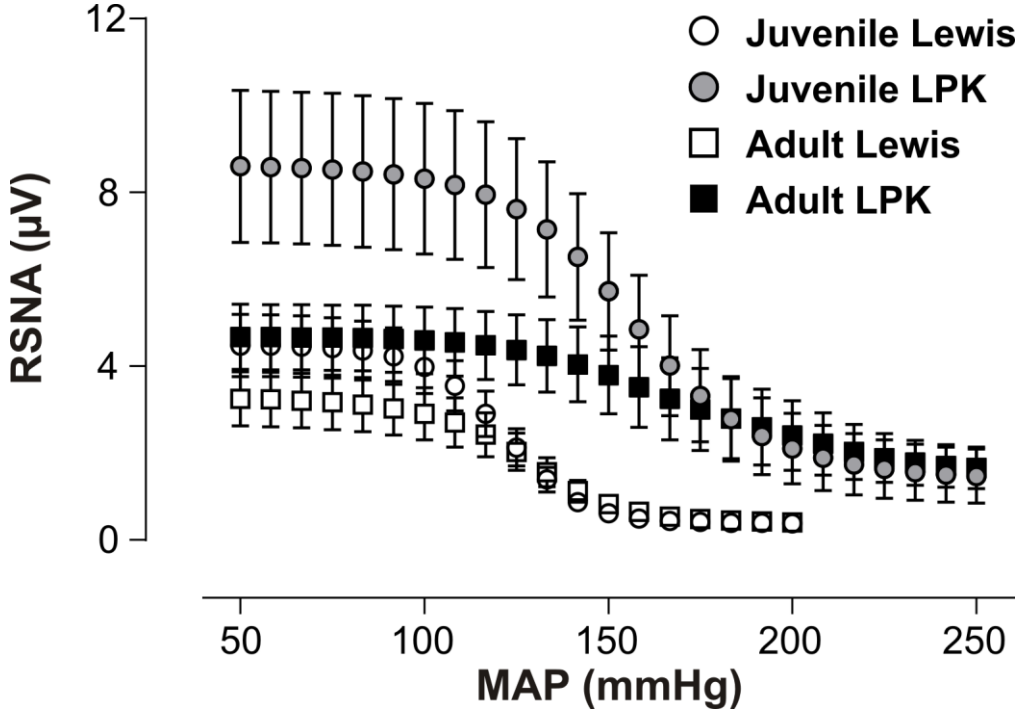

Figure 3.4: Logistic function curves illustrating the relationship between mean arterial pressure (MAP) and renal sympathetic nerve activity (RSNA) expressed in microvolts (μV) in juvenile (7–8 weeks old) and adult (12–13 weeks old) male Lewis and Lewis Polycystic Kidney (LPK) rats. Results are expressed as mean ± SEM. *n* values are as detailed in Table 3.3. (R^2 = 0.94 ± 0.01 all groups).

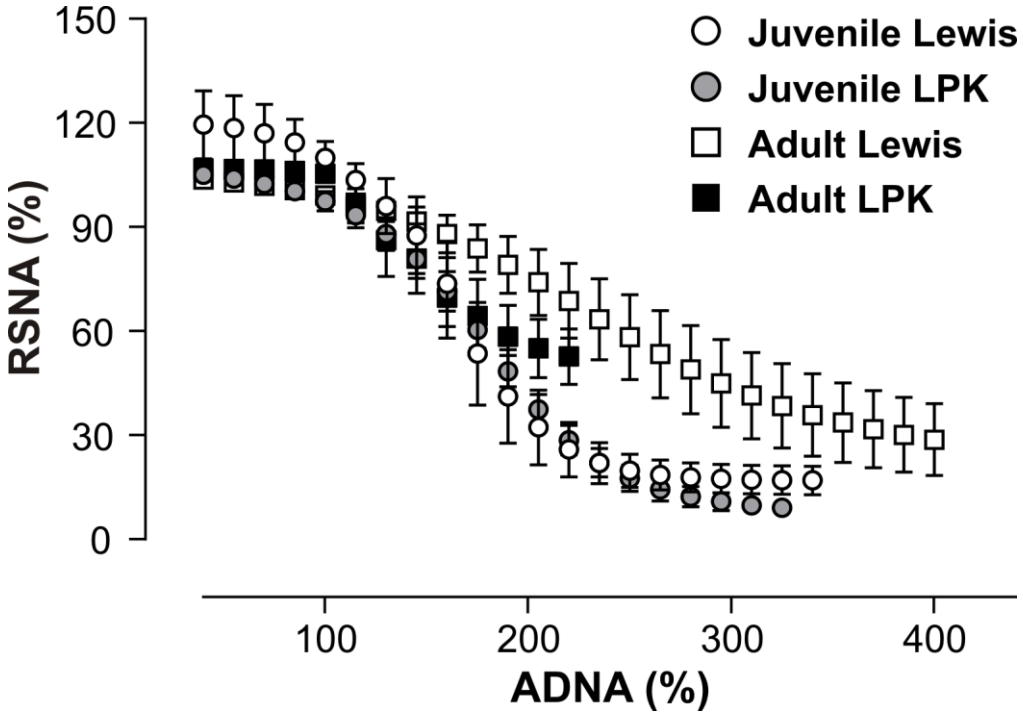

Figure 3.5: Logistic function curves illustrating the relationship between aortic depressor nerve activity (ADNA) and renal sympathetic nerve activity (RSNA) in juvenile (7–8 weeks old) and adult (12–13 weeks old) male Lewis and Lewis Polycystic Kidney (LPK) rats. Results are expressed as mean ± SEM. *n* values are as detailed in Table 3.4. (R^2 = 0.94 ± 0.03 all groups).

Table 3.3: Parameters describing the relationship mean arterial pressure (MAP) and microvolt changes in renal sympathetic nerve activity (RSNA) in the juvenile (7–8 weeks old) and adult (12–13 weeks old) male Lewis and Lewis Polycystic Kidney (LPK) rats

Groups	Juvenile		Adult		Two-way ANOVA adjusted P value	
	Lewis *(8)*	LPK *(9)*	Lewis *(9)*	LPK *(7)*	Strain	Age
Barocurve parameter						
RSNA upper plateau (μV)	4.5 ± 0.7	8.6 ± 1.7*	3.3 ± 0.6	5.0 ± 0.7	0.0143	0.0368
RSNA lower plateau (μV)	0.4 ± 0.1	1.4 ± 0.6	0.4 ± 0.1	1.8 ± 0.5*	0.0050	0.5998
Range (μV)	4.1 ± 0.7	7.2 ± 1.5	2.9 ± 0.6	3.1 ± 0.6†	0.0900	0.0101
Gain (μV/mmHg)	-0.119 ± 0.019	-0.116 ± 0.024	-0.062 ± 0.013	-0.051 ± 0.010†	0.7118	0.0017
MAP_{50} (mmHg)	121 ± 3	157 ± 5*	125 ± 4	167 ± 11*	<0.0001	0.2609
MAP_{thr} (mmHg)	110 ± 4	135 ± 6*	107 ± 6	149 ± 12*	<0.0001	0.4203
RSNA at MAP_{thr} (μV)	3.6 ± 0.6	7.1 ± 1.5*	2.7 ± 0.5	4.3 ± 0.6	0.0102	0.0519
MAP_{sat} (mmHg)	133 ± 3	180 ± 6*	143 ± 2	186 ± 11*	<0.0001	0.1887
RSNA at MAP_{sat} (μV)	1.2 ± 0.2	2.9 ± 0.8*	1.0 ± 0.2	2.5 ± 0.5	0.0029	0.4792
MAP operating range (mmHg)	24 ± 3	45 ± 6*	36 ± 6	37 ± 4	0.0305	0.6697

MAP_{50}, mean arterial pressure at the midpoint of the curve; MAP_{thr}, threshold mean arterial pressure to trigger a change in RSNA; and MAP_{sat}, saturation mean arterial pressure at which there is no further change in RSNA.
Results are expressed as mean ± SEM.
* $P<0.05$ vs. age-matched Lewis.
† $P<0.05$ vs. strain-matched juvenile rat.
(n) values denoted in subscript and represent number in each group.

Table 3.4: Parameters describing the relationship between aortic depressor nerve activity (ADNA) and renal sympathetic nerve activity (RSNA) in the juvenile (7–8 weeks old) and adult (12–13 weeks old) male Lewis and Lewis Polycystic Kidney (LPK) rats

Groups	Juvenile		Adult		Two-way ANOVA adjusted P value	
	Lewis *(5)*	LPK *(4)*	Lewis *(4)*	LPK *(7)*	Strain	Age
Barocurve parameter						
RSNA upper plateau (%)	121 ± 11	108 ± 4	108 ± 4	107 ± 2	0.2854	0.2687
RSNA lower plateau (%)	17 ± 4	7 ± 2	17 ± 8	46 ± 8$^{*\dagger\#}$	0.2070	0.0142
RSNA range (%)	104 ± 12	101 ± 6	91 ± 9	61 ± 8†	0.1166	0.0145
Gain	-0.8 ± 0.2	-0.8 ± 0.1	-0.4 ± 0.1	-2.4 ± 0.8	0.1405	0.3813
$ADNA_{50}$ (%)	165 ± 13	177 ± 6	252 ± 26†	143 ± 14$^{*\#}$	0.0088	0.1211
$ADNA_{thr}$ (%)	111 ± 21	132 ± 13	162 ± 16	115 ± 10$^{\#}$	0.4271	0.2890
RSNA at $ADNA_{thr}$ (%)	99 ± 8	87 ± 3	89 ± 3	94 ± 3	0.5104	0.7892
$ADNA_{sat}$ (%)	219 ± 19	222 ± 8	343 ± 53†	171 ± 26$^{*\#}$	0.0129	0.2477
RSNA at $ADNA_{sat}$ (%)	39 ± 4	28 ± 1	36 ± 6	59 ± 6$^{*\dagger\#}$	0.3073	0.0252
ADNA range (%)	108 ± 30	90 ± 19	181 ± 59	56 ± 27*	0.0594	0.5965

$ADNA_{50}$, aortic depressor nerve activity at the midpoint of the curve; $ADNA_{thr}$, threshold aortic depressor nerve activity to trigger a change in RSNA; and $ADNA_{sat}$, saturation aortic depressor nerve activity at which there is no further change in RSNA.
Results are expressed as mean ± SEM.
$^{*}P<0.05$ vs. age-matched Lewis.
$^{\dagger}P<0.05$ vs. strain-matched juvenile rat.
$^{\#}P<0.05$ indicates strain × age interaction.
(n) values denoted in subscript and represent number in each group.

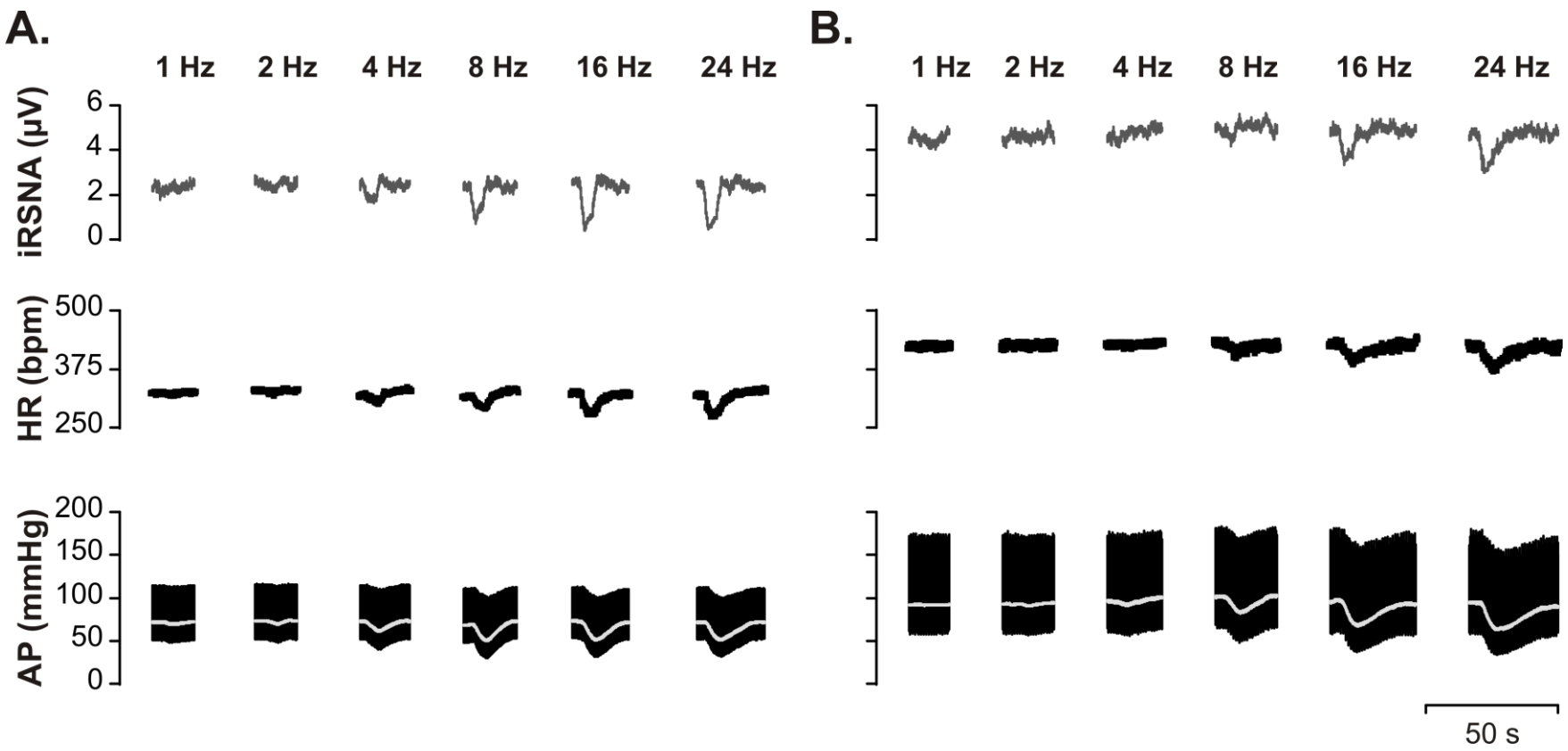

Figure 3.6: Representative data traces, illustrating responses of integrated renal sympathetic nerve activity (iRSNA), heart rate (HR) and arterial pressure (AP) to direct electrical stimulation of the aortic depressor nerve from an adult male (12–13 weeks old) Lewis (left panels) and adult male Lewis Polycystic Kidney (LPK) rat (right panels). bpm: beats per minute.

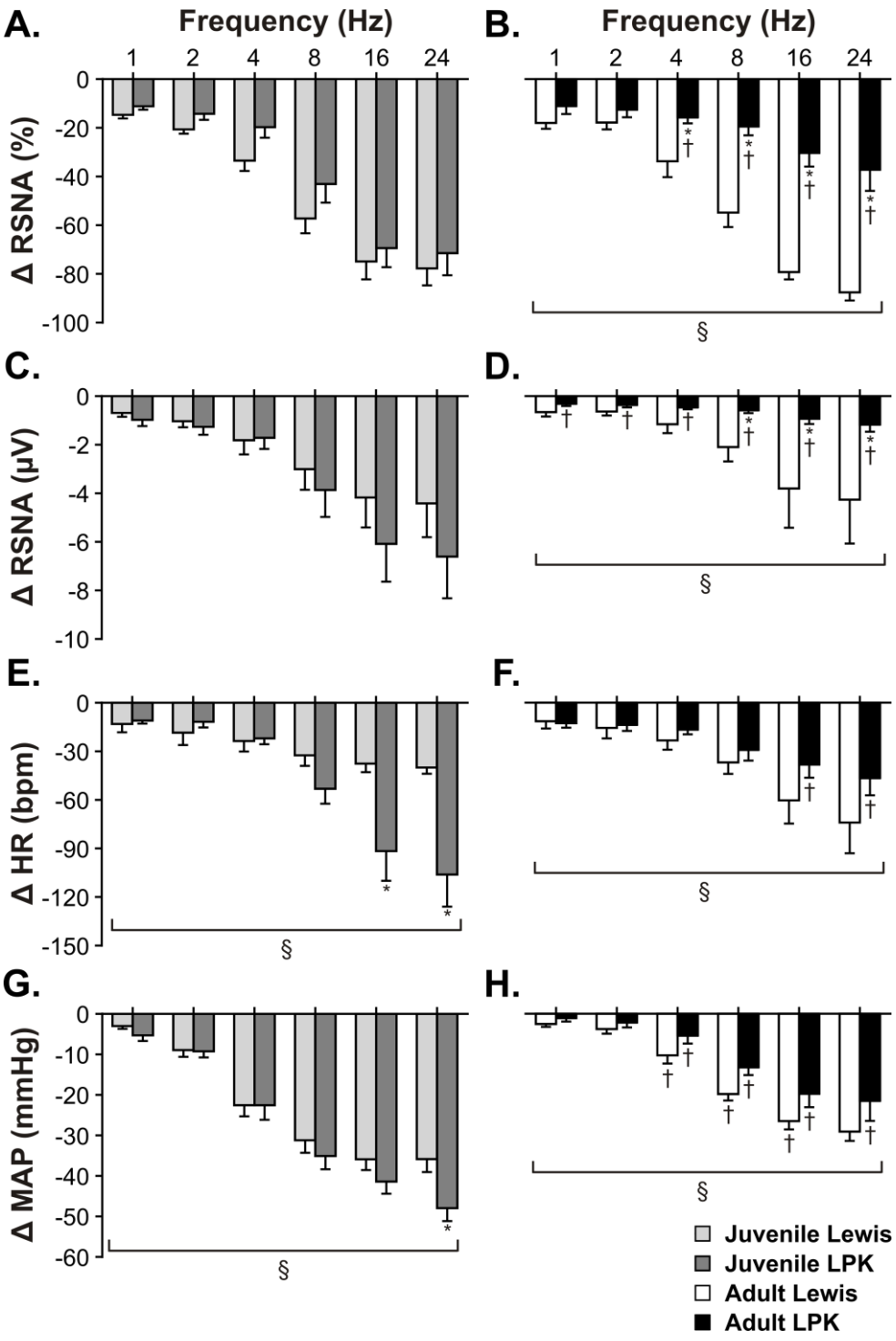

Figure 3.7: Effect of aortic depressor nerve stimulation on renal sympathetic nerve activity (RSNA; A–D), heart rate (HR; E, F) and mean arterial pressure (MAP; G, H) in juvenile (7–8 weeks old; left panel) and adult (12–13 weeks old; right panel) male Lewis and Lewis Polycystic Kidney (LPK) rats. A reduction in RSNA, HR and MAP was observed in all experimental groups. Results are expressed as mean ± SEM. $^{*}P<0.05$ vs. age-matched Lewis, $^{\dagger}P<0.05$ vs. strain-matched juvenile rat and $^{\S}P<0.05$, overall two-way ANOVA strain effect within indicated juvenile or adult age group. *n*/group: juvenile Lewis = 5, juvenile LPK = 5, adult Lewis = 6 and adult LPK = 7. bpm: beats per minute.

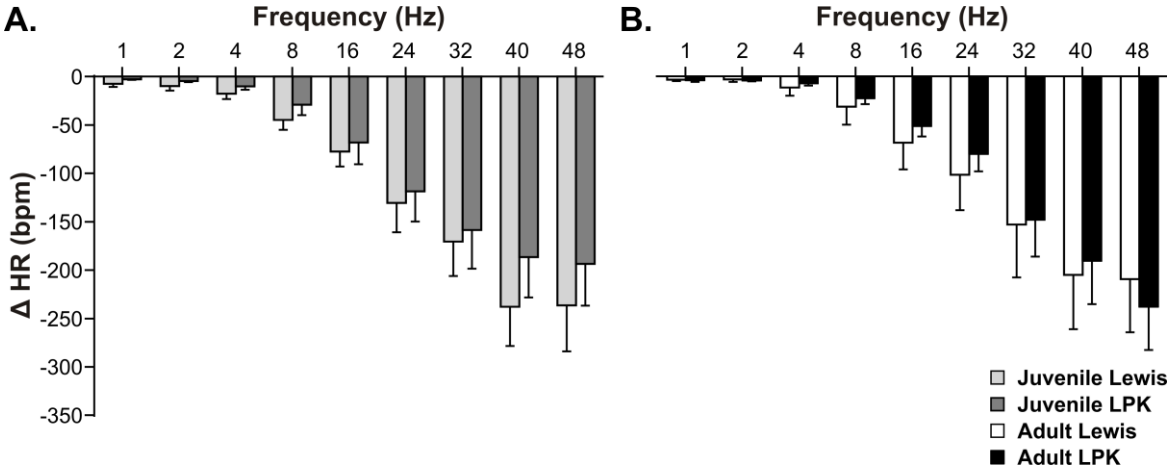

Figure 3.8: Effect of cervical vagal efferent nerve stimulation on heart rate (HR) in juvenile (7–8 weeks old, A) and adult (12–13 weeks old, B) male Lewis and Lewis Polycystic Kidney (LPK) rats. A reduction in HR was observed in all experimental groups. Results are expressed as mean ± SEM. *n*/group: juvenile male Lewis = 8, juvenile male LPK = 8, adult male Lewis = 4 and adult male LPK = 8. bpm: beats per minute.

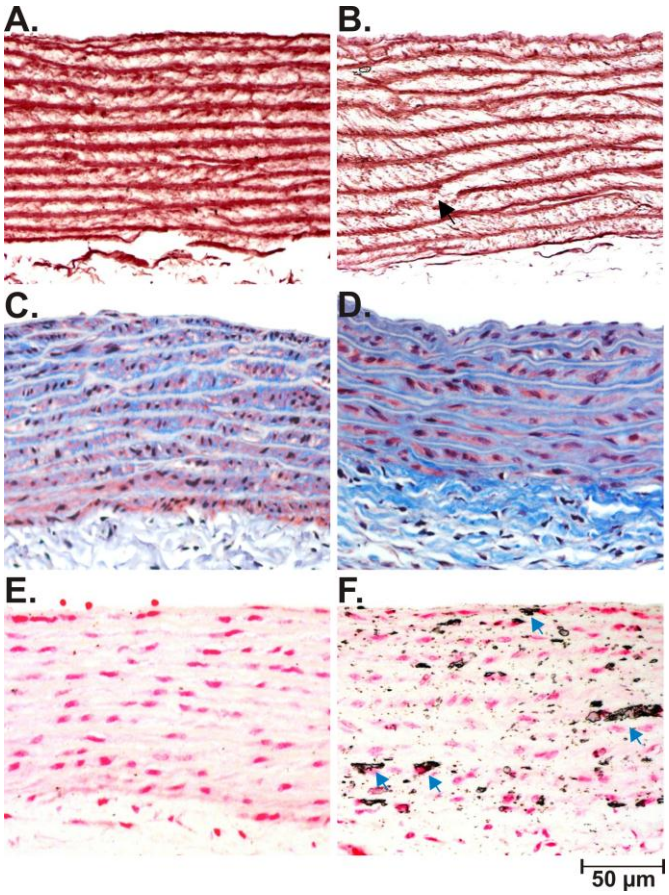

Figure 3.9: Representative histological sections of the aortic arch in adult (12–13 weeks old) male Lewis (left panels) and Lewis Polycystic Kidney rats (right panels), stained with Shikata's orcein (panels A, B) showing the elastin component in red, Martius Scarlet Blue (MSB; panels C, D) showing the collagen component in blue and the nuclei in black and Von Kossa (panels E, F) showing calcification in black. Block arrow in B shows an example of elastic lamellae fracture (point of lamellae discontinuation). Blue arrows in F indicate areas of medial calcification.

Table 3.5: Differentiating histomorphometric variables in the aortic arch of juvenile (7–8 weeks old) and adult (12–13 weeks old) male Lewis and Lewis Polycystic Kidney (LPK) rats

Groups	Juvenile		Adult		Two-way ANOVA adjusted *P* value	
	Lewis *(6)*	LPK *(7)*	Lewis *(5)*	LPK *(6)*	Strain	Age
Morphometric parameter						
Medial thickness (μm)	131 ± 4	166 ± 3*	145 ± 8	222 ± 5$^{*\dagger\#}$	<0.0001	<0.0001
Number of elastin lamellae	12 ± 0.3	11 ± 0.5	11 ± 0.5	13 ± 1.1	0.6073	0.5659
Total elastin density (%)	74 ± 2	61 ± 1*	68 ± 2	44 ± 3$^{*\dagger\#}$	<0.0001	<0.0001
Lamellae elastin density (%)	48± 1	43 ± 1	44 ± 2	34 ± 2*†	0.0001	0.0002
Interlamellae elastin density (%)	25 ± 2	17 ± 0.9*	24 ± 2	10 ± 1$^{*\dagger\#}$	<0.0001	0.0039
Lamellae-to-interlamellae elastin ratio	2.0 ± 0.1	2.6 ± 0.2	1.9 ± 0.2	3.8 ± 0.4$^{*\dagger\#}$	0.0001	0.0517
Thickness of elastin lamellae (μm)	3.9 ± 0.2	4.1 ± 0.1	3.8 ± 0.1	3.2 ± 0.1$^{*\dagger\#}$	0.1500	0.0022
Elastin lamellae spacing (μm)	7.6 ± 0.2	9.9 ± 0.4	9.3 ± 0.3	14.6 ± 1.2$^{*\dagger\#}$	<0.0001	0.0002
Number of elastin lamellae fracture	0.02 ± 0.003	0.05 ± 0.007*	0.02 ± 0.006	0.08 ± 0.011$^{*\dagger\#}$	<0.0001	0.0193
Total collagen density (%)	21 ± 1.6	29 ± 0.5*	23 ± 1.4	34 ± 1.9*†	<0.0001	0.0157
Elastin-to-collagen ratio	3.7 ± 0.4	2.1 ± 0.1*	3.0 ± 0.2	1.3 ± 0.1*†	<0.0001	0.0029
Nuclear density (%)	4.8 ± 0.2	5.8 ± 0.3*	3.7 ± 0.4†	5.0 ± 0.1*	0.0004	0.0032
Nucleus cross-sectional area (μm^2)	9.6 ± 0.5	13.7 ± 1.0*	9.4 ± 1.1	14.2 ± 0.7*	<0.0001	0.8027
Number of nuclei per μm^2	0.10 ± 0.005	0.08 ± 0.008	0.12 ± 0.017	0.07 ± 0.004*	0.0005	0.8233
Calcium density (%)	0.7 ± 0.2	0.9 ± 0.3	1.0 ± 0.2	5.1 ± 1.9*†	0.0369	0.0277
Average size of calcium deposit (μm2)	5.7 ± 0.7	4.0 ± 0.7*	6.4 ± 0.5	8.4 ± 1.7*	0.8544	0.0272

Results are expressed as mean ± SEM.
$^{*}P<0.05$ vs. age-matched Lewis.
$^{\dagger}P<0.05$ vs. strain-matched juvenile rat.
$^{\#}P<0.05$ indicates strain × age interaction.
(n) values denoted in subscript and represent the minimum number in each group.

Table 3.6: Pearson's correlation coefficient (r) for aortic depressor nerve activity (ADNA) baroreceptor afferent function curve parameters relative to vascular structure in juvenile and adult male Lewis and Lewis Polycystic Kidney (LPK) rats

Groups	**MAP-ADNA function curve parameter**	
Morphometric parameter $^{(n)}$	Gain $^{(21)}$	Range $^{(21)}$
Medial thickness (μm)	-0.71 (*P*=0.0005)	-0.58 (*P*=0.0072)
Total elastin density (%)	0.76 (*P*<0.0001)	0.68 (*P*=0.0006)
Number of elastin lamellae fractures (fracture/lamellae/mm)	-0.74 (*P*=0.0001)	-0.69 (*P*=0.0005)
Total collagen density (%)	-0.49 (*P*=0.0201)	ns
Elastin-to-collagen ratio	0.56 (*P*=0.0062)	0.44 (*P*=0.0383)
Nucleus cross-sectional area (μm^2)	-0.58 (*P*=0.0049)	ns
Calcium density (%)	ns	-0.50 (*P*=0.0260)

Correlation analysis of the relationship between the gain/range of aortic depressor nerve activity (ADNA) baroreceptor afferent function and aortic arch vascular remodelling. ns = no significance and *n* = number in each group. Only those parameters for which there was a significant correlation are reported.

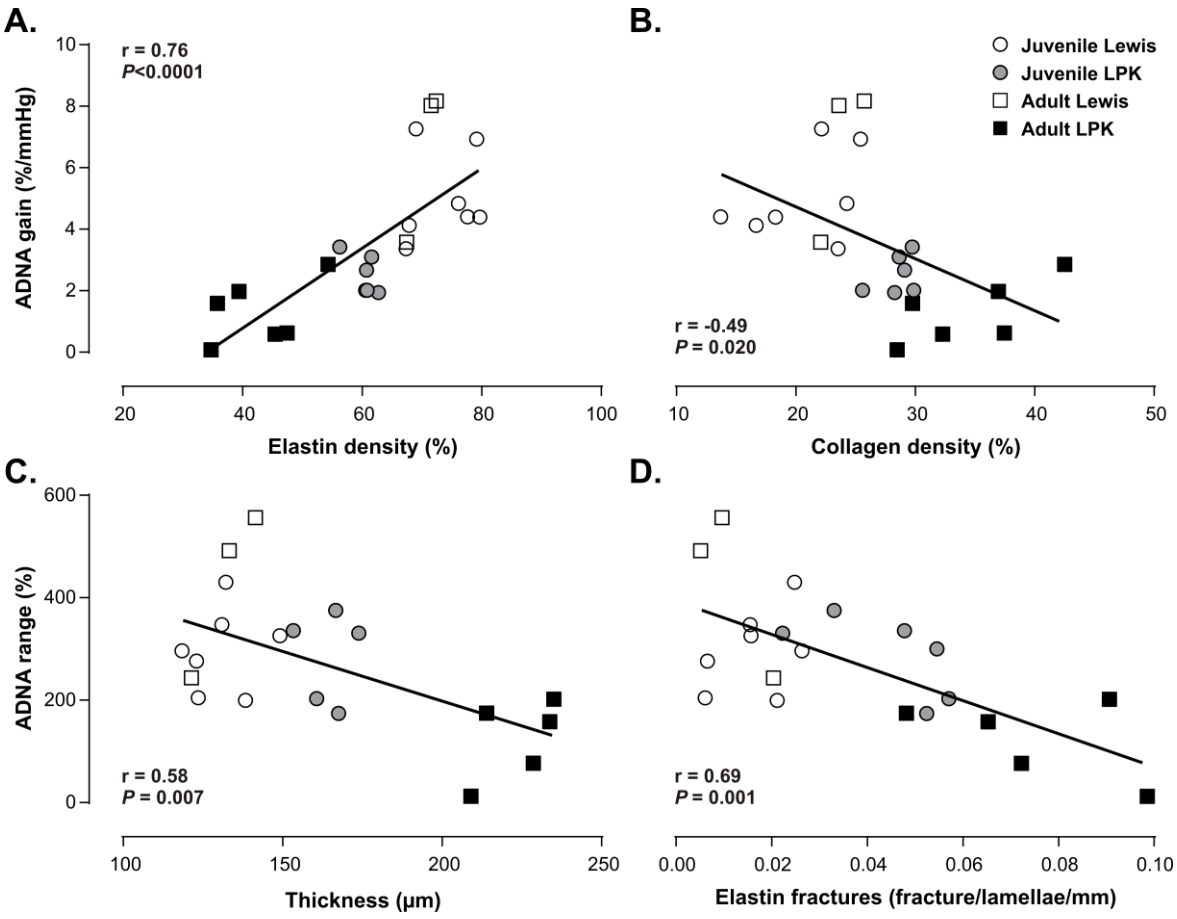

Figure 3.10: Correlation between key histomorphometric variables examined in the aortic arch and afferent baroreceptor function in the juvenile (7–8 weeks old) and adult (12–13 weeks old) male Lewis and Lewis Polycystic Kidney (LPK) rat. (A): elastin density vs. aortic depressor nerve activity (ADNA) gain. (B): collagen density vs. ADNA gain. (C): aortic media thickness vs. ADNA range. (D): number of elastin lamellae fractures vs. ADNA range. *n* = 21.

4 Abnormal Central Control Underlies Impaired Baroreflex Control of Heart Rate and Sympathetic Nerve Activity in Female Lewis Polycystic Kidney Rats

Ibrahim M. Salman, Jacqueline K. Phillips, Omar Z. Ameer, Cara M. Hildreth

Australian School of Advanced Medicine, Macquarie University, Sydney, NSW, Australia

This chapter is currently under revision in *Journal of Hypertension*.

Abstract

We investigated if any temporal changes in baroreflex control of heart rate (HR) and renal sympathetic nerve activity (RSNA) occur in female Lewis Polycystic Kidney (LPK) rats and the underlying mechanism, being any deficit in the afferent, central or efferent components of the reflex pathway. In anaesthetised juvenile and adult LPK and Lewis control rats, baroreflex mediated changes in HR, RSNA and aortic depressor nerve activity (ADNA) were examined. Reflex changes to ADN stimulation and changes in HR in response to vagal efferent nerve stimulation were also determined (n = 64). In the juvenile hypertensive LPK, relative to Lewis controls, both HR and ADNA baroreflex function curves were unaltered. A modest reduction in gain, but not range, of the RSNA baroreflex function curve was observed (-1.8 ± 0.2 vs. -3.2 ± 0.5 %/mmHg, P<0.05). Responses to ADN and vagal efferent nerve stimulation were comparable. In the adult hypertensive LPK, baroreflex control of HR (gain to reflex bradycardia: -0.22 ± 0.04 vs. -0.92 ± 0.15 bpm/mmHg, range: 29 ± 7 vs. 73 ± 9 bpm, P<0.05) and RSNA (gain: -1.1 ± 0.2 vs. -2.6 ± 0.2 %/mmHg, range: 60 ± 7 vs. 80 ± 3%, P<0.05) was reduced. ADNA baroreflex function curves were normal in the adult LPK despite significant vascular remodelling in the aortic arch, while reflex responses to ADN, but not vagal nerve, stimulation were blunted. Our data demonstrates that in female LPK, baroreflex function becomes impaired during adulthood due to impaired central mechanisms that is in parallel with the progression of renal disease. This suggests that renal disease may be triggering central autonomic dysfunction independent of hypertension, sympathetic overactivity or vascular remodelling.

Key words: heart rate, renal sympathetic nerve, aortic depressor nerve, baroreflex, hypertension, chronic kidney disease

4.1 Introduction

Autonomic dysfunction is highly prevalent in chronic kidney disease (CKD) (Dursun et al., 2004, Rubinger et al., 2009) and contributes to an increased risk of cardiovascular morbidity and mortality. This is characterised by sympathetic hyperactivity, which is a powerful predictor of both survival and incidence of cardiovascular complications in CKD patients (Klein et al., 2003, Neumann et al., 2007, Zoccali et al., 2002), and likely underpins the development, maintenance and progression of hypertension in this patient population. Autonomic dysfunction in CKD patients also typically presents as reduced cardiac vagal tone (Harrison et al., 2010, Mircoli et al., 2003) and altered baroreflex regulation of heart rate (HR) (Harrison et al., 2010, Hildreth et al., 2013b, Johansson et al.,

2007, Tinucci et al., 2001) and sympathetic nerve activity (SNA) (Tinucci et al., 2001). The precise underlying cause of altered baroreflex function is currently unknown.

Sex differences exist in both the progression of renal disease, development of cardiovascular disease, and incidence of cardiovascular-related mortality in CKD patients. Female CKD patients often exhibit a slower rate of CKD progression (Eriksen and Ingebretsen, 2006, Xu et al., 2010) and reduced risk of cardiovascular-related mortality (Franczyk-Skora et al., 2012, U.S. renal data system, 2013). Why female sex conveys protection for CKD patients is unknown, with differences in renal structure, systemic and glomerular haemodynamics, lifestyle and the direct effect of sex hormones given as possible causes (Silbiger and Neugarten, 2008). Given the inter-relationship between autonomic dysfunction, particularly baroreflex dysfunction, and an increased risk of cardiovascular and all-cause mortality (Bavanandan et al., 2005, Johansson et al., 2007), it is possible that fundamental differences in the neuroregulatory control of cardiovascular autonomic outflow exist between males and females, and that these differences become more pronounced in the disease state.

Using the Lewis Polycystic Kidney (LPK) rat model of CKD, we recently demonstrated that as renal disease progresses in male rats, a progressive deterioration in both afferent and central functioning of the baroreflex pathway occurs contributing to the temporal decline in baroreflex control of both HR and renal SNA (RSNA), with the progressive deterioration in afferent function related to vascular remodelling in the aortic arch (Chapter 3). In the present study, we therefore hypothesised that female LPK animals would be relatively protected against autonomic dysfunction. Accordingly, the aim of this study was to identify if different temporal changes in the processing of the baroreflex occurs in the female LPK. To achieve this, baroreflex control of both HR and RSNA was assessed in both juvenile and adult female LPK relative to normotensive Lewis female control rats, and the ability of the afferent, central and efferent components of the baroreflex to process information examined.

4.2 Methods

4.2.1 Animals

Juvenile (7–8 weeks old) and adult (12–13 weeks old) female LPK and age-matched Lewis control rats (n = 40 total) were used for surgical in-vivo procedures. In a separate cohort of aged-matched rats (n = 24 total), urinary protein (U_{Pro}), urinary creatinine (U_{Cr}) and urinary protein:creatinine ratio (UPC) were measured using IDEXX VetLab analyser (IDEXX Laboratories Pty Ltd., Australia).

All experiments were approved by the Animal Ethics Committee of Macquarie University and carried out in accordance with the National Health and Medical Research Council of Australia Code of Practice for the Care and Use of Animals for Scientific Purposes (2013).

4.2.2 Surgical Procedures

Animals were anaesthetised with urethane (1.3 g/kg i.p., Sigma Aldrich, Australia) and depth of anaesthesia was confirmed by lack of withdrawal reflexes to corneal stroking and hind-paw pinch.

Supplemental doses of urethane (10–20 mg i.v.) were administered as required. Core body temperature was maintained within the range of 36.5–37.0ºC using a thermostatically controlled electric blanket (Harvard Apparatus Inc., Holliston, MA, USA). The right jugular vein and both femoral veins were cannulated for the administration of fluids (Ringer's solution, 5 ml/kg/hr) and drugs respectively, and right carotid artery cannulated in order to record arterial pressure. A tracheostomy was performed and if required, the animal artificially ventilated with oxygen enriched room air with ventilation rate and volume adjusted to maintain pH at 7.40 ± 0.05 and PCO_2 at 40 ± 5 mmHg. A dorsal cervical incision was made and the left aortic depressor nerve (ADN) and left vagus nerve isolated. The left renal nerve was isolated retroperitoneally. All nerves were placed on bipolar silver wire recording electrodes and maintained in paraffin oil. Nerve recordings were amplified, band-pass filtered (10–1000Hz, CWE Inc., Ardmore, PA, USA) and sampled at 5 kHz using a CED 1401 plus (Cambridge Electronic Designs Ltd, Cambridge, UK) and Spike2 (v7, Cambridge Electronic Designs Ltd., Cambridge, UK), using the same bioamplifier calibrated to a pre-set voltage of 50 µV.

4.2.3 Experimental protocols

Following completion of all surgical procedures, animals were allowed to stabilise for at least 30 minutes. Subsequently, all animals underwent at least one of the following protocols, inclusive of Protocol I.

Protocol I: Assessment of the relationship between blood pressure (BP) and ADN activity (ADNA), RSNA and HR. The vasoactive agents, phenylephrine (PE, 10–50 µg/kg, Sigma Aldrich, Australia) and sodium nitroprusside (SNP, 50–70 µg/kg, Sigma Aldrich, Australia) were administered intravenously over a period of ~5 seconds in order to increase and decrease BP respectively. Corresponding changes in ADNA, RSNA and HR were, where possible, simultaneously recorded. In animals that subsequently underwent Protocol II and/or III, the ADN was cut distal to the recording electrode and background nerve activity recorded. Animals that did not undergo Protocol II and/or III were euthanased with an overdose of sodium pentobarbital (60 mg/kg i.v., Virbac® Pty Ltd., Australia) and background ADNA recorded.

Protocol II: Assessment of the RSNA, HR and BP response to ADN stimulation. The rostral cut end of the ADN was stimulated sequentially using a 5-second train (4.0V, 2.0-ms pulses) of 1, 2, 4, 8, 16 and 24 Hz separated by a period of 3–5 minutes and changes in RSNA, HR and BP recorded. All variables were allowed to return to baseline pre-stimulus levels before application of the next stimulus.

Protocol III: Assessment of HR response to cervical vagal efferent stimulation. The left vagus nerve was cut and the peripheral end was stimulated sequentially using a 5-second train (4.0V, 2.0-ms pulses) of 1, 2, 4, 8, 16, 24, 32, 40 and 48 Hz separated by a period of 3–5 minutes. Heart rate was continuously recorded.

At the end of the final experimental protocol(s), the renal nerve was cut proximally to the recording electrode and RSNA recorded. Animals were euthanased with an overdose of sodium pentobarbital (60 mg/kg i.v.). A cohort of animals was then transcardially perfused with heparinised 0.9% saline followed by 4% formalin in saline. The aortic arch was then removed, post-fixed in 4% formalin for a minimum of 24 hours, dehydrated, paraffin-embedded and 5 µm sections taken and stained with Shikata's orcein, Martius Scarlet Blue (MSB) and Von Kossa in order to quantify total elastin, collagen and calcium densities within the aortic arch as described previously (Ng et al., 2011b).

4.2.4 Data analysis

Baseline data: Baseline measurements of mean arterial pressure (MAP), systolic BP (SBP), diastolic BP (DBP), pulse pressure (PP) and HR were taken over a 30-second period immediately prior to commencement of the experimental protocol. For both RSNA and ADNA, the level of nerve activity following euthanasia or nerve transection was subtracted and the resulting level of nerve activity was averaged over the baseline 30-second period.

Baroreflex function curves: The level of RSNA and ADNA immediately preceding the PE-induced increase in BP and SNP-induced decrease in BP was set as 100% and the level of nerve activity following nerve transection or euthanasia set as 0%. The level of MAP and corresponding level of HR, RSNA (% or µV) and ADNA over the active phase of the pharmacologically induced increase and decrease in BP and the relationship between ADNA and RSNA in response to alterations in MAP were fitted to a four-parameter sigmoid regression curve using the following equation:

$$y = \frac{A_1}{1 + \exp([A_2(MAP - A_3)]} + A_4$$

where A_1 is the y axis range of the curve, A_2 is the gain coefficient, A_3 is midpoint of the curve and A_4 is the lower plateau.

Heart rate baroreflex sensitivity was also examined by separately calculating the sensitivity of the relationship between an increase and decrease in BP and the reciprocal reflex bradycardia (BRS_{PE}) or tachycardia (BRS_{SNP}), respectively, as follows:

$$sensitivity = \frac{\text{change in HR (bpm)}}{\text{change in MAP (mmHg)}}$$

Aortic depressor and vagal nerve stimulation: In response to stimulation of ADN, the absolute change in HR (beats per minute, bpm) and MAP (mmHg), and the percentage change in RSNA, were calculated relative to a 30-second period immediately prior to the application of each stimulus. The HR response to stimulation of the vagus nerve was likewise calculated as an absolute change.

Histomorphometric analysis of the aortic arch: Sections of aortic arch stained with Shikata's orcein, MSB or Von Kossa were imaged using a video camera mounted on a microscope (Carl Zeiss Microimaging, Gottingen, Germany) and processed with Zeiss Axiovision software (AxioVs40

v4.8.2.0, Carl Zeiss Microimaging, Gottingen, Germany). All images were binarized and analysed using Image J (v1.47d, National Institute of Health, USA) in order to quantify the percentage of staining for Shikata's orcein, to identify the elastin component of the aortic arch (red), MSB, to identify the collagen component of the aortic arch (blue), and Von Kossa, to identify calcium deposition within the aortic arch (black), respectively. Nuclei values were determined from brown/black staining on MSB sections. Evaluation of aortic arch thickness, elastin lamellae fracture points, calcium density and average size of calcium deposits was performed on the whole aortic segment (captured at 10x magnification) for each animal. Aortic arch thickness was an average of at least eight measurements distributed around the aortic arch section. All other histomorphometric parameters were calculated from an average of 4 fields equally distributed around the circumference of the aorta from images captured at 20 x magnification. All images were visually inspected by two investigators and compared with the original image to ensure that all parameters were identified accurately.

4.2.5 Statistical analysis

All data are expressed as mean ± standard error of the mean (SEM). Statistical analysis was performed using GraphPad Prism software (GraphPad Prism software v6 Inc., La Jolla, CA, USA). A Brown-Forsythe test was used to determine if there were any differences in the variance, and if so, the data was log-transformed before statistical analysis. All data was analysed using a two-way ANOVA with strain and age as variables. If either strain or age differences were noted, the data was further analysed using a Bonferroni's post-hoc test. The gain and range of the MAP-ADNA function curves were correlated with the aortic arch histomorphometrical indices detailed above. Correlation analysis was performed using a Pearson correlation followed by linear regression. Significance was defined as $P \leq 0.05$ for all analysis.

For more detailed description of the Methods, refer to Chapter (3).

4.3 Results

4.3.1 Baseline data

Baseline measurements of SBP, DBP, PP, MAP, HR and RSNA, but not ADNA, were elevated in both juvenile and adult LPK compared with age-matched Lewis (Table 4.1). Both PP and ADNA showed an overall age effect, being greater in the adult versus juvenile animals.

In the Lewis animals, only 2/6 juvenile and 1/8 adult Lewis had detectable protein levels, while in the LPK animals, 2/5 juvenile LPK and 5/5 adult LPK had detectable protein in their urine. Accordingly, adult LPK had significantly higher U_{Pro} relative to age-matched Lewis and juvenile LPK (Table 4.1). Measurements of U_{Cr} were comparable between juvenile LPK versus Lewis. In adult LPK, however, U_{Cr} was significantly lower compared with adult Lewis (Table 4.1). As U_{Pro} could not be detected in

>2 Lewis and juvenile LPK animals, mean values for UPC were not calculated. In the adult LPK, UPC was 4.4 ± 0.5 (n = 5).

4.3.2 Baroreceptor reflex control of HR, RSNA and ADNA

Reflex HR, RSNA and ADNA responses to pharmacologically-evoked increases and decreases in BP following administration of PE and SNP, respectively, are illustrated in Figure 4.1. Representative curves showing the sigmoidal fit of MAP versus HR, RSNA and ADNA in juvenile and adult Lewis and LPK rats are shown in Figure 4.2, and group data in Figure 4.3.

(i) Baroreflex control of HR: The HR baroreflex function was shifted to the right in both LPK groups (Figure 4.3A), as indicated by an overall increase in MAP_{50} and MAP_{sat} in the LPK versus Lewis (Table 4.2). In the juvenile LPK, these curves were also shifted upward, resulting in a greater upper plateau; however, this parameter decreased with age in the LPK, such that the curve was no longer shifted upward in the adult LPK compared with Lewis (Table 4.2). The lower plateau and range of the reflex were not different between the juvenile groups, but were significantly reduced in the adult female LPK compared with both age-matched Lewis and juvenile LPK. An overall increase in HR levels at MAP_{sat} was also observed in the LPK versus Lewis. There was a trend for the gain of the HR baroreflex function curve to be reduced in the LPK (Table 4.2), however this did not reach statistical significance (P = 0.06). When the reflex bradycardic and tachycardic components were examined separately, BRS_{PE} was reduced in the adult LPK (0.22 ± 0.04 bpm/mmHg) relative to both age-matched Lewis (0.92 ± 0.15 bpm/mmHg, P<0.01) and juvenile LPK (0.80 ± 0.17 bpm/mmHg, P<0.05). Measures of BRS_{SNP}, in contrast, was relatively comparable in the adult LPK (0.28 ± 0.04 bpm/mmHg) in comparisons with either age-matched Lewis (0.56 ± 0.18 bpm/mmHg, P = 0.34) or juvenile LPK (0.34 ± 0.09 bpm/mmHg P > 0.99). In the Lewis, age did not influence both BRS_{PE} and BRS_{SNP} (BRS_{PE}: 1.03 ± 0.18 vs. 0.92 ± 0.15 and BRS_{SNP}: 0.65 ± 0.16 vs. 0.56 ± 0.18 bpm/mmHg, juvenile vs. adult; both P>0.05).

(ii) Baroreflex control of RSNA: Renal sympathetic baroreflex function curves were shifted to the right in both the juvenile and adult LPK (Figure 4.3B). Accordingly, measures of $MAP_{50,}$ MAP_{thr} and/or MAP_{sat} were greater in the LPK compared with age-matched Lewis (Tables 4.2). MAP operating range was only greater in the adult LPK relative to Lewis controls. In juvenile LPK, the upper and lower plateaus were similar, resulting in a comparable range of the relationship in the juvenile LPK versus Lewis (Tables 4.2). In adult LPK, the upper plateau was comparable; however, the lower plateau and therefore RSNA at MAP_{sat} were elevated relative to age-matched Lewis and/or juvenile LPK rats (Table 4.2). This was, consequently, associated with a reduced range of the reflex in adult LPK versus adult Lewis and juvenile LPK (Table 4.2). The gain of the RSNA baroreflex was significantly reduced in both juvenile and adult LPK (Table 4.2) but an age effect was not apparent.

To account for inherent differences in baseline RSNA between the strains, RSNA baroreflex function curves were also constructed using microvolt changes (Figure 4.4). Consistent with an elevated level

of baseline RSNA, the upper and lower plateaus of the reflex and therefore values of RSNA at MAP_{thr} and MAP_{sat} were significantly higher in the juvenile and adult LPK versus age-matched Lewis (Table 4.3). The absolute range and gain of the reflex was greater in the juvenile LPK compared with age-matched Lewis, but these decreased with age such that the range and gain were not different in the adult LPK compared with age-matched Lewis (Table 4.3).

(iii) Baroreflex control of ADNA: Administration of PE increased ADNA while SNP resulted in markedly reduced activity (Figure 4.1). For ADN burst frequency analysis see Appendix 1.

In order to examine whether any deficits in baroreflex control of HR and RSNA were associated with impaired functioning of the afferent component of the baroreflex, the responsiveness of the ADN to changes in BP were examined and ADNA baroreflex function curves generated. As shown in Figure 4.1, administration of PE increased ADNA while SNP resulted in markedly reduced activity. Consistent with an elevated level of resting BP, the ADNA baroreflex function curves (Figure 4.3) were shifted to the right in the LPK in both age groups with a resultant increase in MAP_{50} and MAP_{sat} in the LPK versus Lewis (Table 4.2). While an age-related increase in the lower plateau of the function curve was observed in the LPK ($P = 0.04$), no further strain or age differences were noted in the ability of the ADN to respond to changes in BP in all groups (Table 4.2).

4.3.3 Central component of baroreflex arc

To test whether any difference in baroreflex control of HR or RSNA were associated with a central baroreflex deficit, the central component of the baroreflex arc was tested indirectly by correlating changes in ADNA and RSNA in response to alterations in MAP (Figure 4.5) and directly by measuring reflex changes to direct stimulation of the ADN (Figure 4.6).

(i) Indirect assessment: The ADNA-RSNA relationship was comparable in the juvenile Lewis and LPK and none of the curve parameters differed between the groups (Figure 4.5, Table 4.4). In adult LPK, however, the upper plateau of the relationship was blunted compared with juvenile LPK, whereas the lower plateau and RSNA at $ADNA_{sat}$ were shifted upward relative to adult Lewis and juvenile LPK. Measures of RSNA at $ADNA_{thr}$ were overall significantly greater in the LPK versus Lewis. Consequently, RSNA range was reduced in the adult LPK versus Lewis, and a temporal decline in the LPK was evident. The gain of the relationship was only lower relative to adult Lewis (Table 4.4). Consistent with the comparable ADNA-MAP relationship between female Lewis and LPK, $ADNA_{50}$, $ADNA_{thr}$, $ADNA_{sat}$ and the ADNA range over which reflex control of RSNA was achieved remained unaltered in the adult LPK versus Lewis and an-age related change in these parameters was not observed (Table 4.4).

(ii) Direct assessment: Representative data traces illustrating reflex RSNA, HR and MAP responses to direct electrical stimulation of the ADN in adult female Lewis and LPK rats are shown in Figure 4.6. In both LPK and Lewis, regardless of age, stimulation of the ADN between 1–24 Hz produced

frequency-dependent reductions (P<0.001) in RSNA, HR and MAP (Figure 4.7). In juvenile LPK, the reflex sympathoinhibition (%) was comparable to Lewis controls. An age-related increase in reflex sympathoinhibition in the Lewis (P<0.001) and decrease in the LPK (P<0.05) was observed. Consequently, the reflex sympathoinhibition was reduced in the adult LPK compared with age-matched Lewis controls. Reflex bradycardia remained unchanged in the juvenile LPK versus Lewis and did not alter with age in the Lewis (P = 0.99). In the LPK, however, an age-related decline was noted and consequently, the reflex bradycardic response was reduced in the adult LPK compared with Lewis and juvenile LPK. The reflex depressor response was increased overall in the juvenile LPK compared with age-matched Lewis and declined with age in both LPK and Lewis animals (P<0.01). While there was a tendency for the depressor response to be reduced in the adult LPK compared with Lewis (P = 0.06), this did not attain statistical significance.

Sympathoinhibitory responses to ADN stimulation were also quantified in microvolts (Figure 4.7). Unlike (%) data, the sympathoinhibitory response (μV) was markedly enhanced in the juvenile LPK and this was most noticeable at higher frequencies. Reflex sympathoinhibition expressed in microvolts was not different between the adult LPK and Lewis; however, an age-related reduction was only evident in the LPK.

4.3.4 Efferent baroreflex function

To assess the efficacy of the end-organ to respond to baroreflex-related inputs, the peripheral cut-end of the vagus nerve was stimulated and changes in HR measured. In both LPK and Lewis, regardless of age, stimulation of the vagus nerve produced a frequency-dependent reduction in HR (P<0.001, Figure 4.8). An age-related decline in the bradycardic response to vagal stimulation was observed in both the LPK and Lewis; however, at neither age examined did the bradycardic response differ between the two strains.

4.3.5 Histomorphometry of the aortic arch and correlation with afferent baroreflex function

Typical examples of horizontal sections of the aortic arch stained with Shikata's orcein, MSB and Von Kossa in adult female LPK and Lewis rats are shown in Figure 4.9 and histomorphometric differences presented in Table 4.5. In the juvenile female LPK rats, there was an increase in aortic medial wall thickness, enlargement of the interlamellae elastin spacing, increase in elastin lamellae breaks, increase nuclear cross sectional area and a reduction in the elastin-to-collagen ratio. In the adult LPK, these differences became more pronounced, with an age-related increase in aortic arch medial wall thickness, reduction in elastin density and consequently elastin-to-collagen ratio, and an increase in elastin lamellae spacing and number of elastin lamellae fractures observed. A temporal reduction in elastin density and elastin-to-collagen ratio and increase in elastin lamellae spacing was also noted in the Lewis. None of the changes in the structure of the vascular wall correlated with the MAP-ADNA functional parameters (Table 4.6).

4.4 Discussion

In the present study, we demonstrate that as renal disease progresses in female LPK rats, a temporal decline in baroreflex control of both HR and RSNA results, mediated by a reduced ability of the central component of the baroreflex to produce reflex-evoked changes in both HR and RSNA. Unexpectedly, we saw no deterioration in the capacity of the baroreceptor afferents to respond to changes in BP, despite a marked vasculopathy within the aortic arch. This is in stark contrast to our work in the male LPK rat where we saw not only a decline in the capacity of the central component of the baroreflex, but a strong correlation between aortic arch remodelling and impaired baroreceptor afferent signalling (Chapter 3). As juvenile female LPK were already markedly hypertensive with increased SNA, our results suggest that in this model of CKD, a decline in renal function is the trigger for the change in central processing of the baroreflex in the adult animals.

Here, we demonstrate for the first time that female LPK rats exhibit a temporal decline in baroreflex control of HR and RSNA. In juvenile female rats, where renal function is not overtly compromised, baroreflex control of HR was intact. There was a reduction in the gain of the RSNA baroreflex function curve; however, this is unlikely to be reflective of impaired baroreflex function as it was not associated with any deficit in processing of the baroreflex pathway and analysis of the microvolt RSNA data indicated that both the range and gain of the reflex were enhanced at this age. Instead, it is possible that the reduction in baroreflex gain of the normalised RSNA data reported at this age is biased by the higher level of RSNA exhibited in the LPK. In the adult female LPK, however, as renal function becomes compromised, there was a decline in both baroreflex control of RSNA and HR. With respect to baroreflex control of RSNA, an age-related decline in both the range and gain of the microvolt RSNA baroreflex function curves was also noted, thus supporting our normalised RSNA baroreflex function curve results. On the other hand, while the overall range of the HR baroreflex was reduced, the gain of the reflex bradycardic component only was affected, implying that baroreflex control of cardiac vagal, but not sympathetic, outflow is abnormal in the adult female LPK rats.

While significant remodelling along the aortic arch was noted in both juvenile and adult LPK, which would render the aortic arch stiffer, and the afferent baroreflex function curves were shifted to the right (reflective of the higher resting BP of the LPK), there was no overall difference in functionality of the afferent component of the reflex when compared to the Lewis control strain. This was very surprising given our previous reports of a significant correlation between vascular stiffness in the aortic arch and afferent baroreflex function in the male LPK (Chapter 3), and the known association between baroreflex function and arterial stiffness (Studinger et al., 2006) in end-stage renal disease patients. Notably, the adult female LPK did not exhibit any marked vascular calcification within the aortic arch region. Given that vascular calcification is associated with a decline in the range of the afferent component of the reflex (Chapter 3) and has specifically been shown to be associated with reduced baroreflex function in CKD (Chan et al., 2005, Chesterton and McIntyre, 2005), it is possible

that reduced vascular calcification within the aortic arch of the female LPK was key to preservation of afferent baroreflex function.

While afferent baroreceptor function was unaffected in the female LPK, the central component of the baroreceptor reflex was compromised, and during adulthood reduced HR and RSNA responses to stimulation of the ADN and diminished ADNA-RSNA relationship were observed. The underlying development of impaired central baroreflex function, however, appears to differ depending on the target outflow. With regards to the central regulation of RSNA, this was impaired in the adult female LPK due mainly to an age-related decline in the sympathetic response (both % and μV) to ADN stimulation, which was not observed in the Lewis. A similar age-related decrease in the reflex bradycardic response was also observed in the adult LPK and consequently the reflex bradycardic response was reduced in comparison to both juvenile LPK and adult Lewis. These observations indicate that central baroreflex regulation of HR is also impaired in the adult female LPK. While the central baroreflex control of both HR and RSNA was reduced in the adult LPK, this did not have a major effect on the overall ability to counteract fluctuations in BP, as the overall MAP response to ADN stimulation was not statistically different between adult LPK and Lewis rats. Thus, although changes in central processing of the baroreflex seem to underlie the altered baroreflex control of HR and RSNA observed in the adult female LPK, the fact that this did not lead to an overall reduction in the MAP response suggests that baroreflex control of other sympathetic outflows are not similarly affected. This is supported by our previous work in the adult male LPK rat, where under experimental conditions comparable to this study, baroreflex control of splanchnic SNA is preserved (Harrison et al., 2010).

To strengthen our assertion that the underlying cause of baroreflex dysfunction in the adult female LPK is primarily localised to the central component of the reflex pathway, the ability of the heart to respond to vagal nerve input was examined. Consistent with previous studies examining the age-related change in vagal control of HR (Minami and Head, 2000), we observed an age-related reduction in the HR response to left vagal nerve stimulation in the female Lewis rats. A comparable age-related reduction in the chronotropic responses to vagal efferent nerve stimulation was observed in the female LPK. Importantly, however, both LPK and Lewis rats maintained relatively similar bradycardic response to vagal nerve stimulation at each time point studied, indicating that that in the LPK the responsiveness of the heart to vagal efferent inputs is adequate and is not contributing to the reduced baroreflex control of HR in the adult LPK.

4.5 Limitations

The potential impact of the stage of the oestrous cycle needs to be considered in regards to our findings, as it has previously been reported to impact on baroreflex function (Goldman et al., 2009). While animals used in this study were not matched for the stage of the oestrous cycle, they were, however, matched for age, and clear-cut differences in the measured variables were observed within

the female animals. This therefore indicates that the effect of the oestrus cycle, if any, did not limit our capacity to identify temporal and strain differences between the groups.

4.6 Perspectives and significance

One of the major treatment goals for CKD is to lower BP with a view toward reducing cardiovascular risk and preventing any further deterioration in renal function (Harris and Rangan, 2005, Ravera et al., 2006). In addition to a high resting level of BP (Mazzuchi et al., 2000), the inability to buffer acute changes in BP predicts an increased risk of cardiovascular mortality in people with CKD (Bavanandan et al., 2005, Johansson et al., 2007). In the present study, we demonstrate that reduced baroreflex control of both HR and RSNA in female LPK rats is due to altered processing in the central component of the baroreflex and is not directly related to the presence of a vasculopathy within the aortic arch region, nor hypertension and increased SNA, both of which are elevated in the juvenile animals while central baroreflex function is still intact. Instead, our data suggests that the decline in renal function is the critical trigger. Therefore, in females with CKD, reducing BP alone may not be sufficient to impact baroreflex dysfunction and aggressive preservation of renal function may be paramount to preserving baroreflex function and reducing the associated risk of mortality.

Table 4.1: Baseline parameters in juvenile (7–8 weeks old) and adult (12–13 weeks old) female Lewis and Lewis Polycystic Kidney (LPK) rats

Group	Juvenile		Adult		Two-way ANOVA adjusted *P* value	
	Lewis *(6)*	LPK *(5)*	Lewis *(8)*	LPK *(5)*	Strain	Age
Parameter						
BW (g)	168 ± 4	130 ± 6*	230 ± 3†	166 ± 5$^{*\dagger\#}$	<0.0001	<0.0001
U_{Pro} (g/L)	0.01 ± 0.01	0.11 ± 0.08	0.01 ± 0.01	0.69 ± 0.12$^{*\dagger\#}$	<0.0001	0.0001
U_{Cr} (g/L)	1.05 ± 0.50	0.21 ± 0.04	1.25 ± 0.18	0.16 ± 0.02*	0.0032	0.7998
SBP (mmHg)	121 ± 3	176 ± 7*	127 ± 2	183 ± 5*	<0.0001	0.1316
DBP (mmHg)	61 ± 3	75 ± 4*	59 ± 2	67 ± 4*	0.0012	0.1013
PP (mmHg)	60 ± 3	102 ± 6*	69 ± 2	116 ± 3*†	<0.0001	0.0040
MAP (mmHg)	85 ± 3	116 ± 4*	85 ± 2	107 ± 5*	<0.0001	0.1720
HR (bpm)	340 ± 6	388 ± 12*	323 ± 8	366 ± 14*	<0.0001	0.0572
ADNA (μV)	0.4 ± 0.1	0.5 ± 0.1	1.1 ± 0.3	0.9 ± 0.3	0.9641	0.0330
RSNA (μV)	4.3 ± 1.0	10.0 ± 1.9*	3.9 ± 0.9	9.6 ± 1.2*	<0.0001	0.7560

BW, body weight; U_{Pro}, urinary protein; U_{Cr}, urinary creatinine; MAP, mean arterial pressure; SBP, systolic blood pressure; DBP, diastolic blood pressure; PP, pulse pressure; HR, heart rate; ADNA, aortic depressor nerve activity; and RSNA, renal sympathetic nerve activity.

Results are expressed as mean ± SEM.

$^{*}P<0.05$ vs. age-matched Lewis.

$^{\dagger}P<0.05$ vs. strain-matched juvenile rat.

$^{\#}P<0.05$ for strain × age interaction.

(n) values denoted in subscript and represent the minimum number in each group.

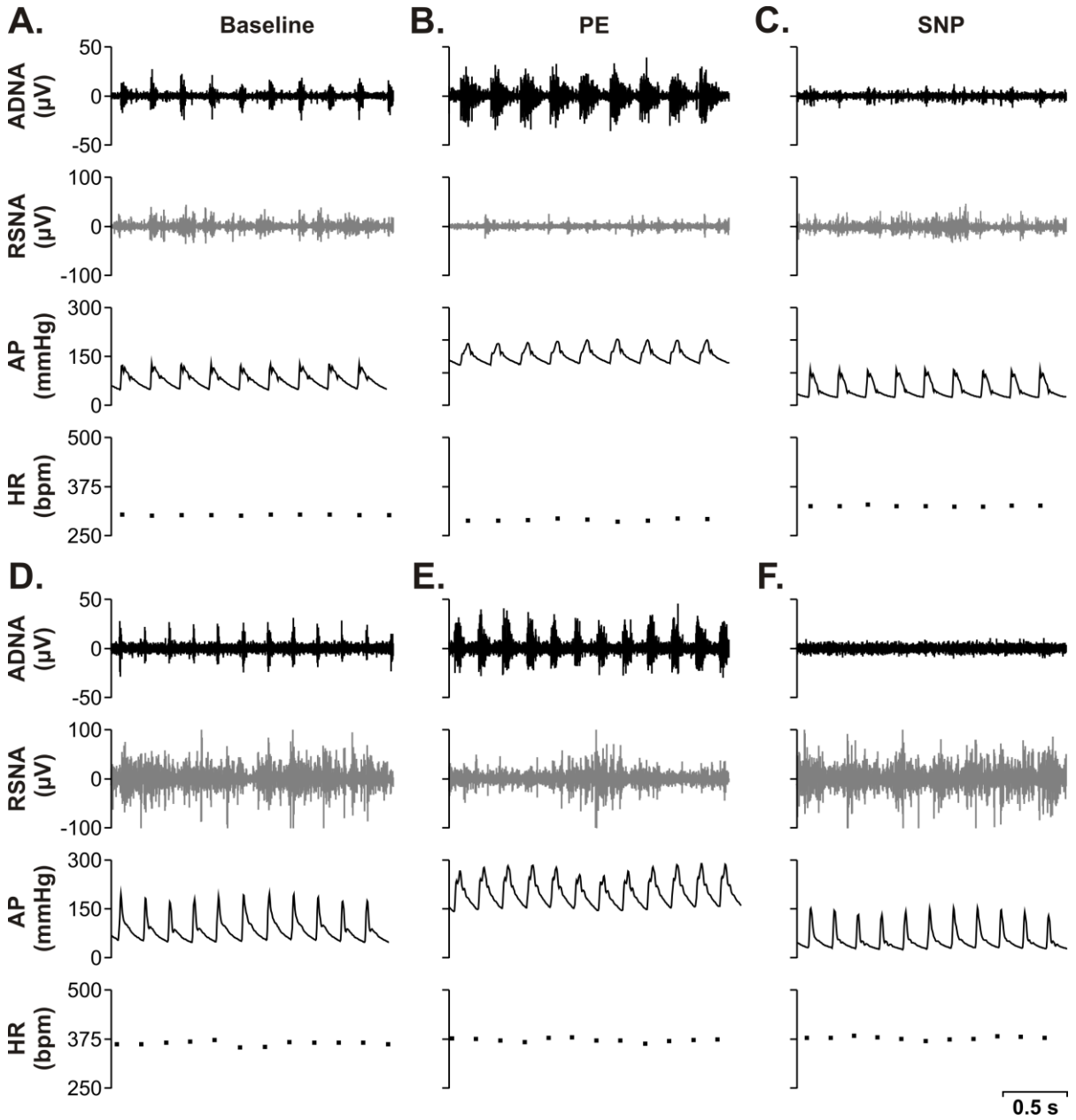

Figure 4.1: Representative raw data traces, illustrating responses of aortic depressor nerve activity (ADNA), renal sympathetic nerve activity (RSNA) and heart rate (HR) to evoked changes in arterial pressure (AP) from an (A–C) adult (12–13 weeks old) female Lewis and (D–E) adult female Lewis Polycystic Kidney (LPK) rat. Bursts of ADNA can be seen in association with each pulse of AP in both Lewis and LPK. In response to phenylephrine (PE, 10–50 μg/kg), RSNA is silenced and HR reduced in the Lewis (B); however, in the LPK (E), reflex sympathoinhibition and bradycardia is reduced. Significant reductions in ADNA and reflex tachycardia are observed when AP is reduced by sodium nitroprusside (SNP, 50–70 μg/kg i.v.; C and F). bpm: beats per minute.

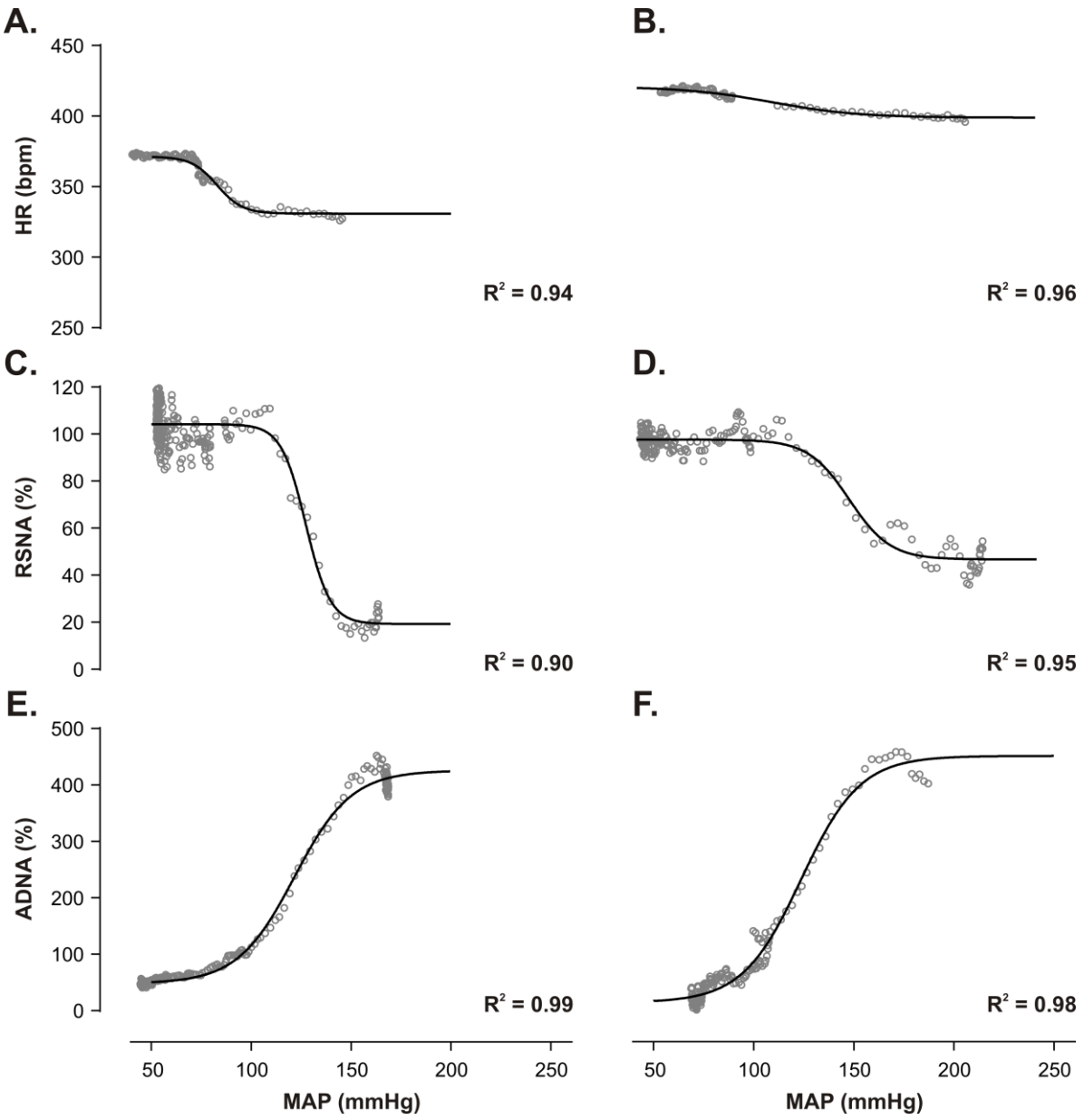

Figure 4.2: Representative raw data curves from individual animals showing the sigmoidal relationship between mean arterial pressure (MAP) and heart rate (HR; A–B), renal sympathetic nerve activity (RSNA; C–D) and aortic depressor nerve activity (ADNA; E–F) in adult female (12–13 weeks old) Lewis (left panels) and Lewis Polycystic Kidney (LPK) rats (right panels).

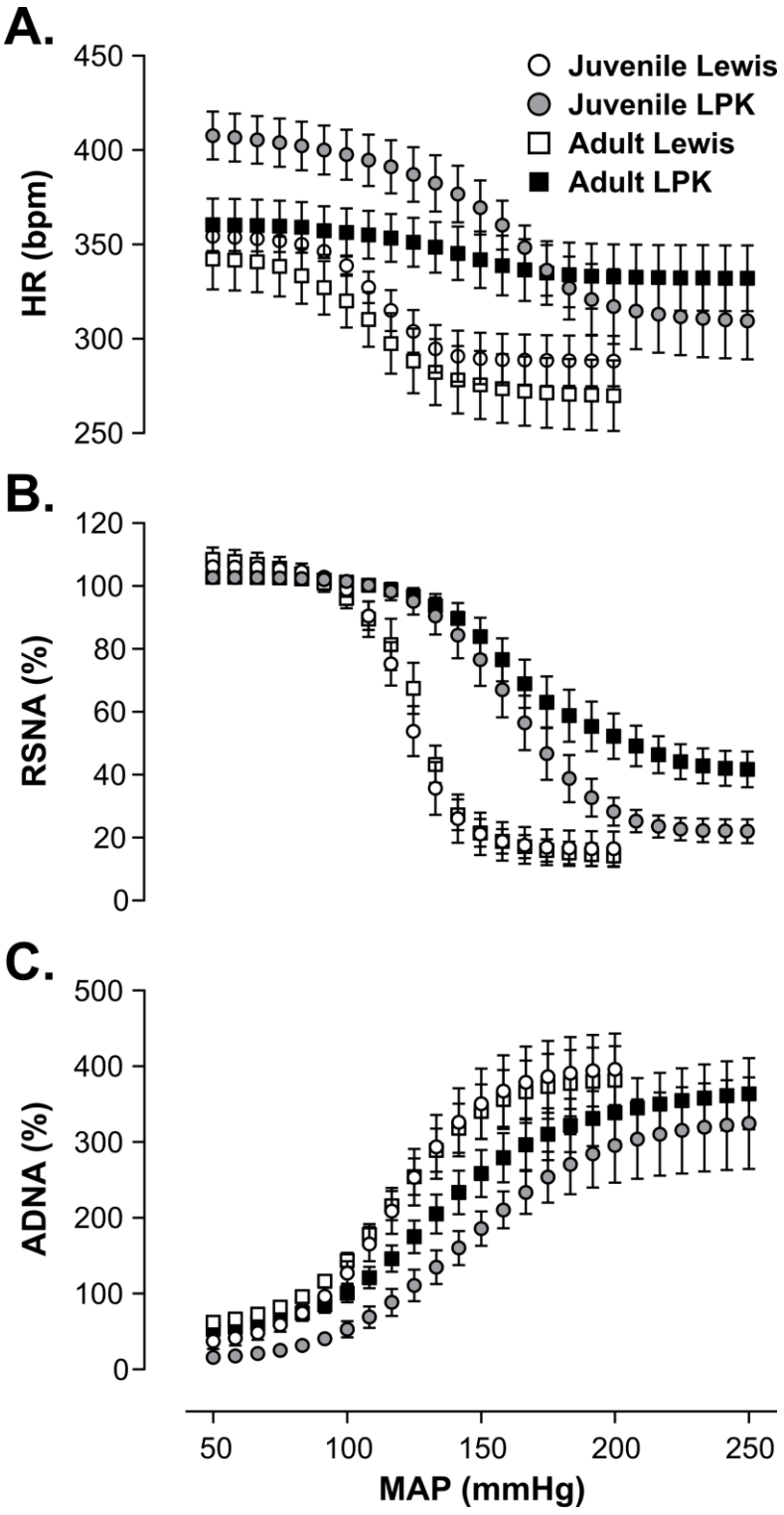

Figure 4.3: Logistic function curves illustrating the relationship between mean arterial pressure (MAP) and heart rate (HR; A), renal sympathetic nerve activity (RSNA; B) and aortic depressor nerve activity (ADNA; C) in juvenile (7–8 weeks old) and adult (12–13 weeks old) female Lewis and Lewis Polycystic Kidney (LPK) rats. Results are expressed as mean ± SEM. *n* values are detailed in Table 4.2. bpm: beats per minute. (HR: $R^2 = 0.95 \pm 0.005$, RSNA: $R^2 = 0.94 \pm 0.009$ and ADNA: $R^2 = 0.98 \pm 0.003$, all groups).

Table 4.2: Parameters describing the relationship between mean arterial pressure (MAP) and heart rate (HR), renal sympathetic nerve activity (RSNA) and aortic depressor nerve activity (ADNA) in the juvenile (7–8 weeks old) and adult (12–13 weeks old) female Lewis and Lewis Polycystic Kidney (LPK) rats

Group	**Juvenile**		**Adult**		**Two-way ANOVA adjusted *P* value**	
	Lewis	LPK	Lewis	LPK	Strain	Age
Parameter						
HR barocurve *(n)*	*8*	*8*	*11*	*7*	-	-
HR upper plateau (bpm)	357 ± 4	413± 14*	342 ± 16	361 ± 14†	0.0110	0.0229
HR lower plateau (bpm)	288 ± 13	306 ± 19	269 ± 19	332 ± 17*	0.0396	0.9552
Range (bpm)	69 ± 14	108 ± 25	73 ± 9	29 ± 7$^{*\dagger\#}$	0.1537	0.0079
Gain (bpm /mmHg)	-2.6 ± 0.8	-1.7 ± 0.8	-2.5 ± 0.6	-0.8 ± 0.2*	0.0087	0.5259
MAP_{50} (mmHg)	107 ± 6	143 ± 9*	111 ± 7	124 ± 10	0.0037	0.3540
MAP_{thr} (mmHg)	92 ± 10	109 ± 13	98 ± 6	106 ± 11	0.2313	0.8745
HR at MAP_{thr} (bpm)	342 ± 4	391 ± 11	327 ± 16	355 ± 15	0.0088	0.0556
MAP_{sat} (mmHg)	121 ± 4	177 ± 11*	124 ± 7	142 ± 11$^{\#}$	0.0002	0.0710
HR at MAP_{sat} (bpm)	302 ± 11	329 ± 15*	285 ± 18	338 ± 17*	0.0203	0.6739
MAP operating range (mmHg)	30 ± 10	68 ± 17	25 ± 4	36 ± 9	0.2313	0.8745
RSNA barocurve *(n)*	*8*	*7*	*9*	*8*	-	-
RSNA upper plateau (%)	107 ± 2	102 ± 2	102 ± 1†	100 ± 1	0.0304	0.0156
RSNA lower plateau (%)	14 ± 4	23 ± 5	22 ± 3	40 ± 7*†	0.0103	0.0126
Range (%)	93 ± 4	80 ± 5	80 ± 3	60 ± 7*†	0.0029	0.0029
Gain (%/mmHg)	-3.2 ± 0.5	-1.8 ± 0.2*	-2.6 ± 0.2	-1.1 ± 0.2*	0.0002	0.0559
MAP_{50} (mmHg)	124 ± 3	162 ± 8*	129 ± 3	154 ± 8*	<0.0001	0.7735
MAP_{thr} (mmHg)	112 ± 4	147 ± 9*	117 ± 3	133 ± 7	<0.0001	0.4679
RSNA at MAP_{thr} (%)	87 ± 2	86 ± 1	85 ± 1	87 ± 2	0.7967	0.9927
MAP_{sat} (mmHg)	134 ± 3	176 ± 8*	140 ± 5	175 ± 4*	<0.0001	0.9459

RSNA at MAP_{sat} (%)	35 ± 4	41 ± 4	39 ± 3	53 ± 5*	0.0157	0.0200
MAP operating range (mmHg)	25 ± 6	29 ± 1	22 ± 3	41 ± 6*	0.0139	0.2986
ADNA barocurve *(n)*	*5*	*7*	*12*	*8*	-	-
ADNA upper plateau (%)	400 ± 47	336 ± 64	385 ± 46	375 ± 55	0.5203	0.8245
ADNA lower plateau (%)	28 ± 11	10 ± 4	53 ± 8	44 ± 12†	0.1777	0.0061
Range (%)	372 ± 53	325 ± 65	331 ± 49	331 ± 64	0.7087	0.7900
Gain (%/mmHg)	5.5 ± 1.0	4.0 ± 0.7	5.4 ± 0.7	4.0 ± 0.7	0.0943	0.9521
MAP_{50} (mmHg)	118 ± 3	142 ± 8*	114 ± 4	136 ± 7*	0.0008	0.3742
MAP_{thr} (mmHg)	95 ± 4	115 ± 6	93 ± 6	108 ± 5	0.0067	0.4565
ADNA at MAP_{thr} (%)	107 ± 10	77 ± 14	123 ± 10	114 ± 7	0.1036	0.0267
MAP_{sat} (mmHg)	141 ± 2	170 ± 11*	135 ± 4	163 ± 10*	0.0013	0.4133
ADNA at MAP_{sat} (%)	321 ± 36	266 ± 50	315 ± 35	305 ± 41	0.4716	0.7148
MAP operating range (mmHg)	46 ± 5	56 ± 9	42 ± 3	56 ± 9	0.1038	0.7495

MAP_{50}, mean arterial pressure at the midpoint of the curve; MAP_{thr}, threshold mean arterial pressure to trigger a change in HR, RSNA or ADNA; and MAP_{sat}, saturation mean arterial pressure at which there is no further change in HR, RSNA or ADNA.
Results are expressed as mean ± SEM.
* $P<0.05$ vs. age-matched Lewis.
† $P<0.05$ vs. strain-matched juvenile rat.
# $P<0.05$ for strain × age interaction.
(n) = number in each group.

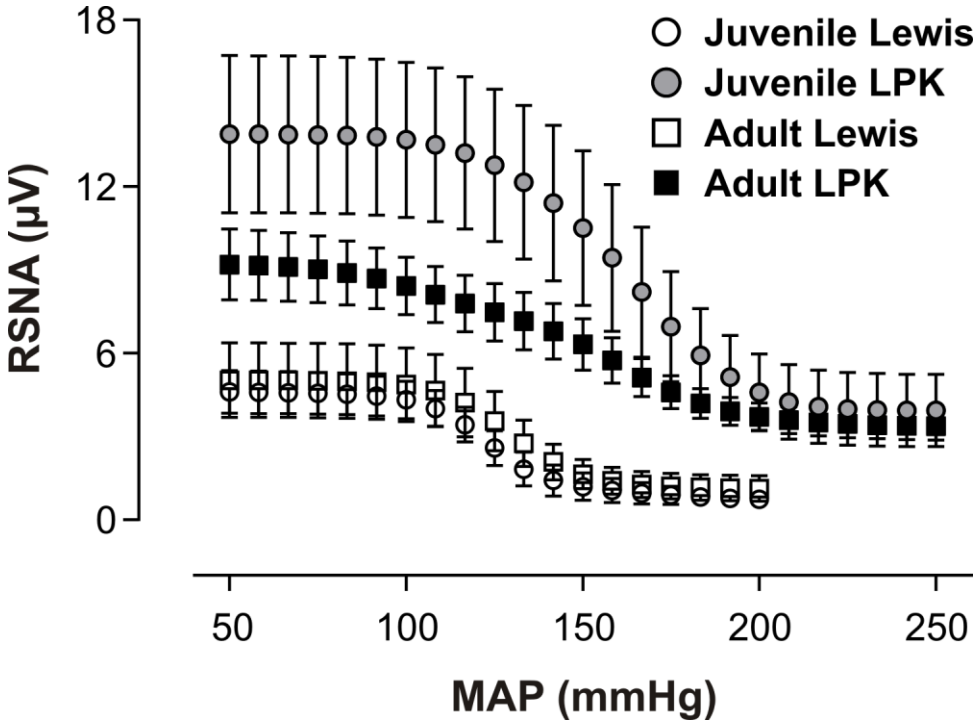

Figure 4.4: Logistic function curves illustrating the relationship between mean arterial pressure (MAP) and renal sympathetic nerve activity (RSNA) expressed in microvolts (μV) in juvenile (7–8 weeks old) and adult (12–13 weeks old) female Lewis and Lewis Polycystic Kidney (LPK) rats. Results are expressed as mean ± SEM. *n* values are as detailed in Table 4.3. (R^2 = 0.93 ± 0.01 all groups).

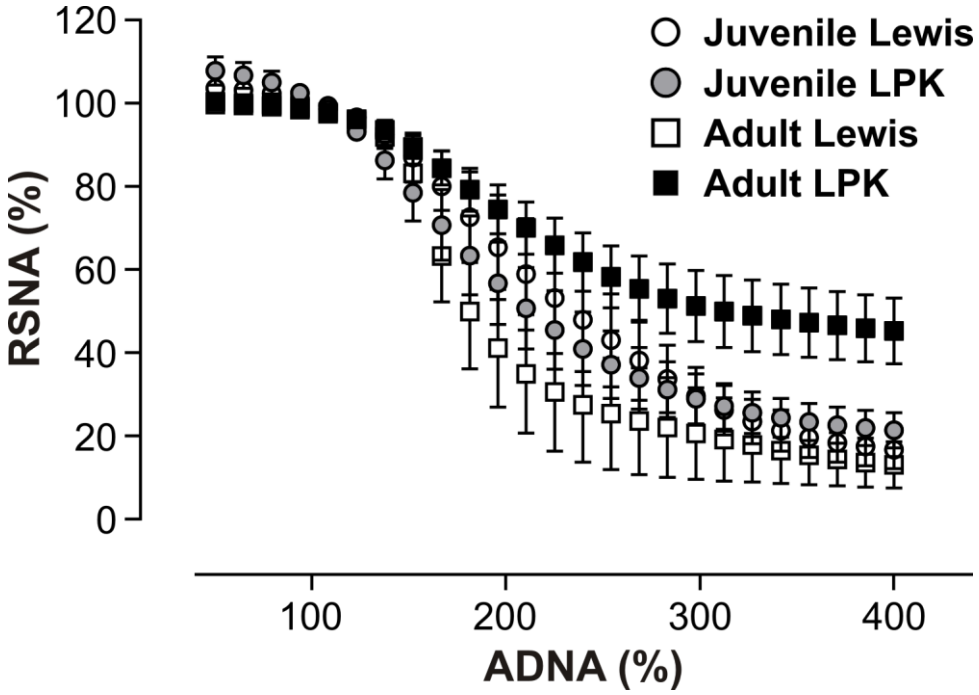

Figure 4.5: Logistic function curves illustrating the relationship between aortic depressor nerve activity (ADNA) and renal sympathetic nerve activity (RSNA) in juvenile (7–8 weeks old) and adult (12–13 weeks old) female Lewis and Lewis Polycystic Kidney (LPK) rats. Results are expressed as mean ± SEM. *n* values are as detailed in Table 4.4. (R^2 = 0.93 ± 0.01 all groups).

Table 4.3: Parameters describing the relationship mean arterial pressure (MAP) and microvolt changes in renal sympathetic nerve activity (RSNA) in the juvenile and adult female Lewis and Lewis Polycystic Kidney (LPK) rats

Group	Juvenile		Adult		Two-way ANOVA adjusted *P* value	
	Lewis *(8)*	LPK *(7)*	Lewis *(9)*	LPK *(8)*	Strain	Age
Barocurve parameter						
RSNA upper plateau (μV)	4.6 ± 0.8	13.9 ± 2.8*	4.7 ± 1.3	9.3 ± 1.3*	<0.0001	0.2773
RSNA lower plateau (μV)	0.6 ± 0.2	3.9 ± 1.3*	1.1 ± 0.5	3.3 ± 0.5*	0.0003	0.9451
Range (μV)	4.0 ± 0.7	10.0 ± 1.6*	3.6 ± 0.8	5.9 ± 1.3†	0.0011	0.0594
Gain (μV/mmHg)	-0.13 ± 0.02	-0.24 ± 0.04*	-0.10 ± 0.03	-0.11 ± 0.03†	0.0387	0.0109
MAP_{50} (mmHg)	126 ± 4	162 ± 8*	129 ± 3	151 ± 9*	0.0001	0.5085
MAP_{thr} (mmHg)	114 ± 2	148 ± 9*	116 ± 2	133 ± 10	0.0006	0.3215
RSNA at MAP_{thr} (μV)	3.8 ± 0.7	11.8 ± 2.5*	3.9 ± 1.1	8.0 ± 1.1*	<0.0001	0.3493
MAP_{sat} (mmHg)	139 ± 8	175 ± 8*	141 ± 5	169 ± 9*	0.0002	0.7845
RSNA at MAP_{sat} (μV)	1.5 ± 0.3	6.0 ± 1.6*	1.9 ± 0.6	4.6 ± 0.5*	0.0002	0.5437
MAP operating range (mmHg)	25 ± 8	28 ± 2	27 ± 4	37 ± 5	0.2131	0.3848

MAP_{50}, mean arterial pressure at the midpoint of the curve; MAP_{thr}, threshold mean arterial pressure to trigger a change in RSNA; and MAP_{sat}, saturation mean arterial pressure at which there is no further change in RSNA.
Results are expressed as mean ± SEM.
* *P*<0.05 vs. age-matched Lewis.
† *P*<0.05 vs. strain-matched juvenile rat.
(n) values denoted in subscript and represent number in each group.

Table 4.4: Parameters describing the relationship between aortic depressor nerve activity (ADNA) and renal sympathetic nerve activity (RSNA) in the juvenile (7–8 weeks old) and adult (12–13 weeks old) female Lewis and Lewis Polycystic Kidney (LPK) rats

Group	Juvenile		Adult		Two-way ANOVA adjusted *P* value	
	Lewis *(5)*	LPK *(7)*	Lewis *(6)*	LPK *(8)*	Strain	Age
Barocurve parameter						
RSNA upper plateau (%)	105 ± 2	111 ± 5	100 ± 1	101 ± 2†	0.2279	0.0190
RSNA lower plateau (%)	15 ± 4	19 ± 4	11 ± 5	40 ± 8*†	0.0166	0.1854
RSNA range (%)	90 ± 5	92 ± 8	89 ± 5	61 ± 9*†	0.1030	0.0451
Gain	-0.7 ± 0.1	-0.7 ± 0.1	-1.7 ± 0.7	-0.5 ± 0.1*	0.1023	0.2969
$ADNA_{50}$ (%)	220 ± 20	191 ± 18	198 ± 24	232 ± 27	0.9217	0.6833
$ADNA_{thr}$ (%)	172 ± 18	139 ± 15	169 ± 20	179 ± 20	0.5666	0.3379
RSNA at $ADNA_{thr}$ (%)	86 ± 2	92 ± 3	81 ± 2	88 ± 2	0.0146	0.1091
$ADNA_{sat}$ (%)	268 ± 28	243 ± 23	228 ± 30	285 ± 35	0.6165	0.9686
RSNA at $ADNA_{sat}$ (%)	34 ± 4	39 ± 3	30 ± 4	53 ± 7*	0.0104	0.2924
ADNA range (%)	96 ± 19	103 ± 19	59 ± 14	107 ± 20	0.1685	0.3674

$ADNA_{50}$, aortic depressor nerve activity at the midpoint of the curve; $ADNA_{thr}$, threshold aortic depressor nerve activity to trigger a change in RSNA; and $ADNA_{sat}$, saturation aortic depressor nerve activity at which there is no further change in RSNA.
Results are expressed as mean ± SEM.
$^{*}P<0.05$ vs. age-matched Lewis.
$^{\dagger}P<0.05$ vs. strain-matched juvenile rat.
(n) values denoted in subscript and represent number in each group.

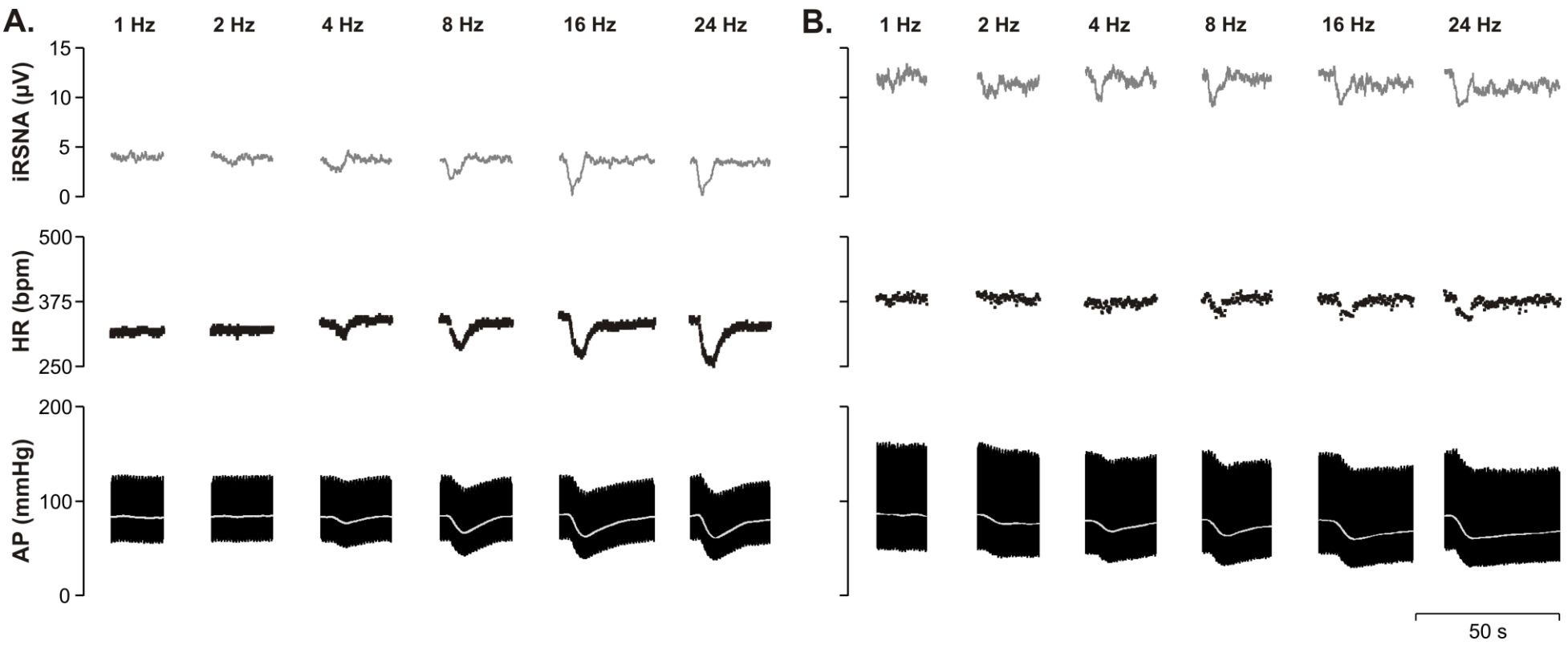

Figure 4.6: Representative data traces, illustrating responses of integrated renal sympathetic nerve activity (iRSNA), heart rate (HR) and arterial pressure (AP) to direct electrical stimulation of the aortic depressor nerve from an adult female (12–13 weeks old) Lewis (left panels) and adult female Lewis Polycystic Kidney (LPK) rat (right panels). bpm: beats per minute.

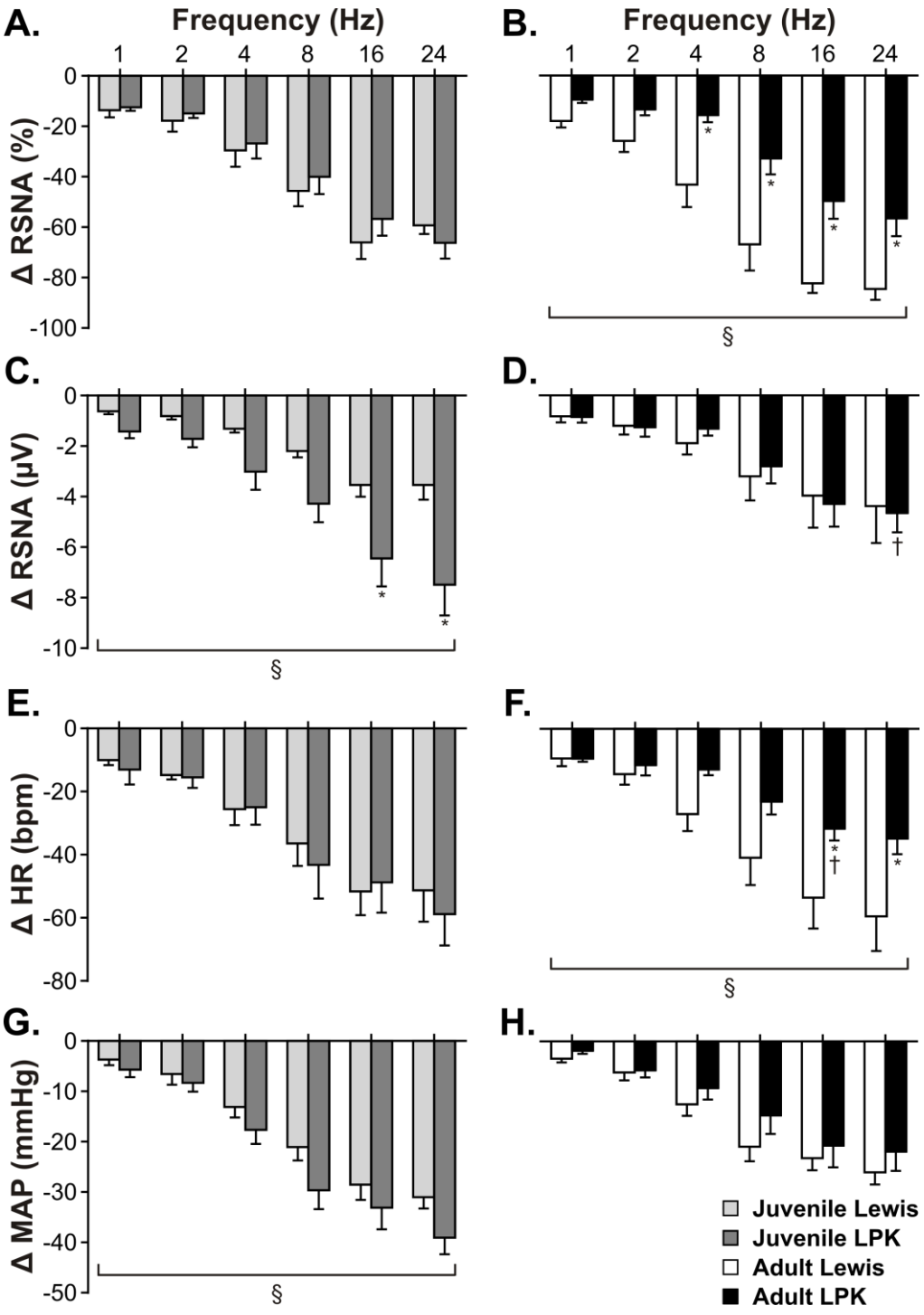

Figure 4.7: Effect of aortic depressor nerve stimulation on renal sympathetic nerve activity (RSNA; A– D), heart rate (HR; G, H) and mean arterial pressure (MAP; I, J) in juvenile (7–8 weeks old; left panel) and adult (12–13 weeks old; right panel) female Lewis and Lewis Polycystic Kidney (LPK) rats. A reduction in RSNA, HR and MAP was observed in all experimental groups. Results are expressed as mean ± SEM. $^{*}P<0.05$ vs. age-matched Lewis and $^{\dagger}P<0.05$ vs. strain-matched juvenile rat. $^{\S}P<0.05$, overall two-way ANOVA strain effect within indicated juvenile or adult age group. Minimum *n*/group: juvenile Lewis = 6, juvenile LPK = 7, adult Lewis = 5 and adult LPK = 8. bpm: beats per minute.

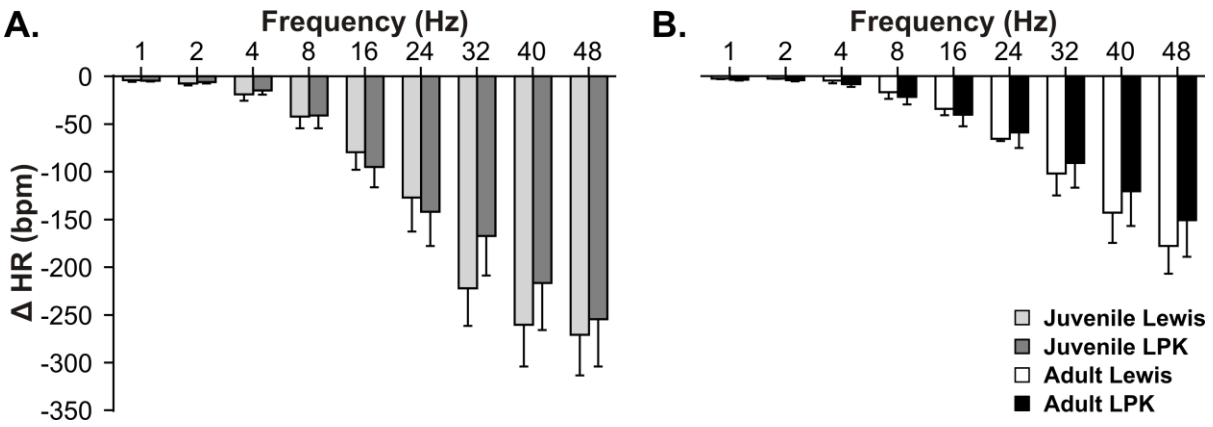

Figure 4.8: Effect of vagal efferent nerve stimulation on heart rate (HR) in juvenile (7–8 weeks old; left panel) and adult (12–13 weeks old; right panel) female Lewis and Lewis Polycystic Kidney (LPK) rats. A reduction in HR was observed in all experimental groups. Results are expressed as mean ± SEM. *n*/group: juvenile Lewis = 8, juvenile LPK = 8, adult Lewis = 5 and adult LPK = 7. bpm: beats per minute.

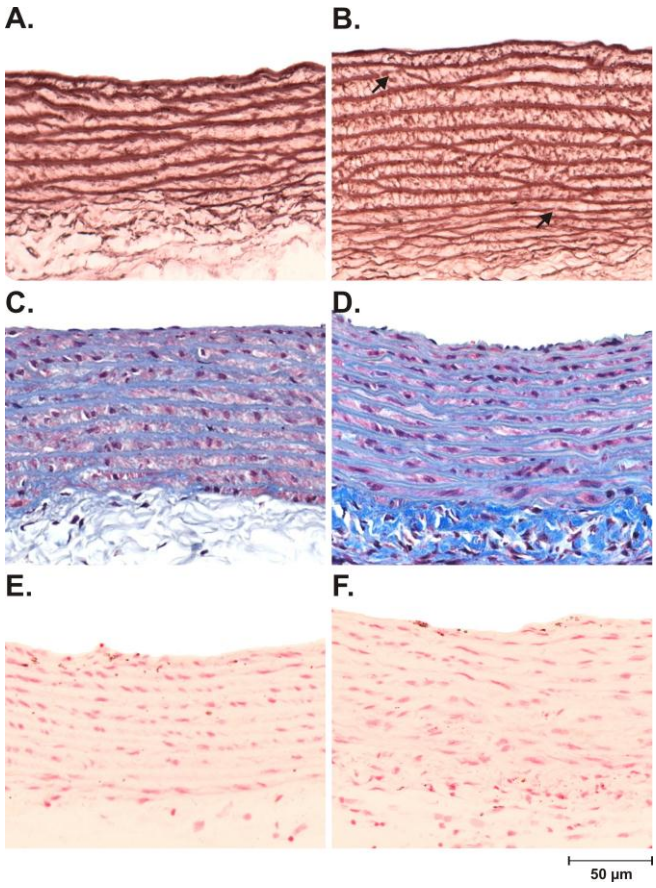

Figure 4.9: Representative histological sections of the aortic arch in adult (12–13 weeks old) female Lewis (left panels) and Lewis Polycystic Kidney rats (right panels), stained with Shikata's orcein (panels A, B), Martius Scarlet Blue (MSB; panels C, D) and Von Kossa (panels E, F), to identify elastin fibres (red staining), collagen fibres (blue staining) and calcification (black staining), respectively. Block arrow in B shows an example of elastic lamellae fracture (point of lamellae discontinuation).

Table 4.5: Differentiating histomorphometric variables in the aortic arch of juvenile (7–8 weeks old) and adult (12–13 weeks old) female Lewis and Lewis Polycystic Kidney (LPK) rats

Group	Juvenile		Adult		Two-way ANOVA adjusted *P* value	
	Lewis *(6)*	LPK *(6)*	Lewis *(6)*	LPK *(5)*	Strain	Age
Morphometric parameter						
Medial thickness (μm)	117 ± 2	150 ± 8*	137 ± 2	190 ± 14*†	<0.0001	0.0005
Number of elastin lamellae	12 ± 0.3	12 ± 0.4	12 ± 0.4	12 ± 0.7	0.4906	0.9631
Total elastin density (%)	75 ± 2	68 ± 5	63 ± 1†	51 ± 2*†	0.0025	<0.0001
Lamellae elastin density (%)	48 ± 1	48 ± 2	46 ± 1	38 ± 1$^{*\dagger\#}$	0.0039	<0.0001
Interlamellae elastin density (%)	27 ± 2	20 ± 3	17 ± 1†	13 ± 1†	0.0169	0.0002
Lamellae-to-interlamellae elastin ratio	1.9 ± 0.1	2.8 ± 0.5	2.9 ± 0.3	3.2 ± 0.3	0.1049	0.0324
Thickness of elastin lamellae (μm)	3.8 ± 0.1	4.2 ± 0.2	3.7 ± 0.1	4.1 ± 0.1	0.0045	0.3173
Elastin lamellae spacing (μm)	6.7 ± 0.3	9.3 ± 0.5*	8.6 ± 0.4†	12.5 ± 0.6*†	<0.0001	<0.0001
Number of elastin lamellae fractures (fracture/lamellae/mm)	0.01 ± 0.002	0.03 ± 0.004*	0.02 ± 0.003	0.05 ± 0.006*†	<0.0001	0.0016
Total collagen density (%)	21 ± 0.4	23 ± 0.6	22 ± 1.0	24 ± 0.7	0.0094	0.0640
Elastin-to-collagen ratio	3.7 ± 0.1	3.0 ± 0.2*	2.8 ± 0.1†	2.1 ± 0.1*†	<0.0001	<0.0001
Nuclear density (%)	4.9 ± 0.3	4.8 ± 0.2	3.8 ± 0.7	4.5 ± 0.2	0.4681	0.1186
Nucleus cross-sectional area (μm^2)	9.0 ± 0.4	12.0 ± 0.9*	9.1 ± 0.9	13.9 ± 0.4*	<0.0001	0.1474
Number of nuclei per μm^2	0.12 ± 0.006	0.09 ± 0.007	0.12 ± 0.013	0.08 ± 0.002*	0.0008	0.3316
Calcium density (%)	0.7 ± 0.2	0.6 ± 0.3	0.5 ± 0.2	1.0 ± 0.5	0.2782	0.1790
Average size of calcium deposit (μm^2)	6.1 ± 1.0	4.8 ± 0.7	4.1 ± 0.6	6.0 ± 0.7	0.6955	0.6034

Results are expressed as mean ± SEM.
$^{*}P$<0.05 vs. age-matched Lewis.
$^{\dagger}P$<0.05 vs. strain-matched juvenile rat.
$^{\#}P$<0.05 for strain × age interaction.
(n) values denoted in subscript and represent the minimum number in each group.

Table 4.6: Pearson's correlation coefficient (r) for aortic depressor nerve activity (ADNA) baroreceptor afferent function curve parameters relative to vascular structure in juvenile and adult female Lewis and Lewis Polycystic Kidney (LPK) rats

Groups	**MAP-ADNA function curve parameter**	
Morphometric parameter *(n)*	Gain *(19)*	Range *(19)*
Medial thickness (μm)	0.11 (*P*=0.6441)	0.15 (*P*=0.5248)
Total elastin density (%)	-0.02 (*P*=0.9492)	-0.14 (*P*=0.566)
Number of elastin lamellae fractures (fracture/lamellae/mm)	-0.22 (*P*=0.3300)	-0.16 (*P*=0.4855)
Total collagen density (%)	-0.26 (*P*=0.2626)	-0.16 (*P*=0.4875)
Elastin-to-collagen ratio	0.09 (*P*=0.7098)	-0.02 (*P*=0.9369)
Nucleus CSA (μm^2)	0.19 (*P*=0.4244)	0.22 (*P*=0.3450)
Calcium density (%)	0.16 (*P*=0.5036)	0.38 (*P*=0.1025)

Example of correlation analysis of the relationship between the gain/range of aortic depressor nerve activity (ADNA) baroreceptor afferent function and aortic arch vascular remodelling. CSA, cross-sectional area. *n* = number in each group. No significant correlations were observed for any of the histomorphometric parameters.

5 Differential Influence of Sex on Expression of Baroreflex Dysfunction in the Lewis Polycystic Kidney Model of Chronic Kidney Disease

Abstract

Current evidence suggests that cardiovascular risk is higher in men with chronic kidney disease (CKD) than women; however, it is unknown if differences are driven by sexual dimorphism in mechanisms controlling autonomic outflows. Accordingly, the results presented in Chapters 3 and 4 are directly compared here, in order to identify if sex differences in the expression of cardiac and sympathetic baroreflex dysfunction exist in CKD, and the differential influence of sex on the functionality of the afferent and central components of the baroreflex arc. In juvenile Lewis Polycystic Kidney (LPK) rats, heart rate (HR), renal sympathetic nerve activity (RSNA) and aortic depressor nerve activity (ADNA) baroreflex function were comparable between males and females, and not dissimilar to Lewis controls. Stimulation of the aortic depressor nerve (ADN) in the juvenile LPK produced similar reflex sympathoinhibition in both males and females; however, greater reflex bradycardic and therefore depressor responses were observed in the male LPK, suggestive of a greater enhancement of the central mediation of vagal outflow in the male LPK at this age. In adult LPK, reductions in HR and RSNA baroreflex gain and range relative to Lewis were comparable in the male versus female. ADNA baroreceptor afferent range, which was blunted in the adult male LPK versus Lewis, was also reduced in the adult male versus female LPK (133 ± 35 vs. 331 ± 64%, $P<0.05$) and greater structural deteriorations of the aortic arch, as evidenced by increased media thickness, lower elastin-to-collagen ratio and higher aortic calcification, were evident. Reductions in the reflex sympthoinhibitory response to ADN stimulation relative to Lewis were greater in the adult male LPK compared to female (overall, -21 ± 4 vs. 30 ± 8%, $P<0.05$), while decreased reflex bradycardic and depressor responses compared with Lewis were comparable in both male and female LPK. This study demonstrates that, upon CKD progression, males and females express similar deficits in the baroreflex control of HR and RSNA despite greater deteriorations in the afferent and central components of the baroreflex arc in the male. Together, this highlights fundamental sex-specific differences in the pathophysiology of autonomic dysfunction in CKD.

Keywords: sexual dimorphism, renal sympathetic nerve, aortic depressor nerve, baroreflex, hypertension, chronic kidney disease

5.1 Introduction

In Chapters 3 and 4, we have investigated the afferent and the central component of the baroreflex arc in both male and female Lewis Polycystic Kidney (LPK) rats relative to normotensive Lewis controls and sought to identify if any temporal changes in the processing of these components of the baroreflex circuit exist that may contribute to or underlie the development of baroreflex dysfunction in both males and females. Our results demonstrated that heart rate (HR) and sympathetic baroreflex dysfunction in the male LPK model of chronic kidney disease (CKD) is related to temporal deficits in the functionality of the afferent and central components of the baroreflex arc (Chapter 3), whereas impaired cardiac and sympathetic baroreflexes in the female appear to be primarily due to a decline in

the central processing of baroreceptor afferent input only (Chapter 4). Given that cardiovascular risk is higher in men with CKD than women (U.S. renal data system, 2013, National Kidney Foundation, 2013), in this chapter the results presented in Chapters 3 and 4 are directly compared, in order to elucidate the degree to which baroreflex dysfunction in the LPK rodent model relates to sex-driven differences in baroreceptor processing.

5.2 Methods

A detailed description of the methodology and the number of animals used in this study are provided in Chapters 3 and 4. All data are expressed as mean ± standard error of the mean (SEM). A two-way ANOVA with Bonferroni's correction was used to identify, within each age group (juvenile and adult animals), if strain and sex differences existed (GraphPad Prism software v6 Inc., La Jolla, CA, USA). As U_{Pro} could not be detected in >2 Lewis and juvenile female LPK animals, mean values for urinary protein:creatinine ratio (UPC) were not calculated, and UPC in adult LPK male and female were compared with a Student's t-test. A Brown-Forsythe test was used to determine if there were any differences in the variance, and if so, the data was log-transformed before statistical analysis. Significance was defined as $P \leq 0.05$.

5.3 Results

5.3.1 Baseline data

Body weight was consistently lower in the LPK relative to Lewis and less in the female animals compared to males. The elevations in baseline measurements of systolic blood pressure (BP), mean arterial pressure (MAP) and/or renal sympathetic nerve activity (RSNA) relative to age-matched Lewis groups were comparable in male and female LPK regardless of age (Table 5.1). An overall sex effect (P = 0.04) influenced pulse pressure in the juvenile group, being greater in the female versus male. This was not evident in the adult group. Male LPK diastolic BP and aortic depressor nerve activity (ADNA) were similar to that of age-matched female LPK (Table 5.1). Juvenile male LPK had higher resting HR than female counterparts and a similar overall sex effect was noted in the adult group (Table 5.1). In juvenile male LPK, urinary protein (U_{Pro}) was significantly higher compared with age-matched female LPK, whereas urinary creatinine (U_{Cr}) was comparable between the two strains. In adult LPK, there was no sex effect on U_{Pro}, U_{Cr} (Table 5.1) or UPC (4.1 ± 0.4 vs. 4.4 ± 0.5, LPK male vs. female, total n = 11, P = 0.85). No sex effect on systolic BP, diastolic BP, MAP, nerve activity and renal function was observed in the Lewis groups of either age (Table 5.1).

5.3.2 Baroreceptor reflex control of HR, RSNA and ADNA

(i) Baroreflex control of HR: consistent with the higher basal HR in the juvenile male LPK relative to females, the HR baroreflex function was shifted upward (Figure 5.1A) in the juvenile male LPK, and

this was reflected by the higher upper plateau of the relationship and HR levels at MAP_{thr} (Table 5.2). In adult LPK, the reduction in HR baroreflex gain and range relative to Lewis (Table 5.2) remained comparable between male and female (Figure 5.1B). There was, however, an overall sex effect on HR upper plateau and HR at MAP_{thr}, being higher in the adult male versus female groups (Table 5.2). All other curve parameters were similar in the Lewis and LPK compared with their strain- and age-matched female counterparts (Table 5.2).

When the reflex bradycardic and tachycardic responses were analysed independently, BRS_{PE} was greater in the juvenile and adult male LPK compared with age-matched female LPK. In contrast, regardless of age, BRS_{SNP} remained uninfluenced by sex (Table 5.5).

(ii) Baroreflex control of RSNA: The rightward shift in the RSNA baroreflex function relative to Lewis controls was similar in both juvenile and adult LPK of either sex (Figure 5.1C & D). Accordingly, the increased measures of $MAP_{50,}$ MAP_{thr} and/or MAP_{sat} compared with age-matched Lewis were comparable between the LPK, and therefore a similar MAP operating range in the male and female LPK was observed (Tables 5.3). In the juvenile LPK, the reduction in RSNA baroreflex gain relative to Lewis did not differ between the male and female. There was, however, a weak overall sex effect (P = 0.05) on RSNA baroreflex range in the juvenile groups, being greater in the male versus female animals (Tables 5.3). In adult LPK, RSNA baroreflex gain and values of the lower plateau, range, and RSNA at MAP_{sat} were reduced to the same levels in both male and female LPK (Tables 5.3).

Comparison of the reflex relationship in microvolts similarly showed a comparable rightward shift in the reflex relationship in the LPK (Figure 5.2), and therefore increases in $MAP_{50,}$ MAP_{thr} and/or MAP_{sat} relative to Lewis were similar in both male and female LPK (Table 5.6). However, there was a greater upward shift in the RSNA baroreflex function in the juvenile and adult female LPK (Figure 5.2), with measures of the lower plateau and/or $RSNA_{thr}$ being significantly higher in the female LPK groups (Table 5.6). In juvenile male LPK, RSNA baroreflex gain was smaller relative to juvenile female LPK. In the adult LPK the gain of the relationship was not influenced by sex, however the upper plateau was significantly blunted in the male LPK compared to female. Accordingly, RSNA baroreflex range tended to be smaller (P = 0.08) in the adult male LPK compared with age-matched female (Table 5.6). Irrespective of age, all other curve parameters expressed in either percentage or microvolts remained comparable among groups and a sex effect was not evident in either strain (Table 5.3 & 5.6).

(iii) Baroreflex control of ADNA: Regardless of age, the rightward shift in the ADNA-MAP relationship relative to Lewis controls was comparable between the male and female LPK (Figure 5.1E & F) and this was indicated by the similar increases in MAP_{50}, MAP_{thr} and/or MAP_{sat} (Table 5.4). An overall sex effect (P = 0.04) influenced ADNA lower plateau in the juvenile groups, such that responses were greater in the male versus female animals. Otherwise, the ADNA baroreceptor afferent

function in juvenile male LPK paralleled those of the female, and no sex differences in any other calculated curve parameters were evident (Table 5.4). In the adult LPK, by contrast, the upper plateau, ADNA at MAP_{sat} and gain tended to be smaller in the male than in female (P = 0.06, 0.05 and 0.08, respectively). Importantly, the range of the ADNA baroreceptor afferent function was markedly blunted in the LPK male compared with LPK female (Table 5.4). No sex differences were identified in the Lewis at either age with respect to this relationship (Table 5.4).

5.3.3 Central component of baroreflex arc

(i) Indirect assessment: Neither strain nor sex influenced the ADNA-RSNA relationship in the juvenile animals (Figure 5.3), as parameters derived from the curve fit were comparable in all groups (Table 5.7). In the adult LPK, however, and consistent with results of the ADNA baroreceptor afferent function (see above), the RSNA-ADNA relationship was shifted leftward in the male LPK compared with female LPK (Figure 5.3B). Accordingly, measures of $ADNA_{50}$ and $ADNA_{sat}$ were markedly smaller in the adult male LPK compared to age-matched female (Table 5.7). Overall reductions (all P<0.01) in RSNA range, lower plateau and RSNA at $ADNA_{sat}$ relative to age- and sex-matched Lewis were comparable between adult male versus female LPK. An overall sex effect influenced measures of RSNA upper plateau and RSNA at $ADNA_{thr}$ in the adult groups, being greater in the male versus female rats. Surprisingly, the gain of the relationship was greater in the adult male LPK versus adult female LPK. With the exception of higher ADNA operating range, no significant differences were found between adult male Lewis versus adult female Lewis with respect to the RSNA-ADNA reflex function (Table 5.7).

(ii) Direct assessment: In juvenile male Lewis, greater reductions in RSNA (%) and MAP, but not HR or RSNA (μV), were able to be evoked compared with female counterparts (Figure 5.4). In juvenile LPK, the reflex sympathoinhibition (% and μV) was not significantly different between the males and the females, however greater bradycardia and hypotension were observed in the males (Figure 5.4). In adult Lewis rats, all reflex responses were similar between in the males and females (Figure 5.5). In contrast, adult male LPK showed smaller reductions in RSNA (%) in responses to aortic depressor nerve (ADN) stimulation relative to age-matched female LPK (Figure 5.5B). This difference was also evident when the sympathoinhibitory responses were expressed in microvolts (Figure 5.5D). The reflex bradycardic response was overall significantly greater (P = 0.05) in the adult LPK male versus female. There was not, however, significant differences in reflex depressor responses in the adult LPK groups (Figure 5.5F& H).

5.3.4 Efferent baroreflex function

In juvenile Lewis and LPK, sex did not influence HR responses to cervical vagal efferent stimulation (Figure 5.6A & B). In contrast, a sex effect on the overall reflex bradycardic response was observed in

both adult groups (minimum $P = 0.02$), with the males showing greater reductions in HR in response to vagal efferent stimulation (Figure 5.6C & D).

5.3.5 Histomorphometry of the aortic arch

As noted in Chapters 3 and 4 and the strain effect reported in Table 5.8, in both juvenile and adult LPK of either sex there were numerous indicators of vascular remodelling relative to the Lewis. When considering sex effects, juvenile male LPK had greater aortic media thickness, lower lamellae elastin density, higher collagen density and increased number of elastin lamellae breaks than female LPK at this age (Table 5.8). A weak overall sex effect ($P = 0.04$) was also noted on elastin lamellae spacing, being larger in the male versus female. All other histomorphometric parameters were comparable in the LPK of either sex and there were no sex differences identified in the juvenile Lewis groups (Table 5.8).

In adult LPK, the aortic arch was 17% thicker in the male than in the females and demonstrated thinner elastin lamellae, greater number of elastin lamellae fractures, higher total collagen density, reduced elastin-to-collagen ratio and increased medial calcification (Table 5.9). Other histomorphometric parameters did not significantly vary between male and female LPK in the adult group. Apart from higher interlamellea elastin density during adulthood, there were no sex effects influencing the Lewis animals in either age group. There was however an overall sex effect on the average size of calcium deposits being greater in male versus female animals (Table 5.9).

5.4 Discussion

It is well established that male sex poses increased risk of cardiovascular mortality in CKD (Chesterton and McIntyre, 2005, Thapa et al., 2010). Accordingly, the aim of this chapter was to compare the male and female data presented in Chapters 3 and 4 to resolve if there was a sex effect in the examined parameters. The main major finding that arose was that male and female LPK express comparatively similar deficits in HR and RSNA baroreflex function by 12 weeks of age; however, in the male LPK, reductions in the functionality of the afferent and central processing of the baroreflex are of markedly larger magnitude. These observations show that, in CKD, there is a relative protection of the afferent and central arms of the baroreflex in the females compared with males of the same age; however, these effects do not appear to proffer preservation of cardiac and sympathetic baroreflex function. Together, this indicates that impaired baroreflexes in CKD likely arise due to sex-dependent deterioration in different components of the baroreflex circuit and highlights fundamental differences in the pathophysiology of autonomic dysfunction in both males and females.

Despite significant vascular remodelling in both male and female LPK relative to Lewis controls, there was a prominent sex difference in the LPK, and afferent baroreceptor function was only compromised

in the male LPK rats, suggesting that the baroreceptor afferent pathway is protected in females. Based on our finding of a significant sex effect in the degree of vascular remodelling in the LPK, altered vessel stretch and impaired mechanosensation are the most likely explanation for this finding, given that altered vascular distensibility has been identified as a key underlying mechanism impairing sensory afferent traffic in hypertension (Andresen, 1984, Sapru and Wang, 1976). Most notably, the male LPK exhibited a greater degree of vascular hypertrophy, decreased aortic elastin-to-collagen and increased calcium density ratio particularly in the adult animals, all suggestive of increased arterial remodelling and stiffness. As discussed in Chapters 3 and 4, pathological changes in aortic media thickness, elastin density, elastin lamellae breaks, elastin-to-collagen ratio, collagen and calcium density and nuclear cross sectional area correlated with reductions in baroreceptor afferent function in the male (Chapter 3), but not female (Chapter 4), cohorts of animals. The molecular and cellular mechanisms pertaining to the relative vascular protection in the female LPK model of CKD were not addressed in this study; however, it may relate to a specific vasoprotective action of female sex hormones on the arterial vasculature (Bakir et al., 2000, Dubey et al., 2002, Xing et al., 2009). Whether comparable deficits in the afferent arm of the baroreflex develop in the female LPK with further aging and progression of CKD is unknown; nevertheless, our observations do suggest that early therapy aimed at staving off vascular remodelling may be an effective treatment for ameliorating at least part of the baroreceptor dysfunction in CKD.

Noteworthy is the fact that vascular-independent mechanisms may also contribute to sexual dimorphism in afferent baroreceptor discharge in CKD. For instance, changes in the expression of voltage-gated ion channels (Tu et al., 2010, Zhang et al., 2014), transient receptor potential vanilloid 1 (TRPV1) (Sun et al., 2009) or P2 purinoceptors (Song et al., 2012), or changes in circulating factors related to inflammation (Santana-Filho et al., 2014), sympathetic nervous system (Munch et al., 1987), renin-angiotensin-aldosterone system (dos Santos et al., 1998) and metabolic status (Gouty et al., 2001) have previously been shown to impact sensory afferent neurotransmission and may therefore be differentially regulated in males and females with CKD. These effects, however, were not examined here and further studies are required to substantiate these assumptions.

Whether improving afferent baroreceptor function alone is sufficient to prevent baroreceptor reflex dysfunction in CKD is debatable. Baroreceptor reflex function was impaired, to a relatively similar degree, in the adult male and female LPK. In the female LPK this is driven solely by a reduction in central processing of the baroreceptor reflex. Whether this central deficit is of comparable magnitude to that observed in the male LPK is unknown. In the present chapter, differences in central baroreceptor function were observed between the male and female LPK, suggesting that sex-specific differences do occur. For example, the recruitment of cardiac vagal outflow in response to stimulation of the ADN, as evidenced by heightened reflex bradycardia, was greater in the juvenile and adult male

LPK. While in the adult LPK, the reflex sympathoinhibition to ADN stimulation was reduced relative to age-matched female LPK. The differences observed in the bradycardic response in the male LPK may reflect an adaptive response to reduced afferent input (Chapter 3), rendering the reflex still functional. Our finding that reflex sympathoinhibition was reduced to a greater extent in adult male LPK rats does suggest that the central deficit is more profound and may involve different brain regions to that occurring in the females. As with the vascular tissue, relative preservation of sympathetic function may relate to a specific action of sex hormones. For instance, it has been shown that intravenous or intracerebral injection of oestrogen suppressed efferent sympathetic nerve activity (SNA) in male rats and ovariectomised females, and that such actions were blunted by selective antagonism of the oestrogen receptors in the brain (Saleh et al., 2000), suggestive of a central action for oestrogen.

While there were notable sex-specific differences in the development of baroreceptor dysfunction in the LPK model of CKD, the net result appears to be relatively comparable and both male and female LPK exhibited similar overall reductions in the gain and range of the HR baroreflex function. However, when the reflex bradycardic response to a rise in BP, reflective of cardiovagal activity (Head and McCarty, 1987), was assessed separately, juvenile and adult male LPK showed greater bradycardia compared with age-matched female animals, suggesting a differential influence for sex on cardiovagal baroreflex in CKD-mediated hypertension. Furthermore, in the presence of greater reflex bradycardic responses to ADN stimulation in the juvenile and adult male LPK relative to females, increased vagal responsiveness of the heart in the male LPK seems to be most likely driven by the enhanced central mediation of cardiac vagal outflow we describe here. A higher HR baroreflex sensitivity has been previously demonstrated in hypertensive female animals compared with males (Johnson et al., 2011, Xue et al., 2005); however, our findings were rather similar to observations describing reduced cardiovagal baroreflex sensitivity in hypertensive women compared with age-matched men (Sevre et al., 2001). The reflex tachycardic response to a fall in BP remained similar between juvenile and adult male and female rats, suggesting a lack of sex influence on sympathetic control of HR.

Baroreflex control of RSNA temporally declined over the same age-range in the male and female LPK. RSNA baroreflex function (μV) was shifted upward in the female LPK relative to male LPK at both time points, as demonstrated by the higher upper or lower plateau of the MAP-RSNA relationship in the females. These observations may predispose females to a reduced ability to attenuate increases or maximally inhibit SNA in CKD. Interestingly, there was a trend of lower RSNA baroreflex range (μV) in the adult male LPK compared with age-matched female LPK, which would have been consistent with the blunted centrally-evoked changes in SNA seen in the male versus female LPK at this age. However, these differences did not approach statistical significance, suggesting that impaired

baroreflex control of RSNA in CKD is relatively uninfluenced by sex, perhaps contributing to similar elevations in SNA in both males and females as we showed here.

Elevated SNA correlates negatively with reductions in the glomerular filtration rate (GFR) and positively with proteinuria in the CKD population (Grassi et al., 2011a, Grassi et al., 2011b). While the underlying pathology driving CKD in the LPK model is the genetic mutation causing cystic kidney disease, it likely that the similar elevations in RSNA seen in both male and female LPK contributes towards the overall progression of renal dysfunction. Whether sexual dimorphism in SNA would be encountered later when rats develop end-stage renal disease remains undetermined.

Clearly, much work remains to be done in this area to identify why, in CKD, males and females express relatively similar deteriorations in overall baroreflex function despite that females show intact sensory afferent neurotransmission and markedly lower impairments of the central pathways of the baroreflex arc. One possible hypothesis is that there might be a non-baroreceptor mediated vagal afferent contribution to the aortic baroreceptor reflex which could have differentially influenced sex differences in HR and RSNA baroreflex function when overall reflex function was assessed in this model. This hypothesis is supported by the fact that bilateral vagotomy was previously shown to reduce baroreflex control of RSNA (Dibner-Dunlap and Thames, 1989, DiBona and Sawin, 1994) and rats in the present study were not vagotomised prior to assessment of baroreflex function. Alternatively, a sex difference in the ability of the heart and vasculature to respond to autonomic inputs (Abdel-Rahman, 1999) may possibly underlie comparable baroreflex function in the adult male and female LPK. Indeed, our data showed that vagal efferent stimulation produced greater reductions in HR in adult male LPK compared with females, suggesting that higher target organ responsiveness to efferent automatic outflow in the males may have relatively offset impairments of the afferent and central pathways and therefore led to similar net changes in the baroreflex function in both male and female LPK. It is unlikely however, that these effects could represent a compensatory response to the observed reductions in the afferent and central baroreflex drives in the adult male LPK, as larger bradycardic responses to vagal efferent stimulation could also be evoked in the adult male versus female Lewis, suggesting a sex-driven rather than CKD-dependent effect.

We have previously shown that renal impairment, as determined by plasma urea and creatinine levels, develops sooner in the male LPK relative to female animals (Phillips et al., 2007). This is keeping with the renal function data we describe in the present chapter, with male LPK showing an earlier elevation of urinary protein. The increased overall severity in male animals, in regards to both onset of baroreflex dysfunction and degree of impairment, would support the underlying premise that kidney function is the primary factor driving the pathology in both autonomic and cardiovascular function in the LPK model. Remaining to be elucidated is why female LPK animals show a slower onset of deterioration of renal function; however, as described elsewhere (Reckelhoff et al., 2000, Stringer et

al., 2005), the presence of male sex hormones (e.g., androgens) and/or deficiency of female sex hormones (e.g., oestrogen) is thought to play a role. Indeed, it has been shown that oestrogen and some of its endogenous metabolites not only exert potentially protective effects on the production, expression and activity of various fibrotic mediators but also attenuate the development of vasoconstriction and preserve GFR (Dubey and Jackson, 2001, Stringer et al., 2005, Williams et al., 1992). Further studies assessing the factors contributing to sex disparity in renal and cardiovascular disease and the effect of sex hormones are therefore warranted.

5.5 Perspectives and significance

The physiological mechanisms contributing to sexual dimorphism in CKD and potential sex-related differences in baroreflex mechanisms are novel areas of research investigation. In favour of the view that cardiovascular disease affects more men than women stands the observation from this study that, in CKD, female sex offers comparatively lower loss in baroreflex processing pathways. However, despite a relative protection of afferent and central function within the baroreceptor reflex in the female, our data clearly demonstrates similar onset of central deficit, comparable impairments of cardiac and sympathetic baroreflex function, and parallel increases in SNA to those of the males, findings perhaps linked to deteriorations in renal functions. Therefore, an appropriate recognition of the complexity of integrated physiological regulation will be a key factor in understanding and developing sex-specific interventional strategies to treat CKD.

Table 5.1: Baseline parameters in the juvenile (7–8 weeks old) and adult (12–13 weeks old) Lewis and Lewis Polycystic Kidney (LPK) rats of either sex

Group	Female		Male		Two-way ANOVA adjusted *P* value	
	Lewis	LPK	Lewis	LPK	Strain	Sex
Parameter						
Juvenile *(n)*	*6*	*5*	*7*	*6*	-	-
BW (g)	168 ± 4	130 ± 6*	214 ± 11‡	167 ± 6*‡	<0.0001	<0.0001
U_{Pro} (g/L)	0.01 ± 0.01	0.11 ± 0.08	0.05 ± 0.00	0.31 ± 0.06*‡	0.0007	0.0137
U_{Cr} (g/L)	1.05 ± 0.50	0.21 ± 0.04	1.30 ± 0.22	0.37 ± 0.08	0.0062	0.4786
SBP (mmHg)	121 ± 3	176 ± 7*	116 ± 5	165 ± 4*	<0.0001	0.0931
DBP (mmHg)	61 ± 3	75 ± 4*	65 ± 3	76 ± 4	0.0015	0.4991
PP (mmHg)	60 ± 3	102 ± 6*	51 ± 4	89 ± 6*	<0.0001	0.0400
MAP (mmHg)	85 ± 3	116 ± 4*	86 ± 3	108 ± 4*	<0.0001	0.3169
HR (bpm)	340 ± 6	388 ± 12*	363 ± 11	439 ± 14*‡	<0.0001	0.0027
RSNA (μV)	4.3 ± 1.0	10.0 ± 1.9*	3.6 ± 0.7	7.3 ± 1.5*	0.0008	0.3145
ADNA (μV)	0.4 ± 0.1	0.5 ± 0.1	0.4 ± 0.1	0.4 ± 0.1	0.2881	0.7150
Adult *(n)*	*8*	*5*	*6*	*6*	-	-
BW (g)	230 ± 3†	166 ± 5*	361 ± 8‡	239 ± 7$^{*‡\#}$	<0.0001	<0.0001
U_{Pro} (g/L)	0.01 ± 0.01	0.69 ± 0.12*	0.05 ± 0.00	1.04 ± 3.130*	0.0007	0.3592
U_{Cr} (g/L)	1.25 ± 0.18	0.16 ± 0.02*	1.10 ± 0.05	0.29 ± 0.07*	<0.0001	0.7192
SBP (mmHg)	127 ± 2	183 ± 5*	123 ± 5	179 ± 6*	<0.0001	0.9548
DBP (mmHg)	59 ± 2	67 ± 4	64 ± 2	69 ± 5	0.0388	0.2197
PP (mmHg)	69 ± 2	116 ± 3*	59 ± 6	111 ± 6*	<0.0001	0.1041
MAP (mmHg)	85 ± 2	107 ± 5*	85 ± 2	111 ± 6*	<0.0001	0.6129
HR (bpm)	323 ± 8	366 ± 14	350 ± 16	402 ± 13*	0.0009	0.0210
RSNA (μV)	3.9 ± 0.9	9.6 ± 1.2*	2.7 ± 0.4	5.3 ± 0.8	0.0002	0.1385
ADNA (μV)	1.1 ± 0.3	0.9 ± 0.3	0.7 ± 0.3	1.2 ± 0.3	0.6037	0.8537

BW, body weight; U_{Pro}, urinary protein; U_{Cr}, urinary creatinine; SBP, systolic blood pressure; DBP, diastolic blood pressure; PP, pulse pressure; MAP, mean arterial pressure; HR, heart rate; RSNA, renal sympathetic nerve activity; and ADNA, aortic depressor nerve activity.
Results are expressed as mean ± SEM.
$^{*}P$<0.05 vs. sex- and age-matched Lewis, $^{‡}P$<0.05 vs. strain-and age-matched female rat and $^{\#}P$<0.05 indicates strain × sex interaction. *(n)* = minimum number in each group.

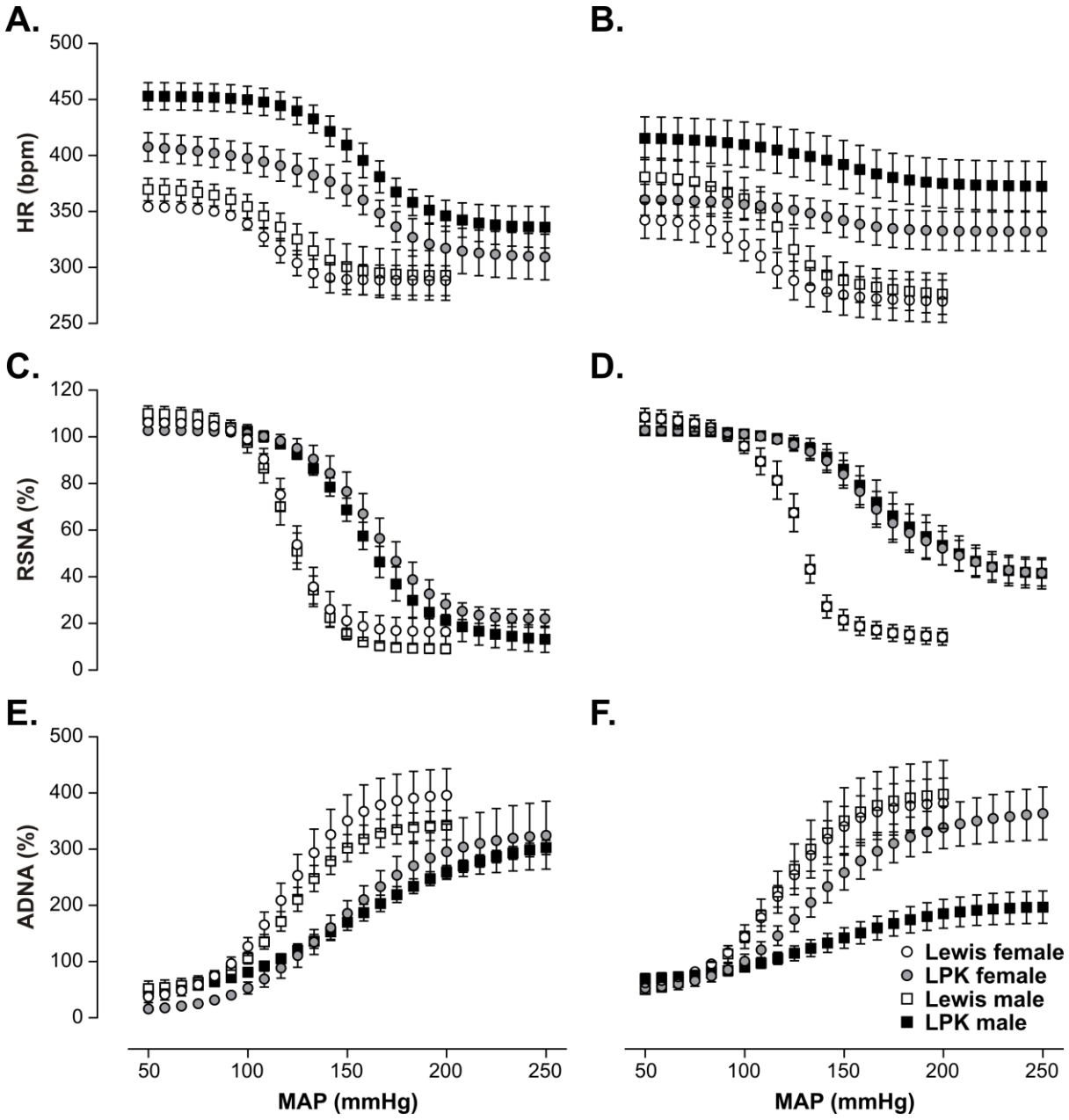

Figure 5.1: Logistic function curves illustrating the relationship between mean arterial pressure (MAP) and heart rate (HR; A & B), renal sympathetic nerve activity (RSNA; C & D) and aortic depressor nerve activity (ADNA; E & F) in juvenile (7–8 weeks old, left panels) and adult (12–13 weeks old, right panels) Lewis and Lewis Polycystic Kidney (LPK) rats of either sex. Results are expressed as mean ± SEM. *n* values are detailed in Tables 5.2, 5.3 and 5.4. bpm: beats per minute.

Table 5.2: Parameters describing the relationship between mean arterial pressure (MAP) and heart rate (HR) in the juvenile (7–8 weeks old) and adult (12–13 weeks old) Lewis and Lewis Polycystic Kidney (LPK) rats of either sex

Group	Female		Male		Two-way ANOVA adjusted *P* value	
	Lewis	LPK	Lewis	LPK	Strain	Sex
Barocurve parameter						
Juvenile *(n)*	*8*	*8*	*7*	*8*	-	-
HR upper plateau (bpm)	357 ± 4	413± 14*	370 ± 10	463 ± 8*‡	<0.0001	0.0030
HR lower plateau (bpm)	288 ± 13	306 ± 19	283 ± 24	331 ± 21	0.0997	0.6082
Range (bpm)	69 ± 14	108 ± 25	88 ± 16	132 ± 24	0.0712	0.2373
Gain (bpm /mmHg)	-2.6 ± 0.8	-1.7 ± 0.8	-3.0 ± 1.3	-2.8 ± 0.6	0.5400	0.3913
MAP_{50} (mmHg)	107 ± 6	143 ± 9*	116 ± 6	153 ± 6*	<0.0001	0.1575
MAP_{thr} (mmHg)	92 ± 10	109 ± 13	102 ± 6	135 ± 8*	0.0144	0.0752
HR at MAP_{thr} (bpm)	342 ± 4	391 ± 11*	352 ± 12	435 ± 7*‡	<0.0001	0.0052
MAP_{sat} (mmHg)	121 ± 4	177 ± 11*	131 ± 7	171 ± 6*	<0.0001	0.7817
HR at MAP_{sat} (bpm)	302 ± 11	329 ± 15	301 ± 8	359 ± 16*	0.0131	0.4528
MAP operating range (mmHg)	30 ± 10	68 ± 17*	29 ± 5	37 ± 5	0.0418	0.1522
Adult *(n)*	*9*	*8*	*11*	*7*	-	-
HR upper plateau (bpm)	342 ± 16	361 ± 14	383 ± 17	415 ± 19	0.1399	0.0101
HR lower plateau (bpm)	269 ± 19	332 ± 17	272 ± 21	372 ± 22*	0.0005	0.3158
Range (bpm)	73 ± 9	29 ± 7*	111 ± 19	44 ± 8*	0.0004	0.0632
Gain (bpm /mmHg)	-2.5 ± 0.6	-0.8 ± 0.2*	-3.5 ± 0.9	-0.7 ± 0.1*	<0.0001	0.4030
MAP_{50} (mmHg)	111 ± 7	124 ± 10	116 ± 6	140 ± 8	0.0244	0.1865
MAP_{thr} (mmHg)	98 ± 6	106 ± 11	101 ± 5	118 ± 10	0.1356	0.3685
HR at MAP_{thr} (bpm)	327 ± 16	355 ± 15	359 ± 16	407 ± 19	0.0359	0.0207
MAP_{sat} (mmHg)	124 ± 7	142 ± 11	131 ± 9	161 ± 9	0.0122	0.1468
HR at MAP_{sat} (bpm)	285 ± 18	338 ± 17	295 ± 18	382 ± 21*	0.0011	0.1751
MAP operating range (mmHg)	25 ± 4	36 ± 9	31 ± 7	44 ± 10	0.1086	0.3941

MAP, mean arterial pressure; MAP_{50}, mean arterial pressure at the midpoint of the curve; MAP_{thr}, threshold mean arterial pressure to trigger a change in HR; MAP_{sat}, saturation mean arterial pressure at which there is no further change in HR, bpm, beat per minute.
Results are expressed as mean ± SEM.
$^{*}P<0.05$ vs. sex- and age-matched Lewis and $^{‡}P<0.05$ vs. strain-and age-matched female rat. *(n)* = number in each group.

Table 5.3: Parameters describing the relationship between mean arterial pressure (MAP) and renal sympathetic nerve activity (RSNA) in the juvenile (7–8 weeks old) and adult (12–13 weeks old) Lewis and Lewis Polycystic Kidney (LPK) rats of either sex

Group	Female		Male		Two-way ANOVA adjusted *P* value	
	Lewis	LPK	Lewis	LPK	Strain	Sex
Barocurve parameter						
Juvenile *(n)*	*8*	*7*	*8*	*9*	-	-
RSNA upper plateau (%)	107 ± 2	102 ± 2	110 ± 3	108 ± 4	0.2816	0.1226
RSNA lower plateau (%)	14 ± 4	23 ± 5	9 ± 2	12 ± 6	0.1838	0.0837
Range (%)	93 ± 4	80 ± 5	101 ± 4	96 ± 8	0.1375	0.0464
Gain (%/mmHg)	-3.2 ± 0.5	-1.8 ± 0.2*	-2.8 ± 0.2	-1.5 ± 0.2*	0.0002	0.2713
MAP_{50} (mmHg)	124 ± 3	162 ± 8*	121 ± 3	159 ± 5*	<0.0001	0.5695
MAP_{thr} (mmHg)	112 ± 4	147 ± 9*	109 ± 4	136 ± 6*	<0.0001	0.2024
RSNA at MAP_{thr} (%)	87 ± 2	86 ± 1	89 ± 3	88 ± 3	0.5635	0.3633
MAP_{sat} (mmHg)	134 ± 3	176 ± 8*	134 ± 3	183 ± 5*	<0.0001	0.8059
RSNA at MAP_{sat} (%)	35 ± 4	41 ± 4	30 ± 2	32 ± 4	0.2332	0.1263
MAP operating range (mmHg)	25 ± 6	29 ± 1	25 ± 2	47 ± 6*	0.0089	0.0744
Adult *(n)*	*9*	*8*	*9*	*7*	-	-
RSNA upper plateau (%)	102 ± 1	100 ± 1	111 ± 5	103 ± 1	0.0799	0.0507
RSNA lower plateau (%)	22 ± 3	40 ± 7*	13 ± 4	41 ± 7*	0.0001	0.4298
Range (%)	80 ± 3	60 ± 7	98 ± 7	62 ± 8*	0.0001	0.1309
Gain (%/mmHg)	-2.6 ± 0.2	-1.1 ± 0.2*	-2.2 ± 0.2	-1.2 ± 0.1*	<0.0001	0.5371
MAP_{50} (mmHg)	129 ± 3	154 ± 8*	127 ± 5	171 ± 11*	<0.0001	0.2906
MAP_{thr} (mmHg)	117 ± 3	133 ± 7	106 ± 7	153 ± 12$^{*\#}$	0.0002	0.5723
RSNA at MAP_{thr} (%)	85 ± 1	87 ± 2	90 ± 4	90 ± 1	0.7339	0.1193
MAP_{sat} (mmHg)	140 ± 5	175 ± 4*	143 ± 2	189 ± 10*	<0.0001	0.2395
RSNA at MAP_{sat} (%)	39 ± 3	53 ± 5*	34 ± 2	54 ± 5*	0.0002	0.6113
MAP operating range (mmHg)	22 ± 3	41 ± 6*	37 ± 8	36 ± 3	0.1083	0.4344

MAP, mean arterial pressure; MAP_{50}, mean arterial pressure at the midpoint of the curve; MAP_{thr}, threshold mean arterial pressure to trigger a change in RSNA; MAP_{sat}, saturation mean arterial pressure at which there is no further change in RSNA.
Results are expressed as mean ± SEM.
$^{*}P<0.05$ vs. sex- and age-matched Lewis, $^{‡}P<0.05$ vs. strain-and age-matched female rat and $^{\#}P<0.05$ indicates strain × sex interaction. *(n)* = number in each group.

Table 5.4: Parameters describing the relationship between mean arterial pressure (MAP) and aortic depressor nerve activity (ADNA) in the juvenile (7–8 weeks old) and adult (12–13 weeks old) Lewis and Lewis Polycystic Kidney (LPK) rats of either sex

Group	Female		Male		Two-way ANOVA adjusted *P* value	
	Lewis	LPK	Lewis	LPK	Strain	Sex
Barocurve parameter						
Juvenile *(n)*	*5*	*7*	*7*	*6*	-	-
ADNA upper plateau (%)	400 ± 47	336 ± 64	346 ± 26	324 ± 26	0.3501	0.4812
ADNA lower plateau (%)	28 ± 11	10 ± 4	48 ± 15	37 ± 8	0.1732	0.0347
Range (%)	372 ± 53	325 ± 65	297 ± 31	287 ± 33	0.5613	0.2612
Gain (%/mmHg)	5.5 ± 1.0	4.0 ± 0.7	5.0 ± 0.6	2.5 ± 0.3*	0.0065	0.1725
MAP_{50} (mmHg)	118 ± 3	142 ± 8*	123 ± 2	155 ± 8*	0.0002	0.1623
MAP_{thr} (mmHg)	95 ± 4	115 ± 6*	103 ± 3	116 ± 7	0.0081	0.4141
ADNA at MAP_{thr} (%)	107 ± 10	77 ± 14	111 ± 11	98 ± 5	0.0803	0.3116
MAP_{sat} (mmHg)	141 ± 2	170 ± 11	143 ± 3	195 ± 13*	0.0002	0.1548
ADNA at MAP_{sat} (%)	321 ± 36	266 ± 50	283 ± 21	263 ± 19	0.3040	0.5650
MAP operating range (mmHg)	46 ± 5	56 ± 9	40 ± 4	80 ± 13*	0.0082	0.3049
Adult *(n)*	*12*	*8*	*7*	*7*	-	-
ADNA upper plateau (%)	385 ± 46	375 ± 55	406 ± 60	199 ± 29*	0.0426	0.1378
ADNA lower plateau (%)	53 ± 8	44 ± 12	40 ± 5	66 ± 9	0.3878	0.6223
Range (%)	331 ± 49	331 ± 64	365 ± 61	133 ± 35$^{*‡\#}$	0.0460	0.1502
Gain (%/mmHg)	5.4 ± 0.7	4.0 ± 0.7	5.2 ± 1.1	1.5 ± 0.4*	0.0043	0.1020
MAP_{50} (mmHg)	114 ± 4	136 ± 7*	119 ± 3	147 ± 9*	0.0002	0.1721
MAP_{thr} (mmHg)	93 ± 6	108 ± 5	93 ± 2	108 ± 11	0.0311	0.9669
ADNA at MAP_{thr} (%)	123 ± 10	114 ± 7	117 ± 12	94 ± 7	0.1144	0.2136
MAP_{sat} (mmHg)	135 ± 4	163 ± 10*	145 ± 6	176 ± 8*	0.0002	0.1220
ADNA at MAP_{sat} (%)	315 ± 35	305 ± 41	328 ± 47	171 ± 22*	0.0425	0.1359
MAP operating range (mmHg)	42 ± 3	56 ± 9	52 ± 6	67 ± 9	0.0308	0.1012

MAP, mean arterial pressure; MAP_{50}, mean arterial pressure at the midpoint of the curve; MAP_{thr}, threshold mean arterial pressure to trigger a change in ADNA; MAP_{sat}, saturation mean arterial pressure at which there is no further change in ADNA.
Results are expressed as mean ± SEM.
$^{*}P<0.05$ vs. sex- and age-matched Lewis, $^{‡}P<0.05$ vs. strain-and age-matched female rat and $^{\#}P<0.05$ indicates strain × sex interaction. *(n)* = number in each group.

Table 5.5: Reflex heart rate responses to evoked increases and decreases in blood pressure using phenylephrine (PE) and sodium nitroprusside (SNP), respectively in the juvenile (7–8 weeks old) and adult (12–13 weeks old) Lewis and Lewis Polycystic Kidney (LPK) rats of either sex

Group	Female		Male		Two-way ANOVA adjusted *P* value	
	Lewis	LPK	Lewis	LPK	Strain	Sex
Baroreflex parameter						
Juvenile *(n)*	*8*	*8*	*7*	*8*	-	-
BRS_{PE} (bpm/mmHg)	1.03 ± 0.18	0.80 ± 0.17	0.99 ± 0.10	1.61 ± 0.23$^{‡\#}$	0.2937	0.0449
BRS_{SNP} (bpm/mmHg)	0.65 ± 0.16	0.34 ± 0.09	0.45 ± 0.08	0.29 ± 0.04	0.0331	0.2312
Adult *(n)*	*11*	*7*	*11*	*7*	-	-
BRS_{PE} (bpm/mmHg)	0.92 ± 0.15	0.22 ± 0.04*	1.38 ± 0.22	0.50 ± 0.10*‡	<0.0001	0.0055
BRS_{SNP} (bpm/mmHg)	0.56 ± 0.18	0.28 ± 0.04	0.59 ± 0.14	0.27 ± 0.05	0.0466	0.9410

BRS_{PE}, heart rate baroreflex sensitivity to PE-induced reflex bradycardia; and BRS_{SNP}, heart rate baroreflex sensitivity to PE-induced reflex tachycardia MAP.
Results are expressed as mean ± SEM.
$^{*}P$<0.05 vs. sex- and age-matched Lewis, $^{‡}P$<0.05 vs. strain-and age-matched female rat and $^{\#}P$<0.05 indicates strain × sex interaction. *(n)* = number in each group.

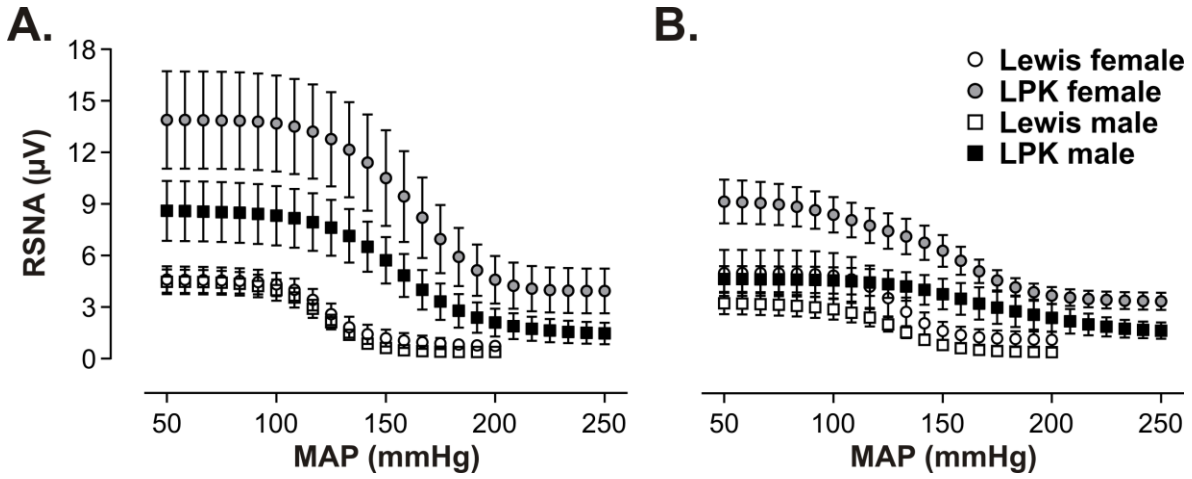

Figure 5.2: Logistic function curves illustrating the relationship between mean arterial pressure (MAP) and renal sympathetic nerve activity (RSNA) expressed in microvolts (μV) in juvenile (7–8 weeks old, A) and adult (12–13 weeks old, B) female Lewis and Lewis Polycystic Kidney (LPK) rats of either sex. Results are expressed as mean ± SEM. *n* values are as detailed in Table 5.6.

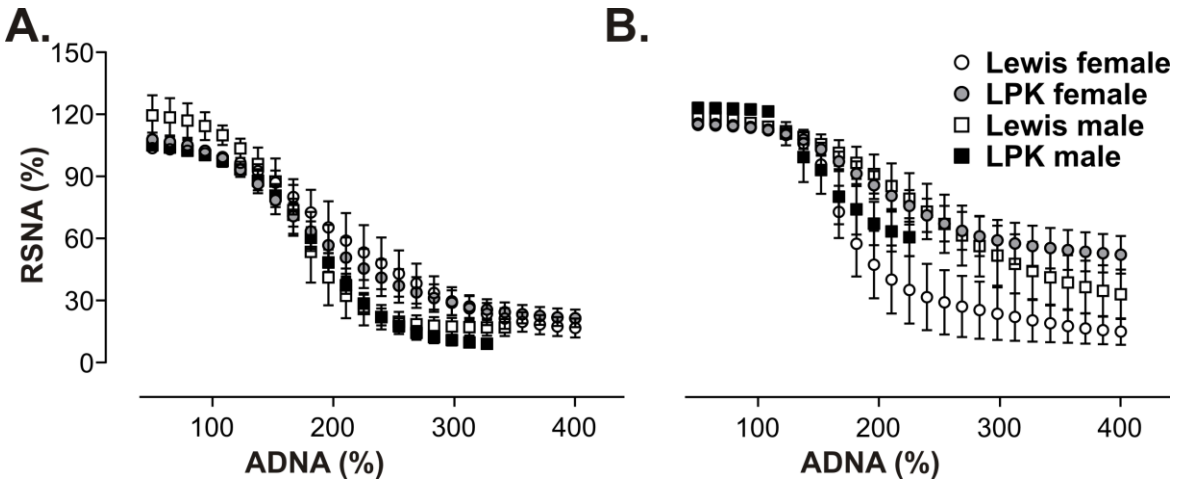

Figure 5.3: Logistic function curves illustrating the relationship between aortic depressor nerve activity (ADNA) and renal sympathetic nerve activity (RSNA) in juvenile (7–8 weeks old, A) and adult (12–13 weeks old, B) female Lewis and Lewis Polycystic Kidney (LPK) rats of either sex. Results are expressed as mean ± SEM. *n* values are as detailed in Table 5.7.

Table 5.6: Parameters describing the relationship between mean arterial pressure (MAP) and renal sympathetic nerve activity (RSNA) expressed in microvolts in the juvenile (7–8 weeks old) and adult (12–13 weeks old) Lewis and Lewis Polycystic Kidney (LPK) rats of either sex

Groups	Female		Male		Two-way ANOVA adjusted *P* value	
	Lewis	LPK	Lewis	LPK	Strain	Sex
Barocurve parameter						
Juvenile *(n)*	*8*	*7*	*8*	*9*	-	-
RSNA upper plateau (μV)	4.6 ± 0.8	13.9 ± 2.8*	4.5 ± 0.7	8.6 ± 1.7*	<0.0001	0.2013
RSNA lower plateau (μV)	0.6 ± 0.2	3.9 ± 1.3*	0.4 ± 0.1	1.4 ± 0.6‡	0.0031	0.0487
Range (μV)	4.0 ± 0.7	10.0 ± 1.6*	4.1 ± 0.7	7.2 ± 1.5*	0.0008	0.2781
Gain (μV/mmHg)	-0.13 ± 0.02	-0.24 ± 0.04*	-0.119 ± 0.019	-0.116 ± 0.024$^{‡\#}$	0.0421	0.0165
MAP_{50} (mmHg)	126 ± 4	162 ± 8*	121 ± 3	157 ± 5*	<0.0001	0.3845
MAP_{thr} (mmHg)	114 ± 2	148 ± 9*	110 ± 4	135 ± 6*	<0.0001	0.1294
RSNA at MAP_{thr} (μV)	3.8 ± 0.7	11.8 ± 2.5*	3.6 ± 0.6	7.1 ± 1.5*	<0.0001	0.1811
MAP_{sat} (mmHg)	139 ± 8	175 ± 8*	133 ± 3	180 ± 6*	<0.0001	0.9086
RSNA at MAP_{sat} (μV)	1.5 ± 0.3	6.0 ± 1.6*	1.2 ± 0.2	2.9 ± 0.8‡	0.0009	0.0575
MAP operating range (mmHg)	25 ± 8	28 ± 2	24 ± 3	45 ± 6*	0.0321	0.1482
Adult *(n)*	*9*	*8*	*9*	*7*	-	-
RSNA upper plateau (μV)	4.7 ± 1.3	9.3 ± 1.3*	3.3 ± 0.6	5.0 ± 0.7‡	0.0060	0.0105
RSNA lower plateau (μV)	1.1 ± 0.5	3.3 ± 0.5*	0.4 ± 0.1	1.8 ± 0.5*‡	0.0001	0.0114
Range (μV)	3.6 ± 0.8	5.9 ± 1.3	2.9 ± 0.6	3.1 ± 0.6	0.1618	0.0580
Gain (μV/mmHg)	-0.10 ± 0.03	-0.11 ± 0.03	-0.062 ± 0.013	-0.051 ± 0.010	0.9728	0.0199
MAP_{50} (mmHg)	129 ± 3	151 ± 9	125 ± 4	167 ± 11*	<0.0001	0.3609
MAP_{thr} (mmHg)	116 ± 2	133 ± 10	107 ± 6	149 ± 12*	0.0008	0.6392
RSNA at MAP_{thr} (μV)	3.9 ± 1.1	8.0 ± 1.1*	2.7 ± 0.5	4.3 ± 0.6‡	0.0031	0.0081
MAP_{sat} (mmHg)	141 ± 5	169 ± 9*	143 ± 2	186 ± 11*	<0.0001	0.1943
RSNA at MAP_{sat} (μV)	1.9 ± 0.6	4.6 ± 0.5*	1.0 ± 0.2	2.5 ± 0.5*	<0.0001	0.0127
MAP operating range (mmHg)	27 ± 4	37 ± 5	36 ± 6	37 ± 4	0.2265	0.2764

MAP, mean arterial pressure; MAP_{50}, mean arterial pressure at the midpoint of the curve; MAP_{thr}, threshold mean arterial pressure to trigger a change in RSNA; MAP_{sat}, saturation mean arterial pressure at which there is no further change in RSNA.
Results are expressed as mean ± SEM.
$^{*}P$<0.05 vs. sex- and age-matched Lewis, $^{‡}P$<0.05 vs. strain-and age-matched female rat and $^{\#}P$<0.05 indicates strain × sex interaction. *(n)* = number in each group.

Table 5.7: Parameters describing the relationship between aortic depressor nerve activity (ADNA) and renal sympathetic nerve activity (RSNA) in the juvenile (7–8 weeks old) and adult (12–13 weeks old) Lewis and Lewis Polycystic Kidney (LPK) rats of either sex

Group	Female		Male		Two-way ANOVA adjusted *P* value	
	Lewis	LPK	Lewis	LPK	Strain	Sex
Barocurve parameter						
Juvenile *(n)*	*5*	*7*	*5*	*4*	-	-
RSNA upper plateau (%)	105 ± 2	111 ± 5	121 ± 11	108 ± 4	0.6302	0.3259
RSNA lower plateau (%)	15 ± 4	19 ± 4	17 ± 4	7 ± 2	0.5875	0.2641
RSNA range (%)	90 ± 5	92 ± 8	104 ± 12	101 ± 6	0.9400	0.2079
Gain	-0.7 ± 0.1	-0.7 ± 0.1	-0.8 ± 0.2	-0.8 ± 0.1	0.8855	0.5299
$ADNA_{50}$ (%)	220 ± 20	191 ± 18	165 ± 13	177 ± 6	0.6342	0.0682
$ADNA_{thr}$ (%)	172 ± 18	139 ± 15	111 ± 21	132 ± 13	0.7561	0.0780
RSNA at $ADNA_{thr}$ (%)	86 ± 2	92 ± 3	99 ± 8	87 ± 3	0.5440	0.4170
$ADNA_{sat}$ (%)	268 ± 28	243 ± 23	219 ± 19	222 ± 8	0.6370	0.1609
RSNA at $ADNA_{sat}$ (%)	34 ± 4	39 ± 3	39 ± 4	28 ± 1	0.4465	0.4323
ADNA range (%)	96 ± 19	103 ± 19	108 ± 30	90 ± 19	0.8099	0.9778
Adult *(n)*	*6*	*8*	*4*	*7*	-	-
RSNA upper plateau (%)	100 ± 1	101 ± 2	108 ± 4	107 ± 2	0.9582	0.0049
RSNA lower plateau (%)	11 ± 5	40 ± 8*	17 ± 8	46 ± 8	0.0020	0.4981
RSNA range (%)	89 ± 5	61 ± 9*	91 ± 9	61 ± 8	0.0030	0.8701
Gain	-1.7 ± 0.7	-0.5 ± 0.1	-0.4 ± 0.1	-2.4 ± 0.8$^{‡\#}$	0.5071	0.6166
$ADNA_{50}$ (%)	198 ± 24	232 ± 27	252 ± 26	143 ± 14$^{*‡\#}$	0.1428	0.4907
$ADNA_{thr}$ (%)	169 ± 20	179 ± 20	162 ± 16	115 ± 10	0.3349	0.0689
RSNA at $ADNA_{thr}$ (%)	81 ± 2	88 ± 2	89 ± 3	94 ± 3	0.0181	0.0108
$ADNA_{sat}$ (%)	228 ± 30	285 ± 35	343 ± 53	171 ± 26$^{*‡\#}$	0.1269	0.9867
RSNA at $ADNA_{sat}$ (%)	30 ± 4	53 ± 7*	36 ± 6	59 ± 6	0.0020	0.3676
ADNA range (%)	59 ± 14	107 ± 20	181 ± 59$^{‡\#}$	56 ± 27*	0.1867	0.2221

$ADNA_{50}$, aortic depressor nerve activity at the midpoint of the curve; $ADNA_{thr}$, threshold aortic depressor nerve activity to trigger a change in RSNA; and $ADNA_{sat}$, saturation aortic depressor nerve activity at which there is no further change in RSNA.
Results are expressed as mean ± SEM.
$^{*}P<0.05$ vs. sex- and age-matched Lewis, $^{‡}P<0.05$ vs. strain-and age-matched female rat and $^{\#}P<0.05$ indicates strain × sex interaction. *(n)* = number in each group.

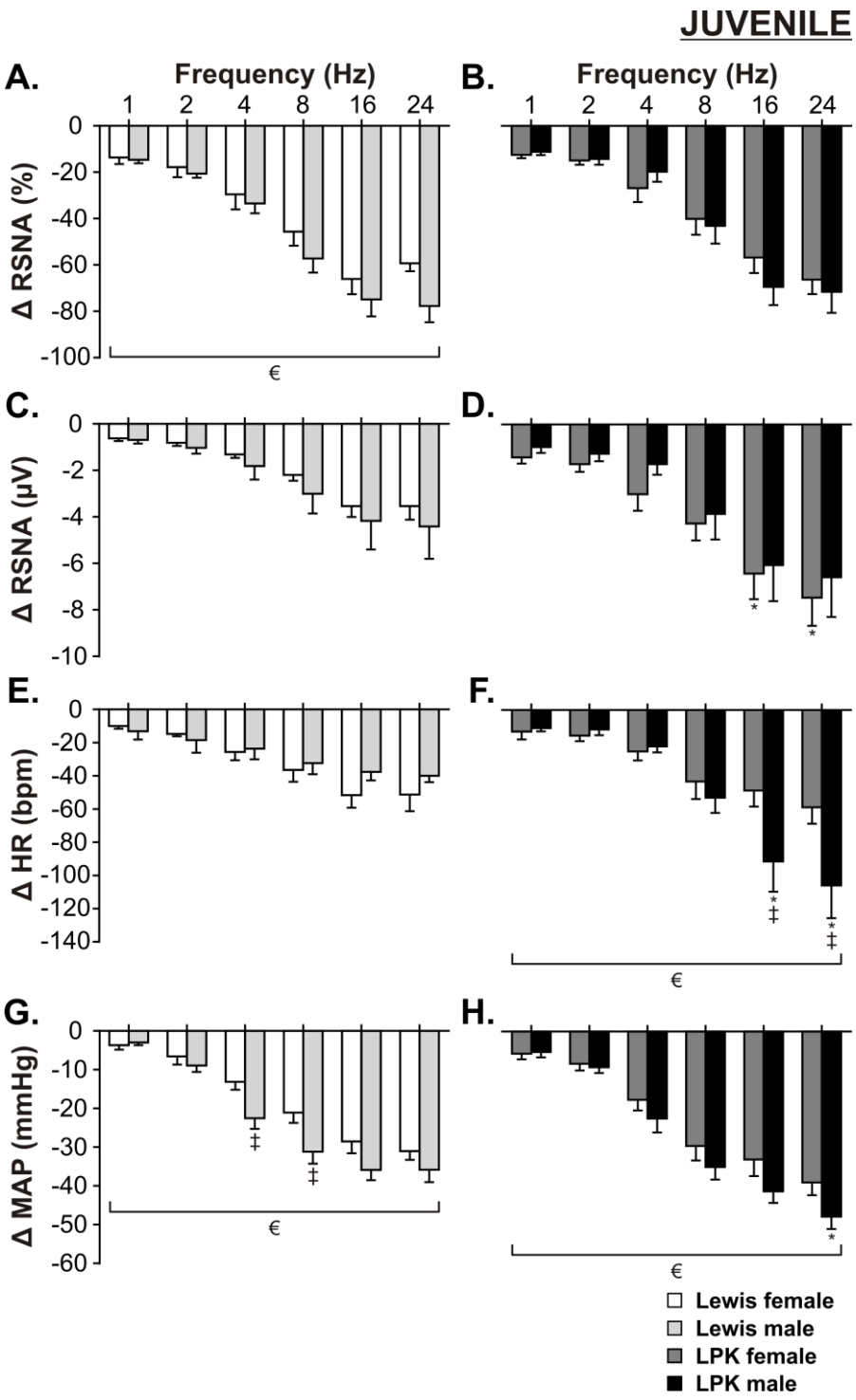

Figure 5.4: Effect of aortic depressor nerve stimulation on renal sympathetic nerve activity (RSNA; A–D), heart rate (HR; E & F) and mean arterial pressure (MAP; G & H) in juvenile (7–8 weeks old) Lewis (left panels) and Lewis Polycystic Kidney (LPK) rats (right panels) of either sex. A reduction in RSNA, HR and MAP was observed in all experimental groups. Results are expressed as mean ± SEM. $^{*}P<0.05$ vs. age-matched Lewis, $^{‡}P<0.05$ vs. strain-matched juvenile female rat and $^{€}P<0.05$, overall two-way ANOVA sex effect within Lewis or LPK. *n*/group: juvenile female Lewis = 6, juvenile female LPK = 7, juvenile male Lewis = 5 and juvenile male LPK = 5. bpm: beats per minute.

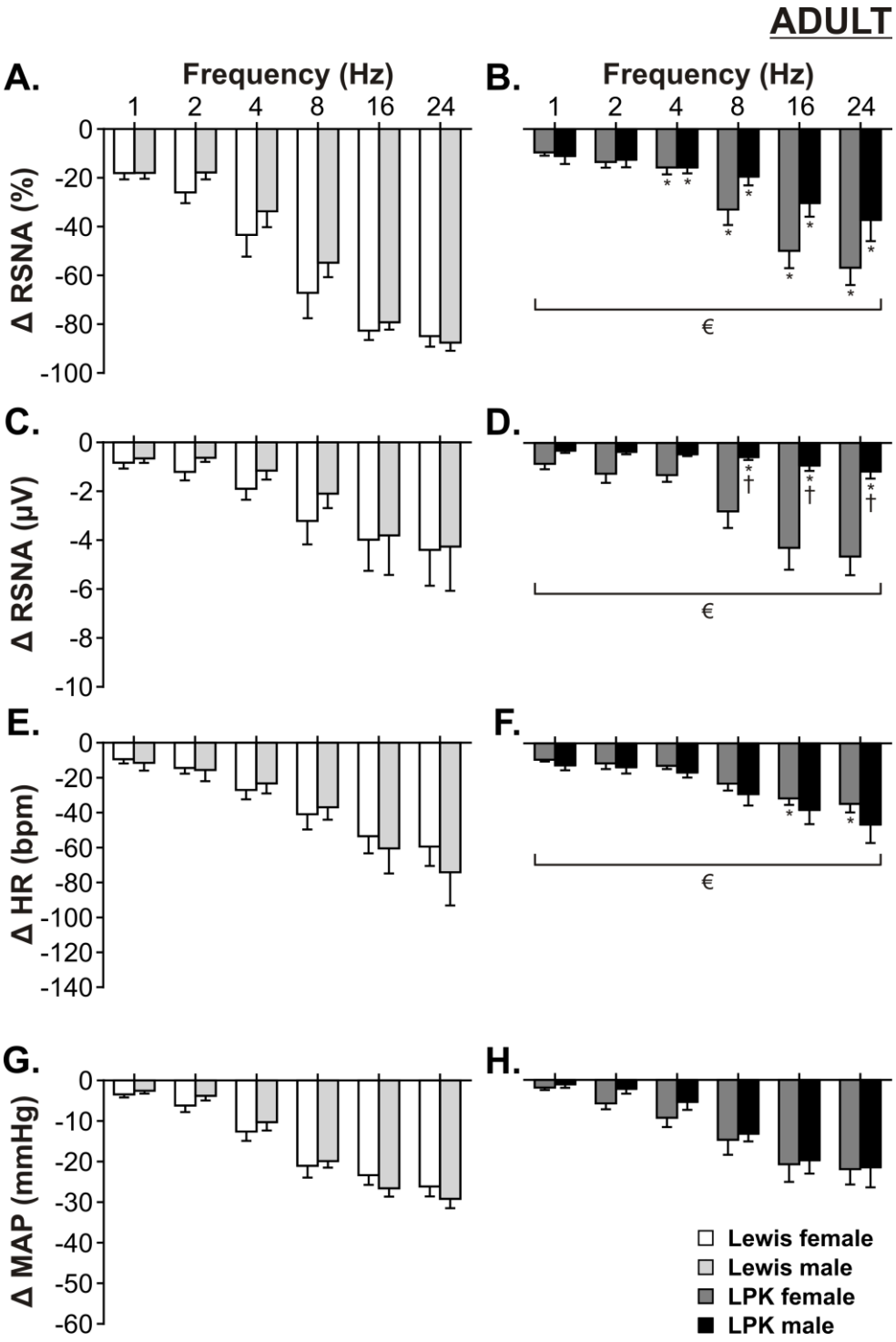

Figure 5.5: Effect of aortic depressor nerve stimulation on renal sympathetic nerve activity (RSNA; A–D), heart rate (HR; E & F) and mean arterial pressure (MAP; G & H) in adult (12–13 weeks old) Lewis (left panels) and Lewis Polycystic Kidney (LPK) rats (right panels) of either sex. A reduction in RSNA, HR and MAP was observed in all experimental groups. Results are expressed as mean ± SEM. $^{*}P<0.05$ vs. age-matched Lewis, $^{‡}P<0.05$ vs. strain-matched juvenile female rat and $^{€}P<0.05$, overall two-way ANOVA sex effect within Lewis or LPK. *n*/group: adult female Lewis = 5, adult female LPK = 8, adult male Lewis = 6 and adult male LPK = 7. bpm: beats per minute.

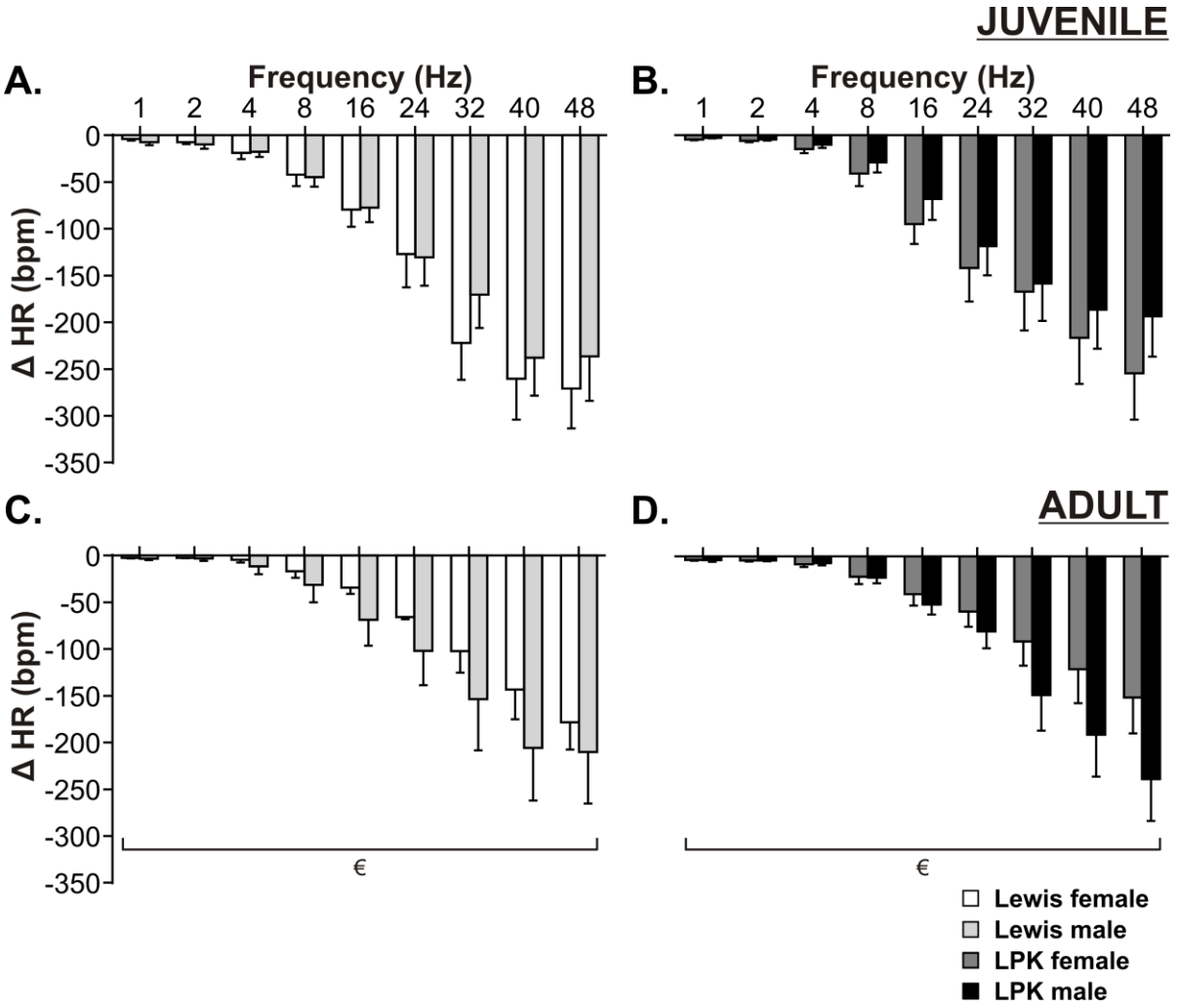

Figure 5.6: Effect of cervical vagal efferent nerve stimulation on heart rate in juvenile (7–8 weeks old, A & B) and adult (12–13 weeks old, C & D) Lewis (left panels) and Lewis Polycystic Kidney (LPK) rats (right panels) of either sex. A reduction in HR was observed in all experimental groups. Results are expressed as mean ± SEM. $^{€}P<0.05$, overall two-way ANOVA sex effect within Lewis or LPK. *n*/group: juvenile female Lewis = 8, juvenile female LPK = 8, juvenile male Lewis = 8, juvenile male LPK = 8, adult female Lewis = 5, adult female LPK = 5, adult male Lewis = 4 and adult male LPK = 8. bpm: beats per minute.

Table 5.8: Differentiating histomorphometric variables in the aortic arch of juvenile (7–8 weeks old) and adult (12–13 weeks old) Lewis and Lewis Polycystic Kidney (LPK) rats of either sex

Group	Female		Male		Two-way ANOVA adjusted *P* value	
	Lewis	LPK	Lewis	LPK	Strain	Sex
Morphometric parameter						
Juvenile *(n)*	*6*	*6*	*6*	*7*	-	-
Medial thickness (μm)	117 ± 2	150 ± 8*	131 ± 4	166 ± 3*‡	<0.0001	0.0018
Number of elastin lamellae	12 ± 0.3	12 ± 0.4	12 ± 0.3	11 ± 0.5	0.2554	0.4975
Total elastin density (%)	75 ± 2	68 ± 5	74 ± 2	61 ± 1*	0.0005	0.0726
Lamellae elastin density (%)	48 ± 1	48 ± 2	48± 1	43 ± 1‡	0.0531	0.0186
Interlamellae elastin density (%)	27 ± 2	20 ± 3	25 ± 2	17 ± 0.9*	0.0007	0.2051
Lamellae-to-interlamellae elastin ratio	1.9 ± 0.1	2.8 ± 0.5	2.0 ± 0.1	2.6 ± 0.2	0.0071	0.8839
Thickness of elastin lamellae (μm)	3.8 ± 0.1	4.2 ± 0.2	3.9 ± 0.2	4.1 ± 0.1	0.0405	0.7977
Elastin lamellae spacing (μm)	6.7 ± 0.3	9.3 ± 0.5*	7.6 ± 0.2	9.9 ± 0.4*	<0.0001	0.0421
Number of elastin lamellae fractures (fracture/lamellae/mm)	0.01 ± 0.002	0.03 ± 0.004*	0.02 ± 0.003	0.05 ± 0.007*‡	<0.0001	0.0123
Total collagen density (%)	21 ± 0.4	23 ± 0.6	21 ± 1.6	29 ± 0.5$^{*‡#}$	<0.0001	0.0080
Elastin-to-collagen ratio	3.7 ± 0.1	3.0 ± 0.2*	3.7 ± 0.4	2.1 ± 0.1*	<0.0001	0.0778
Nuclear density (%)	4.9 ± 0.3	4.8 ± 0.2	4.8 ± 0.2	5.8 ± 0.3	0.1424	0.1522
Nucleus cross-sectional area (μm^2)	9.0 ± 0.4	12.0 ± 0.9*	9.6 ± 0.5	13.7 ± 1.0*	<0.0001	0.1409
Number of nuclei per μm^2	0.12 ± 0.006	0.09 ± 0.007	0.10 ± 0.005	0.08 ± 0.008*	0.0015	0.0875
Calcium density (%)	0.7 ± 0.2	0.6 ± 0.3	0.7 ± 0.2	0.9 ± 0.3	0.9352	0.5056
Average size of calcium deposit (μm^2)	6.1 ± 1.0	4.8 ± 0.7	5.7 ± 0.7	4.0 ± 0.7	0.0980	0.4634
Adult *(n)*	*5*	*5*	*5*	*6*	-	-
Medial thickness (μm)	137 ± 2	190 ± 14*	145 ± 8	222 ± 5*‡	<0.0001	0.0357
Number of elastin lamellae	12 ± 0.4	12 ± 0.7	11 ± 0.5	13 ± 1.1	0.5355	0.8372
Total elastin density (%)	63 ± 1	51 ± 2*	68 ± 2	44 ± 3$^{*#}$	<0.0001	0.6707
Lamellae elastin density (%)	46 ± 1	38 ± 1*	44 ± 2	34 ± 2*	<0.0001	0.0803
Interlamellae elastin density (%)	17 ± 1	13 ± 1	24 ± 2‡	10 ± 1$^{*#}$	<0.0001	0.1061
Lamellae-to-interlamellae elastin ratio	2.9 ± 0.3	3.2 ± 0.3	1.9 ± 0.2	3.8 ± 0.4$^{*#}$	0.0049	0.5898
Thickness of elastin lamellae (μm)	3.7 ± 0.1	4.1 ± 0.1*	3.8 ± 0.1	3.2 ± 0.1$^{*‡#}$	0.5459	0.0094
Elastin lamellae spacing (μm)	8.6 ± 0.4	12.5 ± 0.6*	9.3 ± 0.3	14.6 ± 1.2*	<0.0001	0.0946
Number of elastin lamellae fractures (fracture/lamellae/mm)	0.02 ± 0.003	0.05 ± 0.006*	0.02 ± 0.006	0.08 ± 0.011*‡	<0.0001	0.0359

Total collagen density (%)	22 ± 1.0	24 ± 0.7	23 ± 1.4	34 ± 1.9$^{*‡\#}$	0.0002	0.0035
Elastin-to-collagen ratio	2.8 ± 0.1	2.1 ± 0.1*	3.0 ± 0.2	1.3 ± 0.1$^{*‡\#}$	<0.0001	0.0311
Nuclear density (%)	3.8 ± 0.7	4.5 ± 0.2	3.7 ± 0.4	5.0 ± 0.1	0.0284	0.6559
Nucleus cross-sectional area (μm^2)	9.1 ± 0.9	13.9 ± 0.4*	9.4 ± 1.1	14.2 ± 0.7*	<0.0001	0.7931
Number of nuclei per μm^2	0.12 ± 0.013	0.08 ± 0.002*	0.12 ± 0.017	0.07 ± 0.004*	0.0005	0.8320
Calcium density (%)	0.5 ± 0.2	1.0 ± 0.5	1.0 ± 0.2	5.1 ± 1.9‡	0.0567	0.0500
Average size of calcium deposit (μm^2)	4.1 ± 0.6	6.0 ± 0.7	6.4 ± 0.5	8.4 ± 1.7	0.0789	0.0421

Results are expressed as mean ± SEM.
$^{*}P<0.05$ vs. sex- and age-matched Lewis, $^{‡}P<0.05$ vs. strain-and age-matched female rat and $^{\#}P<0.05$ indicates strain × sex interaction. *(n)* = minimum number in each group.

6 Dysfunctional Reflex Cardiac and Sympathetic Responses to Vagal Afferent Stimulation in Chronic Kidney Disease

Ibrahim M. Salman, Cara M. Hildreth, and Jacqueline K. Phillips

[1] *Australian School of Advanced Medicine, Macquarie University, Sydney, NSW, Australia*

This chapter is currently in preparation for publication.

Abstract

We investigated reflex changes in heart rate (HR) and renal sympathetic nerve activity (RSNA) in response to vagal afferent stimulation in chronic kidney disease (CKD), and changes associated with age and sex. In anaesthetised juvenile (7–8 weeks old) and adult (12–13 weeks old) Lewis Polycystic Kidney (LPK) and Lewis control rats of either sex (n = 63), reflex changes in HR, RSNA and mean arterial pressure (MAP) to vagal afferent stimulation (4.0V, 2.0-ms, at 1–16 Hz) were measured. In all groups, stimulation of the vagal afferents below 16 Hz produced frequency-dependent reductions in RSNA, HR and MAP, while a 16 Hz stimulus produced an initial sympathoinhibition followed by sustained sympathoexcitation. Juvenile LPK showed comparable reductions in RSNA (μV), but not RSNA (%), and relatively higher bradycardic and/or depressor responses compared to age-matched Lewis. In adult LPK, the reflex sympathoinhibition (both μV and %) was blunted by at least 22% (P<0.05) in the LPK of either sex, while reflex reductions in HR (25 ± 11 vs. 89 ± 21 beat per minute at 8 Hz, P<0.05) and MAP (9 ± 4 vs. 24 ± 2 mmHg at 8 Hz, P<0.05) were only diminished in the adult female LPK versus Lewis. Regardless of age, reflex sympathoexcitation at 16 Hz expressed as area under the curve was greater in the LPK versus Lewis (overall, 9 ± 1 vs. 19 ± 3 μV.s, P<0.05), suggestive of enhanced sympathoexcitatory drive in the LPK. Our data demonstrates temporal deficits in the central processing of vagal afferent input in the LPK model of CKD and highlights a differential sex influence on altered reflex regulation of autonomic outflows. An inability to reflexively control autonomic activity may contribute to altered blood pressure homeostasis observed in CKD.

Key words: vagal afferents, sympathetic nerve activity, cardiac vagal outflow, hypertension, chronic kidney disease

6.1 Introduction

It is well established that the reflex regulation of cardiovascular function is altered in chronic kidney disease (CKD), with cumulative evidence demonstrating dysfunctional baroreflex (Johansson et al., 2007, Tinucci et al., 2001), chemoreflex (Despas et al., 2009, Rassaf et al., 2012) and cardiopulmonary reflex (Frank et al., 2004, Neahring et al., 1995) control of autonomic outflows. We have now shown that the decline in baroreceptor reflex control of both heart rate (HR) and sympathetic nerve activity (SNA) that occurs in the rodent model of CKD, the Lewis Polycystic Kidney (LPK) rat, is primarily driven by a temporal decline in the central processing of the baroreceptor afferent input (Chapters 3 &

4). However, whether a similar temporal change in the central processing of other afferent inputs exists in CKD is still unknown.

In addition to the baroreceptor afferents, which in the rat are communicated via the aortic depressor and carotid sinus nerves (Ninomiya et al., 1971), the vagal afferent neurons, mainly those mediating cardiopulmonary reflexes, communicate information to the brain that reflexively alters autonomic outflows and regulate blood pressure (BP) (Hainsworth, 1991, Hainsworth, 2014). Vagal afferent neurons, which can be distinguished based on nerve conduction velocities into slow conducting unmyelinated C-fibres and fast conducting myelinated A-fibers (Bennett et al., 1985, Hainsworth, 2014), terminate in the nucleus tractus solitarius (NTS) (Kalia and Sullivan, 1982, Sun and Guyenet, 1987, Vardhan et al., 1993). The unmyelinated C-fibre vagal afferents share a common central pathway with the baroreceptor reflex within the brainstem, and therefore use a similar relay circuit to regulate efferent sympathetic and parasympathetic nerve activity (Kashihara, 2009, Lee et al., 1972, Sun and Guyenet, 1987, Verberne and Guyenet, 1992). Sympathetic outflow to the heart and vasculature is modulated via the caudal ventrolateral medulla (CVLM), rostral ventrolateral medulla (RVLM) and sympathetic preganglionic neurons in the spinal cord (Su et al., 1996, Sun and Guyenet, 1987, Verberne and Guyenet, 1992, Verberne et al., 1999). Efferent parasympathetic outflow to the heart is modulated through the nucleus ambiguus and dorsal motor nucleus of the vagus (Lee et al., 1972, Toader et al., 2007). Like baroreceptor afferents, activation of the unmyelinated C-fibre vagal afferent evokes sympathoinhibition, bradycardia and hypotension (Merrill et al., 1999, Vardhan et al., 1993), with the reflex bradycardia specifically indicative of cardiovagal outflow (Chianca and Machado, 1996, Sharkey et al., 1991). In contrast to the unmyelinated C-fibre vagal afferents, the myelinated A-fibre type is thought to regulate sympathetic vasomotor tone through an excitatory projection from the NTS to the RVLM (Sun and Guyenet, 1987), and therefore its activation evokes sympathoexcitation, vasoconstriction and hypertension (Huber and Schreihofer, 2010, Sun and Guyenet, 1987). There is also evidence that vagal afferents terminating in the NTS project to the paraventricular nucleus and elicit a differential response in sympathetic outflow (Deering and Coote, 2000, Higuchi et al., 1988). A deficit in the central processing of vagal afferent input and an inability of the medullary relay nuclei to produce changes in vagal or sympathetic outflow could potentially result in an inability to effectively regulate circulatory function. A large body of evidence indicates that cardiovascular reflexes mediated via the vagal afferent fibres are impaired in a number of different hypertensive conditions (Ferrari et al., 1984, Huber and Schreihofer, 2010, Verberne et al., 1988). However, whether similar impairments can be identified in CKD-related hypertension remains undetermined.

Given that the LPK rat model of CKD exhibits a temporal decline in central processing of baroreflex-related information and that baroreflex dysfunction is associated with blunted afferent traffic in the

males and impaired central drives in males and females (Chapters 3 & 4), we hypothesised that a similar age- and sex-dependent decline in the central integration of vagal afferent input and consequent deficits in the reflex efferent autonomic activity would be seen in the LPK. Accordingly, in the present study we examined the ability of the central component of the vagal afferent pathway to evoke baroreceptor-independent changes in autonomic outflows in CKD, and determined the impact of age and sex.

6.2 Methods

6.2.1 Ethical approval

All protocols were approved by the Animal Ethics Committees of Macquarie University and conducted in agreement with the Australian Code of Practice for the Care and Use of Animals for Scientific Purposes.

6.2.2 Animals

Studies described in the present chapter were carried out in a cohort of mixed sex juvenile (7–8 weeks old) and adult (12–13 weeks old) LPK and Lewis rats (total n = 63). Animals were part of a larger overall study and underwent in-vivo protocols as described in Chapters 3 and 4 prior to the experiments described below. All animals were purchased from the Animal Resource Centre (ARC) in Western Australia and housed in the Animal House Facility of Macquarie University. Rats were allowed to acclimatise for at least a week prior to the conduction of any experimental procedure. All animals were maintained under a 12-hour light/dark cycle and fed with rat chow and water *ad libitum*.

6.2.3 Surgical procedures and experimental protocols

Animals (male, n = 29 and female, n = 34) were anaesthetised with ethyl carbamate (urethane, 1.3 g/kg i.p., Sigma Aldrich, Australia). Initial adequacy of anaesthesia was confirmed by lack of withdrawal to a firm toe pinch and corneal stocking. Supplemental doses of urethane (10–20 mg) were injected intravenously as required. Following induction of anaesthesia, rectal temperature was monitored and maintained at 36.5–37.0ºC using a thermostatically controlled heating blanket and infrared heating source, and supplemental oxygen provided. A tracheostomy was performed and if required, the animal was artificially ventilated with oxygen enriched room air and ventilation adjusted to maintain pH at 7.40 ± 0.05 and PCO_2 at 40 ± 5 mmHg. The right jugular vein and carotid artery were catheterised for the administration of fluids (Ringer's solution, 5 ml/kg/hr) and recording of BP, respectively. Heart rate was derived from the pulsatile BP signal. A dorsal cervical incision was performed to expose the left vagus nerve. The left renal nerve was isolated retroperitoneally and prepared for whole nerve recordings. All nerves were maintained in paraffin oil. Nerve recording was made using bipolar silver wire recording electrodes, amplified, band-pass filtered (10–1000Hz, CWE Inc., Ardmore, PA, USA) and sampled at 5 kHz using a CED 1401 plus (Cambridge Electronic

Designs Ltd, Cambridge, UK) and Spike2 (v7, Cambridge Electronic Designs Ltd., Cambridge, UK). Renal SNA (RSNA) recordings were made through the same bioamplifier and calibrated according to a pre-set 50 μV voltage on the bioamplifier. Following completion of a prior series of experimental procedures (as detailed in Chapters 3 and 4), the left vagus nerve was isolated, tied with a silk suture then cut. Each animal was allowed to stabilize for a period of 15–30 minutes to obtain resting measurements before the following experimental protocol was begun.

Assessment of the RSNA, HR and BP response to vagal afferent stimulation. The central cut end of the vagus nerve was placed on a bipolar stimulating electrode connected to a stimulator (model 2100; A-M Systems Isolated Pulse Stimulator World Precision Instruments, USA) and stimulated sequentially using a 5-second train (4.0V, 2.0-ms pulses) of 1, 2, 4, 8 and 16 Hz separated by a period of 3–5 minutes. RSNA, HR and BP were continuously recorded. All variables were allowed to return to baseline pre-stimulus levels before the application of the subsequent stimulus. At the end of the experiment, the renal nerve was cut proximal to the recording electrodes and background activity recorded.

6.2.4 Data and statistical analyses

Mean, systolic and diastolic BP and HR were derived from the BP signal. All nerve recordings were rectified and averaged into 1-second bins. The level of nerve activity following transection of the renal nerve was subtracted from nerve recordings to obtain microvolt estimate of RSNA. Resting (unstimulated) measurements were averaged over a 30-second recording period immediately prior to the experimental protocol. RSNA was normalised to a 30-second period immediately prior to the application of each electrical stimulus and set as 100%. The level of nerve activity following transection was set as 0%. Peak changes in RSNA, HR and mean arterial pressure (MAP) were measured in response to the graded electrical stimulations of the vagus nerve. As resting RSNA was elevated in the LPK (see below), the sympathetic responses to vagal afferent stimulation were also expressed in microvolts.

In our study, stimulation of the vagal afferents at 16 Hz evoked a biphasic RSNA response: an initial sympathoinhibition followed by immediate sympathoexcitation. Accordingly, inhibitory and excitatory RSNA, HR and MAP responses at 16 Hz were analysed separately by measuring maximum changes in these variable during each phase. As the time to recovery of excitatory phase was distinct to that of the inhibitory component, the excitatory sympathetic response was additionally analysed as area under the curve (AUC) of the integrated RSNA.

All data are expressed as mean ± SEM. Statistical analysis was performed using GraphPad Prism software (GraphPad Prism software v6 Inc., La Jolla, CA, USA). A two-way ANOVA was used to identify, within each age group, if strain differences at the stimulation frequencies used existed and if,

within each strain, age or sex differences existed. Where ANOVA indicated a strain, age or sex difference a Bonferroni's post-hoc analysis was performed. A Brown-Forsythe test was used to determine if there were any differences in the variance, and if so, the data was log-transformed before statistical analysis. Significance was defined as $P \leq 0.05$.

6.3 Results

6.3.1 Resting measurements in the Lewis and LPK

Resting measurements of systolic BP, pulse pressure, MAP, and RSNA were elevated in both adult and juvenile LPK compared with age-matched Lewis controls. In juvenile LPK of either sex and adult female LPK, diastolic BP was elevated relative to age- and sex-matched Lewis. With the exception of pulse pressure, which was greater in adult versus juvenile male and female LPK rats, no other cardiovascular parameter differed with age (Table 6.1).

A comparison of male versus female data within each age and strain cohort indicated that apart from HR, which was greater in the juvenile male versus female LPK ($P = 0.04$), no other cardiovascular parameter nor RSNA was influenced by sex.

For renal function data, illustrating strain, age and sex differences in this measure, refer to Chapters 3–5.

6.3.2 Reflex responses to vagal afferent stimulation at 1–8 Hz

Representative data traces showing RSNA, HR and MAP responses to vagal afferent stimulation in adult Lewis and LPK rats of either sex are shown in Figure 6.1. As illustrated in Figure 6.2 and 6.3, direct electrical stimulation of the central cut end of the vagus nerve between 1–8 Hz produced a frequency-dependent reduction (all $P<0.001$) in RSNA, HR and MAP in all groups.

In juvenile LPK, renal sympathoinhibitory responses (%) were markedly blunted (all $P<0.001$, ANOVA) in the male and female LPK relative to age- and sex-matched Lewis. This was not observed when RSNA was expressed in microvolts. Reflex bradycardic responses, however, were significantly increased in the juvenile LPK of either sex (all $P<0.001$, ANOVA). Reflex depressor responses were greater overall ($P = 0.002$, ANOVA) in the juvenile female LPK versus Lewis and specifically at 8 Hz; however, this was not observed in the juvenile male groups. In adult LPK of either sex, reflex sympathoinhibitions expressed as both % and µV were reduced (all $P<0.05$, ANOVA) compared with Lewis controls, and an age-related decline (all $P<0.001$, ANOVA) in microvolt measures was also apparent in the LPK. In the male Lewis, an age effect ($P = 0.03$, ANOVA) on the sympathoinhibitory response (%) was also seen. Reflex bradycardic and depressor responses to vagal afferent stimulation were blunted (all $P<0.001$, ANOVA) in the adult female LPK versus Lewis, and age-dependent reductions (all $P \leq 0.001$, ANOVA) in both HR and BP responses in the LPK and the overall depressor

response of the Lewis were evident. Adult male LPK, on the other hand, showed comparable reflex bradycardia and hypotension to those of age- and sex-matched Lewis. Depressor responses in both male LPK and Lewis declined with age (all $P<0.05$, ANOVA).

When comparing both male and female juvenile rats, reflex sympthoinhibitory responses (μV) were overall significantly greater (all $P<0.05$, ANOVA) in the female Lewis and LPK relative to strain-matched male. All other parameters measured in juvenile animals of both strains remained uninfluenced by sex. In the adult groups, with the exception of higher depressor responses ($P = 0.02$, ANOVA) in the male versus female Lewis, sex did not affect any other parameters measured in the Lewis strain. In the adult LPK, sympathetic responses were comparable between the male and female, whereas greater bradycardia and hypotension (all $P<0.001$, ANOVA) could be evoked in the LPK males relative to LPK females.

6.3.3 Reflex responses to vagal afferent stimulation at 16 Hz

Representative data traces showing biphasic sympathetic responses to vagal afferent stimulation at 16 Hz in juvenile and adult Lewis and LPK rats of either sex are shown in Figure 6.4. An initial sympthoinhibitory phase followed by an immediate sympathoexcitatory response was consistently observed in all animals when a 16 Hz stimulus was used to activate the vagal afferent fibres.

In the juvenile rats, the reflex sympathoinhibitory component (%) was reduced in the female LPK versus Lewis but this was not evident when assessed as a microvolt response and there were no strain differences in the juvenile males. In adult male and female rats, RSNA (%) was blunted in the LPK compared with sex-matched Lewis, and an age-dependent reduction in the microvolt measures of the sympathoinhibitory response was observed. No sex differences in the sympathoinhibitory responses at 16 Hz were identified between the groups.

During the sympathoexcitatory phase, apart from a greater ($P<0.05$, ANOVA) RSNA AUC in the LPK versus sex-matched Lewis (Fig. 6.5), no other RSNA parameter measured during the sympathoexcitatory phase of vagal afferent stimulation differed among groups, and an age- or sex-related effect was not evident (Fig. 6.4).

As illustrated in Figure 6.6, reflex bradycardic and depressor responses at 16 Hz were not different in the juvenile male or female LPK versus age- and sex-matched Lewis. Adult female LPK had blunted (all $P<0.05$, ANOVA) bradycardic and depressor responses compared with sex-matched Lewis, and a temporal decline (all $P<0.05$, ANOVA) in both parameters was also seen in the female LPK. Adult male LPK maintained comparable bradycardic and depressor responses to Lewis; however, a temporal decline ($P = 0.03$, ANOVA) in the reflex depressor response was observed in the LPK. In the Lewis, with the exception of an age-related increase in reflex bradycardic response in the males, no other differences in the reflex bradycardic and depressor responses at 16 Hz were noted.

During the sympathoexcitatory phase, there was an age-related increase ($P<0.05$, ANOVA) in the pressor response in the female LPK. No other differences in HR or MAP responses during this stimulation phase were observed among the groups (Fig. 6.6).

When comparing both males and females, there was a greater ($P = 0.02$, ANOVA) depressor response in the adult male versus female LPK during the sympathoinhibitory phase at 16 Hz (Fig. 6.6), but no other sex effects were noted within each strain during both sympthoinhibitory and sympathoexcitatory phases of vagal afferent stimulation at 16 Hz (Fig. 6.4–6.6).

6.4 Discussion

Further to our previous work demonstrating that male and female LPK animals develop impaired central baroreflex function (Chapters 3 & 4), we demonstrate for the first time that altered central processing of autonomic outflows in the LPK also extends to vagal afferent inputs, and that these deficits similarly parallel the decline in renal function. Our data further show that female LPK develop impaired reflex mediation of both sympathetic and cardiovagal outflows whereas in the males deficits within the sympathetic efferent component of the vagal afferent pathway predominate. Together, this indicates that in CKD, impaired central processing of sympathetic and vagal outflows to the heart and vasculature can be driven by pathways that are independent of the baroreflex circuit, and may arise due to sex-dependent deterioration in the central component evoking the vagal afferent reflexes. An inability to adequately suppress RSNA and buffer changes in HR in the LPK may therefore play a role in sustaining hypertension in this model.

Direct stimulation of the vagal afferent eliminates the confounding effects related to peripheral stimulation of the cardiovascular chemosensitive and mechanosensitive receptors (Merrill et al., 1999). A limitation, however, is the inability to ascribe differences in the output responses to a particular vagal reflex as the afferents activated by electrical stimulation of the vagus are varied. Stimulation of the vagal afferents at 1–8 Hz in rats is purported to selectively activate unmyelinated C-fibres, contributing to reflex sympathoinhibition, bradycardia and hypotension (Merrill et al., 1999, Neahring et al., 1995, Oberg and Thoren, 1973). Higher stimulation frequency presumably engages myelinated A-fibres in the vagus nerve and therefore produces an additional sympathoexcitatory phase (Merrill et al., 1999, Oberg and Thoren, 1973, Sun and Guyenet, 1987). By replicating these effects in the Lewis and LPK rats, we were able to identify fundamental differences in the processing of these two separate pathways.

In our experiments, we discount the possibility that intact baroreceptor afferent fibres may have buffered reflex falls in SNA, HR and MAP in response to the stimulation of the vagal afferents and that barodenervation would have markedly enhanced reflex responses. This is mainly because (1) limiting the duration of electrical stimulation to 5 seconds markedly minimises buffering of the reflex

by intact baroreceptor afferent fibres (Salgado et al., 2007); (2) dysfunctional baroreflexes in the LPK (Harrison et al., 2010, Hildreth et al., 2013b, Chapter 3, Chapter 4) would anyhow render any buffering effects offered by intact baroreceptor afferent neurons less effective; and (3) regardless of the presence of buffering nerves, differences in the response variables measured were readily identifiable between the groups.

Inhibitory responses to vagal afferent stimulation

In the LPK, the central processing of vagal afferent input was evidently deteriorating with age yielding a reduced ability to properly restrain SNA and/or maintain optimal HR and BP control in both males and females. When RSNA was normalised to 100%, reflex sympathoinhibitory responses to vagal afferent stimulation were attenuated in the juvenile male and female LPK. We do not believe that this is reflective of a deficit in central regulation of sympathetic outflow at this age, as similar changes in RSNA (μV) were able to be evoked in juvenile Lewis and LPK, suggesting that RSNA (%) data could have been biased by the inherently higher RSNA baseline in the LPK. Furthermore, we observed enhanced bradycardic responses in the juvenile LPK, suggesting that central mediation of vagal efferent outflow is not only intact at this age, but possibly upregulated, driving enhanced depressor responses at least in the females. These observations are consistent with our previous findings of intact and/or enhanced central processing of baroreceptor afferent input in the juvenile male and female LPK (Chapter 3 & 4), reaffirming a lack of a central deficit in the reflex regulation of autonomic outflows at this age.

Stimulation of the vagal afferent pathway in the adult LPK evoked smaller inhibitions of RSNA. We believe this is reflective of a reduced functionality of the reflex at this age, as there was no age-related increase in RSNA that could bias the data, sympthoinhibitory responses to vagal afferent stimulation were reduced when RSNA was expressed in both % and μV units, and an age-related decline in the LPK was evident. The blunted sympthoinhibitory responses in adult female LPK were also associated with diminished bradycardia, suggesting that, in the female LPK, impaired central processing of vagal afferent input does not only impact reflex regulation of SNA but also cardiac vagal outflow. This observation is consistent with our previous finding of impaired central mediation of sympathetic and vagal outflows evoked through activation of the baroreceptor afferent fibres in the female LPK (Chapter 4). In adult male LPK, on the other hand, a blunted bradycardic response was not evident and only a temporal decline in the depressor response, which is likely driven by the age-related attenuation in the reflex mediation of sympathetic vasomotor tone, was seen. This indicates that in adult male LPK, unlike females, baroreceptor-independent reflex regulation of sympathetic outflow, but not cardiac vagal outflow, is impaired. This contrasts with our previous findings in the male LPK, where impaired central processing of baroreceptor afferent input was associated with altered reflex regulation of both sympathetic and parasympathetic outflows (Chapter 3), suggesting that impaired cardiac vagal

outflow observed in males (Harrison et al., 2010, Hildreth et al., 2013) does not arise from deficits within the vagal afferent pathway.

Interestingly, reflex sympathoinhibitory responses (μV) to vagal afferent stimulation in the juvenile animals were always greater in the female sex of both strains, reflecting a sexual dimorphism in the central regulation of sympathetic outflow mediated by this reflex at this age. This data is in keeping with studies reporting greater reflex attenuation of SNA in normotensive and hypertensive females compared with males (Hogarth et al., 2007b, Hogarth et al., 2007a), suggesting that, at least during the early course of CKD, these effects may promote a more effective buffering action on SNA in the females. In adult female LPK, by contrast, stimulation of the vagal afferents evoked comparable sympathetic responses to males, yet smaller reflex bradycardic and depressor responses were seen. This indicates that in adulthood, the enhanced ability of the female LPK to restrain SNA is lost, which together with altered reflex regulation of HR may result in an impaired ability to effectively regulate circulatory function. Specific to this pathway, it appears that impaired central mediation of sympathetic outflow alone, as seen in the males, is insufficient to impact reflex control of BP, and that abnormal sympathetic and vagal components are a prerequisite for altered BP homeostasis in CKD. Alternatively, vagal afferent reflexes may differentially regulate SNA to different vascular beds (Victor et al., 1989) and, while reflex control of RSNA is impaired, intact reflex regulation of other sympathetic outflows may underlie the unaltered BP responses in the male. Of note, the pattern of autonomic deficits we report here compares very closely with those we describe previously within the baroreflex arc (Chapters 3 & 4). This may be due to the fact that the intramedullary neurocircuitry of the cardiovagal and sympathetic components of the baroreflex and C-fibre vagal afferent pathways are similar (Kashihara, 2009, Lee et al., 1972, Sun and Guyenet, 1987, Verberne and Guyenet, 1992). Further studies are required to identify the key medullary nuclei that may be driving altered central processing of vagal afferent input in CKD.

Excitatory responses to vagal afferent stimulation

It is unknown whether impaired reflex SNA and HR responses are due to elevated central excitatory drive or a reduction in the activation of inhibitory pathways. Nonetheless, the patterns of autonomic deficits in the LPK we describe here may provide clues for sources of disrupted autonomic control. Although the sympthoinhibitory responses were markedly blunted in the LPK by 12 weeks of age, the sympathoexcitation evoked by high-frequency stimulation of the vagal afferent fibres at 16 Hz was not. Though peak increases in RSNA were similar in the LPK and Lewis, total nerve activity expressed as AUC was significantly greater, suggesting a more sustained influence of sympathetic activation over the vasculature in the LPK. Interestingly, the reflex sympathoexcitation in the adult female LPK contributed to a significant pressor effect that was not apparent in the male. It is unlikely that this enhanced pressor response in the females was mediated through the heart, owing to the fact

that HR responses at 16 Hz did not differ. In the males, however, the lack of a significant pressor response to high frequency stimulation may be due to sympathetic outflows to other vascular beds not responding in a similar fashion.

Central mechanisms underlying sympathetic responses are anatomically distinct, in such that sympathoinhibitory vagal reflexes are initiated by activation of the NTS and lead to GABAergic inhibition of the RVLM to reduce SNA (Sun and Guyenet, 1987, Verberne and Guyenet, 1992), while sympathoactivation evoked by stimulation of vagal afferent nerves, which is also initiated in the NTS, is produced by glutamatergic activation of the RVLM and withdrawal of GABAergic inhibition (Sun and Guyenet, 1987). Specific to this reflex arc, it is therefore possible that the sympathoexcitatory pathways evoked by glutamatergic activation of the RVLM are upregulated in the LPK, while impaired sympathoinhibitory responses are the result of diminished GABAergic inhibition of the RVLM, contributing to a dominating sympathoexcitatory drive in the LPK. Importantly, a lack of an age-related increase in the sympathoexcitatory component of vagal afferent stimulation in the LPK could suggest an inability to drive any further increases in SNA (ceiling effect) once an elevated adrenergic drive is developed, as described in the ovine heart failure model (Ramchandra et al., 2009a). These findings may contribute to the maintained level of sympathetic overactivity observed in the juvenile and adult LPK model of CKD.

In summary, our study identifies deficits in the central processing of vagal afferent input as a feature of autonomic dysfunction in CKD. This observation, together with our previous demonstration of altered baroreflex mechanisms in the LPK (Chapters 3 & 4), would suggest that impaired autonomic control of cardiovascular function in CKD is not solely contributed to by baroreceptor-dependent mechanisms, but can also be evoked by abnormalities within other reflex pathways.

6.5 Perspectives and significance

Autonomic dysfunction is a major complication of CKD, likely contributing to the increased incidence of cardiovascular mortality in this patient population (Cashion et al., 2000, Dursun et al., 2004, Rubinger et al., 2009), and hence necessitating a better understanding of the neural mechanisms altering sympathetic and parasympathetic tone. Our data provides direct insight into the role of the vagal afferent outflow in the regulation of cardiovascular function in CKD, and how defects within the central processing pathways of this reflex may underpin differential deteriorations of autonomic function in men and women. Our work indicates that the critical involvement of this central control mechanism in the pathogenesis of autonomic dysfunction in CKD should be considered when developing novel therapeutic strategies targeting altered autonomic cardiovascular control in both males and females.

Table 6.1: Baseline parameters in juvenile (7–8 weeks old) and adult (12–13 weeks old) Lewis and Lewis Polycystic Kidney (LPK) rats of either sex

Group	Juvenile		Adult		Two-way ANOVA adjusted *P* value	
	Lewis	LPK	Lewis	LPK	Strain	Age
Parameter						
Males *(n)*	*7*	*6*	*8*	*6*		
SBP (mmHg)	121 ± 4	165 ± 3*	130 ± 4	178 ± 6*	<0.0001	0.0205
DBP (mmHg)	65 ± 3	79 ± 4*	62 ± 3	68 ± 5	0.0155	0.0738
PP (mmHg)	55 ± 4	87 ± 6*	68 ± 3	110 ± 7*†	<0.0001	0.0014
MAP (mmHg)	87 ± 3	110 ± 3*	84 ± 3	111 ± 7*	<0.0001	0.7706
HR (bpm)	369 ± 11	430 ± 15*	344 ± 20	400 ± 12*	0.0010	0.0938
RSNA (μV)	3.1 ± 0.5	7.2 ± 1.7*	2.7 ± 0.4	5.2 ± 1.0*	0.0007	0.3367
Females (*n*)	*5*	*4*	*5*	*4*		
SBP (mmHg)	119 ± 3	174 ± 6*	127 ± 3	184 ± 5*	<0.0001	0.0703
DBP (mmHg)	60 ± 3	75 ± 4*	56 ± 3	69 ± 4*	0.0002	0.1072
PP (mmHg)	59 ± 3	99 ± 6*	72 ± 2	115 ± 4*†	<0.0001	0.0019
MAP (mmHg)	84 ± 3	116 ± 4*	82 ± 3	110 ± 4*	<0.0001	0.3349
HR (bpm)	352 ± 13	384 ± 11	346 ± 13	366 ± 5	0.0362	0.2999
RSNA (μV)	4.5 ± 0.9	9.8 ± 1.6*	3.6 ± 0.8	8.8 ± 1.0*	0.0001	0.4431

BW, body weight; SBP, systolic blood pressure; DBP, diastolic blood pressure; PP, pulse pressure; MAP, mean arterial pressure; HR, heart rate; and RSNA, renal sympathetic nerve activity.
Results are expressed as mean ± SEM.
*P<0.05 vs. age-matched Lewis.
†P<0.05 vs. strain-matched juvenile rat.
n represents the minimum number in each group.

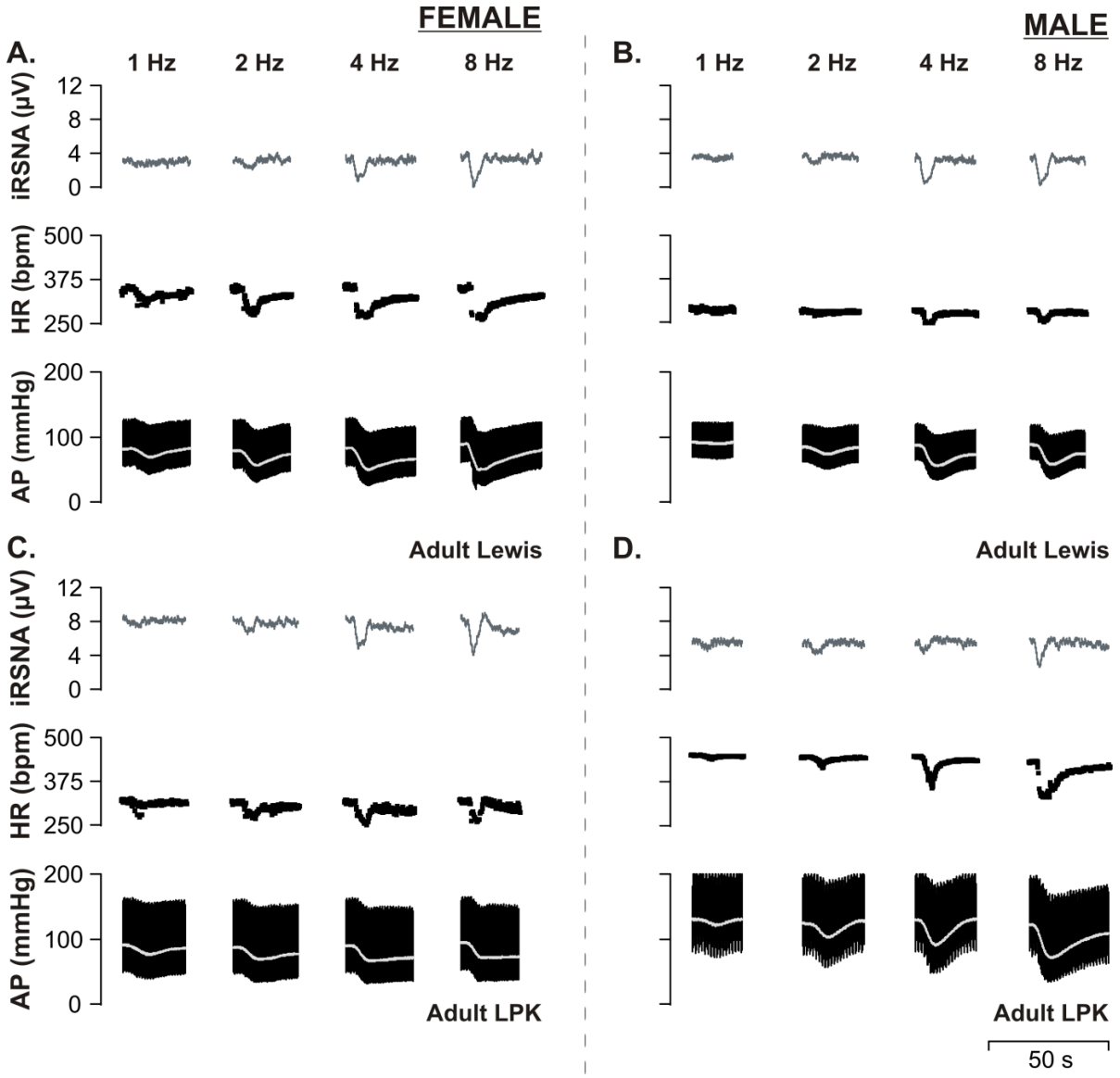

Figure 6.1: Representative data traces, illustrating responses of integrated renal sympathetic nerve activity (iRSNA), heart rate (HR) and arterial pressure (AP) to direct electrical stimulation of the vagal afferent nerve in adult (12–13 weeks old) Lewis and Lewis Polycystic Kidney (LPK) rats of either sex. bpm: beats per minute.

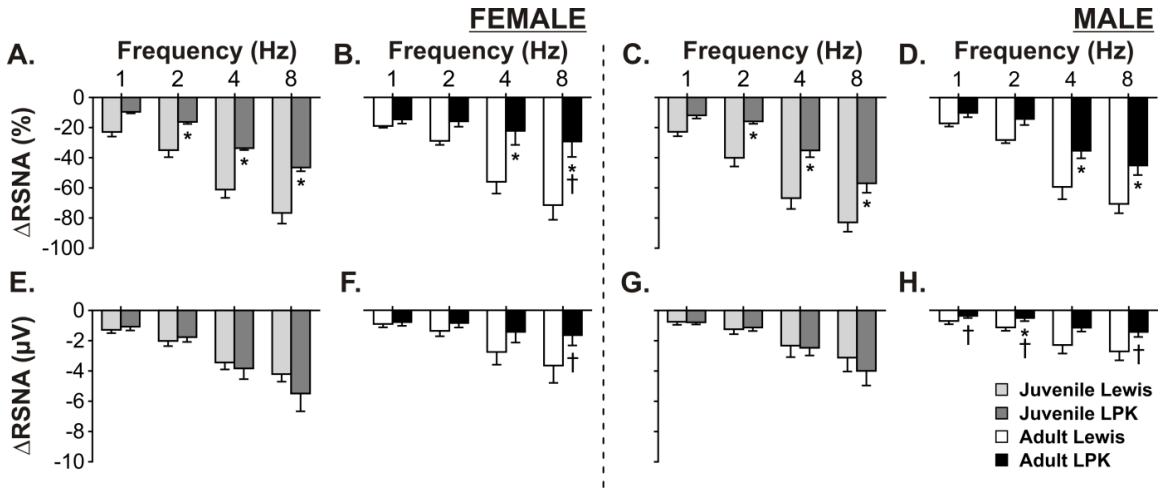

Figure 6.2: Effect of increasing frequency of vagal afferent nerve stimulation on renal sympathetic nerve activity (RSNA: %, A–D and μV, E–H) in juvenile (7–8 weeks old; first and third columns) and adult (12–13 weeks old; second and fourth columns) Lewis and Lewis Polycystic Kidney (LPK) rats of either sex (female, left 2 panels & male, right 2 panels), showing strain and age differences among groups. A reduction in RSNA was observed in all experimental groups. Results are expressed as mean ± SEM. $^{*}P<0.05$ vs. age-matched Lewis and $^{\dagger}P<0.05$ vs. strain-matched juvenile rat. Overall ANOVA strain, age and sex effect is reported within the respective result section. *n*/group: juvenile female Lewis = 9, juvenile female LPK = 8, adult female Lewis = 7, adult female LPK = 6, juvenile male Lewis = 8, juvenile male LPK = 6, adult male Lewis = 7 and adult male LPK = 6. bpm: beats per minute.

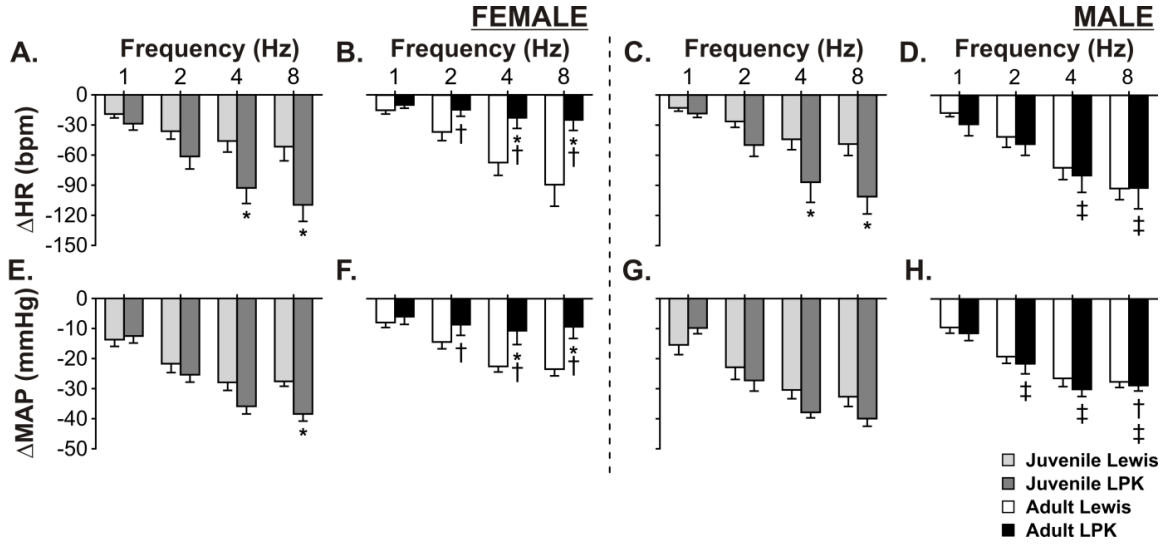

Figure 6.3: Effect of increasing frequency of vagal afferent nerve stimulation on heart rate (HR; A–D) and mean arterial pressure (MAP; E–H) in juvenile (7–8 weeks old; first and third columns) and adult (12–13 weeks old; second and fourth columns) Lewis and Lewis Polycystic Kidney (LPK) rats of either sex (female, left 2 panels & male, right 2 panels), showing strain, age and sex differences among groups. A reduction in HR and MAP was observed in all experimental groups. Results are expressed as mean ± SEM. $^{*}P<0.05$ vs. age-matched Lewis, $^{\dagger}P<0.05$ vs. strain-matched juvenile rat and $^{\ddagger}P<0.05$ vs. strain- and age-matched female rat. Overall ANOVA strain, age and sex effect is reported within the respective result section. *n*/group: juvenile female Lewis = 9, juvenile female LPK = 9, adult female Lewis = 8, adult female LPK = 6, juvenile male Lewis = 8, juvenile male LPK = 7, adult male Lewis = 8 and adult male LPK = 6. bpm: beats per minute.

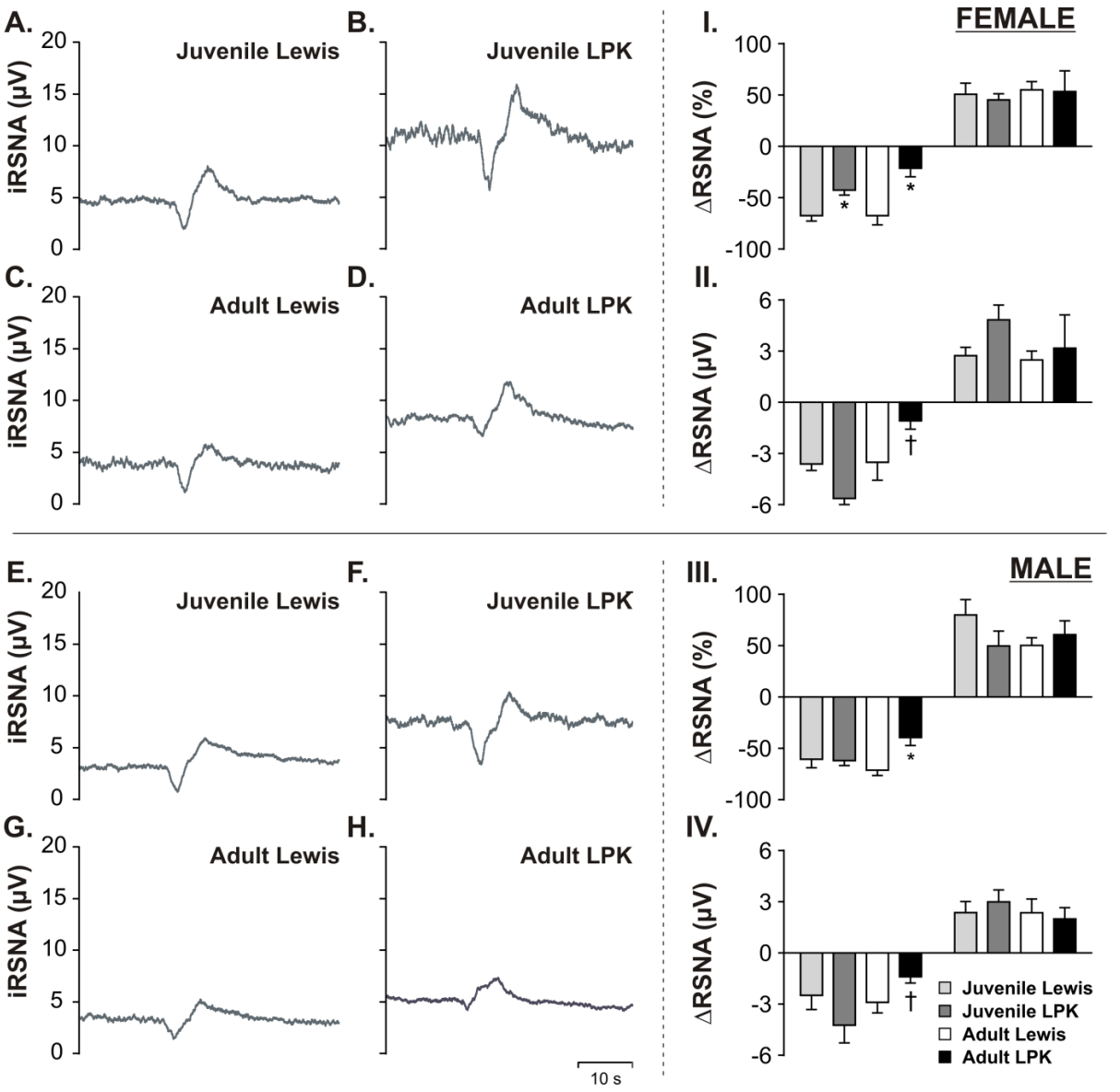

Figure 6.4: Representative data traces (A–H, left panels), illustrating the biphasic renal sympthoinhibitory and sympathoexcitatory responses to vagal afferent nerve stimulation at 16 Hz in female (upper left panels) and male (bottom left panels) juvenile (7–8 weeks old) and adult (12–13 weeks old) Lewis and Lewis Polycystic Kidney (LPK) rats. Right panels (I–IV) present group data (percentage and microvolt change from baseline) characterising the renal sympathetic nerve activity (RSNA) response to a 16 Hz stimulation of the vagal afferents in females (upper panels) and males (lower panels). Negative scale denotes sympathoinhibition while positive scale denotes sympathoexcitation. Results are expressed as mean ± SEM. $^{*}P<0.05$ vs. age-matched Lewis and $^{\dagger}P<0.05$ vs. strain-matched juvenile rat. Overall ANOVA strain, age and sex effect is reported within the respective result section. *n*/group: juvenile female Lewis = 9, juvenile female LPK = 8, adult female Lewis = 8, adult female LPK = 6, juvenile male Lewis = 8, juvenile male LPK = 6, adult male Lewis = 7 and adult male LPK = 6. iRSNA: integrated renal sympathetic nerve activity.

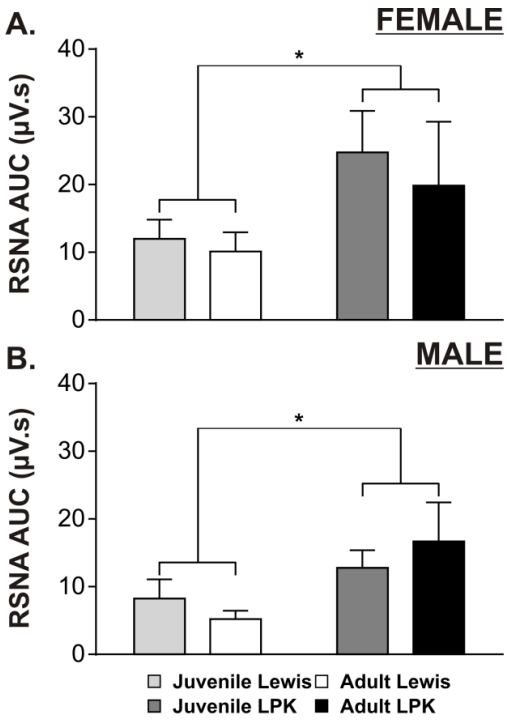

Figure 6.5: Renal sympathetic nerve activity (RSNA) expressed as area under the integrated RSNA curve (AUC) in female (upper panel) and male (bottom panel) juvenile (7–8 weeks old) and adult (12–13 weeks old) Lewis and Lewis Polycystic Kidney (LPK) rats during the sympathoexcitatory phases of vagal afferent nerve stimulation at 16 Hz. Results are expressed as mean ± SEM. $^{*}P<0.05$, overall two-way ANOVA strain effect within indicated sex. *n*/group: juvenile female Lewis = 9, juvenile female LPK = 8, adult female Lewis = 8, adult female LPK = 6, juvenile male Lewis = 6, juvenile male LPK = 7, adult male Lewis = 7 and adult male LPK = 6.

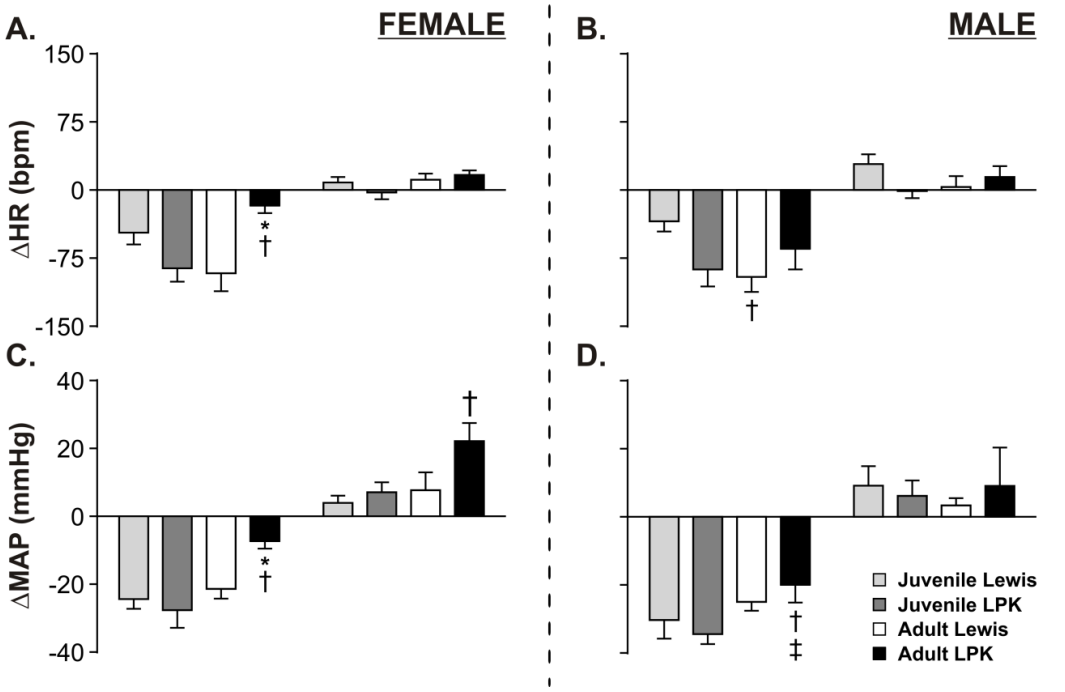

Figure 6.6: Heart rate (HR) and mean arterial pressure (MAP) responses in female (left panels) and male (right panels) juvenile (7–8 weeks old) and adult (12–13 weeks old) Lewis and Lewis Polycystic Kidney (LPK) rats during the sympthoinhibitory and sympathoexcitatory phases of vagal afferent nerve stimulation at 16 Hz. Negative scale denotes bradycardia and hypotension while positive scale denotes tachycardia and hypertension. Results are expressed as mean ± SEM. $^{*}P<0.05$ vs. age-matched Lewis, $^{\dagger}P<0.05$ vs. strain-matched juvenile rat and $^{\ddagger}P<0.05$ vs. strain- and age-matched female rat. Overall ANOVA strain, age and sex effect is reported within the respective result section. *n*/group: juvenile female Lewis = 9, juvenile female LPK = 9, adult female Lewis = 9, adult female LPK = 5, juvenile male Lewis = 9, juvenile male LPK = 7, adult male Lewis = 8 and adult male LPK = 6.

7 Direct Conscious Telemetry Recordings Demonstrate Increased Renal Sympathetic Nerve Activity in Rats with Chronic Kidney Disease

Ibrahim M. Salman[1], Divya S. Kandukuri[1], Cara M. Hildreth[1], Joanna L. Harrison[2] and Jacqueline K. Phillips[1]

[1] *Australian School of Advanced Medicine, Macquarie University, Sydney, NSW, Australia*

[2] *School of Veterinary and Life Sciences, Murdoch University, Perth, WA, Australia*

This chapter is currently in preparation for publication.

Abstract

Chronic kidney disease (CKD) is associated with sympathetic hyperactivity and impaired reflex responses, however direct evidence demonstrating these features of autonomic dysfunction in conscious animals is still lacking. We therefore aimed to measure renal sympathetic nerve activity (RSNA) and mean arterial pressure (MAP) using telemetry based recordings in a rat model of CKD, the Lewis Polycystic Kidney (LPK) rat, and assess responses to chemoreflex activation and acute stress. Adult male LPK and Lewis control animals (10–11 weeks old, total n = 16) were instrumented for telemetric recording of RSNA and MAP. Following recovery, resting RSNA and MAP were recorded (5 minutes every 15 minutes for a 3-hour period during the day, over 48 hours), sympathetic and heamodynamic responses to acute stress (open-field exposure for 40 minutes) and both peripheral and central chemoreflex activation (hypoxia: 10% O_2 and hypercapnia: 7% CO_2, respectively) were tested, and renal function was measured. The quality of the nerve signal was evidenced by pulse modulation of RSNA and/or silencing of nerve activity following ganglionic blockade with hexamethonium (20 mg/kg s.c.). At 12–13 weeks of age, LPK rats had higher resting RSNA (1.2 ± 0.1 vs. 0.6 ± 0.1 µV, P<0.05) and MAP (151 ± 8 vs. 97 ± 2 mmHg, P<0.05) compared to Lewis. MAP positively correlated with RSNA (r = 0.66, P = 0.014) and negatively with urinary creatinine (r = -0.80, P = 0.002). RSNA and MAP responses to activation of the peripheral and central chemoreflex and an open-field stress were reduced (all P<0.05) in the LPK relative to the Lewis. This is the first description of dual conscious telemetry recording of RSNA and MAP in a genetic rodent model of CKD. Conscious LPK show sustained elevated RSNA, which is likely a key contributor to the marked hypertension and to the progressive renal dysfunction in this model. Our demonstration of attenuated RSNA and MAP responses to both chemoreflex activation and acute stress in the LPK indicates possible deficits in the neural processing of autonomic outflows evoked by these sympathoexcitatory pathways.

Keywords: chemoreflex, open-field stress, renal sympathetic nerve activity, hypertension, chronic kidney disease, conscious rat

7.1 Introduction

Sympathetic nervous system (SNS) hyperactivity is a hallmark of chronic kidney disease (CKD), contributing to hypertension, renal disease progression, and consequent cardiovascular morbidity and mortality in this patient population (Grassi et al., 2011a, Penne et al., 2009). Plasma catecholamine levels (Grassi et al., 2011a, Zoccali et al., 2002) and local noradrenaline spillover rate (Schlaich et al., 2013) are drastically increased, and direct measurements of muscle sympathetic nerve activity (SNA) reveal elevated tonic levels (Grassi et al., 2011a, Neumann et al., 2007, Schlaich et al., 2013). Despite various approaches to quantify sympathetic activity in humans and

experimental animals, most measurements share common limitations. Measurement of plasma catecholamine levels does not accurately reflect increases in sympathetic activity when the severity of the disease is much less pronounced (Grassi et al., 2011a). Short-term measurements of SNA may not necessarily reflect sustained levels of adrenergic drive. Interpretation of SNA data acquired from acute recordings in unconscious animals may unavoidably be confounded by the effect of anaesthetic (Shimokawa et al., 1998). Use of pharmacological agents to block the autonomic nervous system and spectral analysis of blood pressure (BP) variability, though commonly used to estimate sympathetic tone in humans and experimental animals, reveal global but not discrete contributions of organ-specific sympathetic nerve beds.

Knowing the baseline level of SNA to specific target organ can be of critical importance. For example, SNA to the kidney has the potential to have a much larger influence on long-term levels of arterial BP in CKD, given the role of renal SNA (RSNA) in not only altering blood flow, but also regulating renin secretion and salt and water reabsorption (Johns et al., 2011). This notion is supported by some recent evidence showing that renal denervation, using a catheter-based approach that disrupts renal sympathetic nerves in the adventitia of the renal arteries, can mitigate sympathetic hyperactivity in CKD patients, contributing to not only reductions in BP but also improving renal haemodynamics, enhancing glomerular filtration rate (GFR) and reducing albuminuria (Hering et al., 2012, Kiuchi et al., 2013, Schlaich et al., 2013). However, our current knowledge of the ongoing levels of RSNA in CKD is still limited, which can perhaps explain why issues pertaining to potential efficacy of renal denervation remain unresolved. This therefore calls for better experimental approaches to enable understanding of modulation of SNA in CKD.

The Lewis Polycystic Kidney (LPK) rat is a model of nephronophthisis, a form of autosomal recessive cystic kidney disease arising from a spontaneous mutation in the *Nek8* gene (McCooke et al., 2012). We have previously demonstrated several indirect modes of evidence consistent with elevated sympathetic drive in the LPK including enhanced hypotensive responses to ganglionic blockade (Phillips et al., 2007), exaggerated bradycardic responses to β_1-adrenoceptor blockade (Harrison et al., 2010) and increased low-frequency power of systolic blood pressure variability (Harrison et al., 2010, Hildreth et al., 2013b). Most recently, we have been able to show that direct recordings of RSNA in anaesthetised animals display elevated baseline tonic levels (Chapters 3 & 4). Given the sympathoexcitatory effects of some anaesthetics (Shimokawa et al., 1998), which may become particularly pronounced in the LPK (Hildreth et al., 2013a), it remains undetermined whether elevated levels of RSNA are sustained in the conscious LPK model of CKD. Accordingly, a key objective of the present study was to record RSNA in conscious unrestrained animals using telemetry, examining the hypothesis that elevated RSNA is a key pathological feature of CKD. We also sought to identify if altered sympathetic activity in the conscious LPK is associated with deficits in regulatory pathways known to impact autonomic neuroregulation of the cardiovascular system including the chemoreceptor reflex and stress inputs. The role of the chemoreceptors in determining sympathetic nerve discharge in

CKD is incompletely understood, with only two reports suggesting tonic activation of excitatory chemoreceptor afferents as one driver of elevated SNA in CKD patients (Despas et al., 2009, Hering et al., 2007). Accordingly, our second aim was to assess RSNA and BP responses to central (hypercapnia) and peripheral (hypoxia) chemoreceptor stimulation in the conscious LPK, assessing the hypothesis that sympathetic activation in the LPK is associated with chemoreflex dysregulation. Another potential contributor to sympathoexcitation in CKD is altered reactivity to or recovery from stress, as in other hypertensive models exaggerated sympathetic responses to acute stress have been reported (D'Angelo et al., 2006, DiBona and Jones, 1995, Head and Burke, 2004). In CKD variable reports of unchanged (Agarwal et al., 1991) or exaggerated (Seliger et al., 2008) haemodynamic response to mental stressors have been previously documented. Therefore, our third aim was to assess sympathetic and BP reactivity to acute stress in the conscious LPK.

7.2 Methods

7.2.1 Animals

Male Lewis (n = 9) and LPK (n = 7) rats were purchased from the Animal Resource Centre (ARC) in Western Australia and housed in the Animal House Facility of Macquarie University. Rats were habituated for at least a week prior to the conduction of any experimental procedure. All animals were kept under a 12-hour light/dark cycle and received a standard pellet diet and water *ad libitum*. All studies were approved by the Animal Ethics committee of Macquarie University and carried out in accordance with the Australian Code of Practice for the Care and Use of Animals for Scientific Purposes.

7.2.2 Radiotelemetry probe implantation

At 10–11 weeks of age, rats were prepared for placement of a telemeter equipped with nerve recording electrodes and arterial catheter (Model TR46SP, Telemetry Research, Auckland, New Zealand) using sterile technique. Animals were anaesthetised with isoflurane (I.S.O. inhalation anaesthetic, Veterinary companies of Australia, 5% in 100% O_2 for induction and 1–3% for maintenance) and pre-operative pain relief [carprofen (Carprieve®,Norbrook laboratories, UK), 2.5 mg/kg s.c.] and antibiotics [cephazolin (DBL Cephazolin sodium®,Hospira Pty Ltd, Australia), 55 mg/kg i.m.] were administered. An abdominal and dorsal skin incision was made and the nerve recording electrode subcutaneously tunnelled from the abdominal through to dorsal incision site. The left kidney was exposed retroperitoneally and a 2-mm portion of the renal nerve, coursing between the abdominal aorta and left renal artery, isolated. The recording electrode was anchored to the aorta and renal artery using non-absorbale 7/0 prolene sutures and the renal nerve gently placed on the electrode and embedded in a silicone elastomer (Kwik-sil®, World Precision Instruments, Sarasota, FL, USA) (Muntzel et al., 2012). The ground electrode was sutured to the flank muscles just exterior to the dorsal incision site and the dorsal incision sutured closed. The BP catheter was placed by one of two methods depending

upon catheter type. Either, the peritoneal cavity was exposed and the catheter (Millar type) was inserted into the abdominal aorta, such that the tip of the catheter was distal to the renal artery. The catheter was secured in place using a plastic mesh (Telemetry Research) and cyanoacrylate cement (Histoacryl®, B Braun, Australia), and lidocaine (1%, Pfizer, Australia) applied to induce vasodilation and improve hindlimb blood flow. Alternatively, the BP catheter (fluid-filled type) was placed into the femoral artery with the probe body placed within the peritoneal cavity as we have described previously (Hildreth et al., 2013b). Supplemental fluids were provided (saline, 6 ml/kg i.p.) and the peritoneal cavity closed. All skin incisions were closed using wound closure clips. Following cessation of anaesthesia, post-operative pain relief was provided [buprenorphine (Temgesic®, Reckitt Benckiser, Australia), 50 µg/kg s.c.]. Rats were allowed to recover for at least one week in order to re-establish circadian rhythms (Hildreth et al., 2013b). Pain relief (carprofen, 2.5 mg/kg, s.c. and/or buprenorphine, 50 µg/kg s.c.) and supplemental fluid therapy (up to 60ml/kg/day 0.9% saline and/or 5% glucose s.c.) were administered as required.

7.2.3 Experimental protocol

All protocols were carried out when animals were aged between 12–13 weeks over a ~7-day period. BP signal was sampled at a minimum of 500 Hz and RSNA at 2 kHz and continuously displayed on Spike 2 (v7, CED Ltd., Cambridge, UK). The original RSNA signal was amplified, filtered between 50–2000 Hz, full-wave rectified and integrated (1 second smoothing constant). All experiments were conducted between 9:00 AM and 5:00 PM. Each rat underwent no more than one study per day. Resting data was collected at the beginning of the experimental period. Chemoreflex and stress response experiments (see below) were performed in random order. Ganglionic blockade was the last protocol undertaken.

Resting data: RSNA and BP were recorded for 5 minutes every 15 minutes for a 3-hour period during the day, over two consecutive days. No experimental intervention was undertaken on these days.

Chemoreceptor Reflex: Animals were placed in a custom-made plexiglass chamber to which they were previously acclimated. The chamber was initially filled with medical grade air [21% O_2 balance N_2 (BOC Ltd, Australia), 0.5–1 L/minute] and O_2 and CO_2 levels continuously monitored (CapStar-100 CO_2 analyser®, CWE Inc., Ardmore, PA, USA and Gas analyser®, ADInstruments Pty Ltd, Australia). Once the animal was resting quietly, as indicated by stable measurements of MAP and RSNA, a 5-minute baseline recording was obtained. Following this, the chamber was flushed with either a hypoxic (10% O_2 balance N_2, BOC Ltd,) or hypercapnic (7% CO_2 balance O_2, BOC Ltd,) gas mixture to activate the peripheral and central chemoreceptors, respectively. Approximately 15 seconds were required to reach target concentration of O_2 (10%) and CO_2 (7%) in the chamber. Animals were exposed to these gas mixtures for no more than 5 minutes, following which the chamber was flushed with medical grade air. Following a 10–20 minutes recovery period, another 5-minute baseline recording was obtained the chamber was filled with the alternate gaseous mixture and RSNA and

MAP recorded for another period of 5 minutes. The order of gas exposure was randomised and at the end of the experiment, the rat was returned to its home cage.

Open-field stress: Baseline levels of MAP and RSNA were recorded for 10 minutes while the animal was in its home cage. The animal was then gently transferred into a brightly lit open field (~90 cm diameter circular container with 40 cm wall) and MAP and RSNA recorded for 40 minutes. The animal was then returned to its home cage.

Ganglionic blockade: Baseline MAP and RSNA was recorded for 5 minutes while the animal was in its home cage. The ganglionic blocker, hexamethonium (20 mg/kg s.c., Sigma Aldrich, Australia) was then administered and RSNA and MAP recorded for at least 30 minutes.

7.2.4 Assessment of kidney function

Animals were individually held in metabolic cages (Tecniplast, Australia) for at least 4 hours to collect urine samples. Urine was then centrifuged at 3000 rpm for 5 minutes and stored at -20^{0}C until further assayed for urinary protein (U_{Pro}) and creatinine (U_{Cr}) using an IDEXX VetLab analyser (IDEXX Laboratories Pty Ltd., NSW, Australia).

7.2.5 Euthanasia

After all protocols had been undertaken, rats were euthanased with an overdose of 60 mg/kg sodium pentobarbital i.v. (Lethabarb Euthanasia®, Virbac Pty Ltd, Australia), and death levels of RSNA were recorded.

7.2.6 Data analysis

All data was analysed offline using Spike 2 software and GraphPad Prism (GraphPad Prism software v6 Inc., La Jolla, CA, USA). Background nerve activity acquired following ganglionic blockade was subtracted from all RSNA recordings. The level of nerve activity following ganglionic blockade was compared against that obtained following euthanasia and the quality of nerve activity verified by assessing the pulse modulation of RSNA (Fig. 7.1) as described previously (Guild et al., 2012, Stocker and Muntzel, 2013).

Resting data: Resting (undisturbed animals in home cage) RSNA and MAP recordings were averaged over the two, 3-hour daytime recording periods to create one RSNA and MAP estimate per animal.

Chemoreflex data: In order to temporally capture changes in the chemoreflex response accurately, RSNA and MAP were averaged into 1-minute bins. The level of RSNA, determined during the 1 minute period immediately prior to exposure to either hypoxic or hypercapnic gas mixture was set as 100%. Maximum changes in RSNA (μV) relative to the 1 minute baseline were also measured. Changes in MAP were expressed relative to the level of MAP 1 minute prior to chemoreflex activation.

Open-field stress: In order to temporally capture changes during the open-field stress accurately, RSNA and MAP were averaged into 2-minute bins. When present, movement artefacts on the RSNA signal acquired during the stress response were excluded from the analysis. The averaged level of RSNA determined during the 2 minutes immediately prior to exposure to the open-field was set as 100% and changes in MAP expressed relative to the level of MAP over that period. Maximum changes in RSNA (μV) relative to the 2 minutes baseline were also measured.

Ganglionic blockade: Maximum RSNA and MAP responses to hexamethonium (20 mg/kg s.c.) were measured (level and time to peak) relative to a 5-minute baseline of these variables. The RSNA baseline data recorded after ganglionic blockade was subsequently compared to the initial resting data to assess stability of RSNA recordings over the experimental period.

Correlation of renal function and autonomic function: Correlation analysis was performed using the 3-hour daytime baseline level of RSNA and MAP and measures of renal function [U_{Pro}, U_{Cr} and urinary protein:creatinine ratio (UPC)]. To determine correlations between MAP, RSNA and urinalysis data, linear regression modelling was undertaken using IBM Statistical Package for the Social Sciences (SPSS; v20, Chicago, Illinois USA). Mean arterial pressure was set as the dependent variable and with RSNA, urinary protein, creatinine and UPC as the independent variables, using a stepwise selection method of entry and listwise exclusion of missing values. Pearson correlation coefficients (r) were derived from the model using a one-tailed test for significance ($P \leq 0.05$) and the adjusted R^2 value and beta standardized regression coefficients (beta) value are provided as an indicator of the relative influence of the predictor variable in the regression model.

7.2.7 Statistical analysis

All data are expressed as mean ± standard error of the mean (SEM). Statistical analysis was performed using GraphPad Prism software (GraphPad Prism software v6 Inc., La Jolla, CA, USA). A Brown-Forsythe test was used to determine if there were any differences in the variance, and if so, the data was log-transformed before statistical analysis. Baseline levels of MAP and RSNA, renal function, maximum RSNA (μV) responses to chemoreflex activation and open-field exposure, responses to ganglionic blockade and stability of RSNA were analysed between strains using two-tailed Student's t-test. The MAP and RSNA (%) responses to chemoreflex activation or exposure to the open-field paradigm were also analysed using a two-way ANOVA, with strain and time as variables. If a strain and/or time difference was noted, a Bonferroni's post-hoc test was performed. When a time effect was noted, the post-hoc was performed within each strain relative to the initial baseline recording of RSNA or MAP. Significance was defined as $P \leq 0.05$.

7.3 Results

7.3.1 Characteristic of the Lewis and LPK rats

Water intake, urine output, U_{Pro}, UPC and resting RSNA and MAP were significantly higher in the LPK versus Lewis (Table 7.1). In contrast, U_{Cr} excretion levels were significantly lower in the LPK compared with Lewis (Table 7.1). Pearson correlation analysis showed a significant positive correlation between MAP and RSNA and a significant negative correlation with urinary creatinine (Fig. 7.2). In the regression model however, urinary creatinine was the only significant predictor variable (adjusted $R^2 = 0.483$, $P = 0.003$, beta -0.723).

7.3.2 Responses to chemoreceptor reflex activation

Peripheral chemoreflex activation: A hypoxic challenge evoked a blunted sympathoexcitatory response ($P<0.01$, ANOVA) in the LPK versus Lewis (Fig. 7.3A). When the RSNA response was expressed in microvolts, 10% O_2 significantly increased RSNA to a maximum level at 5 minutes exposure in the Lewis (baseline: 0.5 ± 0.2 μV vs. 5 minutes exposure: 1.7 ± 0.2 μV, $P = 0.003$). In contrast, there was no significant change in RSNA in the LPK compared to baseline (baseline: 1.3 ± 0.3 μV vs. 5 minutes exposure: 2.0 ± 0.6 μV, $P = 0.35$). The MAP response in both the Lewis and LPK was not significantly different to baseline at any time point, but overall, a reduced MAP response in the LPK was observed during the exposure period (Figure 7.3B).

Central chemoreflex activation: A blunted sympathoexcitatory response to hypercapnia ($P<0.001$, ANOVA) was observed in the LPK versus Lewis (Fig. 7.4A). When the sympathetic response was expressed in microvolts, maximal increase was seen at 5 minutes exposure in the Lewis (baseline: 0.5 ± 0.1 μV vs. at 5 minutes exposure: 1.9 ± 0.3 μV, $P = 0.002$) but there was no significant difference to baseline in the LPK (baseline: 1.5 ± 0.4 μV vs. at 5 minutes exposure: 2.2 ± 0.8 μV, $P = 0.463$). Mean arterial pressure demonstrated a weak time × strain interaction in the response to hypercapnia ($P = 0.04$), with time and strain effects also evident (all $P<0.001$). Post hoc analysis revealed a significant increase in MAP 2 minutes following exposure to CO_2 in both Lewis and LPK (Fig. 7.4B). The pressor response persisted (all $P<0.01$) over the entire exposure period in the Lewis, whereas in the LPK the MAP returned to pre-CO_2 exposure levels by time 4 minutes ($P<0.01$ vs. baseline). Accordingly, MAP responses to central chemoreflex activation were overall significantly attenuated in the LPK compared with Lewis (Fig. 7.4B).

7.3.3 Responses to acute open-field stress

In the Lewis, open-field stress evoked a significant increase in RSNA immediately following exposure to the stressor. This effect persisted for 12 minutes before RSNA returned to levels comparable to baseline at 14 minutes after placement in the open-field (Fig. 7.5A). In the LPK, despite a similar trend to the Lewis, RSNA did not significantly increase beyond baseline levels. Consistent with %

RSNA analysis, a peak in evoked change in RSNA (μV) was seen at 2 minutes exposure in the Lewis (baseline: 0.6 ± 0.1 μV vs. at 2 minutes: 2.7 ± 0.6 μV, $P = 0.006$), but in the LPK there was no time point at which RSNA was significantly different to baseline (baseline: 1.4 ± 0.6 vs. at 4 minutes: 3.7 ± 1.2 μV, $P = 0.13$). Accordingly, the RSNA response to open-field stress was significantly reduced in the LPK versus Lewis ($P<0.001$, ANOVA; Fig. 7.5A). The sympathoexcitatory response to acute stress in the Lewis was associated with a sustained increase in MAP for the first 8 minutes of exposure ($P<0.05$) peaking at time 4 minutes (Fig. 7.5B). There was no significant increase in MAP in the LPK animals (Fig. 7.5B).

7.3.4 Responses to ganglionic blockade

Hexamethonium reduced RSNA and MAP in both Lewis (RSNA: 2.1 ± 0.1 vs. 1.5 ± 0.2 μV, MAP: 105 ± 3 vs. 49 ± 4 mmHg, baseline vs. hexamethonium; all $P<0.05$) and LPK (RSNA: 3.0 ± 0.2 vs. 1.6 ± 0.2 μV, MAP: 157 ± 5 vs. 56 ± 6 mmHg, baseline vs. hexamethonium; all $P<0.05$) over comparable time frame (6.5 ± 1.4 vs. 6.8 ± 0.9 minutes, LPK vs. Lewis, respectively; all $P<0.05$). Relatively larger falls in both RSNA and MAP were observed in the LPK compared with Lewis controls (ΔRSNA: -1.4 ± 0.3 vs. -0.6 ± 0.1 μV and ΔMAP: -105 ± 8 vs. -56 ± 3 mmHg, LPK vs. Lewis; all $P<0.05$). RSNA background activity recorded following administration of hexamethonium was comparable to levels recorded following euthanasia (Lewis: 1.5 ± 0.2 vs. 1.3 ± 0.2 μV and LPK: 1.6 ± 0.2 vs. 1.3 ± 0.2 μV, hexamethonium vs. euthanasia; all $P>0.05$).

7.3.5 Stability of RSNA

Viable SNA recorded over a period of approximately 3 weeks was successfully obtained in ~60% (16 out of 26) of telemetered animals. Levels of RSNA recorded under resting conditions following animal surgical recovery at the start of the 7 day experimental period and immediately prior to the final intervention (ganglionic blockade) did not differ significantly in either the Lewis or LPK animals (Lewis: 0.6 ± 0.1 vs. 0.6 ± 0.1 μV and LPK: 1.2 ± 0.1 vs. 1.4 ± 0.3 μV, 1st RSNA vs. 2nd RSNA, all $P>0.05$).

7.4 Discussion

This is the first description of a conscious concurrent telemetric recording of RSNA and BP in a genetic rodent model of CKD. The major novel findings of the present study are: (1) LPK rats have sustained elevated RSNA under conscious conditions; (2) MAP is positively correlated with RSNA, and significantly negatively correlated with urinary creatinine (3) conscious LPK show reduced RSNA and MAP responses to chemoreceptor reflex activation and acute stress, indicating possible deficits in the neural processing of autonomic outflows evoked by these typically sympathoexcitatory pathways. Together, this shows that in CKD, sympathetic overdrive, as assessed by direct conscious recording of

RSNA, is an archetypal feature, likely contributing to the maintained hypertensive state and altered reactivity to reflexogenic and stressful stimuli.

In the present study, we successfully demonstrated our ability to record reliable RSNA over a sustained period in conscious animals, as bursts of RSNA were clearly visible in the resting rats, activity was strongly coupled to the cardiac cycle as evidenced by the pulse modulation of SNA and the signal was effectively eliminated after ganglionic blockade with hexamethonium (Stocker and Muntzel, 2013). Furthermore, despite that fact that the sample size used in this study was relatively small we were able to show a stable level of RSNA over the entire experimental period.

In our study, microvolt measures and percentage change scores were used to report RSNA. It has been suggested that absolute level of SNA in voltage units cannot be compared between animals, as SNA level is dependent upon conditions at the recording site, the number and size of the nerve fibres and the proximity of the active fibres to the electrode (Burke et al., 2011), which increases variability between different nerve recordings. Normalising nerve activity data by setting baseline to 100% and reporting percentage change scores is proposed to avoid any bias that would therefore otherwise arise from between animal differences in recording technique, and allow for significant differences to be detected in smaller groups of rats. This method, however, does not allow for comparison of baseline activity or maximal changes in absolute units (Burke et al., 2011). This has led some to suggest that reporting properties of nerve activity using both normalised responses and raw rectified voltage is extremely valuable (Huber and Schreihofer, 2010). For this purpose, we determined if microvolt measures were in keeping with data expressed as a percentage change. Indeed, data in microvolt units supported our percentage scores and extended beyond that to show CKD-related baseline differences between the animal groups, suggesting that: (1) errors in sampling did not considerably influence group differences; and (2) percentage change of ongoing activity is still a relevant measure even when differences in baseline activity exist.

In the present work, we recorded SNA to the kidney, given the pivotal role of renal innervation in BP regulation (Johns et al., 2011) and the fact that elevated basal RSNA and impaired RSNA baroreflex function were previously identified in the anaesthetised LPK (Chapters 3 & 4). Whether RSNA measures would still reflect SNA to other vascular beds remains unknown and before data from this study can be extrapolated to other sympathetic outflows, future studies are required to establish the response pattern of other sympathetic nerve beds in CKD. Indeed, current evidence suggests that the contribution of the SNS cannot be simply judged from the recording of a single sympathetic nerve bed (Knuepfer and Osborn, 2010). For example, in Dahl hypertensive rats, targeted sympathetic ablation of the kidneys or the splanchnic vascular beds independently reduces BP (Foss et al., 2013), suggesting a role for renal and splanchnic sympathetic outflow in driving hypertension in this model. In angiotensin II (Ang II)-induced hypertension, by contrast, RSNA is

reduced whereas lumbar SNA is unchanged (Yoshimoto et al., 2010), indicating that SNA to these specific vascular beds are not critically involved in the pathogenesis of Ang II hypertension.

The present study did not account for sex differences in the response variables measured, with only male rats used for the study. With current available technology, the size of the female animals at this age precluded implantation of the radiotelemetry probe. For similar technical reasons, RSNA responses in younger animals prior to deterioration of renal function could not be investigated. With advances in telemetry probe development, for example probes of a size suitable for use in mice, this issue will hopefully be able to be overcome.

We have previously demonstrated evidence of increased sympathetic activity in the LPK. However, these findings were through either indirect measures (Harrison et al., 2010, Hildreth et al., 2013b, Phillips et al., 2007), or when direct recordings were performed (Chapters 3 & 4); measures may have been influenced by the sympathoexcitatory effects of anaesthetics and their ability to dampen cardiovascular responses to various stimuli (Shimokawa et al., 1998). In this study, our direct conscious recording of RSNA confirmed an elevation in SNA in the LPK. These observations unequivocally confirm the LPK as a model of increased SNA and therefore support our previous assertions (Harrison et al., 2010, Hildreth et al., 2013b, Phillips et al., 2007). In the present study, we also confirm our previous finding that the LPK display enhanced depressor responses to ganglionic blockade (Phillips et al., 2007), another indicator of increased sympathetic vasomotor tone (Abdala et al., 2012) in this model. Importantly, we have now extended this observation to show that increased RSNA is a likely contributor to the hypertension observed, as reducing RSNA with hexamethonium resulted in a greater fall in BP in the LPK and a significant positive relationship between RSNA and BP was observed. These key observations conceivably underlie the potential BP lowering effects offered by renal denervation in CKD patients (Hering et al., 2012, Kiuchi et al., 2013, Schlaich et al., 2013). Clinically, elevated SNA in CKD patients is of marked significance being associated with all-cause mortality and nonfatal cardiovascular events (Penne et al., 2009), left ventricular hypertrophy (Guizar-Mendoza et al., 2006) and vascular damage (Bruno et al., 2012).

Apart from its cardiovascular effects in CKD, SNS overactivity is also implicated in the development and progression of renal disease, contributing to upregulated renin release, elevated tubular reabsorption of sodium, high renal vascular resistance with consequent reductions in renal blood flow and GFR and tissue hypoxia, glomerulosclerosis and interstitial fibrosis (DiBona, 2004, Fujita et al., 2012). In the present study, BP was also correlated with urinary creatinine excretion, suggesting that a complex interplay between SNA, BP and renal dysfunction exists in CKD. Previous reports demonstrated a negative association between muscle SNA and GFR in patients with chronic renal insufficiency (Grassi et al., 2011a, Grassi et al., 2011b), indicating a significant contribution of SNA to driving renal pathology and highlights a critical role for renal innervation in the manifestation of renal dysfunction in CKD. In support of this view are the observations that

significant enhancements in renal haemodynamics and GFR are observed in CKD patients treated with renal denervation (Kiuchi et al., 2013) or a centrally acting sympatholytic drug (Vonend et al., 2003).

The pathophysiologic basis for sympathetic activation in CKD is poorly understood. However, a number of not mutually exclusive mechanisms including activation of the renal afferents (Ye et al., 1997b), upregulation of the renin-angiotensin-aldosterone system (RAAS) (Neumann et al., 2007) and reductions in central nitric oxide availability (Ye et al., 1997a) have been forwarded. We have previously demonstrated that elevated sympathetic drive in the LPK is associated with an inability to effectively restrain SNA by the baroreflex (Chapters 3 & 4) and vagal afferent pathways (Chapter 6). A key objective of the present work was to assess if the LPK display abnormalities in other neuronal pathways known to modulate SNA, including activation of the chemoreceptor reflex and stress pathways. Irrespective of the stimulus being either peripheral (hypoxia) or central (hypercapnia), activation of the chemoreflex pathway in the LPK produced blunted RSNA and BP responses. The association between hypoxia, sympathoexcitation and hypertension (Hedner et al., 1988, Huang et al., 2009, Sobajima et al., 2011) is well established, and current evidence suggests that nocturnal hypoxic exposure typical of obstructive sleep apnea is common in CKD and a contributing risk factor for hypertension in this patient group (Adeseun and Rosas, 2010). Given this association, our observation of attenuated chemoreflex control of SNA and resulting reduced BP responses in the conscious LPK was perhaps counterintuitive. The mechanisms underlying these effects were not examined in this study; however, it is possible that tonic activation of the chemoreflex pathway in CKD may impair the ability of this reflex to drive further increases in SNA, such that diminished SNA and BP responses are observed in the LPK when this mechanism is triggered. In support of this view were the observations that (1) central and peripheral chemoreflex activation was able to evoke a significant increase in SNA in the Lewis control group but not in the LPK; and (2) deactivation of the chemoreflex pathway using 100% O_2 in CKD patients produces exaggerated falls in SNA and pulse pressure that were not observed in the control group (Hering et al., 2007). Nonetheless, a role for increased chemoreflex activity as an instigating factor for high SNA and BP in the younger LPK cannot be ruled out and warrants future investigation.

Like chemoreflex activation, altered cardiovascular responses to emotional stress have been implicated in the setting of high BP (Ming et al., 2004) and are often evident in different models of hypertension (D'Angelo et al., 2006, DiBona and Jones, 1995, Head and Burke, 2004). The principal response of the body to a stressful stimulus involves the activation of the SNS, release of catecholamines from the adrenal medulla and activation of the hypothalamic-pituitary-adrenocortical axis (Fontes et al., 2011), mechanisms which may become altered during disease. Comparable to our chemoreflex response, we observed diminution of the sympathetic responses to acute stress in the LPK relative to Lewis, such that an acute rise in RSNA and BP was only evident in the Lewis. In CKD, previous studies have shown that sympathetic reactivity to mental stress was either unchanged

(Agarwal et al., 1991) or exaggerated (Seliger et al., 2008). In these studies, however, sympathetic reactivity was inferred indirectly from assessing differences in the haemodynamic response to stress in test subjects. To our knowledge, this is the first report to show sympathetic responses to stress in CKD using direct recording of both SNA and BP. Our observations do however parallel findings in rabbits fed with high fat diets, in which a similar attenuation in sympathetic and BP responses was observed when air-jet stress was used (Armitage et al., 2012). Although the mechanism underlying this reduction in the response to stress is not known, one possible scenario is that the persistent elevation in BP and RSNA observed with CKD may be contributed to by upregulation of endogenous stress pathways (Armitage et al., 2012). Therefore, when these pathways are activated by external factors, the net increase to maximal response is proportionally less.

Of note were the observations that activation of both chemoreflex and stress pathways produced attenuated sympathetic and BP responses in the LPK. It is possible that this could have been the result of an effective activation of the baroreflex to buffer the triggered rise in RSNA and BP; however, we believe this is unlikely because we have shown that baroreflex control of RSNA and heart rate are markedly impaired in the LPK at this age (Chapters 3).

7.5 Perspectives and significance

Direct conscious recording of SNA in undisturbed freely moving rats overcomes many of the limitations that other indirect or anaesthetised assessments of sympathetic activity are associated with. In a conscious rodent model of CKD, we describe for the first time direct telemetric recording of SNA to the kidney and provide evidence that high BP is significantly correlated with increased RSNA and renal dysfunction, thus supporting the clinical use of renal denervation as a treatment for limiting hypertension and renal disease progression in CKD. The study further shows that the renal disease is associated with both reduced chemosensitive and stress-induced regulation of RSNA and MAP, indicating that the ability of the CNS to regulate sympathetic outflow and BP is compromised in CKD, and therefore emphasizing the complexity of this pathological condition. Findings from the present study are relevant to better understanding the complex nature of this global clinical problem and future understanding of therapies such as renal denervation targeting increased sympathetic activity to specific organs to limit cardiovascular disease in CKD.

Table 7.1: Characteristics of Lewis and Lewis Polycystic Kidney (LPK) rats

Parameter *(n)*	**Lewis** *(8)*	**LPK** *(6)*	***P* value**
Body weight (g)	332 ± 8	254 ± 8*	<0.0001
Water intake (ml/24h)	25 ± 1	50 ± 3*	<0.0001
Urine output (ml/24h)	11 ± 1	51 ± 3*	<0.0001
U_{Pro} (g/L)	0.05 ± 0.01	0.89 ± 0.41*	<0.0001
U_{Cr} (g/L)	1.2 ± 0.2	0.2 ± 0.1*	0.0006
UPC	0.06 ± 0.02	5.9 ± 3.2*	<0.0001
RSNA (μV)	0.6 ± 0.1	1.2 ± 0.1*	0.0190
MAP (mmHg)	97 ± 2	151 ± 8*	<0.0001

U_{Pro}, urinary total protein; U_{Cr}, urinary creatinine; UPC, urinary protein-to-creatinine ratio; RSNA, renal sympathetic nerve activity and MAP, mean arterial pressure. Results are expressed as mean ± SEM. In the Lewis, UPC was not calculated in 3/9 animals due to lack of detectable protein levels in the urine. Accordingly, only 6 Lewis animals were used to compare mean values of UPC. *P<0.05 vs. Lewis control. *(n)* values denoted in subscript and represent the minimum number in each group.

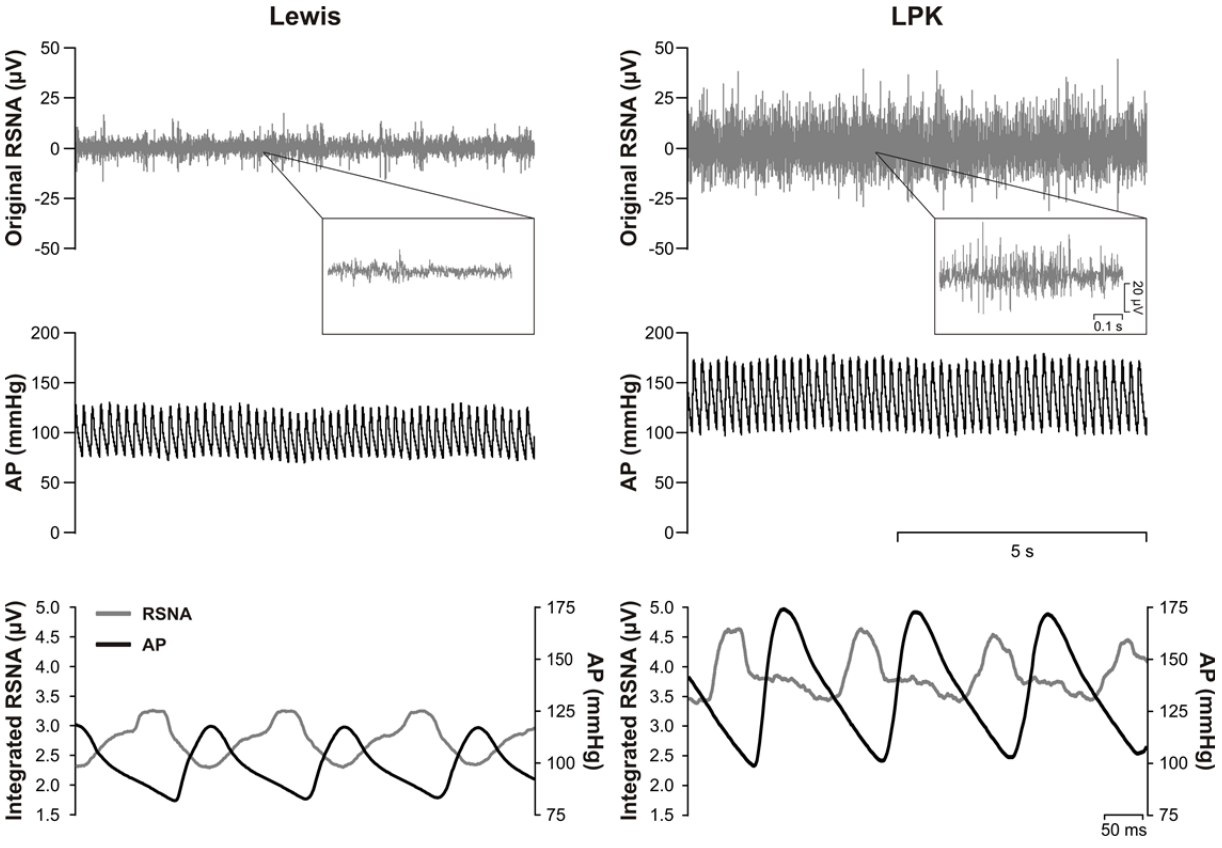

Figure 7.1: Top, representative raw data traces of original renal sympathetic nerve activity (RSNA) and arterial pressure (AP) from conscious Lewis (left) and Lewis Polycystic Kidney (LPK, right) rats. Bottom, pulse modulation of RSNA using pulse triggered averages of AP and integrated RSNA (solid lines) from the same Lewis (left) and LPK (right) animals. Note the inverse phasic relationship between AP and RSNA in the pulse triggered averages, typical of pulse modulation of RSNA.

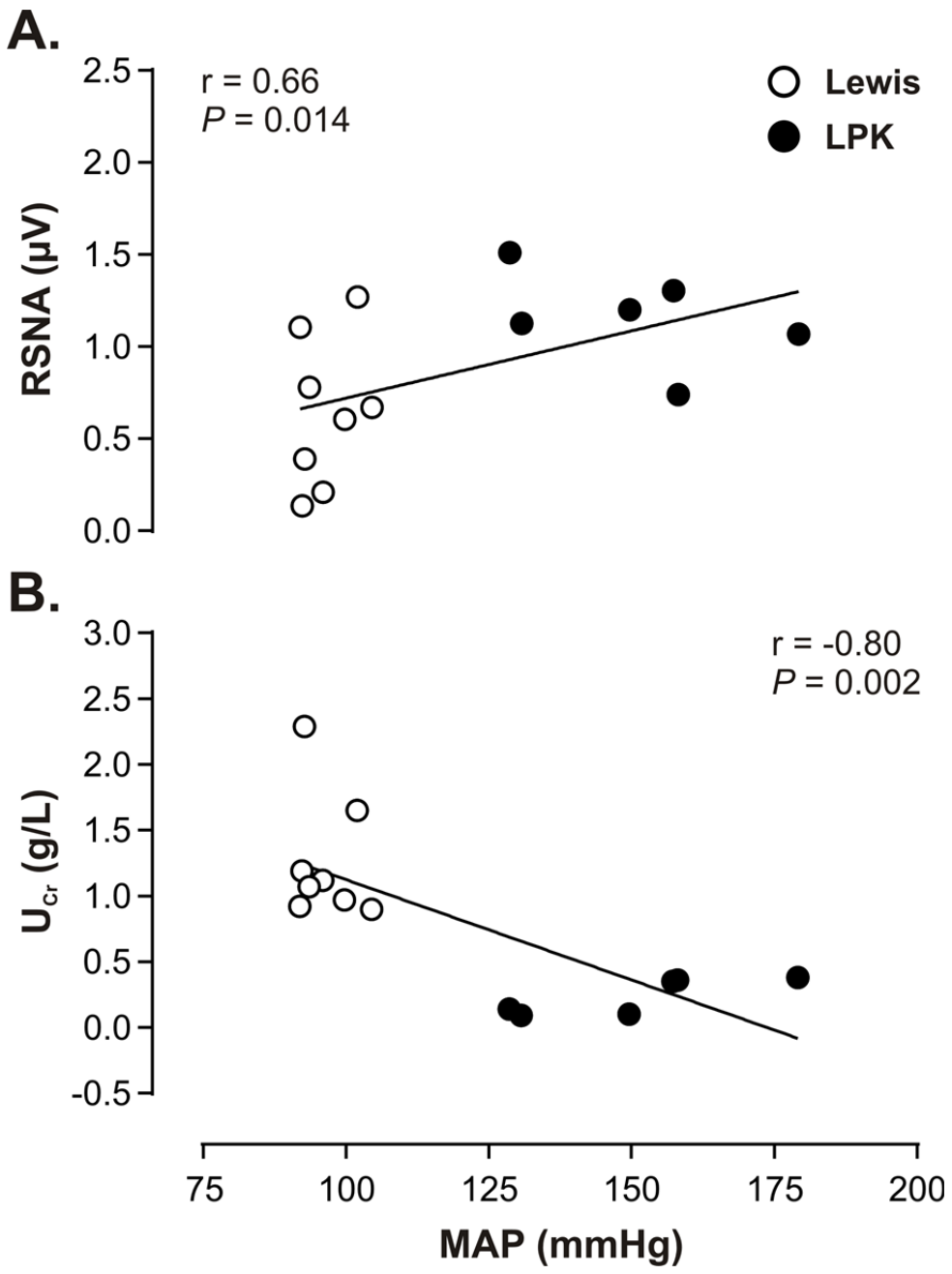

Figure 7.2: Correlations of (A) mean arterial pressure (MAP) versus renal sympathetic nerve activity (RSNA) and (B) MAP versus urinary creatinine (U_{Cr}) in Lewis and Lewis Polycystic Kidney (LPK) rats. *n* = 14. Note the positive association between MAP and RSNA and the negative association between MAP and U_{Cr}.

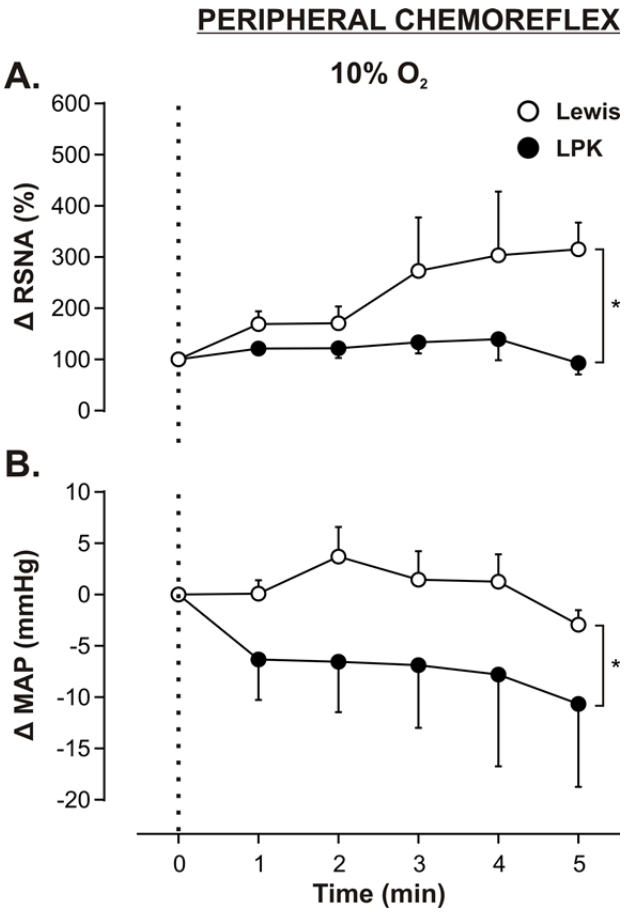

Figure 7.3: Renal sympathetic nerve activity (RSNA, A) and mean arterial pressure (MAP, B) responses to peripheral chemoreflex activation in Lewis and Lewis Polycystic Kidney (LPK) rats. Data points are 1-minute averages of RSNA and MAP measured for 1 minutes before (time zero, dashed vertical line) and 5 minutes during a hypoxic challenge (10% O_2). Results are expressed as mean ± SEM. $^{*}P<0.05$ versus Lewis control rat. Minimum *n*/group = 4.

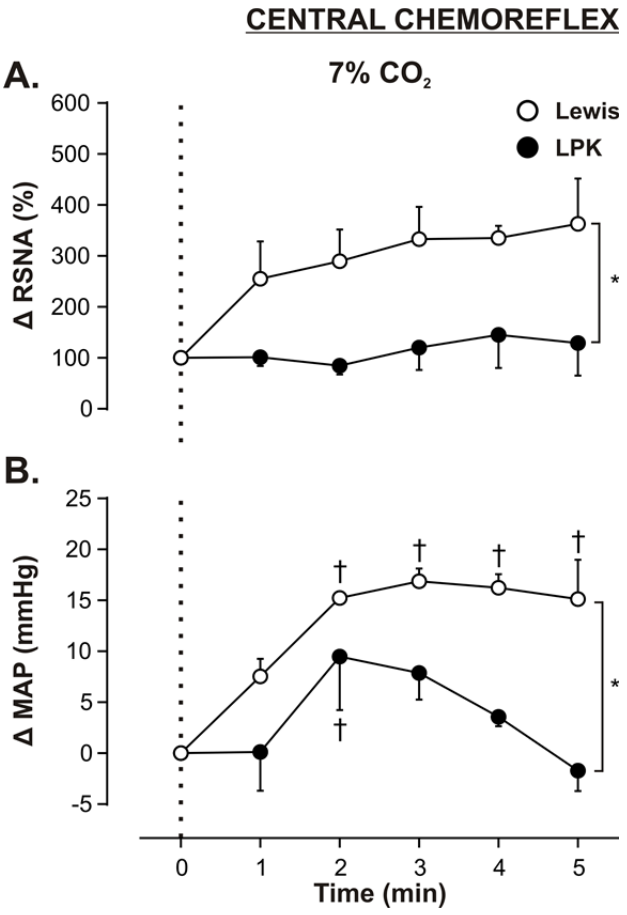

Figure 7.4: Renal sympathetic nerve activity (RSNA, A) and mean arterial pressure (MAP, B) responses to central chemoreflex activation in Lewis and Lewis Polycystic Kidney (LPK) rats. Data points are 1-minute averages of RSNA and MAP measured for 1 minute before (time zero, dashed vertical line) and 5 minutes during a hypcapnic challenge (7% CO_2). Results are expressed as mean ± SEM. $^{\dagger}P<0.05$ versus time zero within each strain and $^{*}P<0.05$ versus Lewis control rat. Minimum *n*/group = 4.

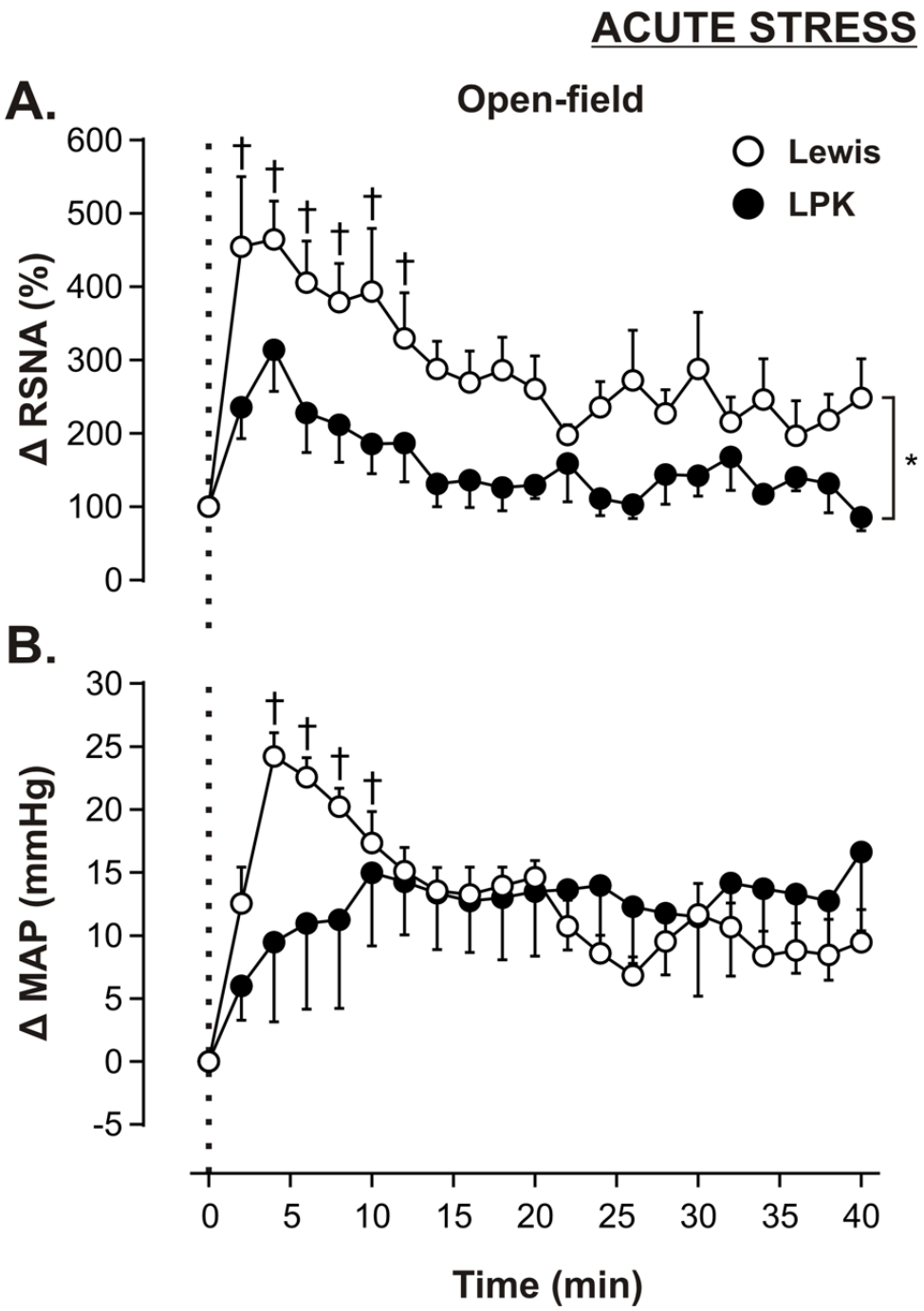

Figure 7.5: Renal sympathetic nerve activity (RSNA, A) and mean arterial pressure (MAP, B) responses to acute open-field stress in Lewis and Lewis Polycystic Kidney (LPK) rats. Data points are 2-minute averages of RSNA and MAP measured for 2 minutes before (time zero, dashed line) and 40 minutes during acute stress exposure. Results are expressed as mean±SEM. $^{\dagger}P<0.05$ versus time zero within each strain and $^{*}P<0.05$ versus Lewis control rat. Minimum *n*/group = 6.

8 Final Discussion

Hypertension is a critical clinical issue in patients with chronic kidney disease (CKD), as it plays a key role in the progression of renal damage and forms the basis for excessive cardiovascular complications and mortality. Although this point is widely recognized, blood pressure (BP) control in CKD patients is often poor, whether in an early or advanced stage or when receiving dialysis therapy, suggesting a limited knowledge of the principle underlying aetiologies. Therefore, the overarching topic of this thesis was the examination of altered tonic and reflex control of autonomic outflows in association with the cardiovascular disease phenotype of CKD. In view of this, the present thesis aimed to provide answers to the following questions:

1. Is baroreflex control of sympathetic nerve activity impaired in CKD, and associated with an elevated sympathetic drive?
2. What are the mechanisms that underlie altered cardiac and sympathetic baroreflex function in CKD?
3. Do females express baroreflex dysfunction differently to males, and if so are the mechanisms contributing to those deficits similar?
4. Is altered reflex control of autonomic outflow associated with dysregulations of other baroreflex-independent mechanisms?
5. Is sympathetic overactivity a consistent feature of CKD when measurements are performed under both unconscious and conscious conditions?

8.1 Increased sympathetic nerve activity in chronic kidney disease: A new research dimension

Sympathetic activation is associated with both BP increase and high cardiovascular morbidity and mortality in CKD and end-stage renal disease (ESRD). Human studies utilising indirect measurements of plasma noradrenaline (Grassi et al., 2011a, Levitan et al., 1984, Masuo et al., 1995, Zoccali et al., 2002), spectral analysis of BP and heart rate (HR) (Lewanski and Chrzanowski, 2003), or assessment of haemodynamic responses to sympatholytic drugs (Badve et al., 2011, Furgeson and Chonchol, 2008, Levitan et al., 1984, Schohn et al., 1985), alongside direct recording of muscle sympathetic nerve activity (SNA) (Grassi et al., 2011b, Klein et al., 2003, Neumann et al., 2007) have definitively established that there is altered activity of the sympathetic nervous system (SNS) in CKD. Despite the valuable information these studies have yielded, it is difficult in human clinical research for specific mechanisms to be tested within the CKD population. In our studies, we chose to record renal sympathetic nerve activity (RSNA) given the pivotal role of the kidney and its innervation in the regulation of arterial resistance, blood flow, glomerular filtration rate, renin secretion, salt/water excretion and therefore long-term BP homeostasis (DiBona, 2000b, DiBona, 2000a, DiBona and Kopp, 1997, Johns et al., 2011). Furthermore, current evidence suggests that renal denervation appears

to lower BP in the CKD population (Hering et al., 2012, Kiuchi et al., 2013, Schlaich et al., 2013), supporting a role for elevated renal sympathetic tone to play a significant role in driving CKD mediated hypertension. Indeed, findings from this thesis do not only confirm the presence of an elevated renal sympathetic drive in the LPK model of CKD, but also show that RSNA levels increase early on when renal impairments are minimal. Surprisingly, and despite a temporal decline in renal function, RSNA did not increase further and both male and female LPK rats expressed comparable elevations in RSNA over the same time frame. These observations show that: 1) analogous to the human condition, SNA is increased early in the disease-course and may contribute to the further deterioration in renal function (Grassi et al., 2011a); and 2) sex does not appear to influence tonic levels of SNA in male and female models of CKD.

It might be argued that interpretation of SNA data acquired from acute recordings in unconscious animals may be confounded by the effect of anaesthetic. Indeed, Shimokawa and others have previously demonstrated that urethane anaesthesia, the same anaesthesia used in our unconscious RSNA recordings, evoked a marked increase in RSNA in Wistar rats without altering sympathetic baroreflex gain (Shimokawa et al., 1998). Notwithstanding the value of experimental data that can only be obtained in anaesthetised non-recovery protocols, this does pose a technical challenge that has required development of equipment and devices designed for reliable and accurate measurement of SNA in conscious animals. With the advent of radiotelemetry, it is now possible to directly record SNA in conscious unrestrained rats. The success of this approach is still constrained by a number of factors, including surgical approach, electrode leads/nerve stability and long-term preservation of viable nerve bursts. Using direct telemetric recordings of SNA in undisturbed freely moving Lewis and LPK rats, this work was able to establish the capability of this technique to determine with high fidelity ongoing changes in SNA in CKD. Indeed, when recorded at 12–13 weeks of age, RSNA was not only higher in the LPK relative to the Lewis controls, but also showed a positive correlation with mean arterial BP. These observations therefore supported our previous findings of increased SNA as assessed by direct recording of RSNA under urethane anaesthesia (Chapters 3 and 4) and through indirect measures such as enhanced depressor responses to ganglionic blockade, increased low-frequency (LF) power of systolic blood pressure variability (SBPV) and heightened bradycardic responses to selective β_1-adrenoceptor blockade in the LPK (Harrison et al., 2010, Hildreth et al., 2013b, Phillips et al., 2007). The observations made herein further highlighted a likely role for renal sympathetic innervation as a key player in the hypertension in CKD. However, whether female LPK or juvenile LPK of either sex show similar elevated levels of RSNA under conscious conditions is yet to be determined. Interestingly, in conscious LPK, however, the LF component of SBPV is reduced at 10 weeks of age but becomes elevated at 12 weeks of age (Hildreth et al., 2013b). This observation, while consistent with the demonstration of increased RSNA levels in the conscious LPK at 12 weeks of age, suggests that sympathetic activity may not be as elevated in the conscious juvenile LPK and that differences in RSNA levels acquired by direct recordings in anaesthetised animals at this age

perhaps relate to a differential vulnerability to the sympathoexcitatory effect of anaesthetics in the Lewis and LPK (Hildreth et al., 2013a). Alternatively, the LF component of SBPV provides a rough estimate of overall sympathetic tone and SNA to the kidney may still be elevated relative to sympathetic outflow to other vascular beds.

Thus far, it appears clear that a complex set of events governs the pathophysiological basis of sympathetic hyperactivity in CKD. The novel findings from the present work will help open a new avenue of research in conscious animals which will potentially enable better understanding of the role of SNA in modulation of cardiovascular function in CKD, and resolve long-standing debates over how the hormonal system interacts with sympathetic activity.

8.2 Cardiovascular autonomic dysfunction in chronic kidney disease

Cardiovascular autonomic dysfunction is a serious yet poorly understood pathological manifestation of CKD, contributing to a high incidence of cardiovascular morbidity and mortality in this patient population (Di Leo et al., 2005, Dursun et al., 2004, Rubinger et al., 2009). In most cases, sympathetic activity is elevated and associated with a hypoactive parasympathetic nervous system and impaired baroreflex sensitivity (BRS) (Grassi et al., 2011a, Johansson et al., 2007, Neumann et al., 2007, Zoccali et al., 2002). However, the conundrum has been to identify the principle underlying aetiology. Empirically, sympathovagal imbalance has been recognised as a major mechanism underlying many cardiovascular morbidities and comorbidities in general (Thayer et al., 2010), and could possibly be the final common pathway of sudden cardiac death in CKD in particular (Cashion et al., 2000, Dursun et al., 2004, Ranpuria et al., 2008).

Normal levels of SNA are dependent upon a balance between the regulatory influence of sympathoexcitatory and sympathoinhibitory pathways. For example, in salt-sensitive hypertension, it has been proposed that dietary salt intake exerts its effect on the SNS by disturbing the balance between sympathoexcitatory and sympathoinhibitory inputs to the rostral ventrolateral medulla (RVLM) (Brooks et al., 2005, Brooks et al., 2001). In obese-hypertensive Zucker rats, Huber and Schreihofer showed that, while sympathoinhibitory reflexes evoked by low-frequency stimulation of the vagal afferents were attenuated, sympathoexcitatory reflexes to high-frequency activation were exaggerated (Huber and Schreihofer, 2010). We therefore predicted that elevated SNA in CKD might similarly have a basis in reflex responses and could be contributed to by: 1) a reduction in the physiological restraint on SNA exerted by sympathoinhibitory pathways such as the baroreceptor reflex or C-fiber vagal afferents; 2) upregulation of sympathoexcitatory drive due to activation of the chemoreceptor reflex, stress inputs or A-fiber vagal afferents; or 3) a combination of both. Observations from the present study showed that the ability to evoke maximal sympathoinhibition in the LPK was attenuated, as SNA responses to a pharmacologically evoked increase in BP, stimulation of the aortic depressor nerve (ADN) and low frequency stimulation of the vagal afferent nerve yielded blunted reductions in SNA in the LPK relative to controls. In contrast,

sympathoexcitatory responses evoked by high frequency stimulation of the vagal afferents produced sustained sympathoexcitations in the LPK. Together, this indicates that baroreceptor-dependent and -independent control of SNA is disrupted in the LPK, such that a combination of mechanisms that impair sympathoinhibition and those which promote sympathoexcitation are possibly driving elevated RSNA in CKD. On the other hand, our results indicate it is unlikely that sympathoexcitation evoked by activation of the chemoreflex and stress pathways is involved in driving sympathoexcitation in the LPK at this stage of the disease, as sympathetic responses evoked by the activation of those pathways produced blunted renal sympathetic responses. Nonetheless, a role for increased stress reactivity and chemoreflex activity as instigating factors for high SNA in the younger LPK cannot be ruled out, with persistent tonic activation of these pathways (Armitage et al., 2012, Despas et al., 2009, Hering et al., 2007) perhaps underling diminished sympathetic responses seen later during the course of CKD. Most importantly, however, the ability to trigger more sympathoexcitation by one pathway but not by another suggests a differential ceiling effect through different cardiovascular regulatory pathways and the capacity for further increases in SNA and subsequently detrimental effects on the heart and blood vessels as the disease progresses.

As described throughout this thesis, altered baroreflex function is a key contributor to autonomic dysfunction in CKD. Observations from this thesis indicated that deficits within the LPK baroreflex arc were not only age-related and associated with progressive decline in renal function, but also contingent upon sex. In the male LPK, cardiac and sympathetic baroreflex dysfunction was contributed to by deficits in both the afferent and central components of the baroreflex arc. In female LPK, by contrast, baroreflex dysfunction was solely driven by deficits within the central component of baroreflex pathway. To our knowledge, this is the first report to provide a comprehensive investigation of the baroreceptor reflex in CKD and account for sex differences in the neuroregulation of autonomic functions.

A large body of evidence demonstrates a direct association between vasculopathy and impaired BRS in CKD (Chan et al., 2005, Chesterton et al., 2005, Studinger et al., 2006). Observations from the present work are in keeping with those reports, showing that where baroreceptor afferent neurotransmission was impaired in the LPK, deficits were significantly correlated with the progressive deteriorations in vascular structure. Interestingly, however, impairments within the sensory afferent arm of the baroreceptor reflex appear to have a minimal contribution to the development of baroreflex dysfunction in CKD, as despite an age-related decline in the functionality of the afferent drive in the male LPK, this was not observed in the female LPK, and yet both male and female LPK rats exhibited comparable deficits in cardiac and sympathetic baroreflex function by 12 weeks of age. We therefore believe that a central deficit in the processing of autonomic outflows to the heart and vasculature, which is perhaps linked to a complex interplay between high BP and loss of renal function, primarily underpins autonomic dysfunction in CKD, as there was not only an attenuation of the baroreceptor-dependent central processing of efferent sympathetic and

vagal nerve traffic, but there was also a diminution of central mediation of autonomic outflows driven by the vagal afferents, central chemoreflex and stress inputs, which are mediated independently of the baroreceptors. Taken together, it appears that CKD promotes a state of generalised central dysfunction, which begs the question of whether or not deficits within neuroanatomical elements common to these cardiovascular modulatory pathways may drive autonomic dysfunction in CKD.

Central regulation of the cardiovascular system is a complex integrated process, with the CNS additionally critically involved in the release and modulation of hormonal factors that influence BP control over the short and long term. Neurocardiovascular dysregulation is clearly implicated in a number of pathophysiological states, including hypertension (Gonzalez et al., 1983, Koepke and DiBona, 1985, Salgado et al., 2007), heart failure (Dibner-Dunlap and Thames, 1992), and obesity (Huber and Schreihofer, 2010). Therefore, by recognising the critical involvement of central mechanisms in the pathogenesis of autonomic dysfunction in CKD, this work lays the foundation for identifying the precise CNS mechanisms underlying the development and progression of autonomic dysfunction and cardiovascular disease in CKD.

An interesting observation from this study was that deficits in the baroreceptor-dependent central processing of sympathetic outflow were relatively less pronounced in the female LPK relative to males. In striking contrast, baroreceptor-independent mediation of cardiovagal outflow driven by central integration of vagal afferent input was impaired in the female LPK but not in the male. This raises the hypothesis that a complex crosstalk between different neuroregulatory pathways exists in CKD, such that impairments within one reflex mechanism may become compensated for by upregulation of other cardiovascular reflexes to maintain autonomic outflows. Alternatively, CKD may differentially influence central processing of autonomic outflows within each sex, with different integrated physiological mechanisms being relied upon to maintain arterial BP within a narrow range. It can be further speculated that abnormalities within the central pathways regulating BP are driven by different anatomical regions within the brain in the male and female, or may relate to fundamental sex-based differences in how medullary nuclei responsible for the generation of efferent autonomic activity process the afferent input. In favour of sexual dimorphism in the neurochemical signalling of brainstem neurons is the observation that female rats have more angiotensin type 1 (AT_1) receptors in RVLM neurons and less NADPH oxidase subunit P47 levels relative to males (Wang et al., 2008). Our intriguing observations therefore of a sex difference in the central handling of sympathetic and cardiovagal outflow certainly warrants further investigation in order to understand the principle underlying mechanisms that may differentially promote CKD-mediated hypertension in both males and females.

Many of the current therapeutics primarily target the vasculature to lower BP in CKD. However, impaired baroreflex function remains a major risk factor for cardiovascular morbidity and mortality

in CKD patients, despite BP control with antihypertensive medications. This indicates that other factors contributing to this risk are being overlooked in clinical practice and/or are not well accounted for. Our results clearly show that autonomic dysfunction in CKD is not directly related to the effect of hypertension on the vasculature and pathways that signal BP changes to the brain; rather, it is mainly driven by altered central control of the autonomic nervous system, suggesting that treatments which target the CNS are underutilised in the CKD population. Current evidence suggests that central sympatholytic drugs can provide pronounced therapeutic advantages in CKD patients. In hypertensive patients with advanced renal failure, treatment with standard antihypertensive therapy and adjunctive treatment with moxonidine, a central sympatholytic, was predicted to reduce the number of new ESRD cases over three years compared to adjunctive treatment with nitrendipine, a calcium channel blocker (Littlewood et al., 2007). In CKD patients treated with eprosartan, an AT_1 receptor antagonist, the angiotensin II-independent sympathetic overactivity was normalized by the addition of moxonidine therapy (Neumann et al., 2004). More recently, Palkovits and colleagues showed that CKD-triggered activation of central sympathetic, stress- and pain-related brain areas, as well as the limbic system, was ameliorated by the AT_1 receptor antagonist losartan but more vigorously by moxonidine monotherpay (Palkovits et al., 2013). While these reports fit in well with the demonstrated central deficit outlined in this thesis, current interventional strategies remain non-specific, and identifying critical brain regions promoting abnormal autonomic control of cardiovascular function is warranted and importantly could facilitate the development of a more target-specific treatment to alleviate autonomic dysregulation in CKD.

8.3 Perspectives

The relationship between hypertension and CKD is complex and multifactorial. A better understanding of these pathological processes is imperative to improve our treatment strategies and reduce the number of cardiovascular adverse events reported within the CKD population. Findings from the present thesis identify neurogenic mechanisms as a potential driver of increased SNA, autonomic dysfunction and hypertension in CKD, and highlight a critical role for central pathways regulating tonic and reflex function in promoting those deficits. This work further stresses the importance of sexual dimorphism when investigating pathophysiological mechanisms relating to CKD, and that the female sex should not be underrepresented in research investigations or clinical trials. Regardless of the underlying aetiology, the LPK model appears to reproduce many aspects of the human pathophysiological course of CKD (see Chapter 1). It is, therefore, possible that the mechanisms of autonomic dysfunction outlined in this work may well be applicable to other variations of CKD in both humans and experimental animals. An important continuation of the present work therefore will be to determine if there is a prevalent pathophysiological mechanism underlying CKD-related hypertension; what are the best antihypertensive therapies for CKD patients; and, should sex dictate the treatment approach to be used?

9 References

ABDALA, A. P., MCBRYDE, F. D., MARINA, N., HENDY, E. B., ENGELMAN, Z. J., FUDIM, M., SOBOTKA, P. A., GOURINE, A. V. & PATON, J. F. 2012. Hypertension is critically dependent on the carotid body input in the spontaneously hypertensive rat. *J Physiol,* 590**,** 4269-77.

ABDEL-RAHMAN, A. A. 1999. Gender difference in baroreflex-mediated bradycardia in young rats: role of cardiac sympathetic and parasympathetic components. *Can J Physiol Pharmacol,* 77**,** 358-66.

ADAMCZAK, M., ZEIER, M., DIKOW, R. & RITZ, E. 2002. Kidney and hypertension. *Kidney Int Suppl***,** 62-7.

ADESEUN, G. A. & ROSAS, S. E. 2010. The impact of obstructive sleep apnea on chronic kidney disease. *Curr Hypertens Rep,* 12**,** 378-83.

AGARWAL, A., ANAND, I. S., SAKHUJA, V. & CHUGH, K. S. 1991. Effect of dialysis and renal transplantation on autonomic dysfunction in chronic renal failure. *Kidney Int,* 40**,** 489-95.

AGARWAL, S. K., GELSEMA, A. J. & CALARESU, F. R. 1989. Neurons in rostral VLM are inhibited by chemical stimulation of caudal VLM in rats. *Am J Physiol,* 257**,** R265-70.

AICHER, S. A., SARAVAY, R. H., CRAVO, S., JESKE, I., MORRISON, S. F., REIS, D. J. & MILNER, T. A. 1996. Monosynaptic projections from the nucleus tractus solitarii to C1 adrenergic neurons in the rostral ventrolateral medulla: comparison with input from the caudal ventrolateral medulla. *J Comp Neurol,* 373**,** 62-75.

AKEMI SATO, M., VANDERLEI MENANI, J., UBRIACO LOPES, O. & COLOMBARI, E. 2001. Lesions of the commissural nucleus of the solitary tract reduce arterial pressure in spontaneously hypertensive rats. *Hypertension,* 38**,** 560-4.

AKIBA, T., TACHIBANA, K., TOGASHI, K., HIROE, M. & MARUMO, F. 1995. Plasma human brain natriuretic peptide in chronic renal failure. *Clin Nephrol,* 44 Suppl 1**,** S61-4.

ALA-MELLO, S., KIVIVUORI, S. M., RONNHOLM, K. A., KOSKIMIES, O. & SIIMES, M. A. 1996. Mechanism underlying early anaemia in children with familial juvenile nephronophthisis. *Pediatr Nephrol,* 10**,** 578-81.

AL-NIMRI, M. A., KOMERS, R., OYAMA, T. T., SUBRAMANYA, A. R., LINDSLEY, J. N. & ANDERSON, S. 2003. Endothelial-derived vasoactive mediators in polycystic kidney disease. *Kidney Int,* 63**,** 1776-84.

AMANN, K., KOCH, A., HOFSTETTER, J., GROSS, M. L., HAAS, C., ORTH, S. R., EHMKE, H., RUMP, L. C. & RITZ, E. 2001. Glomerulosclerosis and progression: effect of subantihypertensive doses of alpha and beta blockers. *Kidney Int,* 60**,** 1309-23.

AMANN, K., RUMP, L. C., SIMONAVICIENE, A., OBERHAUSER, V., WESSELS, S., ORTH, S. R., GROSS, M. L., KOCH, A., BIELENBERG, G. W., VAN KATS, J. P., EHMKE, H., MALL, G. & RITZ, E. 2000. Effects of low dose sympathetic inhibition on glomerulosclerosis and albuminuria in subtotally nephrectomized rats. *J Am Soc Nephrol,* 11**,** 1469-78.

ANDRESEN, M. C. 1984. Short- and long-term determinants of baroreceptor function in aged normotensive and spontaneously hypertensive rats. *Circ Res,* 54**,** 750-9.

ANDRESEN, M. C., DOYLE, M. W., JIN, Y. H. & BAILEY, T. W. 2001. Cellular mechanisms of baroreceptor integration at the nucleus tractus solitarius. *Ann N Y Acad Sci,* 940**,** 132-41.

ANDRESEN, M. C., KRAUHS, J. M. & BROWN, A. M. 1978. Relationship of aortic wall and baroreceptor properties during development in normotensive and spontaneously hypertensive rats. *Circ Res,* 43**,** 728-38.

ANZDATA REGISTRY 2012. ANZ data 35th annaul report. *In:* MCDONALD, S., CLAYTON, P. & HURST, K. (eds.). Adelaide, South Australia.

ARDELL, J. L., RANDALL, W. C., CANNON, W. J., SCHMACHT, D. C. & TASDEMIROGLU, E. 1988. Differential sympathetic regulation of automatic, conductile, and contractile tissue in dog heart. *Am J Physiol,* 255**,** H1050-9.

ARMITAGE, J. A., BURKE, S. L., PRIOR, L. J., BARZEL, B., EIKELIS, N., LIM, K. & HEAD, G. A. 2012. Rapid onset of renal sympathetic nerve activation in rabbits fed a high-fat diet. *Hypertension,* 60**,** 163-71.

ASANOI, H. 2009. Application of microneurography to circulatory disorders. *Brain Nerve,* 61**,** 270-6.

ASHTON, J. H. & CASSIDY, S. S. 1985. Reflex depression of cardiovascular function during lung inflation. *J Appl Physiol (1985),* 58**,** 137-45.

ATALA, A., FREEMAN, M. R., MANDELL, J. & BEIER, D. R. 1993. Juvenile cystic kidneys (jck): a new mouse mutation which causes polycystic kidneys. *Kidney Int,* 43**,** 1081-5.

AUGUSTYNIAK, R. A., TUNCEL, M., ZHANG, W., TOTO, R. D. & VICTOR, R. G. 2002. Sympathetic overactivity as a cause of hypertension in chronic renal failure. *J Hypertens,* 20**,** 3-9.

AUSTRALIAN BUREAU OF STATISTICS 2013. Australian Health Survey: Biomedical Results for Chronic Diseases, 2011-12. Australian Bureau of Statistics. Report number: 4364.0.55.005.

AUSTRALIAN INSTITUTE OF HEALTH AND WELFARE 2011. The health and welfare of Australia's Aboriginal and Torres Strait Islander people: an overview.

AVIADO, D. M. & GUEVARA AVIADO, D. 2001. The Bezold-Jarisch reflex. A historical perspective of cardiopulmonary reflexes. *Ann N Y Acad Sci,* 940**,** 48-58.

BADVE, S. V., ROBERTS, M. A., HAWLEY, C. M., CASS, A., GARG, A. X., KRUM, H., TONKIN, A. & PERKOVIC, V. 2011. Effects of beta-adrenergic antagonists in patients with chronic kidney disease: a systematic review and meta-analysis. *J Am Coll Cardiol,* 58**,** 1152-61.

BAILEY, T. W. & DIMICCO, J. A. 2001. Chemical stimulation of the dorsomedial hypothalamus elevates plasma ACTH in conscious rats. *Am J Physiol Regul Integr Comp Physiol,* 280**,** R8-15.

BAILEY, T. W., HERMES, S. M., ANDRESEN, M. C. & AICHER, S. A. 2006. Cranial visceral afferent pathways through the nucleus of the solitary tract to caudal ventrolateral medulla or paraventricular hypothalamus: target-specific synaptic reliability and convergence patterns. *J Neurosci,* 26**,** 11893-902.

BAINBRIDGE, F. A. 1915. The influence of venous filling upon the rate of the heart. *J Physiol,* 50**,** 65-84.

BAKIR, S., MORI, T., DURAND, J., CHEN, Y. F., THOMPSON, J. A. & OPARIL, S. 2000. Estrogen-induced vasoprotection is estrogen receptor dependent: evidence from the balloon-injured rat carotid artery model. *Circulation,* 101**,** 2342-4.

BAKRIS, G. L., HART, P. & RITZ, E. 2006. Beta blockers in the management of chronic kidney disease. *Kidney Int,* 70**,** 1905-13.

BARAJAS, L. & WANG, P. 1978. Myelinated nerves of the rat kidney. A light and electron microscopic autoradiographic study. *J Ultrastruct Res,* 65**,** 148-62.

BARDAJI, A., MARTINEZ-VEA, A., VALERO, A., GUTIERREZ, C., GARCIA, C., RIDAO, C., OLIVER, J. A. & RICHART, C. 2001. Cardiac involvement in autosomal-dominant polycystic kidney disease: a hypertensive heart disease. *Clin Nephrol,* 56**,** 211-20.

BARROS, R. C., BONAGAMBA, L. G., OKAMOTO-CANESIN, R., DE OLIVEIRA, M., BRANCO, L. G. & MACHADO, B. H. 2002. Cardiovascular responses to chemoreflex

activation with potassium cyanide or hypoxic hypoxia in awake rats. *Auton Neurosci,* 97**,** 110-5.

BAVANANDAN, S., AJAYI, S., FENTUM, B., PAUL, S. K., CARR, S. J. & ROBINSON, T. G. 2005. Cardiac baroreceptor sensitivity: a prognostic marker in predialysis chronic kidney disease patients? *Kidney Int,* 67**,** 1019-27.

BELARDINELLI, L. & ISENBERG, G. 1983. Isolated atrial myocytes: adenosine and acetylcholine increase potassium conductance. *Am J Physiol,* 244**,** H734-7.

BENNETT, J. A., GOODCHILD, C. S., KIDD, C. & MCWILLIAM, P. N. 1985. Neurones in the brain stem of the cat excited by vagal afferent fibres from the heart and lungs. *J Physiol,* 369**,** 1-15.

BENNETT, K. L., LINDEN, R. J. & MARY, D. A. S. G. 1983. The effect of stimulation of atrial receptors on the plasma concentration of vasopressin. *Exp Physiol,* 68**,** 579-589.

BERGER, A., EDELSBERG, J., INGLESE, G. W., BHATTACHARYYA, S. K. & OSTER, G. 2009. Cost comparison of peritoneal dialysis versus hemodialysis in end-stage renal disease. *Am J Manag Care,* 15**,** 509-18.

BERTRAM, D., OREA, V., CHAPUIS, B., BARRES, C. & JULIEN, C. 2005. Differential responses of frequency components of renal sympathetic nerve activity to arterial pressure changes in conscious rats. *Am J Physiol Regul Integr Comp Physiol,* 289**,** R1074-82.

BEVAN, J. A. & SU, C. 1971. Distribution theory of resistance of neurogenic vasoconstriction to alpha-receptor blockade in the rabbit. *Circ Res,* 28**,** 179-87.

BHATT, D. L., KANDZARI, D. E., O'NEILL, W. W., D'AGOSTINO, R., FLACK, J. M., KATZEN, B. T., LEON, M. B., LIU, M., MAURI, L., NEGOITA, M., COHEN, S. A., OPARIL, S., ROCHA-SINGH, K., TOWNSEND, R. R. & BAKRIS, G. L. 2014. A controlled trial of renal denervation for resistant hypertension. *N Engl J Med,* 370**,** 1393-401.

BIAGGIONI, I., WHETSELL, W. O., JOBE, J. & NADEAU, J. H. 1994. Baroreflex failure in a patient with central nervous system lesions involving the nucleus tractus solitarii. *Hypertension,* 23**,** 491-5.

BIGAZZI, R., KOGOSOV, E. & CAMPESE, V. M. 1994. Altered norepinephrine turnover in the brain of rats with chronic renal failure. *J Am Soc Nephrol,* 4**,** 1901-7.

BLACHER, J., GUERIN, A. P., PANNIER, B., MARCHAIS, S. J. & LONDON, G. M. 2001. Arterial calcifications, arterial stiffness, and cardiovascular risk in end-stage renal disease. *Hypertension,* 38**,** 938-42.

BLACHER, J., SAFAR, M. E., GUERIN, A. P., PANNIER, B., MARCHAIS, S. J. & LONDON, G. M. 2003. Aortic pulse wave velocity index and mortality in end-stage renal disease. *Kidney Int,* 63**,** 1852-60.

BLACK, P. H. 2002. Stress and the inflammatory response: a review of neurogenic inflammation. *Brain Behav Immun,* 16**,** 622-53.

BOERO, R., PIGNATARO, A., FERRO, M. & QUARELLO, F. 2001. Sympathetic nervous system and chronic renal failure. *Clin Exp Hypertens,* 23**,** 69-75.

BOOTH, L. C., RAMCHANDRA, R., CALZAVACCA, P. & MAY, C. N. 2014. Role of prostaglandins in determining the increased cardiac sympathetic nerve activity in ovine sepsis. *Am J Physiol Regul Integr Comp Physiol*. (in press)

BRAGA, V. A., BURMEISTER, M. A., SHARMA, R. V. & DAVISSON, R. L. 2008. Cardiovascular responses to peripheral chemoreflex activation and comparison of different methods to evaluate baroreflex gain in conscious mice using telemetry. *Am J Physiol Regul Integr Comp Physiol,* 295**,** R1168-74.

BRAGA, V. A., SORIANO, R. N. & MACHADO, B. H. 2006. Sympathoexcitatory response to peripheral chemoreflex activation is enhanced in juvenile rats exposed to chronic intermittent hypoxia. *Exp Physiol,* 91**,** 1025-31.

BRAUN, C., LUDICKE, C., REBSCH, W., GRETZ, N., VAN DER WOUDE, F. J. & ROHMEISS, P. 1996. Autoregulation of renal blood flow and pressure-dependent renin release in autosomal dominant polycystic kidney disease of rats. *Nephrol Dial Transplant,* 11 (Suppl) 6**,** 52-7.

BREWSTER, U. C. & PERAZELLA, M. A. 2004. The renin-angiotensin-aldosterone system and the kidney: effects on kidney disease. *Am J Med,* 116**,** 263-72.

BRINKMANN, J., HEUSSER, K., SCHMIDT, B. M., MENNE, J., KLEIN, G., BAUERSACHS, J., HALLER, H., SWEEP, F. C., DIEDRICH, A., JORDAN, J. & TANK, J. 2012. Catheter-based renal nerve ablation and centrally generated sympathetic activity in difficult-to-control hypertensive patients: prospective case series. *Hypertension,* 60**,** 1485-90.

BRODDE, O. E., BRUCK, H., LEINEWEBER, K. & SEYFARTH, T. 2001. Presence, distribution and physiological function of adrenergic and muscarinic receptor subtypes in the human heart. *Basic Res Cardiol,* 96**,** 528-38.

BROOKS, D. P., SHORT, B. G., CYRONAK, M. J., CONTINO, L. C., DICRISTO, M., WANG, Y. X. & RUFFOLO, R. R., JR. 1993. Comparison between carvedilol and captopril in rats with partial ablation-induced chronic renal failure. *Br J Pharmacol,* 109**,** 581-6.

BROOKS, V. L., CASSAGLIA, P. A., ZHAO, D. & GOLDMAN, R. K. 2012. Baroreflex function in females: changes with the reproductive cycle and pregnancy. *Gend Med,* 9**,** 61-7.

BROOKS, V. L., HAYWOOD, J. R. & JOHNSON, A. K. 2005. Translation of salt retention to central activation of the sympathetic nervous system in hypertension. *Clin Exp Pharmacol Physiol,* 32**,** 426-32.

BROOKS, V. L., SCROGIN, K. E. & MCKEOGH, D. F. 2001. The interaction of angiotensin II and osmolality in the generation of sympathetic tone during changes in dietary salt intake. An hypothesis. *Ann N Y Acad Sci,* 940**,** 380-94.

BROWN, A. M. 1980. Receptors under pressure. An update on baroreceptors. *Circ Res,* 46**,** 1-10.

BROWN, A. M., SAUM, W. R. & TULEY, F. H. 1976. A comparison of aortic baroreceptor discharge in normotensive and spontaneously hypertensive rats. *Circ Res,* 39**,** 488-96.

BROWN, R., JAMES, C., HENDERSON, L. A. & MACEFIELD, V. G. 2012. Autonomic markers of emotional processing: skin sympathetic nerve activity in humans during exposure to emotionally charged images. *Front Physiol,* 3**,** 394.

BRUNO, R. M., GHIADONI, L., SERAVALLE, G., DELL'ORO, R., TADDEI, S. & GRASSI, G. 2012. Sympathetic regulation of vascular function in health and disease. *Front Physiol,* 3**,** 284.

BURKE, S. L. & HEAD, G. A. 2003. Method for in vivo calibration of renal sympathetic nerve activity in rabbits. *J Neurosci Methods,* 127**,** 63-74.

BURKE, S. L., EVANS, R. G., MORETTI, J. L. & HEAD, G. A. 2008. Levels of renal and extrarenal sympathetic drive in angiotensin II-induced hypertension. *Hypertension,* 51**,** 878-83.

BURKE, S. L., LAMBERT, E. & HEAD, G. A. 2011. New approaches to quantifying sympathetic nerve activity. *Curr Hypertens Rep,* 13**,** 249-57.

BURNS, J., MARY, D. A., MACKINTOSH, A. F., BALL, S. G. & GREENWOOD, J. P. 2004. Arterial pressure lowering effect of chronic atenolol therapy in hypertension and vasoconstrictor sympathetic drive. *Hypertension,* 44**,** 454-8.

BURT, V. L., WHELTON, P., ROCCELLA, E. J., BROWN, C., CUTLER, J. A., HIGGINS, M., HORAN, M. J. & LABARTHE, D. 1995. Prevalence of hypertension in the US adult population. Results from the Third National Health and Nutrition Examination Survey, 1988-1991. *Hypertension,* 25**,** 305-13.

BUSNARDO, C., TAVARES, R. F., RESSTEL, L. B., ELIAS, L. L. & CORREA, F. M. 2010. Paraventricular nucleus modulates autonomic and neuroendocrine responses to acute restraint stress in rats. *Auton Neurosci,* 158**,** 51-7.

CALLERA, J. C., BONAGAMBA, L. G., NOSJEAN, A., LAGUZZI, R. & MACHADO, B. H. 1999. Activation of $GABA_A$ but not $GABA_B$ receptors in the NTS blocked bradycardia of chemoreflex in awake rats. *Am J Physiol,* 276**,** H1902-10.

CALLERA, J. C., BONAGAMBA, L. G., NOSJEAN, A., LAGUZZI, R. & MACHADO, B. H. 2000. Activation of GABA receptors in the NTS of awake rats reduces the gain of baroreflex bradycardia. *Auton Neurosci,* 84**,** 58-67.

CALLERA, J. C., SEVOZ, C., LAGUZZI, R. & MACHADO, B. H. 1997. Microinjection of a serotonin3 receptor agonist into the NTS of unanesthetized rats inhibits the bradycardia evoked by activation of the baro- and chemoreflexes. *J Auton Nerv Syst,* 63**,** 127-36.

CALLISTER, R., SUWARNO, N. O. & SEALS, D. R. 1992. Sympathetic activity is influenced by task difficulty and stress perception during mental challenge in humans. *J Physiol,* 454**,** 373-87.

CAMPAGNA, J. A. & CARTER, C. 2003. Clinical relevance of the Bezold-Jarisch reflex. *Anesthesiology,* 98**,** 1250-60.

CAMPESE, V. M. & KOGOSOV, E. 1995. Renal afferent denervation prevents hypertension in rats with chronic renal failure. *Hypertension,* 25**,** 878-82.

CAMPESE, V. M. & KROL, E. 2002. Neurogenic factors in renal hypertension. *Curr Hypertens Rep,* 4**,** 256-60.

CAMPESE, V. M., KOGOSOV, E. & KOSS, M. 1995. Renal afferent denervation prevents the progression of renal disease in the renal ablation model of chronic renal failure in the rat. *Am J Kidney Dis,* 26**,** 861-5.

CAMPESE, V. M., MOZAYENI, P., YE, S. & GUMBARD, M. 2002. High salt intake inhibits nitric oxide synthase expression and aggravates hypertension in rats with chronic renal failure. *J Nephrol,* 15**,** 407-13.

CAMPOS, R. R. & MCALLEN, R. M. 1997. Cardiac sympathetic premotor neurons. *Am J Physiol,* 272**,** R615-20.

CAO, W. H. & MORRISON, S. F. 2000. Responses of adrenal sympathetic preganglionic neurons to stimulation of cardiopulmonary receptors. *Brain Res,* 887**,** 46-52.

CAO, W. H. & MORRISON, S. F. 2001. Differential chemoreceptor reflex responses of adrenal preganglionic neurons. *Am J Physiol Regul Integr Comp Physiol,* 281**,** R1825-32.

CAO, W. H. & MORRISON, S. F. 2003. Disinhibition of rostral raphe pallidus neurons increases cardiac sympathetic nerve activity and heart rate. *Brain Res,* 980**,** 1-10.

CAPISONDA, R., PHAN, V., TRAUBUCI, J., DANEMAN, A., BALFE, J. W. & GUAY-WOODFORD, L. M. 2003. Autosomal recessive polycystic kidney disease: outcomes from a single-center experience. *Pediatr Nephrol,* 18**,** 119-26.

CARRERO, J. J. 2010. Gender differences in chronic kidney disease: underpinnings and therapeutic implications. *Kidney Blood Press Res,* 33**,** 383-92.

CARSWELL, F., HAINSWORTH, R. & LEDSOME, J. R. 1970a. The effects of distension of the pulmonary vein-atrial junctions upon peripheral vascular resistance. *J Physiol,* 207**,** 1-14.

CARSWELL, F., HAINSWORTH, R. & LEDSOME, J. R. 1970b. The effects of left atrial distension upon urine flow from the isolated perfused kidney. *Q J Exp Physiol Cogn Med Sci,* 55**,** 173-82.

CASHION, A. K., COWAN, P. A., MILSTEAD, E. J., GABER, A. O. & HATHAWAY, D. K. 2000. Heart rate variability, mortality, and exercise in patients with end-stage renal disease. *Prog Transplant,* 10**,** 10-6.

CERASOLA, G., VECCHI, M., MULE, G., COTTONE, S., MANGANO, M. T., ANDRONICO, G., CONTORNO, A., PARRINO, I., RENDA, F. & PAVONE, G. 1998. Sympathetic activity and blood pressure pattern in autosomal dominant polycystic kidney disease hypertensives. *Am J Nephrol,* 18**,** 391-8.

CHAN, C. T., CHERTOW, G. M., DAUGIRDAS, J. T., GREENE, T. H., KOTANKO, P., LARIVE, B., PIERRATOS, A. & STOKES, J. B. 2014. Effects of daily hemodialysis on heart rate variability: results from the Frequent Hemodialysis Network (FHN) Daily Trial. *Nephrol Dial Transplant,* 29**,** 168-78.

CHAN, C. T., HANLY, P., GABOR, J., PICTON, P., PIERRATOS, A. & FLORAS, J. S. 2004. Impact of nocturnal hemodialysis on the variability of heart rate and duration of hypoxemia during sleep. *Kidney Int,* 65**,** 661-5.

CHAN, C. T., JAIN, V., PICTON, P., PIERRATOS, A. & FLORAS, J. S. 2005. Nocturnal hemodialysis increases arterial baroreflex sensitivity and compliance and normalizes blood pressure of hypertensive patients with end-stage renal disease. *Kidney Int,* 68**,** 338-44.

CHAN, C. T., LEVIN, N. W., CHERTOW, G. M., LARIVE, B., SCHULMAN, G. & KOTANKO, P. 2010. Determinants of cardiac autonomic dysfunction in ESRD. *Clin J Am Soc Nephrol,* 5**,** 1821-7.

CHAN, J. Y., WANG, L. L., WU, K. L. & CHAN, S. H. 2001. Reduced functional expression and molecular synthesis of inducible nitric oxide synthase in rostral ventrolateral medulla of spontaneously hypertensive rats. *Circulation,* 104**,** 1676-81.

CHANDOLA, T., BRITTON, A., BRUNNER, E., HEMINGWAY, H., MALIK, M., KUMARI, M., BADRICK, E., KIVIMAKI, M. & MARMOT, M. 2008. Work stress and coronary heart disease: what are the mechanisms? *Eur Heart J,* 29**,** 640-8.

CHAPLEAU, M. W. & SABHARWAL, R. 2011. Methods of assessing vagus nerve activity and reflexes. *Heart Fail Rev,* 16**,** 109-27.

CHAPLEAU, M. W., HAJDUCZOK, G. & ABBOUD, F. M. 1989. Pulsatile activation of baroreceptors causes central facilitation of baroreflex. *Am J Physiol,* 256**,** H1735-41.

CHAPMAN, A. B., JOHNSON, A. M., RAINGUET, S., HOSSACK, K., GABOW, P. & SCHRIER, R. W. 1997. Left ventricular hypertrophy in autosomal dominant polycystic kidney disease. *J Am Soc Nephrol,* 8**,** 1292-7.

CHEN, C. Y. & DICARLO, S. E. 1996. Daily exercise and gender influence arterial baroreflex regulation of heart rate and nerve activity. *Am J Physiol,* 271**,** H1840-8.

CHESTERTON, L. J. & MCINTYRE, C. W. 2005. The assessment of baroreflex sensitivity in patients with chronic kidney disease: implications for vasomotor instability. *Curr Opin Nephrol Hypertens,* 14**,** 586-91.

CHESTERTON, L. J., SELBY, N. M., BURTON, J. O., FIALOVA, J., CHAN, C. & MCINTYRE, C. W. 2010. Categorization of the hemodynamic response to hemodialysis: the importance of baroreflex sensitivity. *Hemodial Int,* 14**,** 18-28.

CHESTERTON, L. J., SIGRIST, M. K., BENNETT, T., TAAL, M. W. & MCINTYRE, C. W. 2005. Reduced baroreflex sensitivity is associated with increased vascular calcification and arterial stiffness. *Nephrol Dial Transplant,* 20**,** 1140-7.

CHEVALIER, R. L. 2006. Pathogenesis of renal injury in obstructive uropathy. *Curr Opin Pediatr,* 18**,** 153-60.

CHIANCA, D. A., JR. & MACHADO, B. H. 1996. Microinjection of NMDA antagonist into the NTS of conscious rats blocks the Bezold-Jarisch reflex. *Brain Res,* 718**,** 185-8.

CICE, G., FERRARA, L., D'ANDREA, A., D'ISA, S., DI BENEDETTO, A., CITTADINI, A., RUSSO, P. E., GOLINO, P. & CALABRO, R. 2003. Carvedilol increases two-year survivalin dialysis patients with dilated cardiomyopathy: a prospective, placebo-controlled trial. *J Am Coll Cardiol,* 41**,** 1438-44.

CIRIELLO, J. & DE OLIVEIRA, C. V. 2002. Renal afferents and hypertension. *Curr Hypertens Rep,* 4**,** 136-42.

COGGINS, C. H., BREYER LEWIS, J., CAGGIULA, A. W., CASTALDO, L. S., KLAHR, S. & WANG, S. R. 1998. Differences between women and men with chronic renal disease. *Nephrol Dial Transplant,* 13**,** 1430-7.

COLEMAN, T. G. 1980. Arterial baroreflex control of heart rate in the conscious rat. *Am J Physiol,* 238**,** H515-20.

COLLINS, A. J. 2003. Cardiovascular mortality in end-stage renal disease. *Am J Med Sci,* 325**,** 163-7.

COLLINS, A. J., FOLEY, R. N., GILBERTSON, D. T. & CHEN, S. C. 2009. The state of chronic kidney disease, ESRD, and morbidity and mortality in the first year of dialysis. *Clin J Am Soc Nephrol,* 4 Suppl 1**,** S5-11.

COLLINS, A. J., LI, S., MA, J. Z. & HERZOG, C. 2001. Cardiovascular disease in end-stage renal disease patients. *Am J Kidney Dis,* 38**,** S26-9.

COMPERAT, E., FERLICOT, S., CAMPARO, P., ESCHWEGE, P., BA, N., BENOIT, G., BEDOSSA, P. & PARADIS, V. 2006. Expression of epidermal growth factor receptor and proliferative activity of cyst epithelium in human renal cystic diseases. *Urol Int,* 76**,** 269-73.

CONVERSE, R. L., JR., JACOBSEN, T. N., TOTO, R. D., JOST, C. M., COSENTINO, F., FOUAD-TARAZI, F. & VICTOR, R. G. 1992. Sympathetic overactivity in patients with chronic renal failure. *N Engl J Med,* 327**,** 1912-8.

CONVERTINO, V. A. 1998. Gender differences in autonomic functions associated with blood pressure regulation. *Am J Physiol,* 275**,** R1909-20.

COOPER, V. L. & HAINSWORTH, R. 2008. Head-up sleeping improves orthostatic tolerance in patients with syncope. *Clin Auton Res,* 18**,** 318-24.

COOTE, J. H. & BOTHAMS, V. F. 2001. Cardiac vagal control before, during and after exercise. *Exp Physiol,* 86**,** 811-5.

COOTE, J. H. 2005. A role for the paraventricular nucleus of the hypothalamus in the autonomic control of heart and kidney. *Exp Physiol,* 90**,** 169-73.

COSTA, F., DIEDRICH, A., JOHNSON, B., SULUR, P., FARLEY, G. & BIAGGIONI, I. 2001. Adenosine, a metabolic trigger of the exercise pressor reflex in humans. *Hypertension,* 37**,** 917-22.

COUSER, W. G., REMUZZI, G., MENDIS, S. & TONELLI, M. 2011. The contribution of chronic kidney disease to the global burden of major noncommunicable diseases. *Kidney Int,* 80**,** 1258-70.

COWLEY, B. D., JR., RUPP, J. C., MUESSEL, M. J. & GATTONE, V. H., 2ND 1997. Gender and the effect of gonadal hormones on the progression of inherited polycystic kidney disease in rats. *Am J Kidney Dis,* 29**,** 265-72.

CRAVO, S. L. & MORRISON, S. F. 1993. The caudal ventrolateral medulla is a source of tonic sympathoinhibition. *Brain Res,* 621**,** 133-6.

CROFTON, J. T., OTA, M. & SHARE, L. 1993. Role of vasopressin, the renin-angiotensin system and sex in Dahl salt-sensitive hypertension. *J Hypertens,* 11**,** 1031-8.

CROFTON, J. T., SHARE, L. & BROOKS, D. P. 1988. Pressor responsiveness to and secretion of vasopressin during the estrous cycle. *Am J Physiol,* 255**,** R1041-8.

CULLINAN, W. E., HELMREICH, D. L. & WATSON, S. J. 1996. Fos expression in forebrain afferents to the hypothalamic paraventricular nucleus following swim stress. *J Comp Neurol,* 368**,** 88-99.

CUNHA, R. S., CABRAL, A. M. & VASQUEZ, E. C. 1993. Evidence that the autonomic nervous system plays a major role in the L-NAME-induced hypertension in conscious rats. *Am J Hypertens,* 6**,** 806-9.

DAMPNEY, R. A. 1994. Functional organization of central pathways regulating the cardiovascular system. *Physiol Rev,* 74**,** 323-64.

DAMPNEY, R. A., COLEMAN, M. J., FONTES, M. A., HIROOKA, Y., HORIUCHI, J., LI, Y. W., POLSON, J. W., POTTS, P. D. & TAGAWA, T. 2002. Central mechanisms underlying short- and long-term regulation of the cardiovascular system. *Clin Exp Pharmacol Physiol,* 29**,** 261-8.

DAMPNEY, R. A., TAGAWA, T., HORIUCHI, J., POTTS, P. D., FONTES, M. & POLSON, J. W. 2000. What drives the tonic activity of presympathetic neurons in the rostral ventrolateral medulla? *Clin Exp Pharmacol Physiol,* 27**,** 1049-53.

D'ANGELO, G., MINTZ, J. D., TIDWELL, J. E., SCHREIHOFER, A. M., POLLOCK, D. M. & STEPP, D. W. 2006. Exaggerated cardiovascular stress responses and impaired beta-adrenergic-mediated pressor recovery in obese Zucker rats. *Hypertension,* 48**,** 1109-15.

DAUGIRDAS, J. T. 2001. Pathophysiology of dialysis hypotension: an update. *Am J Kidney Dis,* 38**,** S11-7.

DE BURGH DALY, M. & SCOTT, M. J. 1962. An analysis of the primary cardiovascular reflex effects of stimulation of the carotid body chemoreceptors in the dog. *J Physiol,* 162**,** 555-73.

DE FERRARI, G. M., VANOLI, E., STRAMBA-BADIALE, M., HULL, S. S., JR., FOREMAN, R. D. & SCHWARTZ, P. J. 1991. Vagal reflexes and survival during acute myocardial ischemia in conscious dogs with healed myocardial infarction. *Am J Physiol,* 261**,** H63-9.

DE PAULA, P. M., CASTANIA, J. A., BONAGAMBA, L. G., SALGADO, H. C. & MACHADO, B. H. 1999. Hemodynamic responses to electrical stimulation of the aortic depressor nerve in awake rats. *Am J Physiol,* 277**,** R31-8.

DEERING, J. & COOTE, J. H. 2000. Paraventricular neurones elicit a volume expansion-like change of activity in sympathetic nerves to the heart and kidney in the rabbit. *Exp Physiol,* 85**,** 177-86.

DESIR, G. V. & PEIXOTO, A. J. 2014. Renalase in hypertension and kidney disease. *Nephrol Dial Transplant,* 29**,** 22-8.

DESPAS, F., DETIS, N., DUMONTEIL, N., LABRUNEE, M., BELLON, B., FRANCHITTO, N., GALINIER, M., SENARD, J. M. & PATHAK, A. 2009. Excessive sympathetic activation in heart failure with chronic renal failure: role of chemoreflex activation. *J Hypertens,* 27**,** 1849-54.

DI LEO, R., VITA, G., MESSINA, C. & SAVICA, V. 2005. Autonomic function in elderly uremics studied by spectral analysis of heart rate. *Kidney Int,* 67**,** 1521-5.

DI RIENZO, M., PARATI, G., CASTIGLIONI, P., TORDI, R., MANCIA, G. & PEDOTTI, A. 2001. Baroreflex effectiveness index: an additional measure of baroreflex control of heart rate in daily life. *Am J Physiol Regul Integr Comp Physiol,* 280**,** R744-51.

DIBNER-DUNLAP, M. E. & THAMES, M. D. 1989. Baroreflex control of renal sympathetic nerve activity is preserved in heart failure despite reduced arterial baroreceptor sensitivity. *Circ Res,* 65**,** 1526-35.

DIBNER-DUNLAP, M. E. & THAMES, M. D. 1992. Control of sympathetic nerve activity by vagal mechanoreflexes is blunted in heart failure. *Circulation,* 86**,** 1929-34.

DIBONA, G. F. & JONES, S. Y. 1995. Analysis of renal sympathetic nerve responses to stress. *Hypertension,* 25**,** 531-8.

DIBONA, G. F. & JONES, S. Y. 2003a. Effect of sodium intake on sympathetic and hemodynamic response to thermal receptor stimulation. *Hypertension,* 41**,** 261-5.

DIBONA, G. F. & JONES, S. Y. 2003b. Endogenous angiotensin affects responses to stimulation of baroreceptor afferent nerves. *J Hypertens,* 21**,** 1539-46.

DIBONA, G. F. & KOPP, U. C. 1997. Neural control of renal function. *Physiol Rev,* 77**,** 75-197.

DIBONA, G. F. & SAWIN, L. L. 1985. Renal nerve activity in conscious rats during volume expansion and depletion. *Am J Physiol,* 248**,** F15-23.

DIBONA, G. F. & SAWIN, L. L. 1994. Reflex regulation of renal nerve activity in cardiac failure. *Am J Physiol,* 266**,** R27-39.

DIBONA, G. F. 1994. Neural control of renal function in health and disease. *Clin Auton Res,* 4**,** 69-74.

DIBONA, G. F. 2000a. Nervous kidney. Interaction between renal sympathetic nerves and the renin-angiotensin system in the control of renal function. *Hypertension,* 36**,** 1083-8.

DIBONA, G. F. 2000b. Neural control of the kidney: functionally specific renal sympathetic nerve fibers. *Am J Physiol Regul Integr Comp Physiol,* 279**,** R1517-24.

DIBONA, G. F. 2004. The sympathetic nervous system and hypertension: recent developments. *Hypertension,* 43**,** 147-50.

DIBONA, G. F., JONES, S. Y. & SAWIN, L. L. 1997. Reflex influences on renal nerve activity characteristics in nephrosis and heart failure. *J Am Soc Nephrol,* 8**,** 1232-9.

DIEDRICH, A., JORDAN, J., TANK, J., SHANNON, J. R., ROBERTSON, R., LUFT, F. C., ROBERTSON, D. & BIAGGIONI, I. 2003. The sympathetic nervous system in hypertension: assessment by blood pressure variability and ganglionic blockade. *J Hypertens,* 21**,** 1677-86.

DIMICCO, J. A., GALE, K., HAMILTON, B. & GILLIS, R. A. 1979. GABA receptor control of parasympathetic outflow to heart: characterization and brainstem localization. *Science,* 204**,** 1106-9.

DIMICCO, J. A., SAMUELS, B. C., ZARETSKAIA, M. V. & ZARETSKY, D. V. 2002. The dorsomedial hypothalamus and the response to stress: part renaissance, part revolution. *Pharmacol Biochem Behav,* 71**,** 469-80.

DING, A., KALAIGNANASUNDARAM, P., RICARDO, S. D., ABDELKADER, A., WITTING, P. K., BROUGHTON, B. R., KIM, H. B., WYSE, B. F., PHILLIPS, J. K. & EVANS, R. G. 2012. Chronic treatment with tempol does not significantly ameliorate renal tissue hypoxia or disease progression in a rodent model of polycystic kidney disease. *Clin Exp Pharmacol Physiol,* 39**,** 917-29.

DIWAN, V., GOBE, G. & BROWN, L. 2014. Glibenclamide improves kidney and heart structure and function in the adenine-diet model of chronic kidney disease. *Pharmacol Res,* 79**,** 104-10.

DONOVAN, M. K., WYSS, J. M. & WINTERNITZ, S. R. 1983. Localization of renal sensory neurons using the fluorescent dye technique. *Brain Res,* 259**,** 119-22.

DORWARD, P. K., BURKE, S. L., JANIG, W. & CASSELL, J. 1987. Reflex responses to baroreceptor, chemoreceptor and nociceptor inputs in single renal sympathetic neurones in the rabbit and the effects of anaesthesia on them. *J Auton Nerv Syst,* 18**,** 39-54.

DOS SANTOS, C. M., MOREIRA, E. D., KRIEGER, E. M. & MICHELINI, L. C. 1998. Chronic AT1 receptor blockade alters aortic nerve activity in hypertension. *Hypertension,* 31**,** 973-7.

DOUMAS, M., FASELIS, C., KOKKINOS, P., ANYFANTI, P., TSIOUFIS, C. & PAPADEMETRIOU, V. 2014. Carotid baroreceptor stimulation: a promising approach for the management of resistant hypertension and heart failure. *Curr Vasc Pharmacol,* 12**,** 30-7.

DRINKHILL, M. J. & MARY, D. A. 1989. The effect of stimulation of the atrial receptors on plasma cortisol level in the dog. *J Physiol,* 413**,** 299-313.

DRINKHILL, M. J., HICKS, M. N., MARY, D. A. & PEARSON, M. J. 1988. The effect of stimulation of the atrial receptors on plasma renin activity in the dog. *J Physiol,* 398**,** 411-21.

DU, X. J., DART, A. M. & RIEMERSMA, R. A. 1994. Sex differences in the parasympathetic nerve control of rat heart. *Clin Exp Pharmacol Physiol,* 21**,** 485-93.

DUBEY, R. K. & JACKSON, E. K. 2001. Estrogen-induced cardiorenal protection: potential cellular, biochemical, and molecular mechanisms. Am J Physiol Renal Physiol, 280, F365-88.

DUBEY, R. K., OPARIL, S., IMTHURN, B. & JACKSON, E. K. 2002. Sex hormones and hypertension. *Cardiovasc Res,* 53**,** 688-708.

DURSUN, B., DEMIRCIOGLU, F., VARAN, H. I., BASARICI, I., KABUKCU, M., ERSOY, F., ERSEL, F. & SULEYMANLAR, G. 2004. Effects of different dialysis modalities on cardiac autonomic dysfunctions in end-stage renal disease patients: one year prospective study. *Ren Fail,* 26**,** 35-8.

EASTON, J. & HOWE, A. 1983. The distribution of thoracic glomus tissue (aortic bodies) in the rat. *Cell Tissue Res,* 232**,** 349-56.

ECDER, T. & SCHRIER, R. W. 2004. Hypertension and left ventricular hypertrophy in autosomal dominant polycystic kidney disease. *Expert Rev Cardiovasc Ther,* 2**,** 369-74.

EDWARDS, N. C., STEEDS, R. P., STEWART, P. M., FERRO, C. J. & TOWNEND, J. N. 2009. Effect of spironolactone on left ventricular mass and aortic stiffness in early-stage chronic kidney disease: a randomized controlled trial. *J Am Coll Cardiol,* 54**,** 505-12.

ELECTROPHYSIOLOGY, 1996. Heart rate variability: standards of measurement, physiological interpretation and clinical use. Task Force of the European Society of Cardiology and the North American Society of Pacing and Electrophysiology. *Circulation,* 93, 1043-65.

ENDEMANN, D. H. & SCHIFFRIN, E. L. 2004. Endothelial dysfunction. *J Am Soc Nephrol,* 15**,** 1983-92.

ERAMI, C., ZHANG, H., HO, J. G., FRENCH, D. M. & FABER, J. E. 2002. Alpha(1)-adrenoceptor stimulation directly induces growth of vascular wall in vivo. *Am J Physiol Heart Circ Physiol,* 283**,** H1577-87.

ERIKSEN, B. O. & INGEBRETSEN, O. C. 2006. The progression of chronic kidney disease: a 10-year population-based study of the effects of gender and age. *Kidney Int,* 69**,** 375-82.

ESLER, M. 1992. The autonomic nervous system and cardiac arrhythmias. *Clin Auton Res,* 2**,** 133-5.

ESLER, M. D., KRUM, H., SCHLAICH, M., SCHMIEDER, R. E., BOHM, M. & SOBOTKA, P. A. 2012. Renal sympathetic denervation for treatment of drug-resistant hypertension: one-year results from the symplicity HTN-2 randomized, controlled trial. *Circulation,* 126**,** 2976-82.

ESLER, M., JENNINGS, G. & LAMBERT, G. 1989. Measurement of overall and cardiac norepinephrine release into plasma during cognitive challenge. *Psychoneuroendocrinology,* 14**,** 477-81.

ESLER, M., JENNINGS, G., LAMBERT, G., MEREDITH, I., HORNE, M. & EISENHOFER, G. 1990. Overflow of catecholamine neurotransmitters to the circulation: source, fate, and functions. *Physiol Rev,* 70**,** 963-85.

ESLER, M., LAMBERT, G., BRUNNER-LA ROCCA, H. P., VADDADI, G. & KAYE, D. 2003. Sympathetic nerve activity and neurotransmitter release in humans: translation from pathophysiology into clinical practice. *Acta Physiol Scand,* 177**,** 275-84.

EVANSON, N. K., VAN HOOREN, D. C. & HERMAN, J. P. 2009. GluR5-mediated glutamate signaling regulates hypothalamo-pituitary-adrenocortical stress responses at the paraventricular nucleus and median eminence. *Psychoneuroendocrinology,* 34**,** 1370-9.

FACCHINI, M., DE FERRARI, G. M., BONAZZI, O., WEISS, T. & SCHWARTZ, P. J. 1991. Effect of reflex vagal activation on frequency of ventricular premature complexes. *Am J Cardiol,* 68**,** 349-54.

FADEL, P. J., ZHAO, W. & THOMAS, G. D. 2003. Impaired vasomodulation is associated with reduced neuronal nitric oxide synthase in skeletal muscle of ovariectomized rats. *J Physiol,* 549**,** 243-53.

FAGIUS, J. & WALLIN, B. G. 1993. Long-term variability and reproducibility of resting human muscle nerve sympathetic activity at rest, as reassessed after a decade. *Clin Auton Res,* 3**,** 201-5.

FALL, P. J. & PRISANT, L. M. 2005. Polycystic kidney disease. *J Clin Hypertens (Greenwich),* 7**,** 617-9, 625.

FAN, W. & ANDRESEN, M. C. 1998. Differential frequency-dependent reflex integration of myelinated and nonmyelinated rat aortic baroreceptors. *Am J Physiol,* 275**,** H632-40.

FAN, W., SCHILD, J. H. & ANDRESEN, M. C. 1999. Graded and dynamic reflex summation of myelinated and unmyelinated rat aortic baroreceptors. *Am J Physiol,* 277**,** R748-56.

FEDECOSTANTE, M., SPANNELLA, F., COLA, G., ESPINOSA, E., DESSI-FULGHERI, P. & SARZANI, R. 2014. Chronic kidney disease is characterized by "double trouble" higher pulse pressure plus night-time systolic blood pressure and more severe cardiac damage. *PLoS One,* 9**,** e86155.

FERRARI, A., GORDON, F. J. & MARK, A. L. 1984. Impairment of cardiopulmonary baroreflexes in Dahl salt-sensitive rats fed low salt. *Am J Physiol,* 247**,** H119-23.

FOLEY, R. N., PARFREY, P. S., HARNETT, J. D., KENT, G. M., MURRAY, D. C. & BARRE, P. E. 1996. Impact of hypertension on cardiomyopathy, morbidity and mortality in end-stage renal disease. *Kidney Int,* 49**,** 1379-85.

FONTES, M. A., TAGAWA, T., POLSON, J. W., CAVANAGH, S. J. & DAMPNEY, R. A. 2001. Descending pathways mediating cardiovascular response from dorsomedial hypothalamic nucleus. *Am J Physiol Heart Circ Physiol,* 280**,** H2891-901.

FONTES, M. A., XAVIER, C. H., DE MENEZES, R. C. & DIMICCO, J. A. 2011. The dorsomedial hypothalamus and the central pathways involved in the cardiovascular response to emotional stress. *Neuroscience,* 184**,** 64-74.

FONTES, M. A., XAVIER, C. H., MARINS, F. R., LIMBORCO-FILHO, M., VAZ, G. C., MULLER-RIBEIRO, F. C. & NALIVAIKO, E. 2014. Emotional stress and sympathetic activity: Contribution of dorsomedial hypothalamus to cardiac arrhythmias. *Brain Res,* 1554, 49-58.

FOSS, J. D., FINK, G. D. & OSBORN, J. W. 2013. Reversal of genetic salt-sensitive hypertension by targeted sympathetic ablation. *Hypertension,* 61**,** 806-11.

FRANCHINI, K. G. & KRIEGER, E. M. 1992. Carotid chemoreceptors influence arterial pressure in intact and aortic-denervated rats. *Am J Physiol,* 262**,** R677-83.

FRANCZYK-SKORA, B., GLUBA, A., BANACH, M., KOZLOWSKI, D., MALYSZKO, J. & RYSZ, J. 2012. Prevention of sudden cardiac death in patients with chronic kidney disease. *BMC Nephrol,* 13**,** 162.

FRANK, H., HEUSSER, K., HOFFKEN, B., HUBER, P., SCHMIEDER, R. E. & SCHOBEL, H. P. 2004. Effect of erythropoietin on cardiovascular prognosis parameters in hemodialysis patients. *Kidney Int,* 66**,** 832-40.

FRANK, V., HABBIG, S., BARTRAM, M. P., EISENBERGER, T., VEENSTRA-KNOL, H. E., DECKER, C., BOORSMA, R. A., GOBEL, H., NURNBERG, G., GRIESSMANN, A., FRANKE, M., BORGAL, L., KOHLI, P., VOLKER, L. A., DOTSCH, J., NURNBERG, P., BENZING, T., BOLZ, H. J., JOHNSON, C., GERKES, E. H., SCHERMER, B. &

BERGMANN, C. 2013. Mutations in NEK8 link multiple organ dysplasia with altered Hippo signalling and increased c-MYC expression. *Hum Mol Genet,* 22**,** 2177-85.

FREY, M. A., TOMASELLI, C. M. & HOFFLER, W. G. 1994. Cardiovascular responses to postural changes: differences with age for women and men. *J Clin Pharmacol,* 34**,** 394-402.

FUJITA, M., ANDO, K., KAWARAZAKI, H., KAWARASAKI, C., MURAOKA, K., OHTSU, H., SHIMIZU, H. & FUJITA, T. 2012. Sympathoexcitation by brain oxidative stress mediates arterial pressure elevation in salt-induced chronic kidney disease. *Hypertension,* 59**,** 105-12.

FURCHGOTT, R. F. & JOTHIANANDAN, D. 1991. Endothelium-dependent and -independent vasodilation involving cyclic GMP: relaxation induced by nitric oxide, carbon monoxide and light. *Blood Vessels,* 28**,** 52-61.

FURGESON, S. B. & CHONCHOL, M. 2008. Beta-blockade in chronic dialysis patients. *Semin Dial,* 21**,** 43-8.

FURLONG, T. M., MCDOWALL, L. M., HORIUCHI, J., POLSON, J. W. & DAMPNEY, R. A. 2014. The effect of air puff stress on c-Fos expression in rat hypothalamus and brainstem: central circuitry mediating sympathoexcitation and baroreflex resetting. *Eur J Neurosci.*

FURNIVAL, C. M., LINDEN, R. J. & SNOW, H. M. 1971. Reflex effects on the heart of stimulating left atrial receptors. *J Physiol,* 218**,** 447-63.

FURUKAWA, Y., WALLICK, D. W., MARTIN, P. J. & LEVY, M. N. 1990. Chronotropic and dromotropic responses to stimulation of intracardiac sympathetic nerves to sinoatrial or atrioventricular nodal region in anesthetized dogs. *Circ Res,* 66**,** 1391-9.

GABOW, P. A., CHAPMAN, A. B., JOHNSON, A. M., TANGEL, D. J., DULEY, I. T., KAEHNY, W. D., MANCO-JOHNSON, M. & SCHRIER, R. W. 1990. Renal structure and hypertension in autosomal dominant polycystic kidney disease. *Kidney Int,* 38**,** 1177-80.

GAGNADOUX, M. F., BACRI, J. L., BROYER, M. & HABIB, R. 1989. Infantile chronic tubulo-interstitial nephritis with cortical microcysts: variant of nephronophthisis or new disease entity? *Pediatr Nephrol,* 3**,** 50-5.

GAO, L., WANG, W. Z., WANG, W. & ZUCKER, I. H. 2008. Imbalance of angiotensin type 1 receptor and angiotensin II type 2 receptor in the rostral ventrolateral medulla: potential mechanism for sympathetic overactivity in heart failure. *Hypertension,* 52**,** 708-14.

GAO, L., WANG, W., LI, Y. L., SCHULTZ, H. D., LIU, D., CORNISH, K. G. & ZUCKER, I. H. 2005. Sympathoexcitation by central ANG II: roles for AT1 receptor upregulation and NAD(P)H oxidase in RVLM. *Am J Physiol Heart Circ Physiol,* 288**,** H2271-9.

GARCIA PEREZ, M. & JORDAN, D. 2001. Effect of stimulating non-myelinated vagal axons on atrio-ventricular conduction and left ventricular function in anaesthetized rabbits. *Auton Neurosci,* 86**,** 183-91.

GATTONE, V. H., 2ND, SIQUEIRA, T. M., JR., POWELL, C. R., TRAMBAUGH, C. M., LINGEMAN, J. E. & SHALHAV, A. L. 2008. Contribution of renal innervation to hypertension in rat autosomal dominant polycystic kidney disease. *Exp Biol Med (Maywood),* 233**,** 952-7.

GILBEY, M. P. 2007. Sympathetic rhythms and nervous integration. *Clin Exp Pharmacol Physiol,* 34**,** 356-61.

GIORDANO, M., MANZELLA, D., PAOLISSO, G., CALIENDO, A., VARRICCHIO, M. & GIORDANO, C. 2001. Differences in heart rate variability parameters during the post-dialytic period in type II diabetic and non-diabetic ESRD patients. *Nephrol Dial Transplant,* 16**,** 566-73.

GODDARD, J. & TURNER, A. N. 2014. Kidney and urinary tract disease *In:* WALKER, B. R., COLLEDGE, N. R., RALSTON, S. H. & PENMAN, I. D. (eds.) *Davidson's Principles and Practice of Medicine.* 22th ed. Philadelphia, USA: Churchill Livingstone Elsevier.

GOLDMAN, R. K., AZAR, A. S., MULVANEY, J. M., HINOJOSA-LABORDE, C., HAYWOOD, J. R. & BROOKS, V. L. 2009. Baroreflex sensitivity varies during the rat estrous cycle: role of gonadal steroids. Am J Physiol Regul Integr Comp Physiol, 296, R1419-26.

GONZALEZ, C., ALMARAZ, L., OBESO, A. & RIGUAL, R. 1994. Carotid body chemoreceptors: from natural stimuli to sensory discharges. *Physiol Rev,* 74**,** 829-98.

GONZALEZ, E. R., KRIEGER, A. J. & SAPRU, H. N. 1983. Central resetting of baroreflex in the spontaneously hypertensive rat. *Hypertension,* 5**,** 346-52.

GONZALO, A., GALLEGO, A., RIVERA, M., ORTE, L. & ORTUNO, J. 1996. Influence of hypertension on early renal insufficiency in autosomal dominant polycystic kidney disease. *Nephron,* 72**,** 225-30.

GORDON, F. J. & MARK, A. L. 1984. Mechanism of impaired baroreflex control in prehypertensive Dahl salt-sensitive rats. *Circ Res,* 54**,** 378-87.

GOUTY, S., REGALIA, J. & HELKE, C. J. 2001. Attenuation of the afferent limb of the baroreceptor reflex in streptozotocin-induced diabetic rats. *Auton Neurosci,* 89**,** 86-95.

GRASSI, G. 2001. Renin-angiotensin-sympathetic crosstalks in hypertension: reappraising the relevance of peripheral interactions. *J Hypertens,* 19**,** 1713-6.

GRASSI, G., BERTOLI, S. & SERAVALLE, G. 2012. Sympathetic nervous system: role in hypertension and in chronic kidney disease. *Curr Opin Nephrol Hypertens,* 21**,** 46-51.

GRASSI, G., GIANNATTASIO, C., CLEROUX, J., CUSPIDI, C., SAMPIERI, L., BOLLA, G. B. & MANCIA, G. 1988. Cardiopulmonary reflex before and after regression of left ventricular hypertrophy in essential hypertension. *Hypertension,* 12**,** 227-37.

GRASSI, G., PARATI, G., POMIDOSSI, G., GIANNATTASIO, C., CASADEI, R., BOLLA, G. B., CASATI, S., GRAZIANI, G. & MANCIA, G. 1987. Effects of haemodialysis and kidney transplantation on carotid and cardiopulmonary baroreflexes in uremic patients. *J Hypertens,* 5**,** S367–9.

GRASSI, G., QUARTI-TREVANO, F., SERAVALLE, G., ARENARE, F., VOLPE, M., FURIANI, S., DELL'ORO, R. & MANCIA, G. 2011a. Early sympathetic activation in the initial clinical stages of chronic renal failure. *Hypertension,* 57**,** 846-51.

GRASSI, G., SERAVALLE, G., GHIADONI, L., TRIPEPI, G., BRUNO, R. M., MANCIA, G. & ZOCCALI, C. 2011b. Sympathetic nerve traffic and asymmetric dimethylarginine in chronic kidney disease. *Clin J Am Soc Nephrol,* 6**,** 2620-7.

GRASSI, G., TREVANO, F. Q., SERAVALLE, G., SCOPELLITI, F. & MANCIA, G. 2006. Baroreflex function in hypertension: consequences for antihypertensive therapy. *Prog Cardiovasc Diss,* 48**,** 407-15.

GRAY, A. L., JOHNSON, T. A., ARDELL, J. L. & MASSARI, V. J. 2004. Parasympathetic control of the heart. II. A novel interganglionic intrinsic cardiac circuit mediates neural control of heart rate. *J Appl Physiol (1985),* 96**,** 2273-8.

GREENWOOD, J. P., STOKER, J. B. & MARY, D. A. 1999. Single-unit sympathetic discharge : quantitative assessment in human hypertensive disease. *Circulation,* 100**,** 1305-10.

GRISK, O. & RETTIG, R. 2004. Interactions between the sympathetic nervous system and the kidneys in arterial hypertension. *Cardiovasc Res,* 61**,** 238-46.

GU, H., ZHANG, Z. H., EPSTEIN, P. N., LI, L., HARDEN, S. W., WURSTER, R. D. & CHENG, Z. J. 2009. Impaired baroreflex control of renal sympathetic nerve activity in type 1 diabetic mice (OVE26). *Neuroscience,* 161**,** 78-85.

GU, R., LU, W., XIE, J., BAI, J. & XU, B. 2011. Renalase deficiency in heart failure model of rats-a potential mechanism underlying circulating norepinephrine accumulation. *PLoS One,* 6**,** e14633.

GUAY-WOODFORD, L. M. 2003. Murine models of polycystic kidney disease: molecular and therapeutic insights. *Am J Physiol Renal Physiol,* 285**,** F1034-49.

GUILD, S. J., MCBRYDE, F. D., MALPAS, S. C. & BARRETT, C. J. 2012. High dietary salt and angiotensin II chronically increase renal sympathetic nerve activity: a direct telemetric study. *Hypertension,* 59**,** 614-20.

GUIMARAES, S. & MOURA, D. 2001. Vascular adrenoceptors: an update. *Pharmacol Rev,* 53**,** 319-56.

GUIZAR-MENDOZA, J. M., AMADOR-LICONA, N., LOZADA, E. E., RODRIGUEZ, L., GUTIERREZ-NAVARRO, M., DUBEY-ORTEGA, L. A., TREJO-BELLIDO, J., ENCARNACION JDE, J. & RUIZ-JARAMILLO MDE, L. 2006. Left ventricular mass and heart sympathetic activity after renal transplantation in children and young adults. *Pediatr Nephrol,* 21**,** 1413-8.

GULATI, A., REBELLO, S. & KUMAR, A. 1997. Role of sympathetic nervous system in cardiovascular effects of centrally administered endothelin-1 in rats. *Am J Physiol,* 273**,** H1177-86.

GUYENET, P. & KOSHIYA, N. 1992. Respiratory-Sympathetic Integration in the Medulla Oblongata. *In:* KUNOS, G. & CIRIELLO, J. (eds.) *Central Neural Mechanisms in Cardiovascular Regulation.* Birkhäuser Boston.

GUYENET, P. G. & KOSHIYA, N. 1995. Working model of the sympathetic chemoreflex in rats. *Clin Exp Hypertens,* 17**,** 167-79.

GUYENET, P. G. 2006. The sympathetic control of blood pressure. *Nat Rev Neurosci,* 7**,** 335-46.

GUYENET, P. G., BAYLISS, D. A., STORNETTA, R. L., FORTUNA, M. G., ABBOTT, S. B. & DEPUY, S. D. 2009. Retrotrapezoid nucleus, respiratory chemosensitivity and breathing automaticity. *Respir Physiol Neurobiol,* 168**,** 59-68.

GUYENET, P. G., DARNALL, R. A. & RILEY, T. A. 1990. Rostral ventrolateral medulla and sympathorespiratory integration in rats. *Am J Physiol,* 259**,** R1063-74.

GUYENET, P. G., FILTZ, T. M. & DONALDSON, S. R. 1987. Role of excitatory amino acids in rat vagal and sympathetic baroreflexes. *Brain Res,* 407**,** 272-84.

GUYENET, P. G., STORNETTA, R. L., ABBOTT, S. B., DEPUY, S. D., FORTUNA, M. G. & KANBAR, R. 2010. Central CO2 chemoreception and integrated neural mechanisms of cardiovascular and respiratory control. *J Appl Physiol (1985),* 108**,** 995-1002.

GUYTON, A. C. & COLEMAN, T. G. 1999. Quantitative analysis of the pathophysiology of hypertension. 1969. *J Am Soc Nephrol,* 10**,** 2248-58.

HABLER, H. J., JANIG, W., KRUMMEL, M. & PETERS, O. A. 1994. Reflex patterns in postganglionic neurons supplying skin and skeletal muscle of the rat hindlimb. *J Neurophysiol,* 72**,** 2222-36.

HAGBARTH, K. E., HALLIN, R. G., HONGELL, A., TOREBJORK, H. E. & WALLIN, B. G. 1972. General characteristics of sympathetic activity in human skin nerves. *Acta Physiol Scand,* 84**,** 164-76.

HAIBARA, A. S., COLOMBARI, E., CHIANCA, D. A., JR., BONAGAMBA, L. G. & MACHADO, B. H. 1995. NMDA receptors in NTS are involved in bradycardic but not in pressor response of chemoreflex. *Am J Physiol,* 269**,** H1421-7.

HAINSWORTH, R. 1991. Reflexes from the heart. *Physiol Rev,* 71**,** 617-58.

HAINSWORTH, R. 2014. Cardiovascular control from cardiac and pulmonary vascular receptors. *Exp Physiol,* 99**,** 312-9.

HALL, J. E., BRANDS, M. W., ZAPPE, D. H. & ALONSO GALICIA, M. 1995. Insulin resistance, hyperinsulinemia, and hypertension: causes, consequences, or merely correlations? *Proc Soc Exp Biol Med,* 208**,** 317-29.

HAMZA, S. M. & HALL, J. E. 2012. Direct recording of renal sympathetic nerve activity in unrestrained, conscious mice. *Hypertension,* 60**,** 856-64.

HARADA, S., TOKUNAGA, S., MOMOHARA, M., MASAKI, H., TAGAWA, T., IMAIZUMI, T. & TAKESHITA, A. 1993. Inhibition of nitric oxide formation in the nucleus tractus solitarius increases renal sympathetic nerve activity in rabbits. *Circ Res,* 72**,** 511-6.

HARRIS, D. C. & RANGAN, G. K. 2005. Retardation of kidney failure - applying principles to practice. *Ann Acad Med Singapore,* 34**,** 16-23.

HARRISON, J. L., HILDRETH, C. M., CALLAHAN, S. M., GOODCHILD, A. K. & PHILLIPS, J. K. 2010. Cardiovascular autonomic dysfunction in a novel rodent model of polycystic kidney disease. *Auton Neurosci,* 152**,** 60-6.

HART, E. C., MCBRYDE, F. D., BURCHELL, A. E., RATCLIFFE, L. E., STEWART, L. Q., BAUMBACH, A., NIGHTINGALE, A. & PATON, J. F. 2013. Translational examination of changes in baroreflex function after renal denervation in hypertensive rats and humans. *Hypertension,* 62**,** 533-41.

HATTON, D. C., BROOKS, V., QI, Y. & MCCARRON, D. A. 1997. Cardiovascular response to stress: baroreflex resetting and hemodynamics. *Am J Physiol,* 272**,** R1588-94.

HAUSBERG, M., KOSCH, M., HARMELINK, P., BARENBROCK, M., HOHAGE, H., KISTERS, K., DIETL, K. H. & RAHN, K. H. 2002. Sympathetic nerve activity in end-stage renal disease. *Circulation,* 106**,** 1974-9.

HAUSBERG, M., TOKMAK, F., PAVENSTADT, H., KRAMER, B. K. & RUMP, L. C. 2010. Effects of moxonidine on sympathetic nerve activity in patients with end-stage renal disease. *J Hypertens,* 28**,** 1920-7.

HAYANO, J., YASUMA, F., OKADA, A., MUKAI, S. & FUJINAMI, T. 1996. Respiratory sinus arrhythmia. A phenomenon improving pulmonary gas exchange and circulatory efficiency. *Circulation,* 94**,** 842-7.

HAYWOOD, J. R. & HINOJOSA-LABORDE, C. 1997. Sexual dimorphism of sodium-sensitive renal-wrap hypertension. *Hypertension,* 30**,** 667-71.

HAYWOOD, J. R., WILLIAMS, S. F. & BALL, N. A. 1984. Contribution of sodium to the mechanism of one-kidney, renal-wrap hypertension. *Am J Physiol,* 247**,** H797-803.

HEAD, G. A. & BURKE, S. L. 2001. Renal and cardiac sympathetic baroreflexes in hypertensive rabbits. *Clin Exp Pharmacol Physiol,* 28**,** 972-5.

HEAD, G. A. & BURKE, S. L. 2004. Sympathetic responses to stress and rilmenidine in 2K1C rabbits: evidence of enhanced nonvascular effector mechanism. *Hypertension,* 43**,** 636-42.

HEAD, G. A. & MCCARTY, R. 1987. Vagal and sympathetic components of the heart rate range and gain of the baroreceptor-heart rate reflex in conscious rats. *J Auton Nerv Syst,* 21**,** 203-13.

HEAD, G. A. 2003. The sympathetic nervous system in hypertension: assessment by blood pressure variability and ganglionic blockade. *J Hypertens,* 21**,** 1619-21.

HEDNER, J., EJNELL, H., SELLGREN, J., HEDNER, T. & WALLIN, G. 1988. Is high and fluctuating muscle nerve sympathetic activity in the sleep apnoea syndrome of pathogenetic importance for the development of hypertension? *J Hypertens Suppl,* 6**,** S529-31.

HEIDBREDER, E., SCHAFFERHANS, K. & HEIDLAND, A. 1985. Disturbances of peripheral and autonomic nervous system in chronic renal failure: effects of hemodialysis and transplantation. *Clin Nephrol,* 23**,** 222-8.

HERING, D., LAMBERT, E. A., MARUSIC, P., WALTON, A. S., KRUM, H., LAMBERT, G. W., ESLER, M. D. & SCHLAICH, M. P. 2013. Substantial reduction in single sympathetic nerve firing after renal denervation in patients with resistant hypertension. *Hypertension,* 61**,** 457-64.

HERING, D., MAHFOUD, F., WALTON, A. S., KRUM, H., LAMBERT, G. W., LAMBERT, E. A., SOBOTKA, P. A., BOHM, M., CREMERS, B., ESLER, M. D. & SCHLAICH, M. P. 2012. Renal denervation in moderate to severe CKD. *J Am Soc Nephrol,* 23**,** 1250-7.

HERING, D., MARUSIC, P., WALTON, A. S., LAMBERT, E. A., KRUM, H., NARKIEWICZ, K., LAMBERT, G. W., ESLER, M. D. & SCHLAICH, M. P. 2014. Sustained sympathetic and blood pressure reduction 1 year after renal denervation in patients with resistant hypertension. *Hypertension,* 64**,** 118-24.

HERING, D., ZDROJEWSKI, Z., KROL, E., KARA, T., KUCHARSKA, W., SOMERS, V. K., RUTKOWSKI, B. & NARKIEWICZ, K. 2007. Tonic chemoreflex activation contributes to the elevated muscle sympathetic nerve activity in patients with chronic renal failure. *J Hypertens,* 25**,** 157-61.

HERZOG, C. A. 2003. Cardiac arrest in dialysis patients: approaches to alter an abysmal outcome. *Kidney Int Suppl,* 84**,** S197-200.

HERZOG, C. A., MA, J. Z. & COLLINS, A. J. 1998. Poor long-term survival after acute myocardial infarction among patients on long-term dialysis. *N Engl J Med,* 339**,** 799-805.

HEUSSER, K., TANK, J., ENGELI, S., DIEDRICH, A., MENNE, J., ECKERT, S., PETERS, T., SWEEP, F. C., HALLER, H., PICHLMAIER, A. M., LUFT, F. C. & JORDAN, J. 2010. Carotid baroreceptor stimulation, sympathetic activity, baroreflex function, and blood pressure in hypertensive patients. *Hypertension,* 55**,** 619-26.

HIGUCHI, S., MORGAN, D. A. & MARK, A. L. 1988. Contrasting reflex effects of chemosensitive and mechanosensitive vagal afferents. *Hypertension,* 11**,** 674-9.

HILDEBRANDT, F. & OTTO, E. 2005. Cilia and centrosomes: a unifying pathogenic concept for cystic kidney disease? *Nat Rev Genet,* 6**,** 928-40.

HILDEBRANDT, F. & ZHOU, W. 2007. Nephronophthisis-associated ciliopathies. *J Am Soc Nephrol,* 18**,** 1855-71.

HILDEBRANDT, F., ATTANASIO, M. & OTTO, E. 2009. Nephronophthisis: disease mechanisms of a ciliopathy. *J Am Soc Nephrol,* 20**,** 23-35.

HILDEBRANDT, F., WALDHERR, R., KUTT, R. & BRANDIS, M. 1992. The nephronophthisis complex: clinical and genetic aspects. *Clin Investig,* 70**,** 802-8.

HILDRETH, C. M. 2011. Prognostic indicators of cardiovascular risk in renal disease. *Front Physiol,* 2**,** 121.

HILDRETH, C. M., GOODCHILD, A. K. & PHILLIPS, J. K. 2013a. Insight into Autonomic Nervous System Control of Heart Rate in the Rat Using Analysis of Heart Rate Variability and Baroreflex Sensitivity. *In:* PILOWSKY, P. M., FARNHAM, M. M. J. & FONG, A. Y. (eds.) *Stimulation and Inhibition of Neurons.* New York, USA: Humana Press.

HILDRETH, C. M., KANDUKURI, D. S., GOODCHILD, A. K. & PHILLIPS, J. K. 2013b. Temporal development of baroreceptor dysfunction in a rodent model of chronic kidney disease. *Clinical and Experimental Pharmacology and Physiology,* 40**,** 458-65.

HINOJOSA-LABORDE, C., JONES, S. Y. & DIBONA, G. F. 1994. Hemodynamics and baroreflex function in rats with nephrotic syndrome. *Am J Physiol,* 267**,** R953-64.

HIRAKAWA, N., MORIMOTO, M. & TOTOKI, T. 1993. Sympathetic innervation of the young canine heart using antero- and retrograde axonal tracer methods. *Brain Res Bull,* 31**,** 673-80.

HIROOKA, Y., KISHI, T., SAKAI, K., TAKESHITA, A. & SUNAGAWA, K. 2011. Imbalance of central nitric oxide and reactive oxygen species in the regulation of sympathetic activity and neural mechanisms of hypertension. *Am J Physiol Regul Integr Comp Physiol,* 300**,** R818-26.

HJEMDAHL, P., FAGIUS, J., FREYSCHUSS, U., WALLIN, B. G., DALESKOG, M., BOHLIN, G. & PERSKI, A. 1989. Muscle sympathetic activity and norepinephrine release during mental challenge in humans. *Am J Physiol,* 257**,** E654-64.

HÖCHT, C. 2013. Blood Pressure Variability: Prognostic Value and Therapeutic Implications. *ISRN Hypertension,* 2013**,** 16.

HOGARTH, A. J., MACKINTOSH, A. F. & MARY, D. A. 2007a. The effect of gender on the sympathetic nerve hyperactivity of essential hypertension. *J Hum Hypertens,* 21**,** 239-45.

HOGARTH, A. J., MACKINTOSH, A. F. & MARY, D. A. 2007b. Gender-related differences in the sympathetic vasoconstrictor drive of normal subjects. *Clin Sci,* 112**,** 353-61.

HOOD, S. G. & WOODS, R. L. 2004. Vagal reflex actions of atrial natriuretic peptide survive physiological but not pathological cardiac hypertrophy in rat. *Exp Physiol,* 89**,** 445-54.

HORIUCHI, J., KILLINGER, S. & DAMPNEY, R. A. 2004. Contribution to sympathetic vasomotor tone of tonic glutamatergic inputs to neurons in the RVLM. *Am J Physiol Regul Integr Comp Physiol,* 287**,** R1335-43.

HUANG, J., LUSINA, S., XIE, T., JI, E., XIANG, S., LIU, Y. & WEISS, J. W. 2009. Sympathetic response to chemostimulation in conscious rats exposed to chronic intermittent hypoxia. *Respir Physiol Neurobiol,* 166**,** 102-6.

HUBER, D. A. & SCHREIHOFER, A. M. 2010. Attenuated baroreflex control of sympathetic nerve activity in obese Zucker rats by central mechanisms. *J Physiol,* 588**,** 1515-25.

HUIKURI, H. V., PIKKUJAMSA, S. M., AIRAKSINEN, K. E., IKAHEIMO, M. J., RANTALA, A. O., KAUMA, H., LILJA, M. & KESANIEMI, Y. A. 1996. Sex-related differences in autonomic modulation of heart rate in middle-aged subjects. *Circulation,* 94**,** 122-5.

HUNT, B. E. & FARQUHAR, W. B. 2005. Nonlinearities and asymmetries of the human cardiovagal baroreflex. *Am J Physiol Regul Integr Comp Physiol,* 288**,** R1339-46.

HUNT, B. E., TAYLOR, J. A., HAMNER, J. W., GAGNON, M. & LIPSITZ, L. A. 2001. Estrogen replacement therapy improves baroreflex regulation of vascular sympathetic outflow in postmenopausal women. *Circulation,* 103**,** 2909-14.

ICHINOSE, M., SAITO, M., KONDO, N. & NISHIYASU, T. 2006. Time-dependent modulation of arterial baroreflex control of muscle sympathetic nerve activity during isometric exercise in humans. *Am J Physiol Heart Circ Physiol,* 290**,** H1419-26.

IGARASHI, P. & SOMLO, S. 2002. Genetics and pathogenesis of polycystic kidney disease. *J Am Soc Nephrol,* 13**,** 2384-98.

IRIUCHIJIMA, J. 1997. Why is the hypotensive effect of clonidine greater in hypertensive rats? *Tohoku J Exp Med,* 182**,** 271-6.

ISEKI, K. 2008. Gender differences in chronic kidney disease. *Kidney Int,* 74**,** 415-7.

ISEKI, K., ISEKI, C., IKEMIYA, Y. & FUKIYAMA, K. 1996. Risk of developing end-stage renal disease in a cohort of mass screening. *Kidney Int,* 49**,** 800-5.

IZZO, P. N., DEUCHARS, J. & SPYER, K. M. 1993. Localization of cardiac vagal preganglionic motoneurones in the rat: immunocytochemical evidence of synaptic inputs containing 5-hydroxytryptamine. *J Comp Neurol,* 327**,** 572-83.

JAFAR, T. H., SCHMID, C. H., STARK, P. C., TOTO, R., REMUZZI, G., RUGGENENTI, P., MARCANTONI, C., BECKER, G., SHAHINFAR, S., DE JONG, P. E., DE ZEEUW, D., KAMPER, A. L., STRANGAARD, S. & LEVEY, A. S. 2003. The rate of progression of renal disease may not be slower in women compared with men: a patient-level meta-analysis. *Nephrol Dial Transplant,* 18**,** 2047-53.

JAMES, C., HENDERSON, L. & MACEFIELD, V. G. 2013a. Real-time imaging of brain areas involved in the generation of spontaneous skin sympathetic nerve activity at rest. *Neuroimage,* 74**,** 188-94.

JAMES, C., MACEFIELD, V. G. & HENDERSON, L. A. 2013b. Real-time imaging of cortical and subcortical control of muscle sympathetic nerve activity in awake human subjects. *Neuroimage,* 70**,** 59-65.

JANES, R. D., BRANDYS, J. C., HOPKINS, D. A., JOHNSTONE, D. E., MURPHY, D. A. & ARMOUR, J. A. 1986. Anatomy of human extrinsic cardiac nerves and ganglia. *Am J Cardiol,* 57**,** 299-309.

JÄNIG, W. & HABLER, H. J. 2003. Neurophysiological analysis of target-related sympathetic pathways - from animal to human: similarities and differences. *Acta Physiol Scand,* 177**,** 255-74.

JESKE, I., REIS, D. J. & MILNER, T. A. 1995. Neurons in the barosensory area of the caudal ventrolateral medulla project monosynaptically on to sympathoexcitatory bulbospinal neurons in the rostral ventrolateral medulla. *Neuroscience,* 65**,** 343-53.

JIA, T., OLAUSON, H., LINDBERG, K., AMIN, R., EDVARDSSON, K., LINDHOLM, B., ANDERSSON, G., WERNERSON, A., SABBAGH, Y., SCHIAVI, S. & LARSSON, T. E. 2013. A novel model of adenine-induced tubulointerstitial nephropathy in mice. *BMC Nephrol,* 14**,** 116.

JIN, Y., PERSU, A. & STAESSEN, J. A. 2013. Renal denervation in the management of resistant hypertension: current evidence and perspectives. *Curr Opin Nephrol Hypertens,* 22**,** 511-8.

JOHANSSON, M., ELAM, M., RUNDQVIST, B., EISENHOFER, G., HERLITZ, H., LAMBERT, G. & FRIBERG, P. 1999. Increased sympathetic nerve activity in renovascular hypertension. *Circulation,* 99**,** 2537-42.

JOHANSSON, M., GAO, S. A., FRIBERG, P., ANNERSTEDT, M., BERGSTROM, G., CARLSTROM, J., IVARSSON, T., JENSEN, G., LJUNGMAN, S., MATHILLAS, O., NIELSEN, F. D. & STROMBOM, U. 2005. Reduced baroreflex effectiveness index in hypertensive patients with chronic renal failure. *Am J Hypertens,* 18**,** 995-1000; discussion 1016.

JOHANSSON, M., GAO, S. A., FRIBERG, P., ANNERSTEDT, M., CARLSTROM, J., IVARSSON, T., JENSEN, G., LJUNGMAN, S., MATHILLAS, O., NIELSEN, F. D. & STROMBOM, U. 2007. Baroreflex effectiveness index and baroreflex sensitivity predict all-cause mortality and sudden death in hypertensive patients with chronic renal failure. *J Hypertens,* 25**,** 163-8.

JOHNS, E. J., KOPP, U. C. & DIBONA, G. F. 2011. Neural control of renal function. *Compr Physiol,* 1**,** 731-67.

JOHNSON, M. S., DEMARCO, V. G., HEESCH, C. M., WHALEY-CONNELL, A. T., SCHNEIDER, R. I., REHMER, N. T., TILMON, R. D., FERRARIO, C. M. & SOWERS, J. R. 2011. Sex differences in baroreflex sensitivity, heart rate variability, and end organ damage in the TGR(mRen2)27 rat. *Am J Physiol Heart Circ Physiol,* 301**,** H1540-50.

JOHNSON, P. L. & SHEKHAR, A. 2006. Panic-prone state induced in rats with GABA dysfunction in the dorsomedial hypothalamus is mediated by NMDA receptors. *J Neurosci,* 26**,** 7093-104.

JONES, C. L., BUCH, S., POST, M., MCCULLOCH, L., LIU, E. & EDDY, A. A. 1991. Pathogenesis of interstitial fibrosis in chronic purine aminonucleoside nephrosis. *Kidney Int,* 40**,** 1020-31.

JONES, J. F., WANG, Y. & JORDAN, D. 1998. Activity of C fibre cardiac vagal efferents in anaesthetized cats and rats. *J Physiol,* 507**,** 869-80.

JONES, P. P., SNITKER, S., SKINNER, J. S. & RAVUSSIN, E. 1996. Gender differences in muscle sympathetic nerve activity: effect of body fat distribution. *Am J Physiol,* 270**,** E363-6.

KALIA, M. & SULLIVAN, J. M. 1982. Brainstem projections of sensory and motor components of the vagus nerve in the rat. *J Comp Neurol,* 211**,** 248-65.

KANBAR, R., OREA, V., BARRES, C. & JULIEN, C. 2007. Baroreflex control of renal sympathetic nerve activity during air-jet stress in rats. *Am J Physiol Regul Integr Comp Physiol,* 292**,** R362-7.

KAPLAN, N. M. 2006. Treatment of Hypertension: Drug Therapy. *In:* KAPLAN, N. M. & FLYNN, J. T. (eds.) *Clinical Hypertension.* Philadelphia, USA: Lippincott Williams and Wilkins.

KARIM, F., KIDD, C., MALPUS, C. M. & PENNA, P. E. 1972. The effects of stimulation of the left atrial receptors on sympathetic efferent nerve activity. *J Physiol,* 227**,** 243-60.

KASHIHARA, K. 2009. Roles of arterial baroreceptor reflex during bezold-jarisch reflex. *Curr Cardiol Rev,* 5**,** 263-7.

KASHIHARA, N. & SATOH, M. 2008. Molecular pathogenesis of chronic kidney disease. *Nihon Rinsho,* 66**,** 1671-7.

KATHOLI, R. E., WHITLOW, P. L., WINTERNITZ, S. R. & OPARIL, S. 1982. Importance of the renal nerves in established two-kidney, one clip Goldblatt hypertension. *Hypertension,* 4**,** 166-74.

KAUFMAN, M. P., BAKER, D. G., COLERIDGE, H. M. & COLERIDGE, J. C. 1980. Stimulation by bradykinin of afferent vagal C-fibers with chemosensitive endings in the heart and aorta of the dog. *Circ Res,* 46**,** 476-84.

KAWABE, T., CHITRAVANSHI, V. C., KAWABE, K. & SAPRU, H. N. 2008. Cardiovascular function of a glutamatergic projection from the hypothalamic paraventricular nucleus to the nucleus tractus solitarius in the rat. *Neuroscience,* 153**,** 605-17.

KAWADA, T., SUGIMACHI, M., SHISHIDO, T., MIYANO, H., SATO, T., YOSHIMURA, R., MIYASHITA, H., NAKAHARA, T., ALEXANDER, J., JR. & SUNAGAWA, K. 1999. Simultaneous identification of static and dynamic vagosympathetic interactions in regulating heart rate. *Am J Physiol,* 276**,** R782-9.

KELLETT, D. O., RAMAGE, A. G. & JORDAN, D. 2005. Central 5-HT7 receptors are critical for reflex activation of cardiac vagal drive in anaesthetized rats. *J Physiol,* 563**,** 319-31.

KELLY, D. J., WILKINSON-BERKA, J. L., ALLEN, T. J., COOPER, M. E. & SKINNER, S. L. 1998. A new model of diabetic nephropathy with progressive renal impairment in the transgenic (mRen-2)27 rat (TGR). *Kidney Int,* 54**,** 343-52.

KENT, B. B., DRANE, J. W., BLUMENSTEIN, B. & MANNING, J. W. 1972. A mathematical model to assess changes in the baroreceptor reflex. *Cardiology,* 57**,** 295-310.

KHURANA, R. K. & WU, R. 2006. The cold face test: a non-baroreflex mediated test of cardiac vagal function. *Clin Auton Res,* 16**,** 202-7.

KIDNEY HEALTH AUSTRALIA 2012. *Chronic Kidney Disease (CKD) Management in General Practice (2nd edition),* Melbourne, Kidney Health Australia.

KIM, A., DEO, S. H., VIANNA, L. C., BALANOS, G. M., HARTWICH, D., FISHER, J. P. & FADEL, P. J. 2011. Sex differences in carotid baroreflex control of arterial blood pressure in humans: relative contribution of cardiac output and total vascular conductance. *Am J Physiol Heart Circ Physiol,* 301**,** H2454-65.

KINZLER, G. J., HOLMES, E. W., RECKARD, C. R., JABLOKOW, V. R., FRESCO, R. & FLANIGAN, R. C. 1991. The effect of chronic renal insufficiency on cyclosporine nephrotoxicity. *J Urol,* 145**,** 179-83.

KIUCHI, M. G., MAIA, G. L., DE QUEIROZ CARREIRA, M. A., KIUCHI, T., CHEN, S., ANDREA, B. R., GRACIANO, M. L. & LUGON, J. R. 2013. Effects of renal denervation with a standard irrigated cardiac ablation catheter on blood pressure and renal function in patients with chronic kidney disease and resistant hypertension. *Eur Heart J,* 34**,** 2114-21.

KLEIN, I. H., LIGTENBERG, G., NEUMANN, J., OEY, P. L., KOOMANS, H. A. & BLANKESTIJN, P. J. 2003a. Sympathetic nerve activity is inappropriately increased in chronic renal disease. *J Am Soc Nephrol,* 14**,** 3239-44.

KLEIN, I. H., LIGTENBERG, G., OEY, P. L., KOOMANS, H. A. & BLANKESTIJN, P. J. 2001. Sympathetic activity is increased in polycystic kidney disease and is associated with hypertension. *J Am Soc Nephrol,* 12**,** 2427-33.

KLEIN, I. H., LIGTENBERG, G., OEY, P. L., KOOMANS, H. A. & BLANKESTIJN, P. J. 2003b. Enalapril and losartan reduce sympathetic hyperactivity in patients with chronic renal failure. *J Am Soc Nephrol,* 14**,** 425-30.

KNUEPFER, M. M. & OSBORN, J. W. 2010. Direct assessment of organ specific sympathetic nervous system activity in normal and cardiovascular disease states. *Exp Physiol,* 95**,** 32-3.

KOCAMAN, O., OFLAZ, H., YEKELER, E., DURSUN, M., ERDOGAN, D., DEMIREL, S., ALISIR, S., TURGUT, F., MERCANOGLU, F. & ECDER, T. 2004. Endothelial dysfunction and increased carotid intima-media thickness in patients with autosomal dominant polycystic kidney disease. *Am J Kidney Dis,* 43**,** 854-60.

KOCYIGIT, I., KAYA, M. G., ORSCELIK, O., KAYA, C., AKPEK, M., ZENGIN, H., SIPAHIOGLU, M. H., UNAL, A., YILMAZ, M. I., TOKGOZ, B., OYMAK, O. & AXELSSON, J. 2012. Early arterial stiffness and inflammatory bio-markers in normotensive polycystic kidney disease patients. *Am J Nephrol,* 36**,** 11-8.

KOEGLER-MULY, S. M., OWENS, M. J., ERVIN, G. N., KILTS, C. D. & NEMEROFF, C. B. 1993. Potential corticotropin-releasing factor pathways in the rat brain as determined by bilateral electrolytic lesions of the central amygdaloid nucleus and the paraventricular nucleus of the hypothalamus. *J Neuroendocrinol,* 5**,** 95-8.

KOEPKE, J. P. & DIBONA, G. F. 1985. Central beta-adrenergic receptors mediate renal nerve activity during stress in conscious spontaneously hypertensive rats. *Hypertension,* 7**,** 350-6.

KOOMANS, H. A., BLANKESTIJN, P. J. & JOLES, J. A. 2004. Sympathetic hyperactivity in chronic renal failure: a wake-up call. *J Am Soc Nephrol,* 15**,** 524-37.

KOPP, U. C. & BUCKLEY-BLEILER, R. L. 1989. Impaired renorenal reflexes in two-kidney, one clip hypertensive rats. *Hypertension,* 14**,** 445-52.

KOPP, U. C., SMITH, L. A. & DIBONA, G. F. 1985. Renorenal reflexes: neural components of ipsilateral and contralateral renal responses. *Am J Physiol,* 249**,** F507-17.

KOPP, U. C., SMITH, L. A. & DIBONA, G. F. 1987. Facilitatory role of efferent renal nerve activity on renal sensory receptors. *Am J Physiol,* 253**,** F767-77.

KOREJWO, G., HERMANN, A., ZDROJEWSKI, Z., DEBSKA-SLIZIEN, A. & RUTKOWSKI, B. 2002. Improved autonomic function after kidney transplantation. *Transplant Proc,* 34**,** 601-3.

KOSCH, M., BARENBROCK, M., KISTERS, K., RAHN, K. H. & HAUSBERG, M. 2002. Relationship between muscle sympathetic nerve activity and large artery mechanical vessel wall properties in renal transplant patients. *J Hypertens,* 20**,** 501-8.

KOSHIYA, N., HUANGFU, D. & GUYENET, P. G. 1993. Ventrolateral medulla and sympathetic chemoreflex in the rat. *Brain Res,* 609**,** 174-84.

KOTANKO, P. 2006. Cause and consequences of sympathetic hyperactivity in chronic kidney disease. *Blood Purif,* 24**,** 95-9.

KOUIDI, E., KARAGIANNIS, V., GREKAS, D., IAKOVIDES, A., KAPRINIS, G., TOURKANTONIS, A. & DELIGIANNIS, A. 2010. Depression, heart rate variability, and exercise training in dialysis patients. *Eur J Cardiovasc Prev Rehabil,* 17**,** 160-7.

KRAUHS, J. M. 1979. Structure of rat aortic baroreceptors and their relationship to connective tissue. *J Neurocytol,* 8**,** 401-14.

KRIEGER, E. M. 1988. Mechanisms of complete baroreceptor resetting in hypertension. *Drugs,* 35 Suppl 6**,** 98-103.

KSIAZEK, A. & ZALUSKA, W. 2008. Sympathetic overactivity in uremia. *J Ren Nutr,* 18**,** 118-21.

KUMADA, M., TERUI, N. & KUWAKI, T. 1990. Arterial baroreceptor reflex: its central and peripheral neural mechanisms. *Prog Neurobiol,* 35**,** 331-61.

KUNOS, G. & VARGA, K. 1995. The tachycardia associated with the defense reaction involves activation of both GABAA and GABAB receptors in the nucleus tractus solitarii. *Clin Exp Hypertens,* 17**,** 91-100.

LA ROVERE, M. T., BIGGER, J. T., JR., MARCUS, F. I., MORTARA, A. & SCHWARTZ, P. J. 1998. Baroreflex sensitivity and heart-rate variability in prediction of total cardiac mortality after myocardial infarction. ATRAMI (Autonomic Tone and Reflexes After Myocardial Infarction) Investigators. *Lancet,* 351**,** 478-84.

LACY, P., CARR, S. J., O'BRIEN, D., FENTUM, B., WILLIAMS, B., PAUL, S. K. & ROBINSON, T. G. 2006. Reduced glomerular filtration rate in pre-dialysis non-diabetic chronic kidney disease patients is associated with impaired baroreceptor sensitivity and reduced vascular compliance. *Clin Sci (Lond),* 110**,** 101-8.

LAGER, D. J., QIAN, Q., BENGAL, R. J., ISHIBASHI, M. & TORRES, V. E. 2001. The pck rat: a new model that resembles human autosomal dominant polycystic kidney and liver disease. *Kidney Int,* 59**,** 126-36.

LAUDE, D., ELGHOZI, J. L., GIRARD, A., BELLARD, E., BOUHADDI, M., CASTIGLIONI, P., CERUTTI, C., CIVIDJIAN, A., DI RIENZO, M., FORTRAT, J. O., JANSSEN, B., KAREMAKER, J. M., LEFTHERIOTIS, G., PARATI, G., PERSSON, P. B., PORTA, A., QUINTIN, L., REGNARD, J., RUDIGER, H. & STAUSS, H. M. 2004. Comparison of various techniques used to estimate spontaneous baroreflex sensitivity (the EuroBaVar study). *Am J Physiol Regul Integr Comp Physiol,* 286**,** R226-31.

LEDOUX, J. 2007. The amygdala. *Curr Biol,* 17**,** R868-74.

LEDSOME, J. R. & LINDEN, R. J. 1964. A reflex increase in heart rate from distension of the pulmonary-vein-atrial junctions. *J Physiol,* 170**,** 456-73.

LEE, T. M., KUO, J. S. & CHAI, C. Y. 1972. Central integrating mechanism of the Bezold-Jarisch and baroceptor reflexes. *Am J Physiol,* 222**,** 713-20.

LEONE, C. & GORDON, F. J. 1989. Is L-glutamate a neurotransmitter of baroreceptor information in the nucleus of the tractus solitarius? *J Pharmacol Exp Ther,* 250**,** 953-62.

LERMA, C., MINZONI, A., INFANTE, O. & JOSE, M. V. 2004. A mathematical analysis for the cardiovascular control adaptations in chronic renal failure. *Artif Organs,* 28**,** 398-409.

LEVEY, A. S. & CORESH, J. 2012. Chronic kidney disease. *Lancet,* 379**,** 165-80.

LEVITAN, D., MASSRY, S. G., ROMOFF, M. & CAMPESE, V. M. 1984. Plasma catecholamines and autonomic nervous system function in patients with early renal insufficiency and hypertension: effect of clonidine. *Nephron,* 36**,** 24-9.

LEWANSKI, R. & CHRZANOWSKI, W. 2003. Assessment of autonomic nervous system by spectral analysis of heart rate and blood pressure in hemodialysed patients. *Pol Merkur Lekarski,* 15**,** 391-3.

LI, G., XU, J., WANG, P., VELAZQUEZ, H., LI, Y., WU, Y. & DESIR, G. V. 2008. Catecholamines regulate the activity, secretion, and synthesis of renalase. *Circulation,* 117**,** 1277-82.

LI, Y. F., WANG, W., MAYHAN, W. G. & PATEL, K. P. 2006. Angiotensin-mediated increase in renal sympathetic nerve discharge within the PVN: role of nitric oxide. *Am J Physiol Regul Integr Comp Physiol,* 290**,** R1035-43.

LI, Y.-L. 2011. Cardiovascular Autonomic Dysfunction in Diabetes as a Complication: Cellular and Molecular Mechanisms. *In:* WAGNER, D. (ed.) *Type 1 Diabetes Complication* Rijeka, Croatia: InTech.

LIGTENBERG, G. 1999. Regulation of blood pressure in chronic renal failure: determinants of hypertension and dialysis-related hypotension. *Neth J Med,* 55**,** 13-8.

LIGTENBERG, G., BLANKESTIJN, P. J., OEY, P. L., KLEIN, I. H., DIJKHORST-OEI, L. T., BOOMSMA, F., WIENEKE, G. H., VAN HUFFELEN, A. C. & KOOMANS, H. A. 1999. Reduction of sympathetic hyperactivity by enalapril in patients with chronic renal failure. *N Engl J Med,* 340**,** 1321-8.

LIPSKI, J., KANJHAN, R., KRUSZEWSKA, B. & RONG, W. F. 1995. Criteria for intracellular identification of pre-sympathetic neurons in the rostral ventrolateral medulla in the rat. *Clin Exp Hypertens,* 17**,** 51-65.

LITTLEWOOD, K. J., GREINER, W., BAUM, D. & ZOELLNER, Y. 2007. Adjunctive treatment with moxonidine versus nitrendipine for hypertensive patients with advanced renal failure: a cost-effectiveness analysis. *BMC Nephrol,* 8**,** 9.

LIU, S., LU, W., OBARA, T., KUIDA, S., LEHOCZKY, J., DEWAR, K., DRUMMOND, I. A. & BEIER, D. R. 2002. A defect in a novel Nek-family kinase causes cystic kidney disease in the mouse and in zebrafish. *Development,* 129**,** 5839-46.

LIU, Z. C., CHOW, K. M. & CHANG, T. M. 2003. Evaluation of two protocols of uremic rat model: partial nephrectomy and infarction. *Ren Fail,* 25**,** 935-43.

LOCATELLI, F., BOMMER, J., LONDON, G. M., MARTIN-MALO, A., WANNER, C., YAQOOB, M. & ZOCCALI, C. 2001. Cardiovascular disease determinants in chronic renal failure: clinical approach and treatment. *Nephrol Dial Transplant,* 16**,** 459-68.

LOCATELLI, F., POZZONI, P., TENTORI, F. & DEL VECCHIO, L. 2003. Epidemiology of cardiovascular risk in patients with chronic kidney disease. *Nephrol Dial Transplant,* 18 (Suppl 7)**,** vii2-9.

LOEWY, A. D. & SPYER, K. M. 1990. *Central Regulation of Autonomic Functions,* Oxford University Press, USA.

LOHMEIER, T. E., DWYER, T. M., IRWIN, E. D., ROSSING, M. A. & KIEVAL, R. S. 2007. Prolonged activation of the baroreflex abolishes obesity-induced hypertension. *Hypertension,* 49**,** 1307-14.

LOHMEIER, T. E., ILIESCU, R., DWYER, T. M., IRWIN, E. D., CATES, A. W. & ROSSING, M. A. 2010. Sustained suppression of sympathetic activity and arterial pressure during chronic activation of the carotid baroreflex. *Am J Physiol Heart Circ Physiol,* 299**,** H402-9.

LOVICK, T. A. & COOTE, J. H. 1988. Effects of volume loading on paraventriculo-spinal neurones in the rat. *J Auton Nerv Syst,* 25**,** 135-40.

LOW, D. A., KELLER, D. M., WINGO, J. E., BROTHERS, R. M. & CRANDALL, C. G. 2011. Sympathetic nerve activity and whole body heat stress in humans. *J Appl Physiol (1985),* 111**,** 1329-34.

LUGON, J. R., WARRAK, E. A., LUGON, A. S., SALVADOR, B. A. & NOBREGA, A. C. 2003. Revisiting autonomic dysfunction in end-stage renal disease patients. *Hemodial Int,* 7**,** 198-203.

MA, D., CHAKRABARTI, M. K. & WHITWAM, J. G. 1999. Propofol, bradycardia and the Bezold-Jarisch reflex in rabbits. *Br J Anaesth,* 82**,** 412-7.

MA, X., ABBOUD, F. M. & CHAPLEAU, M. W. 2002. Analysis of afferent, central, and efferent components of the baroreceptor reflex in mice. *Am J Physiol Regul Integr Comp Physiol,* 283**,** R1033-40.

MACE, S. E. & LEVY, M. N. 1983. Neural control of heart rate: a comparison between puppies and adult animals. *Pediatr Res,* 17**,** 491-5.

MACEFIELD, V. G., WALLIN, B. G. & VALLBO, A. B. 1994. The discharge behaviour of single vasoconstrictor motoneurones in human muscle nerves. *J Physiol,* 481 (Pt 3)**,** 799-809.

MACHADO, B. H. & BONAGAMBA, L. G. 2005. Antagonism of glutamate receptors in the intermediate and caudal NTS of awake rats produced no changes in the hypertensive response to chemoreflex activation. *Auton Neurosci,* 117**,** 25-32.

MAILLOUX, L. U. 2000. The overlooked role of salt restriction in dialysis patients. *Semin Dial,* 13**,** 150-1.

MAKARA, G. B., STARK, E., KAPOCS, G. & ANTONI, F. A. 1986. Long-term effects of hypothalamic paraventricular lesion on CRF content and stimulated ACTH secretion. *Am J Physiol,* 250**,** E319-24.

MAKEHAM, J. M., GOODCHILD, A. K. & PILOWSKY, P. M. 2005. NK1 receptor activation in rat rostral ventrolateral medulla selectively attenuates somato-sympathetic reflex while antagonism attenuates sympathetic chemoreflex. *Am J Physiol Regul Integr Comp Physiol,* 288**,** R1707-15.

MALLAT, Z., VICAUT, E., SANGARE, A., VERSCHUEREN, J., FONTAINE, G. & FRANK, R. 1997. Prediction of head-up tilt test result by analysis of early heart rate variations. *Circulation,* 96**,** 581-4.

MANCIA, G., GRASSI, G., FERRARI, A. & ZANCHETTI, A. 1985. Reflex cardiovascular regulation in humans. *J Cardiovasc Pharmacol,* 7 Suppl 3**,** S152-9.

MARIC, C. 2005. Sex differences in cardiovascular disease and hypertension: involvement of the renin-angiotensin system. *Hypertension,* 46**,** 475-6.

MARSHALL, J. M. 1994. Peripheral chemoreceptors and cardiovascular regulation. *Physiol Rev,* 74**,** 543-94.

MASUO, K., LAMBERT, G. W., ESLER, M. D., RAKUGI, H., OGIHARA, T. & SCHLAICH, M. P. 2010. The role of sympathetic nervous activity in renal injury and end-stage renal disease. *Hypertens Res,* 33**,** 521-8.

MASUO, K., MIKAMI, H., OGIHARA, T. & TUCK, M. 1995. Hormonal mechanisms in blood pressure reduction during hemodialysis in patients with chronic renal failure. *Hypertens Res,* 18 Suppl 1**,** S201-3.

MATHIAS, C. J. 2003. Autonomic diseases: clinical features and laboratory evaluation. *J Neurol Neurosurg Psychiatry,* 74 (Suppl 3)**,** iii31-41.

MATTHEWS, K. A., WOODALL, K. L. & ALLEN, M. T. 1993. Cardiovascular reactivity to stress predicts future blood pressure status. *Hypertension,* 22**,** 479-85.

MAZZUCHI, N., CARBONELL, E. & FERNANDEZ-CEAN, J. 2000. Importance of blood pressure control in hemodialysis patient survival. *Kidney Int,* 58**,** 2147-54.

MCALLEN, R. M. & DAMPNEY, R. A. 1990. Vasomotor neurons in the rostral ventrolateral medulla are organized topographically with respect to type of vascular bed but not body region. *Neurosci Lett,* 110**,** 91-6.

MCALLEN, R. M., MAY, C. N. & SHAFTON, A. D. 1995. Functional anatomy of sympathetic premotor cell groups in the medulla. *Clin Exp Hypertens,* 17**,** 209-21.

MCCOOKE, J., APPELS, R., BARRERO, R., DING, A., OZIMEK-KULIK, J., BELLGARD, M., MORAHAN, G. & PHILLIPS, J. 2012. A novel mutation causing nephronophthisis in the Lewis polycystic kidney rat localises to a conserved RCC1 domain in Nek8. *BMC Genomics,* 13**,** 1-17.

MCCUBBIN, J. W., GREEN, J. H. & PAGE, I. H. 1956. Baroceptor Function in Chronic Renal Hypertension. *Circulation Research,* 4**,** 205-210.

MCCULLOCH, P. F., DINOVO, K. M. & CONNOLLY, T. M. 2010. The cardiovascular and endocrine responses to voluntary and forced diving in trained and untrained rats. *Am J Physiol Regul Integr Comp Physiol,* 298**,** R224-34.

MELCHER, A. & DONALD, D. E. 1981. Maintained ability of carotid baroreflex to regulate arterial pressure during exercise. *Am J Physiol,* 241**,** H838-49.

MENCARELLI, F., FABI, M., CORAZZI, V., DOYON, A., MASETTI, R., BONETTI, S., CASTIGLIONI, L., PESSION, A. & MONTINI, G. 2013. Left ventricular mass and cardiac function in a population of children with chronic kidney disease. *Pediatr Nephrol,* 29, 893-900.

MENDELOWITZ, D., YANG, M., ANDRESEN, M. C. & KUNZE, D. L. 1992. Localization and retention in vitro of fluorescently labeled aortic baroreceptor terminals on neurons from the nucleus tractus solitarius. *Brain Res,* 581**,** 339-43.

MENG, L., FU, B., ZHANG, T., HAN, Z. & YANG, M. 2014. Salt sensitivity of blood pressure in non-dialysis patients with chronic kidney disease. *Ren Fail,* 36**,** 345-50.

MENNE, J., JORDAN, J., LINNENWEBER-HELD, S. & HALLER, H. 2013. Resistant hypertension: baroreflex stimulation as a new tool. *Nephrol Dial Transplant,* 28**,** 288-95.

MERCHENTHALER, I., HYNES, M. A., VIGH, S., SCHALLY, A. V. & PETRUSZ, P. 1984. Corticotropin releasing factor (CRF): origin and course of afferent pathways to the median eminence (ME) of the rat hypothalamus. *Neuroendocrinology,* 39**,** 296-306.

MERRILL, D. C., SEGAR, J. L., MCWEENY, O. J. & ROBILLARD, J. E. 1999. Sympathetic responses to cardiopulmonary vagal afferent stimulation during development. *Am J Physiol,* 277**,** H1311-6.

MEYER, C., SCHUELLER, P., BALZER, J., LAUER, T., WESTENFELD, R., SCHAUERTE, P., HENNERSDORF, M., STEINER, S., KELM, M. & RASSAF, T. 2009. Sympathetic hyperactivity influences chemosensor function in patients with end-stage renal disease. *Eur J Med Res,* 4**,** 151-5.

MILLHORN, D. E. 1986. Neural respiratory and circulatory interaction during chemoreceptor stimulation and cooling of ventral medulla in cats. *J Physiol,* 370**,** 217-31.

MINAMI, N. & HEAD, G. A. 2000. Cardiac vagal responsiveness during development in spontaneously hypertensive rats. *Auton Neurosci,* 82**,** 115-22.

MING, E. E., ADLER, G. K., KESSLER, R. C., FOGG, L. F., MATTHEWS, K. A., HERD, J. A. & ROSE, R. M. 2004. Cardiovascular reactivity to work stress predicts subsequent onset of hypertension: the Air Traffic Controller Health Change Study. *Psychosom Med,* 66**,** 459-65.

MIRCOLI, L., RIVERA, R., BONFORTE, G., FEDELE, L., GENOVESI, S., SURIAN, M. & FERRARI, A. U. 2003. Influence of left ventricular mass, uremia and hypertension on vagal tachycardic reserve. *J Hypertens,* 21**,** 1547-53.

MITCHELL, D. A., LAMBERT, G., SECHER, N. H., RAVEN, P. B., VAN LIESHOUT, J. & ESLER, M. D. 2009. Jugular venous overflow of noradrenaline from the brain: a neurochemical indicator of cerebrovascular sympathetic nerve activity in humans. *J Physiol,* 587**,** 2589-97.

MIYAJIMA, E., YAMADA, Y., YOSHIDA, Y., MATSUKAWA, T., SHIONOIRI, H., TOCHIKUBO, O. & ISHII, M. 1991. Muscle sympathetic nerve activity in renovascular hypertension and primary aldosteronism. *Hypertension,* 17**,** 1057-62.

MIYAMOTO, T., INAGAKI, M., TAKAKI, H., KAWADA, T., YANAGIYA, Y., SUGIMACHI, M. & SUNAGAWA, K. 2004. Integrated characterization of the human chemoreflex system controlling ventilation, using an equilibrium diagram. *Eur J Appl Physiol,* 93**,** 340-6.

MIYAWAKI, T., PILOWSKY, P., SUN, Q. J., MINSON, J., SUZUKI, S., ARNOLDA, L., LLEWELLYN-SMITH, I. & CHALMERS, J. 1995. Central inspiration increases barosensitivity of neurons in rat rostral ventrolateral medulla. *Am J Physiol,* 268**,** R909-18.

MIYAWAKI, T., SUZUKI, S., MINSON, J., ARNOLDA, L., CHALMERS, J., LLEWELLYN-SMITH, I. & PILOWSKY, P. 1997. Role of AMPA/kainate receptors in transmission of the sympathetic baroreflex in rat CVLM. *Am J Physiol,* 272**,** R800-12.

MOHAMED, M. K., EL-MAS, M. M. & ABDEL-RAHMAN, A. A. 1999. Estrogen enhancement of baroreflex sensitivity is centrally mediated. *Am J Physiol,* 276**,** R1030-7.

MONTANO, N., FURLAN, R., GUZZETTI, S., MCALLEN, R. M. & JULIEN, C. 2009. Analysis of sympathetic neural discharge in rats and humans. *Philos Trans A Math Phys Eng Sci,* 367**,** 1265-82.

MONTEZANO, A. C. & TOUYZ, R. M. 2012. Oxidative stress, Noxs, and hypertension: experimental evidence and clinical controversies. *Ann Med,* 44 Suppl 1**,** S2-16.

MOODY, W. E., EDWARDS, N. C., CHUE, C. D., FERRO, C. J. & TOWNEND, J. N. 2013. Arterial disease in chronic kidney disease. *Heart,* 99**,** 365-72.

MOORHEAD, J. F., TATLER, G. L., BAILLOD, R. A., VARGHESE, Z., WILLS, M. R. & FARROW, S. C. 1974. Effects of age, sex, and polycystic disease on progressive bone disease of renal failure. *Br Med J,* 4**,** 557-60.

MOREIRA, T. S., TAKAKURA, A. C., COLOMBARI, E. & GUYENET, P. G. 2006. Central chemoreceptors and sympathetic vasomotor outflow. *J Physiol,* 577**,** 369-86.

MORGADO, E. & NEVES, P. L. 2012. Hypertension and Chronic Kidney Disease: Cause and Consequence –Therapeutic Considerations. *In:* BABAEI, H. (ed.) *Antihypertensive Drugs.* Rijeka, Croatia: InTech.

MORRISON, S. F. & CAO, W. H. 2000. Different adrenal sympathetic preganglionic neurons regulate epinephrine and norepinephrine secretion. *Am J Physiol Regul Integr Comp Physiol,* 279**,** R1763-75.

MORTENSEN, L. H. 1999. Endothelin and the central and peripheral nervous systems: a decade of endothelin research. *Clin Exp Pharmacol Physiol,* 26**,** 980-4.

MUELLER, P. J., MISCHEL, N. A. & SCISLO, T. J. 2011. Differential activation of adrenal, renal, and lumbar sympathetic nerves following stimulation of the rostral ventrolateral medulla of the rat. *Am J Physiol Regul Integr Comp Physiol,* 300**,** R1230-40.

MULKEY, D. K., STORNETTA, R. L., WESTON, M. C., SIMMONS, J. R., PARKER, A., BAYLISS, D. A. & GUYENET, P. G. 2004. Respiratory control by ventral surface chemoreceptor neurons in rats. *Nat Neurosci,* 7**,** 1360-9.

MUNCH, P. A., ANDRESEN, M. C. & BROWN, A. M. 1983. Rapid resetting of aortic baroreceptors in vitro. *Am J Physiol,* 244**,** H672-80.

MUNCH, P. A., THOREN, P. N. & BROWN, A. M. 1987. Dual effects of norepinephrine and mechanisms of baroreceptor stimulation. *Circ Res,* 61**,** 409-19.

MUNTZEL, M. S., AL-NAIMI, O. A., BARCLAY, A. & AJASIN, D. 2012. Cafeteria diet increases fat mass and chronically elevates lumbar sympathetic nerve activity in rats. *Hypertension,* 60**,** 1498-502.

MYLONOPOULOU, M., TENTOLOURIS, N., ANTONOPOULOS, S., MIKROS, S., KATSAROS, K., MELIDONIS, A., SEVASTOS, N. & KATSILAMBROS, N. 2010. Heart rate variability in advanced chronic kidney disease with or without diabetes: midterm effects of the initiation of chronic haemodialysis therapy. *Nephrol Dial Transplant,* 25**,** 3749-54.

NADASDY, T., LASZIK, Z., LAJOIE, G., BLICK, K. E., WHEELER, D. E. & SILVA, F. G. 1995. Proliferative activity of cyst epithelium in human renal cystic diseases. *J Am Soc Nephrol,* 5**,** 1462-8.

NAKAMURA, K., SASAKI, S., MORIGUCHI, J., MORIMOTO, S., MIKI, S., KAWA, T., ITOH, H., NAKATA, T., TAKEDA, K. & NAKAGAWA, M. 1999. Central effects of endothelin and its antagonists on sympathetic and cardiovascular regulation in SHR-SP. *J Cardiovasc Pharmacol,* 33**,** 876-82.

NARKIEWICZ, K., PESEK, C. A., KATO, M., PHILLIPS, B. G., DAVISON, D. E. & SOMERS, V. K. 1998. Baroreflex control of sympathetic nerve activity and heart rate in obstructive sleep apnea. *Hypertension,* 32**,** 1039-43.

NARSIPUR, S. S., SRINIVASAN, B. & SINGH, B. 2011. Effect of simvastatin use on autonomic function in patients with end stage renal disease. *Cardiovasc Hematol Disord Drug Targets,* 11**,** 53-7.

NATIONAL KIDNEY FOUNDATION 2013. Kidney disease outcomes quality initiative (KDOQI) clinical practice guideline for chronic kidney disease care. New York USA: National Kidney Foundation http://www.kidney.org/.

NAUTA, J., GOEDBLOED, M. A., HERCK, H. V., HESSELINK, D. A., VISSER, P., WILLEMSEN, R., DOKKUM, R. P., WRIGHT, C. J. & GUAY-WOODFORD, L. M. 2000. New rat model that phenotypically resembles autosomal recessive polycystic kidney disease. *J Am Soc Nephrol,* 11**,** 2272-84.

NEAHRING, J. C., JONES, S. Y. & DIBONA, G. F. 1995. Cardiopulmonary baroreflex function in nephrotic rats. *J Am Soc Nephrol,* 5**,** 2082-6.

NEFF, R. A., MIHALEVICH, M. & MENDELOWITZ, D. 1998. Stimulation of NTS activates NMDA and non-NMDA receptors in rat cardiac vagal neurons in the nucleus ambiguus. *Brain Research,* 792**,** 277-282.

NEUMANN, J., LIGTENBERG, G., KLEIN, I. H. & BLANKESTIJN, P. J. 2002. Pathogenesis and treatment of hypertension in polycystic kidney disease. *Curr Opin Nephrol Hypertens,* 11**,** 517-21.

NEUMANN, J., LIGTENBERG, G., KLEIN, I. H., BOER, P., OEY, P. L., KOOMANS, H. A. & BLANKESTIJN, P. J. 2007. Sympathetic hyperactivity in hypertensive chronic kidney disease patients is reduced during standard treatment. *Hypertension,* 49**,** 506-10.

NEUMANN, J., LIGTENBERG, G., OEY, L., KOOMANS, H. A. & BLANKESTIJN, P. J. 2004. Moxonidine normalizes sympathetic hyperactivity in patients with eprosartan-treated chronic renal failure. *J Am Soc Nephrol,* 15**,** 2902-7.

NG, A. V., CALLISTER, R., JOHNSON, D. G. & SEALS, D. R. 1993. Age and gender influence muscle sympathetic nerve activity at rest in healthy humans. *Hypertension,* 21**,** 498-503.

NG, K., HILDRETH, C. M., AVOLIO, A. P. & PHILLIPS, J. K. 2011a. Angiotensin-converting enzyme inhibitor limits pulse-wave velocity and aortic calcification in a rat model of cystic renal disease. *Am J Physiol Renal Physiol,* 301**,** F959-66.

NG, K., HILDRETH, C. M., PHILLIPS, J. K. & AVOLIO, A. P. 2011b. Aortic stiffness is associated with vascular calcification and remodeling in a chronic kidney disease rat model. *Am J Physiol Renal Physiol,* 300**,** 6.

NIEBYLSKI, A., BOCCOLINI, A., BENSI, N., BINOTTI, S., HANSEN, C., YACIUK, R. & GAUNA, H. 2012. Neuroendocrine changes and natriuresis in response to social stress in rats. *Stress Health,* 28**,** 179-85.

NIKOLIC, K. & AGBABA, D. 2012. Imidazoline antihypertensive drugs: selective i(1) -imidazoline receptors activation. *Cardiovasc Ther,* 30**,** 209-16.

NILSSON, H., GOLDSTEIN, M. & NILSSON, O. 1986. Adrenergic innervation and neurogenic response in large and small arteries and veins from the rat. *Acta Physiol Scand,* 126**,** 121-33.

NINOMIYA, I., NISIMARU, N. & IRISAWA, H. 1971. Sympathetic nerve activity to the spleen, kidney, and heart in response to baroceptor input. *Am J Physiol,* 221**,** 1346-51.

NOSAKA, S., YAMAMOTO, T. & YASUNAGA, K. 1979. Localization of vagal cardioinhibitory preganglionic neurons with rat brain stem. *J Comp Neurol,* 186**,** 79-92.

NURMINEN, M. L., YLIKORKALA, A. & VAPAATALO, H. 1997. Central inhibition of nitric oxide synthesis increases blood pressure and heart rate in anesthetized rats. *Methods Find Exp Clin Pharmacol,* 19**,** 35-41.

OATES, H. F., GRAHAM, R. M. & STOKES, G. S. 1977. Mechanism of the hypotensive action of prazosin. *Arch Int Pharmacodyn Ther,* 227**,** 41-8.

OBERG, B. & THOREN, P. 1973. Circulatory responses to stimulation of medullated and non-medullated afferents in the cardiac nerve in the cat. *Acta Physiol Scand,* 87**,** 121-32.

OMRAN, H., FERNANDEZ, C., JUNG, M., HAFFNER, K., FARGIER, B., VILLAQUIRAN, A., WALDHERR, R., GRETZ, N., BRANDIS, M., RUSCHENDORF, F., REIS, A. & HILDEBRANDT, F. 2000. Identification of a new gene locus for adolescent nephronophthisis, on chromosome 3q22 in a large Venezuelan pedigree. *Am J Hum Genet,* 66**,** 118-27.

ONDOCIN, P. T. & NARSIPUR, S. S. 2006. Influence of angiotensin converting enzyme inhibitor treatment on cardiac autonomic modulation in patients receiving haemodialysis. *Nephrology (Carlton),* 11**,** 497-501.

OOTSUKA, Y., RONG, W., KISHI, E., KOGANEZAWA, T. & TERUI, N. 2002. Rhythmic activities of the sympatho-excitatory neurons in the medulla of rabbits: neurons controlling cutaneous vasomotion. *Auton Neurosci,* 101**,** 48-59.

OPARIL, S., ZAMAN, M. A. & CALHOUN, D. A. 2003. Pathogenesis of hypertension. *Ann Intern Med,* 139**,** 761-76.

O'TOOLE, J. F., LIU, Y., DAVIS, E. E., WESTLAKE, C. J., ATTANASIO, M., OTTO, E. A., SEELOW, D., NURNBERG, G., BECKER, C., NUUTINEN, M., KARPPA, M., IGNATIUS, J., UUSIMAA, J., PAKANEN, S., JAAKKOLA, E., VAN DEN HEUVEL, L. P., FEHRENBACH, H., WIGGINS, R., GOYAL, M., ZHOU, W., WOLF, M. T., WISE, E., HELOU, J., ALLEN, S. J., MURGA-ZAMALLOA, C. A., ASHRAF, S., CHAKI, M., HEERINGA, S., CHERNIN, G., HOSKINS, B. E., CHAIB, H., GLEESON, J., KUSAKABE, T., SUZUKI, T., ISAAC, R. E., QUARMBY, L. M., TENNANT, B., FUJIOKA, H., TUOMINEN, H., HASSINEN, I., LOHI, H., VAN HOUTEN, J. L., ROTIG, A., SAYER, J. A., ROLINSKI, B., FREISINGER, P., MADHAVAN, S. M., HERZER, M., MADIGNIER, F., PROKISCH, H., NURNBERG, P., JACKSON, P. K., KHANNA, H., KATSANIS, N. & HILDEBRANDT, F. 2010. Individuals with mutations in XPNPEP3, which encodes a mitochondrial protein, develop a nephronophthisis-like nephropathy. *J Clin Invest,* 120**,** 791-802.

OTTO, E. A., SCHERMER, B., OBARA, T., O'TOOLE, J. F., HILLER, K. S., MUELLER, A. M., RUF, R. G., HOEFELE, J., BEEKMANN, F., LANDAU, D., FOREMAN, J. W., GOODSHIP, J. A., STRACHAN, T., KISPERT, A., WOLF, M. T., GAGNADOUX, M. F., NIVET, H., ANTIGNAC, C., WALZ, G., DRUMMOND, I. A., BENZING, T. & HILDEBRANDT, F. 2003. Mutations in INVS encoding inversin cause nephronophthisis type 2, linking renal cystic disease to the function of primary cilia and left-right axis determination. *Nat Genet,* 34**,** 413-20.

OTTO, E. A., TRAPP, M. L., SCHULTHEISS, U. T., HELOU, J., QUARMBY, L. M. & HILDEBRANDT, F. 2008. NEK8 mutations affect ciliary and centrosomal localization and may cause nephronophthisis. *J Am Soc Nephrol,* 19**,** 587-92.

OUCHI, Y., SHARE, L., CROFTON, J. T., IITAKE, K. & BROOKS, D. P. 1987. Sex difference in the development of deoxycorticosterone-salt hypertension in the rat. *Hypertension,* 9**,** 172-7.

PABLO HUIDOBRO-TORO, J. & VERONICA DONOSO, M. 2004. Sympathetic co-transmission: the coordinated action of ATP and noradrenaline and their modulation by neuropeptide Y in human vascular neuroeffector junctions. *Eur J Pharmacol,* 500**,** 27-35.

PAI, A., LEAF, E. M., EL-ABBADI, M. & GIACHELLI, C. M. 2011. Elastin degradation and vascular smooth muscle cell phenotype change precede cell loss and arterial medial calcification in a uremic mouse model of chronic kidney disease. *Am J Pathol,* 178**,** 764-73.

PAL, G. K., PAL, P., NANDA, N., AMUDHARAJ, D. & ADITHAN, C. 2013. Cardiovascular dysfunctions and sympathovagal imbalance in hypertension and prehypertension: physiological perspectives. *Future Cardiol,* 9**,** 53-69.

PALKOVITS, M., SEBEKOVA, K., KLENOVICS, K. S., KEBIS, A., FAZELI, G., BAHNER, U. & HEIDLAND, A. 2013. Neuronal activation in the central nervous system of rats in the initial stage of chronic kidney disease-modulatory effects of losartan and moxonidine. *PLoS One,* 8**,** e66543.

PARATI, G., DI RIENZO, M. & MANCIA, G. 2000. How to measure baroreflex sensitivity: from the cardiovascular laboratory to daily life. *J Hypertens,* 18**,** 7-19.

PARMAR, M. S. 2002. Chronic renal disease. *BMJ,* 325**,** 85-90.

PASSAUER, J., PISTROSCH, F., BUSSEMAKER, E., LASSIG, G., HERBRIG, K. & GROSS, P. 2005. Reduced agonist-induced endothelium-dependent vasodilation in uremia is attributable to an impairment of vascular nitric oxide. *J Am Soc Nephrol,* 16**,** 959-65.

PATEL, K. P., LI, Y. F. & HIROOKA, Y. 2001. Role of nitric oxide in central sympathetic outflow. *Exp Biol Med (Maywood),* 226**,** 814-24.

PATON, J. F., DEUCHARS, J., AHMAD, Z., WONG, L. F., MURPHY, D. & KASPAROV, S. 2001a. Adenoviral vector demonstrates that angiotensin II-induced depression of the cardiac baroreflex is mediated by endothelial nitric oxide synthase in the nucleus tractus solitarii of the rat. *J Physiol,* 531**,** 445-58.

PATON, J. F., DEUCHARS, J., LI, Y. W. & KASPAROV, S. 2001b. Properties of solitary tract neurones responding to peripheral arterial chemoreceptors. *Neuroscience,* 105**,** 231-48.

PAVITHRAN, P., MADANMOHAN, T. & NANDEESHA, H. 2008. Sex differences in short-term heart rate variability in patients with newly diagnosed essential hypertension. *J Clin Hypertens,* 10**,** 904-10.

PENG, N., OPARIL, S., MENG, Q. C. & WYSS, J. M. 1996. Atrial natriuretic peptide regulation of noradrenaline release in the anterior hypothalamic area of spontaneously hypertensive rats. *J Clin Invest,* 98**,** 2060-5.

PENNE, E. L., NEUMANN, J., KLEIN, I. H., OEY, P. L., BOTS, M. L. & BLANKESTIJN, P. J. 2009. Sympathetic hyperactivity and clinical outcome in chronic kidney disease patients during standard treatment. *J Nephrol,* 22**,** 208-15.

PETI-PETERDI, J. & HARRIS, R. C. 2010. Macula densa sensing and signaling mechanisms of renin release. *J Am Soc Nephrol,* 21**,** 1093-6.

PHILLIPS, J. K. 2012. Autonomic dysfunction in heart failure and renal disease. *Front Physiol,* 3**,** 219.

PHILLIPS, J. K., HOPWOOD, D., LOXLEY, R. A., GHATORA, K., COOMBES, J. D., TAN, Y. S., HARRISON, J. L., MCKITRICK, D. J., HOLOBOTVSKYY, V., ARNOLDA, L. F. & RANGAN, G. K. 2007. Temporal relationship between renal cyst development, hypertension and cardiac hypertrophy in a new rat model of autosomal recessive polycystic kidney disease. *Kidney Blood Press Res,* 30**,** 129-44.

PICKERING, A. E., SIMMS, A. E. & PATON, J. F. 2008. Dominant role of aortic baroreceptors in the cardiac baroreflex of the rat in situ. *Auton Neurosci,* 142**,** 32-9.

PILOWSKY, P. M. & GOODCHILD, A. K. 2002. Baroreceptor reflex pathways and neurotransmitters: 10 years on. *J Hypertens,* 20**,** 1675-88.

POTTS, J. T., PATON, J. F., MITCHELL, J. H., GARRY, M. G., KLINE, G., ANGUELOV, P. T. & LEE, S. M. 2003. Contraction-sensitive skeletal muscle afferents inhibit arterial baroreceptor

signalling in the nucleus of the solitary tract: role of intrinsic GABA interneurons. *Neuroscience,* 119**,** 201-14.

PREJBISZ, A., KADZIELA, J., LEWANDOWSKI, J., FLORCZAK, E., ZYLINSKA, E., KLOPOTOWSKI, M., WITKOWSKI, A. & JANUSZEWICZ, A. 2014. Effect of percutaneous renal denervation on blood pressure level and sympathetic activity in a patient with polycystic kidney disease. *Clin Res Cardiol,* 103**,** 251-3.

PYNER, S., DEERING, J. & COOTE, J. H. 2002. Right atrial stretch induces renal nerve inhibition and c-fos expression in parvocellular neurones of the paraventricular nucleus in rats. *Exp Physiol,* 87**,** 25-32.

RAIZADA, V., HILLERSON, D., AMARAM, J. S. & SKIPPER, B. 2012. Angiotensin II-mediated left ventricular abnormalities in chronic kidney disease. *J Investig Med,* 60**,** 785-91.

RAMCHANDRA, R., BARRETT, C. J., GUILD, S. J. & MALPAS, S. C. 2006. Evidence of differential control of renal and lumbar sympathetic nerve activity in conscious rabbits. *Am J Physiol Regul Integr Comp Physiol,* 290**,** 20.

RAMCHANDRA, R., HOOD, S. G., DENTON, D. A., WOODS, R. L., MCKINLEY, M. J., MCALLEN, R. M. & MAY, C. N. 2009a. Basis for the preferential activation of cardiac sympathetic nerve activity in heart failure. *Proc Natl Acad Sci USA,* 106**,** 924-8.

RAMCHANDRA, R., HOOD, S. G., FRITHIOF, R., MCKINLEY, M. J. & MAY, C. N. 2013. The role of the paraventricular nucleus of the hypothalamus in the regulation of cardiac and renal sympathetic nerve activity in conscious normal and heart failure sheep. *J Physiol,* 591**,** 93-107.

RAMCHANDRA, R., HOOD, S. G., WATSON, A. M., ALLEN, A. M. & MAY, C. N. 2012. Central angiotensin type 1 receptor blockade decreases cardiac but not renal sympathetic nerve activity in heart failure. *Hypertension,* 59**,** 634-41.

RAMCHANDRA, R., WAN, L., HOOD, S. G., FRITHIOF, R., BELLOMO, R. & MAY, C. N. 2009b. Septic shock induces distinct changes in sympathetic nerve activity to the heart and kidney in conscious sheep. *Am J Physiol Regul Integr Comp Physiol,* 297**,** R1247-53.

RANPURIA, R., HALL, M., CHAN, C. T. & UNRUH, M. 2008. Heart rate variability (HRV) in kidney failure: measurement and consequences of reduced HRV. *Nephrol Dial Transplant.* , 23**,** 444-9.

RASSAF, T., SCHUELLER, P., WESTENFELD, R., FLOEGE, J., EICKHOLT, C., HENNERSDORF, M., MERX, M. W., SCHAUERTE, P., KELM, M. & MEYER, C. 2012. Peripheral chemosensor function is blunted in moderate to severe chronic kidney disease. *Int J Cardiol,* 155**,** 201-5.

RASSAF, T., WESTENFELD, R., BALZER, J., LAUER, T., MERX, M., FLOEGE, J., STEINER, S., HEISS, C., KELM, M. & MEYER, C. 2010. Modulation of peripheral chemoreflex by neurohumoral adaptations after kidney transplantation. *Eur J Med Res,* 15 Suppl 2**,** 83-7.

RAVERA, M., RE, M., DEFERRARI, L., VETTORETTI, S. & DEFERRARI, G. 2006. Importance of blood pressure control in chronic kidney disease. *J Am Soc Nephrol,* 17**,** S98-103.

RECKELHOFF, J. F. 2001. Gender differences in the regulation of blood pressure. *Hypertension,* 37**,** 1199-208.

RECKELHOFF, J. F., ZHANG, H. & SRIVASTAVA, K. 2000. Gender differences in development of hypertension in spontaneously hypertensive rats: role of the renin-angiotensin system. *Hypertension,* 35**,** 480-3.

RECORDATI, G., MOSS, N. G., GENOVESI, S. & ROGENES, P. 1981. Renal chemoreceptors. *J Auton Nerv Syst,* 3**,** 237-51.

REID, I. A. 1992. Interactions between ANG II, sympathetic nervous system, and baroreceptor reflexes in regulation of blood pressure. *Am J Physiol.,* 262**,** E763-78.

RICHERSON, G. B., WANG, W., HODGES, M. R., DOHLE, C. I. & DIEZ-SAMPEDRO, A. 2005. Homing in on the specific phenotype(s) of central respiratory chemoreceptors. *Exp Physiol,* 90**,** 259-66; discussion 266-9.

RICKSTEN, S. E., LUNDIN, S. & THOREN, P. 1984. Spontaneous variations in arterial blood pressure, heart rate and sympathetic nerve activity in conscious normotensive and spontaneously hypertensive rats. *Acta Physiol Scand,* 120**,** 595-600.

RIDAO, N., LUNO, J., GARCIA DE VINUESA, S., GOMEZ, F., TEJEDOR, A. & VALDERRABANO, F. 2001. Prevalence of hypertension in renal disease. *Nephrol Dial Transplant,* 16 Suppl 1**,** 70-3.

ROBINSON, T. G. & CARR, S. J. 2002. Cardiovascular autonomic dysfunction in uremia. *Kidney Int,* 62**,** 1921-32.

ROSENMANN, E., YANKO, L. & COHEN, A. M. 1984. Female sex hormone and nephropathy in Cohen diabetic rat (genetically selected sucrose-fed). *Horm Metab Res,* 16**,** 11-6.

RUBINGER, D., BACKENROTH, R. & SAPOZNIKOV, D. 2009. Restoration of baroreflex function in patients with end-stage renal disease after renal transplantation. *Nephrol Dial Transplant,* 24**,** 1305-13.

RUMP, L. C., AMANN, K., ORTH, S. & RITZ, E. 2000. Sympathetic overactivity in renal disease: a window to understand progression and cardiovascular complications of uraemia? *Nephrol Dial Transplant,* 15**,** 1735-8.

RYAN, J. P., SHEU, L. K., VERSTYNEN, T. D., ONYEWUENYI, I. C. & GIANAROS, P. J. 2013. Cerebral blood flow links insulin resistance and baroreflex sensitivity. *PLoS One,* 8**,** e83288.

SABINO, J. P., DA SILVA, C. A., GIUSTI, H., GLASS, M. L., SALGADO, H. C. & FAZAN, R., JR. 2013. Parasympathetic activation by pyridostigmine on chemoreflex sensitivity in heart-failure rats. *Auton Neurosci,* 179**,** 43-8.

SAHIN, M., KAYATAS, M., URUN, Y., SENNAROGLU, E. & AKDUR, S. 2006. Performing only one cardiovascular reflex test has a high positive predictive value for diagnosing autonomic neuropathy in patients with chronic renal failure on hemodialysis. *Ren Fail,* 28**,** 383-7.

SAINO, A., POMIDOSSI, G., PERONDI, R., MORGANTI, A., TUROLO, L. & MANCIA, G. 2000. Modulation of sympathetic coronary vasoconstriction by cardiac renin-angiotensin system in human coronary heart disease. *Circulation,* 101**,** 2277-83.

SAINO, A., POMIDOSSI, G., PERONDI, R., VALENTINI, R., RIMINI, A., DI FRANCESCO, L. & MANCIA, G. 1997. Intracoronary angiotensin II potentiates coronary sympathetic vasoconstriction in humans. *Circulation,* 96**,** 148-53.

SAKUMA, I., TOGASHI, H., YOSHIOKA, M., SAITO, H., YANAGIDA, M., TAMURA, M., KOBAYASHI, T., YASUDA, H., GROSS, S. S. & LEVI, R. 1992. NG-methyl-L-arginine, an inhibitor of L-arginine-derived nitric oxide synthesis, stimulates renal sympathetic nerve activity in vivo. A role for nitric oxide in the central regulation of sympathetic tone? *Circ Res,* 70**,** 607-11.

SALEH, M. C., CONNELL, B. J. & SALEH, T. M. 2000. Medullary and intrathecal injections of 17beta-estradiol in male rats. *Brain Res,* 867**,** 200-9.

SALEH, T. M. & CONNELL, B. J. 2000. 17beta-estradiol modulates baroreflex sensitivity and autonomic tone of female rats. *J Auton Nerv Syst,* 80**,** 148-61.

SALGADO, H. C., BARALE, Á. R., CASTANIA, J. A., MACHADO, B. H., CHAPLEAU, M. W. & FAZAN, R. 2007. Baroreflex responses to electrical stimulation of aortic depressor nerve in conscious SHR. *Am J Physiol Heart Circ Physiol,* 292**,** H593-600.

SALOMON, R., SAUNIER, S. & NIAUDET, P. 2009. Nephronophthisis. *Pediatr Nephrol,* 24**,** 2333-44.

SAMUELS, B. C., ZARETSKY, D. V. & DIMICCO, J. A. 2002. Tachycardia evoked by disinhibition of the dorsomedial hypothalamus in rats is mediated through medullary raphe. *J Physiol,* 538**,** 941-6.

SANDER, M., HANSEN, P. G. & VICTOR, R. G. 1995. Sympathetically mediated hypertension caused by chronic inhibition of nitric oxide. *Hypertension,* 26**,** 691-5.

SANDERS, J. S., MARK, A. L. & FERGUSON, D. W. 1989. Evidence for cholinergically mediated vasodilation at the beginning of isometric exercise in humans. *Circulation,* 79**,** 815-24.

SANTANA-FILHO, V. J., DAVIS, G. J., CASTANIA, J. A., MA, X., SALGADO, H. C., ABBOUD, F. M., FAZAN, R., JR. & CHAPLEAU, M. W. 2014. Autocrine/paracrine modulation of baroreceptor activity after antidromic stimulation of aortic depressor nerve in vivo. *Auton Neurosci,* 180**,** 24-31.

SAPRU, H. N. & KRIEGER, A. J. 1977. Carotid and aortic chemoreceptor function in the rat. *J Appl Physiol,* 42**,** 344-8.

SAPRU, H. N. & WANG, S. C. 1976. Modification of aortic barorecptor resetting in the spontaneously hypertensive rat. *Am J Physiol,* 230**,** 664-74.

SAPRU, H. N., GONZALEZ, E. & KRIEGER, A. J. 1981. Aortic nerve stimulation in the rat: cardiovascular and respiratory responses. *Brain Res Bull,* 6**,** 393-8.

SARNAK, M. J., LEVEY, A. S., SCHOOLWERTH, A. C., CORESH, J., CULLETON, B., HAMM, L. L., MCCULLOUGH, P. A., KASISKE, B. L., KELEPOURIS, E., KLAG, M. J., PARFREY, P., PFEFFER, M., RAIJ, L., SPINOSA, D. J. & WILSON, P. W. 2003. Kidney disease as a risk factor for development of cardiovascular disease: a statement from the American Heart Association Councils on Kidney in Cardiovascular Disease, High Blood Pressure Research, Clinical Cardiology, and Epidemiology and Prevention. *Hypertension,* 42**,** 1050-65.

SATO, R., MIZUNO, M., MIURA, T., KATO, Y., WATANABE, S., FUWA, D., OGIYAMA, Y., TOMONARI, T., OTA, K., ICHIKAWA, T., SHIRASAWA, Y., ITO, A., YOSHIDA, A., FUKUDA, M. & KIMURA, G. 2013. Angiotensin receptor blockers regulate the synchronization of circadian rhythms in heart rate and blood pressure. *J Hypertens,* 31**,** 1233-8.

SCHALLER, B. 2004. Trigeminocardiac reflex. A clinical phenomenon or a new physiological entity? *J Neurol,* 251**,** 658-65.

SCHEFFERS, I. J., KROON, A. A., SCHMIDLI, J., JORDAN, J., TORDOIR, J. J., MOHAUPT, M. G., LUFT, F. C., HALLER, H., MENNE, J., ENGELI, S., CERAL, J., ECKERT, S., ERGLIS, A., NARKIEWICZ, K., PHILIPP, T. & DE LEEUW, P. W. 2010. Novel baroreflex activation therapy in resistant hypertension: results of a European multi-center feasibility study. *J Am Coll Cardiol,* 56**,** 1254-8.

SCHIFFRIN, E. L., LIPMAN, M. L. & MANN, J. F. 2007. Chronic kidney disease: effects on the cardiovascular system. *Circulation,* 116**,** 85-97.

SCHLAICH, M. P., BART, B., HERING, D., WALTON, A., MARUSIC, P., MAHFOUD, F., BOHM, M., LAMBERT, E. A., KRUM, H., SOBOTKA, P. A., SCHMIEDER, R. E., IKA-SARI, C., EIKELIS, N., STRAZNICKY, N., LAMBERT, G. W. & ESLER, M. D. 2013. Feasibility of catheter-based renal nerve ablation and effects on sympathetic nerve activity and blood pressure in patients with end-stage renal disease. *Int J Cardiol,* 168**,** 2214-20.

SCHLAICH, M. P., HERING, D., SOBOTKA, P., KRUM, H., LAMBERT, G. W., LAMBERT, E. & ESLER, M. D. 2012. Effects of renal denervation on sympathetic activation, blood pressure, and glucose metabolism in patients with resistant hypertension. *Front Physiol,* 3**,** 10.

SCHLAICH, M. P., KAYE, D. M., LAMBERT, E., SOMMERVILLE, M., SOCRATOUS, F. & ESLER, M. D. 2003. Relation between cardiac sympathetic activity and hypertensive left ventricular hypertrophy. *Circulation,* 108**,** 560-5.

SCHLAICH, M. P., LAMBERT, E. A., SOBOTKA, P. A., LAMBERT, G. W. & ESLER, M. D. 2007. Sympathetic hyperactivity in hypertensive chronic kidney disease patients is reduced during standard treatment. *Hypertension,* 49**,** e27; author reply e28.

SCHLAICH, M. P., SOBOTKA, P. A., KRUM, H., LAMBERT, E. & ESLER, M. D. 2009a. Renal sympathetic-nerve ablation for uncontrolled hypertension. *N Engl J Med,* 361**,** 932-4.

SCHLAICH, M. P., SOCRATOUS, F., HENNEBRY, S., EIKELIS, N., LAMBERT, E. A., STRAZNICKY, N., ESLER, M. D. & LAMBERT, G. W. 2009b. Sympathetic activation in chronic renal failure. *J Am Soc Nephrol,* 20**,** 933-9.

SCHMIDT, R. J. & BAYLIS, C. 2000. Total nitric oxide production is low in patients with chronic renal disease. *Kidney Int,* 58**,** 1261-6.

SCHNEIDER, M. P. & MANN, J. F. 2014. Endothelin antagonism for patients with chronic kidney disease: still a hope for the future. *Nephrol Dial Transplant,* 29 Suppl 1**,** i69-73.

SCHOHN, D., WEIDMANN, P., JAHN, H. & BERETTA-PICCOLI, C. 1985. Norepinephrine-related mechanism in hypertension accompanying renal failure. *Kidney Int,* 28**,** 814-22.

SCHREIHOFER, A. M. & GUYENET, P. G. 1997. Identification of C1 presympathetic neurons in rat rostral ventrolateral medulla by juxtacellular labeling in vivo. *J Comp Neurol,* 387**,** 524-36.

SCHREIHOFER, A. M. & GUYENET, P. G. 2002. The baroreflex and beyond: control of sympathetic vasomotor tone by GABAergic neurons in the ventrolateral medulla. *Clin Exp Pharmacol Physiol,* 29**,** 514-21.

SCHROEDER, C., ADAMS, F., BOSCHMANN, M., TANK, J., HAERTTER, S., DIEDRICH, A., BIAGGIONI, I., LUFT, F. C. & JORDAN, J. 2004. Phenotypical evidence for a gender difference in cardiac norepinephrine transporter function. *Am J Physiol Regul Integr Comp Physiol,* 286**,** R851-6.

SCHULER, J. L. & O'BRIEN, W. H. 1997. Cardiovascular recovery from stress and hypertension risk factors: a meta-analytic review. *Psychophysiology,* 34**,** 649-59.

SCHULTZ, H. D. 2001. Cardiac vagal chemosensory afferents. Function in pathophysiological states. *Ann N Y Acad Sci,* 940**,** 59-73.

SCISLO, T. J. & DICARLO, S. E. 1994. Gender difference in cardiopulmonary reflex inhibition of sympathetic nerve activity. *Am J Physiol,* 267**,** H1537-43.

SCISLO, T. J., AUGUSTYNIAK, R. A. & O'LEARY, D. S. 1998. Differential arterial baroreflex regulation of renal, lumbar, and adrenal sympathetic nerve activity in the rat. *Am J Physiol,* 275**,** R995-1002.

SELIGER, S. L., KATZEL, L. I., FINK, J. C., WEIR, M. R. & WALDSTEIN, S. R. 2008. Renal function and cardiovascular response to mental stress. *Am J Nephrol,* 28**,** 304-10.

SEVRE, K., LEFRANDT, J. D., NORDBY, G., OS, I., MULDER, M., GANS, R. O., ROSTRUP, M. & SMIT, A. J. 2001. Autonomic function in hypertensive and normotensive subjects: the importance of gender. *Hypertension,* 37**,** 1351-6.

SHAMSEDDIN, M. K. & PARFREY, P. S. 2011. Sudden cardiac death in chronic kidney disease: epidemiology and prevention. *Nat Rev Nephrol,* 7**,** 145-54.

SHARKEY, K. A., OLAND, L. D., KIRK, D. R. & DAVISON, J. S. 1991. Capsaicin-sensitive vagal stimulation-induced gastric acid secretion in the rat: evidence for cholinergic vagal afferents. *Br J Pharmacol,* 103**,** 1997-2003.

SHEPHERD, J. T. 1981. The lungs as receptor sites for cardiovascular regulation. *Circulation,* 63**,** 1-10.

SHICHIRI, M., HIRATA, Y., ANDO, K., EMORI, T., OHTA, K., KIMOTO, S., OGURA, M., INOUE, A. & MARUMO, F. 1990. Plasma endothelin levels in hypertension and chronic renal failure. *Hypertension,* 15**,** 493-6.

SHIMOKAWA, A., KUNITAKE, T., TAKASAKI, M. & KANNAN, H. 1998. Differential effects of anesthetics on sympathetic nerve activity and arterial baroreceptor reflex in chronically instrumented rats. *J Auton Nerv Syst,* 72**,** 46-54.

SHINOHARA, K., HIROOKA, Y., KISHI, T. & SUNAGAWA, K. 2012. Reduction of nitric oxide-mediated gamma-amino butyric acid release in rostral ventrolateral medulla is involved in superoxide-induced sympathoexcitation of hypertensive rats. *Circ J,* 76**,** 2814-21.

SHOEMAKER, J. K., HOGEMAN, C. S., KHAN, M., KIMMERLY, D. S. & SINOWAY, L. I. 2001. Gender affects sympathetic and hemodynamic response to postural stress. *Am J Physiol Heart Circ Physiol,* 281**,** H2028-35.

SIDDIQI, L., OEY, P. L. & BLANKESTIJN, P. J. 2011. Aliskiren reduces sympathetic nerve activity and blood pressure in chronic kidney disease patients. *Nephrol Dial Transplant,* 26**,** 2930-4.

SILBIGER, S. & NEUGARTEN, J. 2008. Gender and human chronic renal disease. *Gend Med,* 5 (Suppl A), S3-10.

SILVA, A. Q. & SCHREIHOFER, A. M. 2011. Altered sympathetic reflexes and vascular reactivity in rats after exposure to chronic intermittent hypoxia. *J Physiol,* 589**,** 1463-76.

SINSKI, M., LEWANDOWSKI, J., ABRAMCZYK, P., NARKIEWICZ, K. & GACIONG, Z. 2006. Why study sympathetic nervous system? *J Physiol Pharmacol,* 57 (Suppl 11)**,** 79-92.

SIT, D., KADIROGLU, A. K., KAYABASI, H. & YILMAZ, M. E. 2006. The prevalence of insulin resistance in nondiabetic nonobese patients with chronic kidney disease. *Adv Ther,* 23**,** 988-98.

SMIRNOV, A. V., PETRISHCHEV, N. N., PANINA, I., MNUSKINA, M. M., ACHKASOVA, V. V., RUMIANTSEV, A. & MENSHUTINA, M. A. 2011. The level of endothelin-1 and reactivity of skin microvessels in patients with early stages of chronic kidney disease. *Ter Arkh,* 83**,** 13-8.

SMITH, J. K. & BARRON, K. W. 1990. GABAergic responses in ventrolateral medulla in spontaneously hypertensive rats. *Am J Physiol,* 258**,** R450-6.

SMITH, L. A., BUKANOV, N. O., HUSSON, H., RUSSO, R. J., BARRY, T. C., TAYLOR, A. L., BEIER, D. R. & IBRAGHIMOV-BESKROVNAYA, O. 2006. Development of polycystic kidney disease in juvenile cystic kidney mice: insights into pathogenesis, ciliary abnormalities, and common features with human disease. *J Am Soc Nephrol,* 17**,** 2821-31.

SMITH, S. A., QUERRY, R. G., FADEL, P. J., GALLAGHER, K. M., STROMSTAD, M., IDE, K., RAVEN, P. B. & SECHER, N. H. 2003. Partial blockade of skeletal muscle somatosensory afferents attenuates baroreflex resetting during exercise in humans. *J Physiol,* 551**,** 1013-21.

SMITH, S. M. & VALE, W. W. 2006. The role of the hypothalamic-pituitary-adrenal axis in neuroendocrine responses to stress. *Dialogues Clin Neurosci,* 8**,** 383-95.

SMITHWICK, R. H. & THOMPSON, J. E. 1953. Splanchnicectomy for essential hypertension; results in 1,266 cases. *J Am Med Assoc,* 152**,** 1501-4.

SMYTH, H. S., SLEIGHT, P. & PICKERING, G. W. 1969. Reflex regulation of arterial pressure during sleep in man. A quantitative method of assessing baroreflex sensitivity. *Circ Res,* 24**,** 109-21.

SOBAJIMA, M., NOZAWA, T., NAKADATE, T., SHIDA, T., OHORI, T., SUZUKI, T., MATSUKI, A., HIRAI, T. & INOUE, H. 2011. Transient hypercapnic stress causes exaggerated and prolonged elevation of cardiac and renal interstitial norepinephrine levels in conscious hypertensive rats. *Am J Physiol Heart Circ Physiol,* 300**,** H2214-20.

SOLANO-FLORES, L. P., ROSAS-ARELLANO, M. P. & CIRIELLO, J. 1997. Fos induction in central structures after afferent renal nerve stimulation. *Brain Res,* 753**,** 102-19.

SOLTIS, R. P., COOK, J. C., GREGG, A. E., STRATTON, J. M. & FLICKINGER, K. A. 1998. EAA receptors in the dorsomedial hypothalamic area mediate the cardiovascular response to activation of the amygdala. *Am J Physiol,* 275**,** R624-31.

SOMERS, V. K., MARK, A. L. & ABBOUD, F. M. 1991. Interaction of baroreceptor and chemoreceptor reflex control of sympathetic nerve activity in normal humans. *J Clin Invest,* 87**,** 1953-7.

SONG, X., GAO, X., GUO, D., YU, Q., GUO, W., HE, C., BURNSTOCK, G. & XIANG, Z. 2012. Expression of P2X(2) and P2X (3) receptors in the rat carotid sinus, aortic arch, vena cava, and heart, as well as petrosal and nodose ganglia. *Purinergic Signal,* 8**,** 15-22.

SPIEKER, L. E., CORTI, R., BINGGELI, C., LUSCHER, T. F. & NOLL, G. 2000. Baroreceptor dysfunction induced by nitric oxide synthase inhibition in humans. *J Am Coll Cardiol,* 36**,** 213-8.

STAUSS, H. M. 2007. Identification of blood pressure control mechanisms by power spectral analysis. *Clin Exp Pharmacol Physiol,* 34**,** 362-8.

STAUSS, H. M., MOFFITT, J. A., CHAPLEAU, M. W., ABBOUD, F. M. & JOHNSON, A. K. 2006. Baroreceptor reflex sensitivity estimated by the sequence technique is reliable in rats. *Am J Physiol Heart Circ Physiol,* 291**,** H482-3.

STEINBACK, C. D., SALZER, D., MEDEIROS, P. J., KOWALCHUK, J. & SHOEMAKER, J. K. 2009. Hypercapnic vs. hypoxic control of cardiovascular, cardiovagal, and sympathetic function. *Am J Physiol Regul Integr Comp Physiol,* 296**,** R402-10.

STOCKER, S. D. & MUNTZEL, M. S. 2013. Recording sympathetic nerve activity chronically in rats: surgery techniques, assessment of nerve activity, and quantification. *Am J Physiol Heart Circ Physiol,* 305**,** H1407-16.

STOTZ-POTTER, E. H., WILLIS, L. R. & DIMICCO, J. A. 1996. Muscimol acts in dorsomedial but not paraventricular hypothalamic nucleus to suppress cardiovascular effects of stress. *J Neurosci,* 16**,** 1173-9.

STRAMBA-BADIALE, M., VANOLI, E., DE FERRARI, G. M., CERATI, D., FOREMAN, R. D. & SCHWARTZ, P. J. 1991. Sympathetic-parasympathetic interaction and accentuated antagonism in conscious dogs. *Am J Physiol,* 260**,** H335-40.

STRAZZULLO, P., BARBATO, A., VUOTTO, P. & GALLETTI, F. 2001. Relationships between salt sensitivity of blood pressure and sympathetic nervous system activity: a short review of evidence. *Clin Exp Hypertens,* 23**,** 25-33.

STRINGER, K. D., KOMERS, R., OSMAN, S. A., OYAMA, T. T., LINDSLEY, J. N. & ANDERSON, S. 2005. Gender hormones and the progression of experimental polycystic kidney disease. *Kidney Int,* 68**,** 1729-39.

STROJEK, K., GRZESZCZAK, W., GORSKA, J., LESCHINGER, M. I. & RITZ, E. 2001. Lowering of microalbuminuria in diabetic patients by a sympathicoplegic agent: novel approach to prevent progression of diabetic nephropathy? *J Am Soc Nephrol,* 12**,** 602-5.

STUDINGER, P., LENARD, Z., MERSICH, B., REUSZ, G. S. & KOLLAI, M. 2006. Determinants of baroreflex function in juvenile end-stage renal disease. *Kidney Int,* 69**,** 2236-42.

STUESSE, S. L. 1982. Origins of cardiac vagal preganglionic fibers: a retrograde transport study. *Brain Res,* 236**,** 15-25.

SU, J. D., HUANG, Z. S., WANG, S. L. & LU, J. 1996. [Medullary mechanism of the inhibition on renal sympathetic efferent activities by stimulation of the cervical vagal afferent nerve in rabbits]. *Sheng Li Xue Bao,* 48**,** 410-4.

SUN, H., LI, D. P., CHEN, S. R., HITTELMAN, W. N. & PAN, H. L. 2009. Sensing of blood pressure increase by transient receptor potential vanilloid 1 receptors on baroreceptors. *J Pharmacol Exp Ther,* 331**,** 851-9.

SUN, M. K. & GUYENET, P. G. 1985. GABA-mediated baroreceptor inhibition of reticulospinal neurons. *Am J Physiol,* 249**,** R672-80.

SUN, M. K. & GUYENET, P. G. 1987. Arterial baroreceptor and vagal inputs to sympathoexcitatory neurons in rat medulla. *Am J Physiol,* 252**,** R699-709.

SUN, Q., GOODCHILD, A. K. & PILOWSKY, P. M. 2001. Firing patterns of pre-Botzinger and Botzinger neurons during hypocapnia in the adult rat. *Brain Res,* 903**,** 198-206.

SUNDLOF, G. & WALLIN, B. G. 1977. The variability of muscle nerve sympathetic activity in resting recumbent man. *J Physiol,* 272**,** 383-97.

SUTLIFF, R. L., WALP, E. R., EL-ALI, A. M., ELKHATIB, S., LOMASHVILI, K. A. & O'NEILL, W. C. 2011. Effect of medial calcification on vascular function in uremia. *Am J Physiol Renal Physiol,* 301**,** F78-83.

SUZUKI, H., MORIWAKI, K., KANNO, Y., NAKAMOTO, H., OKADA, H. & CHEN, X. M. 2001. Comparison of the effects of an ACE inhibitor and alphabeta blocker on the progression of renal failure with left ventricular hypertrophy: preliminary report. *Hypertens Res,* 24**,** 153-8.

SVED, A. F., ITO, S. & MADDEN, C. J. 2000. Baroreflex dependent and independent roles of the caudal ventrolateral medulla in cardiovascular regulation. *Brain Res Bull,* 51**,** 129-33.

SVENSSON, M. & ERIKSSON, J. W. 2006. Insulin resistance in diabetic nephropathy--cause or consequence? *Diabetes Metab Res Rev,* 22**,** 401-10.

SWEENEY, H. L., BOWMAN, B. F. & STULL, J. T. 1993. Myosin light chain phosphorylation in vertebrate striated muscle: regulation and function. *Am J Physiol,* 264**,** C1085-95.

SWEENEY, W. E., JR. & AVNER, E. D. 2006. Molecular and cellular pathophysiology of autosomal recessive polycystic kidney disease (ARPKD). *Cell Tissue Res,* 326**,** 671-85.

TAGAWA, T. & DAMPNEY, R. A. 1999. AT(1) receptors mediate excitatory inputs to rostral ventrolateral medulla pressor neurons from hypothalamus. *Hypertension,* 34**,** 1301-7.

TALMAN, W. T., PERRONE, M. H. & REIS, D. J. 1980. Evidence for L-glutamate as the neurotransmitter of baroreceptor afferent nerve fibers. *Science,* 209**,** 813-5.

TANK, J., DIEDRICH, A., SZCZECH, E., LUFT, F. C. & JORDAN, J. 2005. Baroreflex regulation of heart rate and sympathetic vasomotor tone in women and men. *Hypertension,* 45**,** 1159-64.

TEMMAR, M., LIABEUF, S., RENARD, C., CZERNICHOW, S., ESPER, N. E., SHAHAPUNI, I., PRESNE, C., MAKDASSI, R., ANDREJAK, M., TRIBOUILLOY, C., GALAN, P., SAFAR, M. E., CHOUKROUN, G. & MASSY, Z. 2010. Pulse wave velocity and vascular calcification at different stages of chronic kidney disease. *J Hypertens,* 28**,** 163-9.

THAPA, L., KARKI, P., SHARMA, S. K. & BAJAJ, B. K. 2010. Cardiovascular autonomic neuropathy in chronic kidney diseases. *JNMA J Nepal Med Assoc,* 49**,** 121-8.

THAYER, J. F., YAMAMOTO, S. S. & BROSSCHOT, J. F. 2010. The relationship of autonomic imbalance, heart rate variability and cardiovascular disease risk factors. *Int J Cardiol,* 141**,** 122-31.

THOMAS, G. D. 2011. Neural control of the circulation. *Adv Physiol Educ,* 35**,** 28-32.

TIMMERS, H. J., WIELING, W., KAREMAKER, J. M. & LENDERS, J. W. 2003. Denervation of carotid baro- and chemoreceptors in humans. *J Physiol,* 553**,** 3-11.

TINUCCI, T., ABRAHAO, S. B., SANTELLO, J. L. & MION, D., JR. 2001. Mild chronic renal insufficiency induces sympathetic overactivity. *J Hum Hypertens,* 15**,** 401-6.

TOADER, E., MCALLEN, R. M., CIVIDJIAN, A., WOODS, R. L. & QUINTIN, L. 2007. Effect of systemic B-type natriuretic peptide on cardiac vagal motoneuron activity. *Am J Physiol Heart Circ Physiol,* 293**,** H3465-70.

TOGASHI, H., SAKUMA, I., YOSHIOKA, M., KOBAYASHI, T., YASUDA, H., KITABATAKE, A., SAITO, H., GROSS, S. S. & LEVI, R. 1992. A central nervous system action of nitric oxide in blood pressure regulation. *J Pharmacol Exp Ther,* 262**,** 343-7.

TOMIYAMA, O., SHIIGAI, T., IDEURA, T., TOMITA, K., MITO, Y., SHINOHARA, S. & TAKEUCHI, J. 1980. Baroreflex sensitivity in renal failure. *Clin Sci (Lond),* 58**,** 21-7.

TONELLI, M., WIEBE, N., CULLETON, B., HOUSE, A., RABBAT, C., FOK, M., MCALISTER, F. & GARG, A. X. 2006. Chronic kidney disease and mortality risk: a systematic review. *J Am Soc Nephrol,* 17**,** 2034-47.

TORY, K., HORVATH, E., SUVEGES, Z., FEKETE, A., SALLAY, P., BERTA, K., SZABO, T., SZABO, A. J., TULASSAY, T. & REUSZ, G. S. 2004. Effect of propranolol on heart rate variability in patients with end-stage renal disease: a double-blind, placebo-controlled, randomized crossover pilot trial. *Clin Nephrol,* 61**,** 316-23.

TRAPP, M. L., GALTSEVA, A., MANNING, D. K., BEIER, D. R., ROSENBLUM, N. D. & QUARMBY, L. M. 2008. Defects in ciliary localization of Nek8 is associated with cystogenesis. *Pediatr Nephrol,* 23**,** 377-87.

TROMBETTA, I. C., MAKI-NUNES, C., TOSCHI-DIAS, E., ALVES, M. J., RONDON, M. U., CEPEDA, F. X., DRAGER, L. F., BRAGA, A. M., LORENZI-FILHO, G. & NEGRAO, C. E. 2013. Obstructive sleep apnea is associated with increased chemoreflex sensitivity in patients with metabolic syndrome. *Sleep,* 36**,** 41-9.

TU, H., ZHANG, L., TRAN, T. P., MUELLEMAN, R. L. & LI, Y. L. 2010. Reduced expression and activation of voltage-gated sodium channels contributes to blunted baroreflex sensitivity in heart failure rats. *J Neurosci Res,* 88**,** 3337-49.

TURNER, M. J., KAWADA, T. & SUGIMACHI, M. 2013. Differential dynamic control of cardiac and splanchnic sympathetic nerve activity by the arterial baroreflex. *Conf Proc IEEE Eng Med Biol Soc,* 2013**,** 3809-12.

U.S. RENAL DATA SYSTEM 2013. U.S. renal data system annual data report: atlas of chronic kidney disease and end-stage renal disease in the United States. National Institutes of Health, National Institute of Diabetes and Digestive and Kidney Diseases, Bethesda, MD.

UGGERE, T. A., ABREU, G. R., SAMPAIO, K. N., CABRAL, A. M. & BISSOLI, N. S. 2000. The cardiopulmonary reflexes of spontaneously hypertensive rats are normalized after regression of left ventricular hypertrophy and hypertension. *Braz J Med Biol Res,* 33**,** 589-94.

UIJTDEHAAGE, S. H. & THAYER, J. F. 2000. Accentuated antagonism in the control of human heart rate. *Clin Auton Res,* 10**,** 107-10.

ULRICH-LAI, Y. M. & HERMAN, J. P. 2009. Neural regulation of endocrine and autonomic stress responses. *Nat Rev Neurosci,* 10**,** 397-409.

VALVO, E., GAMMARO, L., TESSITORE, N., PANZETTA, G., LUPO, A., LOSCHIAVO, C., OLDRIZZI, L., FABRIS, A., RUGIU, C., ORTALDA, V. & ET AL. 1985. Hypertension of polycystic kidney disease: mechanisms and hemodynamic alterations. *Am J Nephrol,* 5**,** 176-81.

VARDHAN, A., KACHROO, A. & SAPRU, H. N. 1993. Excitatory amino acid receptors in the nucleus tractus solitarius mediate the responses to the stimulation of cardio-pulmonary vagal afferent C fiber endings. *Brain Res,* 618**,** 23-31.

VASQUEZ, E. C., MEYRELLES, S. S., MAUAD, H. & CABRAL, A. M. 1997. Neural reflex regulation of arterial pressure in pathophysiological conditions: interplay among the baroreflex, the cardiopulmonary reflexes and the chemoreflex. *Braz J Med Biol Res,* 30**,** 521-32.

VATTA, M. S., PAPOUCHADO, M. L., BIANCIOTTI, L. G. & FERNANDEZ, B. E. 1993. Atrial natriuretic factor inhibits noradrenaline release in the presence of angiotensin II and III in the rat hypothalamus. *Comp Biochem Physiol C,* 106**,** 545-8.

VAZIRI, N. D., NI, Z., OVEISI, F., LIANG, K. & PANDIAN, R. 2002. Enhanced nitric oxide inactivation and protein nitration by reactive oxygen species in renal insufficiency. *Hypertension,* 39**,** 135-41.

VERBERNE, A. J. & GUYENET, P. G. 1992. Medullary pathway of the Bezold-Jarisch reflex in the rat. *Am J Physiol,* 263**,** R1195-202.

VERBERNE, A. J., STORNETTA, R. L. & GUYENET, P. G. 1999. Properties of C1 and other ventrolateral medullary neurones with hypothalamic projections in the rat. *J Physiol,* 517 (Pt 2)**,** 477-94.

VERBERNE, A. J., YOUNG, N. A. & LOUIS, W. J. 1988. Impairment of inhibitory cardiopulmonary vagal reflexes in spontaneously hypertensive rats. *J Auton Nerv Syst,* 23**,** 63-8.

VICTOR, R. G., THOREN, P., MORGAN, D. A. & MARK, A. L. 1989. Differential control of adrenal and renal sympathetic nerve activity during hemorrhagic hypotension in rats. *Circ Res,* 64**,** 686-94.

VINK, E. E., DE JAGER, R. L. & BLANKESTIJN, P. J. 2013. Sympathetic hyperactivity in chronic kidney disease: pathophysiology and (new) treatment options. *Curr Hypertens Rep,* 15**,** 95-101.

VITA, G., BELLINGHIERI, G., TRUSSO, A., COSTANTINO, G., SANTORO, D., MONTELEONE, F., MESSINA, C. & SAVICA, V. 1999. Uremic autonomic neuropathy studied by spectral analysis of heart rate. *Kidney Int,* 56**,** 232-7.

VITA, G., SAVICA, V., PUGLISI, R. M., MARABELLO, L., BELLINGHIERI, G. & MESSINA, C. 1992. The course of autonomic neural function in chronic uraemic patients during haemodialysis treatment. *Nephrol Dial Transplant,* 7**,** 1022-5.

VITELA, M., HERRERA-ROSALES, M., HAYWOOD, J. R. & MIFFLIN, S. W. 2005. Baroreflex regulation of renal sympathetic nerve activity and heart rate in renal wrap hypertensive rats. *Am J Physiol Regul Integr Comp Physiol,* 288**,** R856-62.

VLACHOJANNIS, J. G., TSAKAS, S., ALEXANDRI, S., PETROPOULOU, C. & GOUMENOS, D. S. 2000. Continuous ambulatory peritoneal dialysis is responsible for an increase in plasma norepinephrine. *Perit Dial Int,* 20**,** 322-7.

VOLLENWEIDER, P., TAPPY, L., RANDIN, D., SCHNEITER, P., JEQUIER, E., NICOD, P. & SCHERRER, U. 1993. Differential effects of hyperinsulinemia and carbohydrate metabolism on sympathetic nerve activity and muscle blood flow in humans. *J Clin Invest,* 92**,** 147-54.

VONEND, O., MARSALEK, P., RUSS, H., WULKOW, R., OBERHAUSER, V. & RUMP, L. C. 2003. Moxonidine treatment of hypertensive patients with advanced renal failure. *J Hypertens,* 21**,** 1709-17.

WALLIN, B. G. & SUNDLOF, G. 1979. A quantitative study of muscle nerve sympathetic activity in resting normotensive and hypertensive subjects. *Hypertension,* 1**,** 67-77.

WALLIN, B. G., ESLER, M., DORWARD, P., EISENHOFER, G., FERRIER, C., WESTERMAN, R. & JENNINGS, G. 1992. Simultaneous measurements of cardiac noradrenaline spillover and sympathetic outflow to skeletal muscle in humans. *J Physiol,* 453**,** 45-58.

WALLIN, B. G., SUNDLOF, G., STROMGREN, E. & ABERG, H. 1984. Sympathetic outflow to muscles during treatment of hypertension with metoprolol. *Hypertension,* 6**,** 557-62.

WALLIN, B. G., THOMPSON, J. M., JENNINGS, G. L. & ESLER, M. D. 1996. Renal noradrenaline spillover correlates with muscle sympathetic activity in humans. *J Physiol,* 491 (Pt 3)**,** 881-7.

WAMBACH, G., GOTZ, S., SUCKAU, G., BONNER, G. & KAUFMANN, W. 1987. Plasma levels of atrial natriuretic peptide are raised in essential hypertension during low and high sodium intake. *Klin Wochenschr,* 65**,** 232-7.

WANG, A. Y., LI, P. K., LUI, S. F. & SANDERSON, J. E. 2004. Angiotensin converting enzyme inhibition for cardiac hypertrophy in patients with end-stage renal disease: what is the evidence? *Nephrology (Carlton),* 9**,** 190-7.

WANG, D. & STRANDGAARD, S. 1997. The pathogenesis of hypertension in autosomal dominant polycystic kidney disease. *J Hypertens,* 15**,** 925-33.

WANG, G., MILNER, T. A., SPETH, R. C., GORE, A. C., WU, D., IADECOLA, C. & PIERCE, J. P. 2008. Sex differences in angiotensin signaling in bulbospinal neurons in the rat rostral ventrolateral medulla. *Am J Physiol Regul Integr Comp Physiol,* 295**,** R1149-57.

WANG, J., IRNATEN, M., NEFF, R. A., VENKATESAN, P., EVANS, C., LOEWY, A. D., METTENLEITER, T. C. & MENDELOWITZ, D. 2001. Synaptic and neurotransmitter activation of cardiac vagal neurons in the nucleus ambiguus. *Ann N Y Acad Sci,* 940**,** 237-46.

WATKINS, L. L., GROSSMAN, P. & SHERWOOD, A. 1996. Noninvasive assessment of baroreflex control in borderline hypertension. Comparison with the phenylephrine method. *Hypertension,* 28**,** 238-43.

WAUGH, A. & GRANT, A. 2010. *Ross & Wilson Anatomy and Physiology in Health and Illness*, Elsevier Health Sciences UK.

WEINSTOCK, M., GORODETSKY, E. & KALMAN, R. 1996. Renal denervation prevents sodium retention and hypertension in salt-sensitive rabbits with genetic baroreflex impairment. *Clin Sci,* 90**,** 287-93.

WEIR, M. R. 2007. Effects of renin-angiotensin system inhibition on end-organ protection: can we do better? *Clin Ther,* 29**,** 1803-24.

WEIR, M. R. 2009. The renoprotective effects of RAS inhibition: focus on prevention and treatment of chronic kidney disease. *Postgrad Med,* 121**,** 96-103.

WENKER, I. C., SOBRINHO, C. R., TAKAKURA, A. C., MULKEY, D. K. & MOREIRA, T. S. 2013. P2Y1 receptors expressed by C1 neurons determine peripheral chemoreceptor modulation of breathing, sympathetic activity, and blood pressure. *Hypertension,* 62, 263-73.

WEVER, R., BOER, P., HIJMERING, M., STROES, E., VERHAAR, M., KASTELEIN, J., VERSLUIS, K., LAGERWERF, F., VAN RIJN, H., KOOMANS, H. & RABELINK, T. 1999. Nitric oxide production is reduced in patients with chronic renal failure. *Arterioscler Thromb Vasc Biol,* 19**,** 1168-72.

WILLIAMS, J. K., ADAMS, M. R., HERRINGTON, D. M. & CLARKSON, T. B. 1992. Short-term administration of estrogen and vascular responses of atherosclerotic coronary arteries. J Am Coll Cardiol, 20, 452-7.

WOLF, M. T. & HILDEBRANDT, F. 2011. Nephronophthisis. *Pediatr Nephrol,* 26**,** 181-94.

WOLFE, R. A., ASHBY, V. B., MILFORD, E. L., OJO, A. O., ETTENGER, R. E., AGODOA, L. Y., HELD, P. J. & PORT, F. K. 1999. Comparison of mortality in all patients on dialysis, patients on dialysis awaiting transplantation, and recipients of a first cadaveric transplant. *N Engl J Med,* 341**,** 1725-30.

WONG, H., MYLREA, K., FEBER, J., DRUKKER, A. & FILLER, G. 2006. Prevalence of complications in children with chronic kidney disease according to KDOQI. *Kidney Int,* 70**,** 585-90.

WOODS, R. L., COURNEYA, C. A. & HEAD, G. A. 1994. Nonuniform enhancement of baroreflex sensitivity by atrial natriuretic peptide in conscious rats and dogs. *Am J Physiol,* 267**,** R678-86.

WUHL, E. & SCHAEFER, F. 2011. Managing kidney disease with blood-pressure control. *Nat Rev Nephrol,* 7**,** 434-44.

WYSS, J. M., ABOUKARSH, N. & OPARIL, S. 1986. Sensory denervation of the kidney attenuates renovascular hypertension in the rat. *Am J Physiol,* 250**,** H82-6.

XING, D., NOZELL, S., CHEN, Y. F., HAGE, F. & OPARIL, S. 2009. Estrogen and mechanisms of vascular protection. *Arterioscler Thromb Vasc Biol,* 29**,** 289-95.

XU, J., LI, G., WANG, P., VELAZQUEZ, H., YAO, X., LI, Y., WU, Y., PEIXOTO, A., CROWLEY, S. & DESIR, G. V. 2005. Renalase is a novel, soluble monoamine oxidase that regulates cardiac function and blood pressure. *J Clin Invest,* 115**,** 1275-80.

XU, R., ZHANG, L. X., ZHANG, P. H., WANG, F., ZUO, L. & WANG, H. Y. 2010. Gender differences in age-related decline in glomerular filtration rates in healthy people and chronic kidney disease patients. *BMC Nephrol,* 11**,** 20.

XUE, B., PAMIDIMUKKALA, J. & HAY, M. 2005. Sex differences in the development of angiotensin II-induced hypertension in conscious mice. *Am J Physiol Heart Circ Physiol,* 288**,** H2177-84.

YANG, H. C., ZUO, Y. & FOGO, A. B. 2010a. Models of chronic kidney disease. *Drug Discov Today Dis Models,* 7**,** 13-9.

YANG, Y. W., WU, C. H., TSAI, M. K., KUO, T. B., YANG, C. C. & LEE, P. H. 2010b. Heart rate variability during hemodialysis and following renal transplantation. *Transplant Proc,* 42**,** 1637-40.

YANG, Z. & COOTE, J. H. 2003. Role of GABA and NO in the paraventricular nucleus-mediated reflex inhibition of renal sympathetic nerve activity following stimulation of right atrial receptors in the rat. *Exp Physiol,* 88**,** 335-42.

YANG, Z., BERTRAM, D. & COOTE, J. H. 2001. The role of glutamate and vasopressin in the excitation of RVL neurones by paraventricular neurones. *Brain Res,* 908**,** 99-103.

YANG, Z., WHEATLEY, M. & COOTE, J. H. 2002. Neuropeptides, amines and amino acids as mediators of the sympathetic effects of paraventricular nucleus activation in the rat. *Exp Physiol,* 87**,** 663-74.

YE, S., GAMBURD, M., MOZAYENI, P., KOSS, M. & CAMPESE, V. M. 1998. A limited renal injury may cause a permanent form of neurogenic hypertension. *Am J Hypertens,* 11**,** 723-8.

YE, S., NOSRATI, S. & CAMPESE, V. M. 1997a. Nitric oxide (NO) modulates the neurogenic control of blood pressure in rats with chronic renal failure (CRF). *J Clin Invest,* 99**,** 540-8.

YE, S., OZGUR, B. & CAMPESE, V. M. 1997b. Renal afferent impulses, the posterior hypothalamus, and hypertension in rats with chronic renal failure. *Kidney Int,* 51**,** 722-7.

YILDIZ, A., SEVER, M. S., DEMIREL, S., AKKAYA, V., TURK, S., TURKMEN, A., ECDER, T. & ARK, E. 1998. Improvement of uremic autonomic dysfunction after renal transplantation: a heart rate variability study. *Nephron,* 80**,** 57-60.

YOSHIMOTO, M., MIKI, K., FINK, G. D., KING, A. & OSBORN, J. W. 2010. Chronic angiotensin II infusion causes differential responses in regional sympathetic nerve activity in rats. *Hypertension,* 55**,** 644-51.

YOUNG, J. H., KLAG, M. J., MUNTNER, P., WHYTE, J. L., PAHOR, M. & CORESH, J. 2002. Blood pressure and decline in kidney function: findings from the Systolic Hypertension in the Elderly Program (SHEP). *J Am Soc Nephrol,* 13**,** 2776-82.

ZANZINGER, J., CZACHURSKI, J. & SELLER, H. 1995. Inhibition of basal and reflex-mediated sympathetic activity in the RVLM by nitric oxide. *Am J Physiol,* 268**,** R958-62.

ZARETSKY, D. V., ZARETSKAIA, M. V., SAMUELS, B. C., CLUXTON, L. K. & DIMICCO, J. A. 2003. Microinjection of muscimol into raphe pallidus suppresses tachycardia associated with air stress in conscious rats. *J Physiol,* 546**,** 243-50.

ZERRES, K., RUDNIK-SCHONEBORN, S., SENDEREK, J., EGGERMANN, T. & BERGMANN, C. 2003. Autosomal recessive polycystic kidney disease (ARPKD). *J Nephrol,* 16**,** 453-8.

ZHANG, D., LIU, J., TU, H., MUELLEMAN, R. L., CORNISH, K. G. & LI, Y. L. 2014. In vivo transfection of manganese superoxide dismutase gene or nuclear factor kappaB shRNA in nodose ganglia improves aortic baroreceptor function in heart failure rats. *Hypertension,* 63**,** 88-95.

ZHANG, H. & FABER, J. E. 2001. Trophic effect of norepinephrine on arterial intima-media and adventitia is augmented by injury and mediated by different alpha1-adrenoceptor subtypes. *Circ Res,* 89**,** 815-22.

ZHANG, J. & MIFFLIN, S. W. 2000. Integration of Aortic Nerve Inputs in Hypertensive Rats. *Hypertension,* 35**,** 430-6.

ZHANG, K., MAYHAN, W. G. & PATEL, K. P. 1997. Nitric oxide within the paraventricular nucleus mediates changes in renal sympathetic nerve activity. *Am J Physiol,* 273**,** R864-72.

ZHANG, W. & THOREN, P. 1998. Hyper-responsiveness of adrenal sympathetic nerve activity in spontaneously hypertensive rats to ganglionic blockade, mental stress and neuronglucopenia. *Pflugers Arch,* 437**,** 56-60.

ZILCH, O., VOS, P. F., OEY, P. L., CRAMER, M. J., LIGTENBERG, G., KOOMANS, H. A. & BLANKESTIJN, P. J. 2007. Sympathetic hyperactivity in haemodialysis patients is reduced by short daily haemodialysis. *J Hypertens,* 25**,** 1285-9.

ZOCCALI, C., MALLAMACI, F., TRIPEPI, G., PARLONGO, S., CUTRUPI, S., BENEDETTO, F. A., CATALIOTTI, A. & MALATINO, L. S. 2002. Norepinephrine and concentric hypertrophy in patients with end-stage renal disease. *Hypertension,* 40**,** 41-6.

ZOLLINGER, H. U., MIHATSCH, M. J., EDEFONTI, A., GABOARDI, F., IMBASCIATI, E. & LENNERT, T. 1980. Nephronophthisis (medullary cystic disease of the kidney). A study using electron microscopy, immunofluorescence, and a review of the morphological findings. *Helv Paediatr Acta,* 35**,** 509-30.

ZUCKER, I. H. 2006. Novel mechanisms of sympathetic regulation in chronic heart failure. *Hypertension,* 48**,** 1005-11.

ZYGMUNT, A. & STANCZYK, J. 2010. Methods of evaluation of autonomic nervous system function. *Arch Med Sci,* 6**,** 11-8.

Appendix 1

Burst Frequency Analysis of Aortic Depressor Nerve Activity in Chronic Kidney Disease

The following Appendix provides further analysis of the afferent component of the baroreflex arc in animals studied in Chapters 3 & 4.

1. Introduction

Under pathological conditions such as hypertension, a reduction in arterial distensibility due to vascular stiffness and remodelling, is associated with diminished baroreceptor sensitivity and impaired afferent traffic (Andresen et al., 1978). In chronic kidney disease (CKD), baroreflex sensitivity negatively correlates with the magnitude of vascular calcification (Chan et al., 2005, Chesterton et al., 2005) and arterial stiffness (Studinger et al., 2006). As described in Chapters 3 & 4, the adult male, but not female, Lewis Polycystic Kidney (LPK) rat model of CKD show a reduction in the ability to effectively transduce baroreceptor afferent information to the brain. This information was deduced based on analysis of the baroreceptor afferent gain and range of the mean arterial pressure (MAP)-aortic depressor nerve activity (ADNA) relationship in LPK and Lewis control rats, which demonstrated reduced measures in adult male, but not female, LPK. While the range of the relationship was reflective of differences in the aortic depressor nerve (ADN) burst amplitude between groups, it remained undetermined whether this was associated with altered frequency of activation of the baroreceptors. Accordingly, the aim of the present analysis was to identify differences in the ADN burst frequency between the Lewis and LPK, and changes associated with age and sex.

2. Methods

As detailed in Chapters 3 & 4, juvenile and adult Lewis and LPK rats of either sex (total $n = 51$) were prepared for recording of ADNA and blood pressure (BP) and measurement of responses to phenylephrine (PE) and sodium nitroprusside (SNP). Raw ADNA signal was rectified and smoothed (0.02 s time constant) and an algorithm that counts the number of pulse-synchronous ADNA peaks during baseline and PE administration was activated on Spike 2 software. Burst frequency of the ADN was expressed as burst per second (Hz). The ADN burst frequency during SNP administration was not quantified due to a significant reduction in ADN bursting pattern. All data are expressed as mean ± standard error of the mean (SEM). Statistical analysis was performed using GraphPad Prism software (GraphPad Prism software v6 Inc., La Jolla, CA, USA). A two-way ANOVA was used to identify, within each age group, if strain differences existed, and within each strain, if age or sex differences existed. Where ANOVA indicated a strain, age or gender difference a Bonferroni's post-hoc analysis was performed. Significance was defined as $P \leq 0.05$ for all analysis.

3. Results

Figures 1 and 2 show representative data traces of ADNA acquired from juvenile and adult Lewis and LPK rats of either sex, illustrating ADN burst number and systolic triggered averages of ADNA during PE administration. Group data is shown in Table 1.

Regardless of sex, ADN burst frequency was significantly higher (all $P<0.05$) in the LPK versus Lewis at both baseline and when a BP increase with PE was evoked. In the male LPK versus Lewis, ADN burst number during baseline, but not during PE administration, was also greater overall ($P<0.01$). In the female LPK versus Lewis, ADN burst number was always higher regardless of whether measurements were taken at baseline or when BP was increased using PE. Time to reach peak ANDA following PE injection did not differ within the female and male groups, and both age and sex did not influence any of the recorded parameters.

4. Discussion

The major finding of the present analysis was that ADN burst frequency is increased in the LPK rats at both baseline levels or during baroreceptor loading, suggestive of more frequent activation of the baroreceptors in this model. This is consistent with the higher resting HR of the strain, as it is well established that the ADN firing is phasic with the cardiac cycle (Abboud and Chapleau, 1988). In the light of the present results, it is therefore unlikely that a reduction in the frequency of activation of the baroreceptors could have contributed to the observed diminution in the baroreceptor afferent function in the male LPK and that both reductions in the burst amplitude (Figures 1 & 2), evidenced by the blunted range of MAP-ADNA relationship (Chapter 3), and the rate at which the afferent signal travels to the central pathways, indicated by reduced gain of the relationship (Chapter 3), are the primary contributor to the afferent deficit in the male model of CKD. The analysis shown here further adds to the characterisation of the afferent component of the baroreflex circuit in the female LPK, demonstrating that females with CKD do not only exhibit intact signal transduction mechanisms but also preserved ADN firing frequency.

Table 1: Burst frequency analysis of the aortic depressor nerve (ADN) in the juvenile (7–8 weeks old) and adult (12–13 weeks old) female Lewis and Lewis Polycystic Kidney (LPK) rats of either sex

Groups	Juvenile		Adult		Two-way ANOVA adjusted *P* value	
	Lewis	LPK	Lewis	LPK	Strain	Age
Parameters						
Male *(n)*	*7*	*6*	*7*	*7*	-	-
Baseline (Hz)	6.1 ± 0.2	7.2 ± 0.3*	5.6 ± 0.4	6.6 ± 0.2*	0.0014	0.0683
Baseline (burst number)	182 ± 5	212 ± 8	171 ± 10	194 ± 10	0.0058	0.1042
During PE (Hz)	6.0 ± 0.2	6.9 ± 0.3	5.5 ± 0.3	6.3 ± 0.4	0.0113	0.0798
During PE (burst number)	33 ± 3	37 ± 1	24 ± 2	32 ± 6	0.0920	0.0621
Time to PE peak (seconds)	5.5 ± 0.4	5.2 ± 0.1	4.4 ± 0.5	5.0 ± 0.7	0.7731	0.2134
Female *(n)*	*6*	*5*	*8*	*5*		
Baseline (Hz)	5.7 ± 0.1	6.4 ± 0.2	5.4 ± 0.2	6.1 ± 0.2*	0.0035	0.1416
Baseline (burst number)	172 ± 4	193 ± 7	163 ± 5	183 ± 7*	0.0035	0.1416
During PE (Hz)	5.5 ± 0.1	6.2 ± 0.3	5.4 ± 0.2	6.1 ± 0.3	0.0099	0.7696
During PE (burst number)	22 ± 2	30 ± 4	21 ± 2	27 ± 3	0.0198	0.5337
Time to PE peak (seconds)	4.1 ± 0.3	4.8 ± 0.6	4.0 ± 0.3	4.5 ± 0.4	0.1707	0.6866

PE, phenylephrine (10–50 µg/kg i.v.). Baseline measurements were taken over a 30-second period.
Results are expressed as mean ± SEM.
*$P<0.05$ vs. age-matched Lewis under baseline or PE conditions.
n = number in each group.

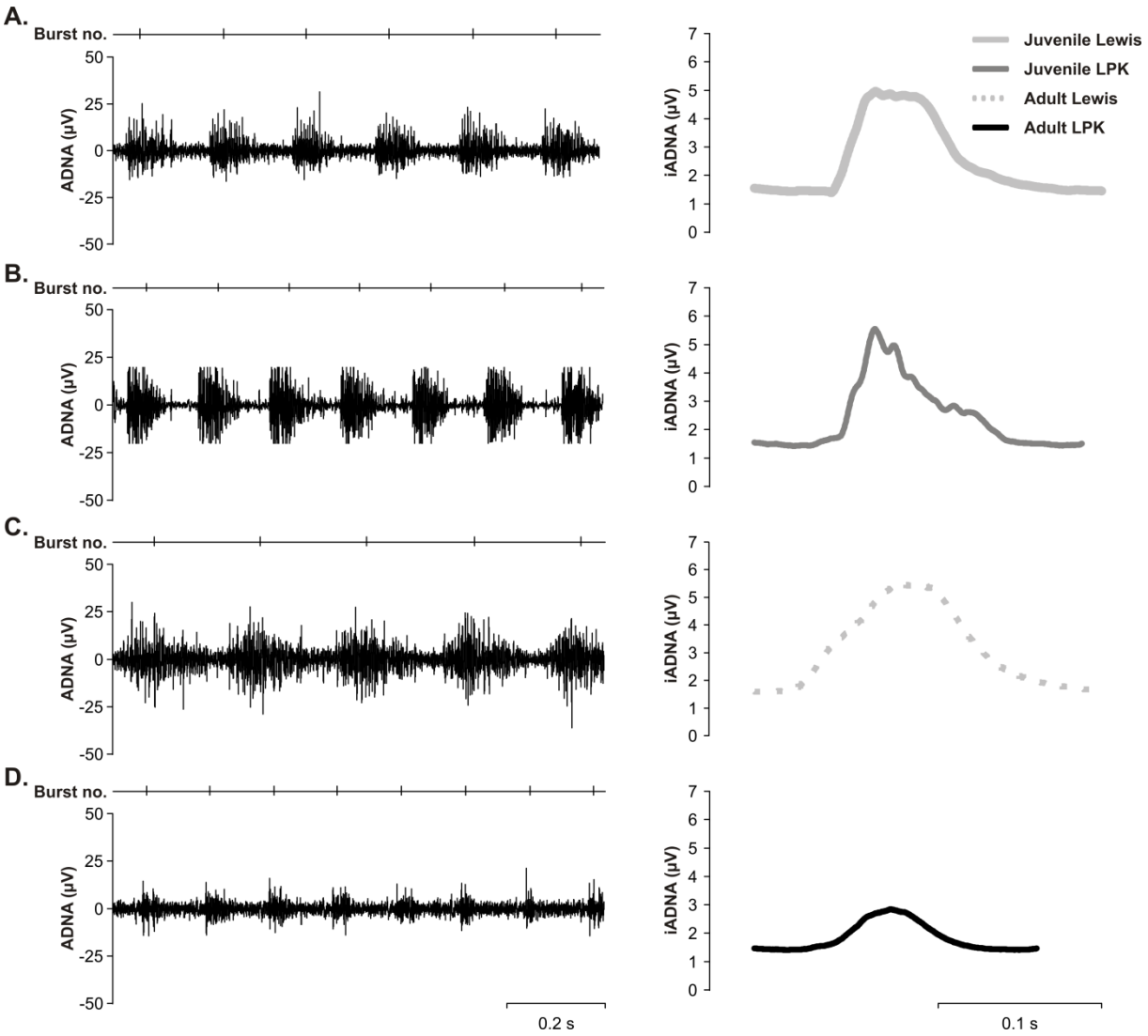

Figure 1: Aortic depressor nerve burst frequency (left panels) and amplitude (right panels) in response to phenylephrine (PE)-induced increase in mean arterial pressure in juvenile (7–8 weeks old, A & B) and adult (12–13 weeks old, C & D) male Lewis (A & C) and male Lewis Polycystic Kidney (LPK) rats (B & D). The left panels show the individual burst count from the original aortic depressor nerve activity (ADNA) signal. Detailed burst frequency analysis is presented in Table 1. The right panels show representative heart rate-triggered averages of the integrated ADNA (iADNA), illustrating the average amplitude of the ADN burst in each group. Note the reduction in burst amplitude in the adult LPK relative to age-matched Lewis and juvenile LPK rats, which is consistent with the reduction in ADNA baroreceptor afferent range in adult male LPK described in Chapter 3.

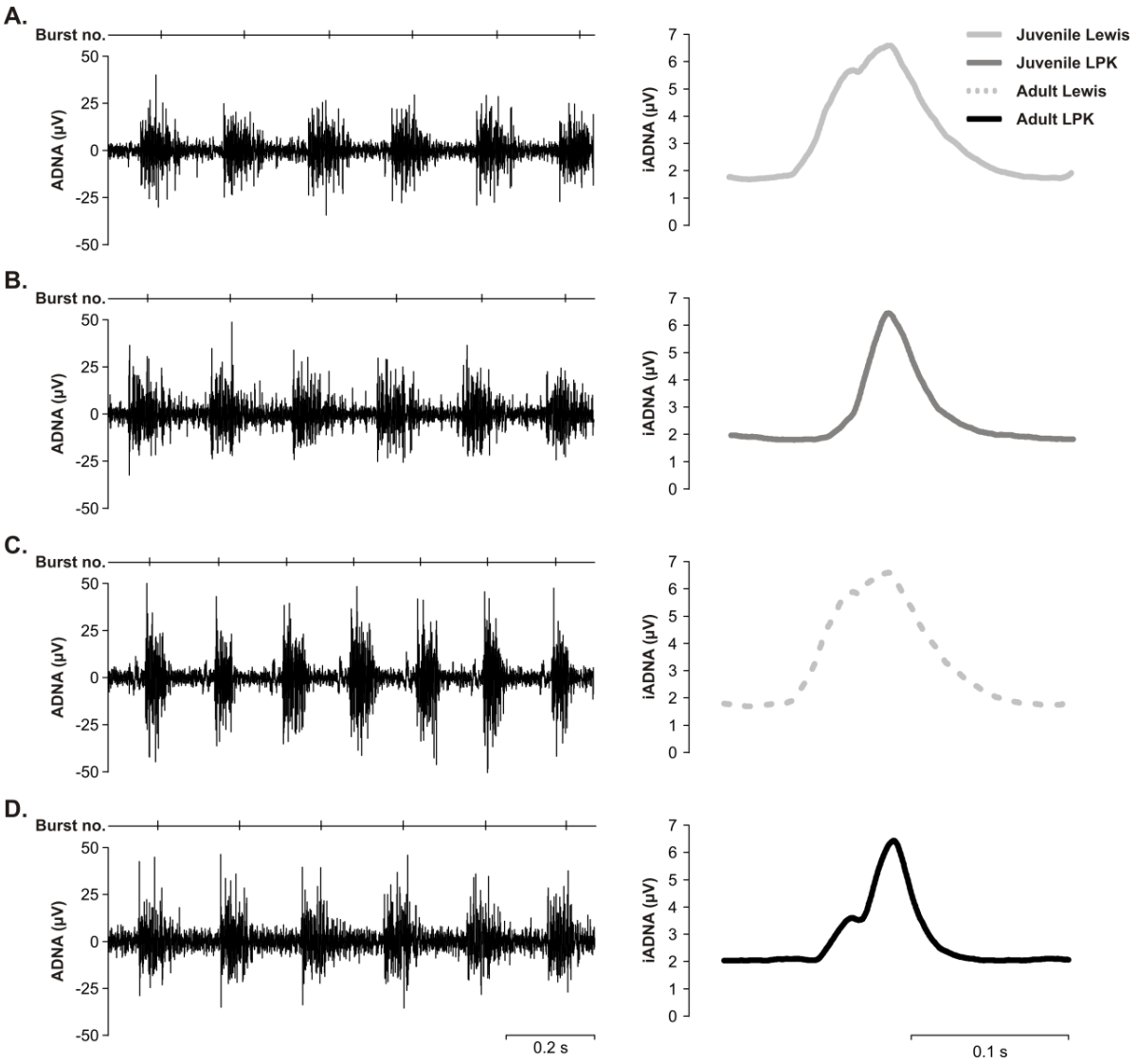

Figure 2: Aortic depressor nerve burst frequency (left panels) and amplitude (right panels) in response to phenylephrine-induced increase in mean arterial pressure in juvenile (7–8 weeks old, A & B) and adult (12–13 weeks old, C & D) female Lewis (A & C) and female Lewis Polycystic Kidney (LPK) rats (B & D). The left panels show the individual burst count from the original aortic depressor nerve activity (ADNA) signal. Detailed burst frequency analysis is presented in Table 1. The right panels show representative heart rate-triggered averages of the integrated ADNA (iADNA), illustrating the average amplitude of the ADN burst in each group. Note the similarity in burst amplitude in the juvenile and adult female Lewis and LPK rats, which is consistent with the comparable ADNA baroreceptor afferent range between the groups described in Chapter 4.

References

ABBOUD, F. M. & CHAPLEAU, M. W. 1988. Effects of pulse frequency on single-unit baroreceptor activity during sine-wave and natural pulses in dogs. *J Physiol,* 401**,** 295-308.

ANDRESEN, M. C., KRAUHS, J. M. & BROWN, A. M. 1978. Relationship of aortic wall and baroreceptor properties during development in normotensive and spontaneously hypertensive rats. *Circ Res,* 43**,** 728-38.

CHAN, C. T., JAIN, V., PICTON, P., PIERRATOS, A. & FLORAS, J. S. 2005. Nocturnal hemodialysis increases arterial baroreflex sensitivity and compliance and normalizes blood pressure of hypertensive patients with end-stage renal disease. *Kidney Int,* 68**,** 338-44.

CHESTERTON, L. J., SIGRIST, M. K., BENNETT, T., TAAL, M. W. & MCINTYRE, C. W. 2005. Reduced baroreflex sensitivity is associated with increased vascular calcification and arterial stiffness. *Nephrol Dial Transplant,* 20**,** 1140-7.

STUDINGER, P., LENARD, Z., MERSICH, B., REUSZ, G. S. & KOLLAI, M. 2006. Determinants of baroreflex function in juvenile end-stage renal disease. *Kidney Int,* 69**,** 2236-42.

Appendix 2

Differential Contribution of Afferent and Central Pathways to the Development of Baroreflex Dysfunction in Chronic Kidney Disease

Ibrahim M. Salman, Cara M. Hildreth, Omar Z. Ameer and Jacqueline K. Phillips

Hypertension. 2014;63:804-810; originally published online December 30, 2013;
doi: 10.1161/HYPERTENSIONAHA.113.02110
Hypertension is published by the American Heart Association, 7272 Greenville Avenue, Dallas, TX 75231

Print ISSN: 0194-911X. Online ISSN: 1524-4563

Pages 231-254 of this thesis have been removed as they contain published material. Please refer to the following citation for details of the article contained in these pages:

Salman, I. M., Hildreth, C. M., Ameer, O. Z., & Phillips, J. K. (2014). Differential contribution of afferent and central pathways to the development of baroreflex dysfunction in chronic kidney disease. Hypertension, 63(4), 804-810. DOI: 10.1161/HYPERTENSIONAHA.113.02110

Appendix 3

Pages 256-264 of this thesis have been removed as they contain published material. Please refer to the following citation for details of the article contained in these pages:

Ameer, O. Z., Salman, I. M., Avolio, A. P., Phillips, J. K., & Butlin, M. (2014). Opposing changes in thoracic and abdominal aortic biomechanical properties in rodent models of vascular calcification and hypertension. American Journal of Physiology-Heart and Circulatory Physiology, 307(2), H143-H151. DOI: 10.1152/ajpheart.00139.2014

Appendix 4

ANIMAL RESEARCH AUTHORITY (ARA)

AEC Reference No.: 2012/060-3 **Date of Expiry:** 9 December 2013

Full Approval Duration: *10 December 2012 to 9 December 2015 (24 Months)*

This ARA remains in force until the Date of Expiry (unless suspended, cancelled or surrendered) **and will only be renewed upon receipt of a satisfactory Progress Report before expiry (see Approval email for submission details).**

Principal Investigator:
Prof Jacqueline Phillips
School of Advanced Medicine
Macquarie University, NSW 2109
jacqueline.phillips@mq.edu.au
0409 225 707

Associate Investigators:
Cara Hildreth 0402 836 705
Yimin Yao 0422 672 507
Other people participating:
Ibrahim Salman 0426 286 182
Divya Sarma Kandukuri 0432 435 596
Rochelle Boyd 0409 322 382

In case of emergency, please contact:
the Principal Investigator / Associate Investigator named above
or Manager, CAF: 9850 7780 / 0428 861 163 and **Animal Welfare Officer**: 9850 7758 / 0439 497 383

The above-named are authorised by MACQUARIE UNIVERSITY ANIMAL ETHICS COMMITTEE to conduct the following research:

Title of the project: **Long term recording of both blood pressure and sympathetic nerve activity in rats with chronic kidney disease**

Purpose: **5 - Research: Human or Animal Health and Welfare**

Aims: **1. To demonstrate that sympathetic nerve activity to different organ beds increases in parallel with increase in blood pressure and decline in renal function in LPK rat**
2. To examine the role of hormonal Renin Angiotensin System (RAS) on causing increased blood pressure and improve nervous function

Surgical Procedures category: 5 - Major Surgery with Recovery

All procedures must be performed as per the AEC-approved protocol, unless stated otherwise by the AEC and/or AWO.

Maximum numbers approved (for the Full Approval Duration):

Species	Strain	Age/Sex/Weight	Total	Supplier/Source
02-Rats	Lewis	4-18 weeks / Mixed / Varied	96	ARC Perth
02-Rats	LPK	4-18 weeks / Mixed / Varied	96	ARC Perth
		TOTAL	192	

Location of research:

Location	*Full street address*
Central Animal Facility	Building F9A, Research Park Drive, Macquarie University, NSW 2109
ASAM	Level 1, F10A, 2 Technology Place, Macquarie University, NSW 2109

Amendments approved by the AEC since initial approval:

1. Increase in the dosage of antihypertensive drug (losartan) administered (Exec approved 9 May 2013, AEC ratified 16 May 2013).
2. Add procedure under anaesthesia prior to euthanasia, as per ASAM/AEC SOP 002 (AEC approved June 2013)

Conditions of Approval: N/A

Being animal research carried out in accordance with the Code of Practice for a recognised research purpose and in connection with animals (other than exempt animals) that have been obtained from the holder of an animal suppliers licence.

Professor Mark Connor (Chair, Animal Ethics Committee) **Approval Date:** 13 June 2013